



# Pol Sci<sup>3</sup> arch

## THE 3<sup>rd</sup> CEEP N WORKSHOP ON POLYMER SCIENCE PROCEEDINGS

23-26 September 2015, Iasi, Romania  
“Petru Poni” Institute of Macromolecular Chemistry  
41A Grigore Ghica Voda Alley, 700487 Iasi, Romania

*Organized under the auspices of the bilateral Romanian-Ukrainian interacademic project  
“Development of multifunctional organic and organic-inorganic polymeric materials on the  
base of components with different chemical nature”, 2012-2016*

**TOPIC OF THE WORKSHOP**

***Polymer Architectures - from concept to design***

**SCIENTIFIC COMMITTEE**

Acad. Bogdan C. SIMIONESCU (Romania)  
Acad. Eugene LEBEDEV (Ukraine)  
Dr. Valeria HARABAGIU (Romania)  
Prof. Yuri SAVELYEV (Ukraine)  
Assoc. Prof. Neli KOSEVA (Bulgaria)  
Dr. Frantisek RYPACEK (Czech Republic)  
Prof. Dr. Bela IVAN (Hungary)  
Prof. Dr. Andrzej DWORAK (Poland)  
Prof. Dr. Marek KOWALCZUK (Poland)  
Prof. Dr. Igor LACIK (Slovakia)  
Prof. Dr. Majda ZIGON (Slovenia)

**ORGANIZING COMMITTEE**

Dr. Madalina ZANOAGA (Romania)  
Dr. Yevgen MAMUNYA (Ukraine)  
Dr. Fulga TANASA (Romania)  
Dr. Maksym IURZHENKO (Ukraine)  
Dr. Marioara NECHIFOR (Romania)  
Dr. Viortica GAINA (Romania)  
Dr. Volodymyr LEVCHENKO (Ukraine)  
Dr. Kristina GUSAKOVA (Ukraine)  
Dr. Liliana ROSU (Romania)  
Dr. Carmen TEACA (Romania)  
Dr. Mirela ZALTARIOV (Romania)

The organizers gratefully acknowledge the assistance of our partner



**Horizon 2020  
WIDESPREAD 2-2014:  
ERA Chairs  
Project no 667387:  
SupraChem Lab**

We thank our sponsors for the financial support:  
**S. C. LABORATORIUM S. R. L. București**  
**S. C. Nitech S. R. L. București**  
**S. C. PTM - Laborator S. R. L. Balotești, Ilfov**  
**S. C. AQUATOR S. R. L. Iași**

# ***PLENARY LECTURES***

## **INNOVATIONS IN PROCESSING OF POLYMERS FOR MEDICAL APPLICATIONS**

**M. Kozłowski**

*Wrocław University of Technology, Poland*

Polymers are widely used in medical applications, both for the diagnostics and therapy. Recently, a special attention attracts biodegradable polymers that degrade in a body after performing their function and do not require a second surgical intervention. Besides standard requirements the biomaterials have to meet (biocompatibility of both the polymer and its degradation products) they should exhibit appropriate engineering properties (function-related properties and shape, the life time, processing properties suited to the manufacturing technology etc.).

In this paper processing technologies of two kinds of medical devices have been discussed: the scaffolds used in tissue engineering and the stents implemented in vascular surgery, urology, and laryngology. These devices represent also different forms of polymers (porous and solid, respectively) and may be manufactured by means of different technologies. Batch foaming, extrusion foaming, 3D printing, electrospinning and laser micromachining have been discussed.

## HYDROGELS BASED ON POLY(2-OXAZOLINE)S

**J. Kronek, A. Zahoranová, M. Mikulec, Z. Kroneková**

*Department for Biomaterials Research, Polymer Institute, Slovak Academy of Sciences, Dúbravská cesta 9, 84541 Bratislava, Slovakia*

[Juraj.kronek@savba.sk](mailto:Juraj.kronek@savba.sk)

Poly(2-oxazoline)s represent versatile polymeric materials for different biomedical applications [1]. The living cationic polymerization of 2-oxazolines enables to prepare the polymers with defined structure, size, functionality, and architecture [2]. It was also shown that poly(2-oxazoline)s do not exhibit any adverse cytotoxic effects towards various cell lines [3,4] and *in vivo* experiments in rodents proved fast clearance time and no accumulation in organs [5,6].

2-Oxazolines can be also used for the preparation of hydrogels using various synthetic routes [7]. In this contribution, two types hydrogels based on poly(2-oxazoline)s have been studied. The first class of hydrogels was prepared by the random copolymerization of 2-ethyl-2-oxazoline with three different aliphatic bis(2-oxazoline)s (Fig. 1a). Second type was based on the crosslinking of poly(2-isopropenyl-2-oxazoline) with different aliphatic dicarboxylic acids (Fig. 1b).

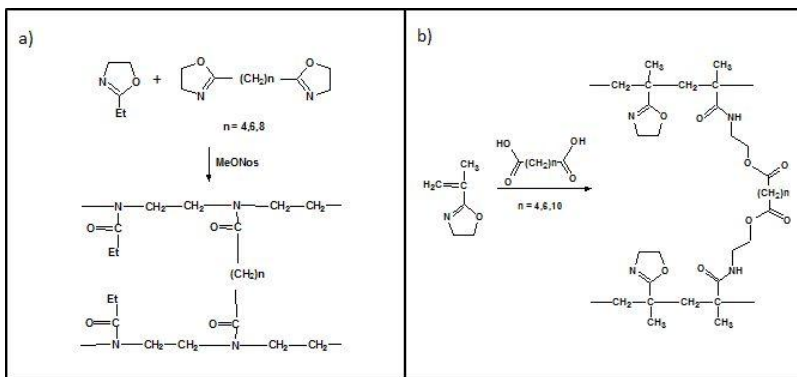


**Fig.1.** Scheme of preparation of hydrogels based on poly(2-oxazoline)s by cationic copolymerization of 2-ethyl-2-oxazoline with aliphatic bis(2-oxazoline)s (a) and polymer-analogous reaction of poly(2-isopropenyl-2-oxazoline) with three different aliphatic dicarboxylic acids (b).

## L2

In both cases, the properties of hydrogels such as polarity, stiffness, swelling ability and porosity have been adjusted by the length of aliphatic chain in crosslinker and the crosslinking density. Beside mentioned properties, we also examined *in vitro* cytotoxicity of all hydrogels using a direct contact method and analysis of hydrogel extracts. Both techniques showed non-toxic character of both types of hydrogels. Moreover, the first cell cultivation studies on the selected hydrogels showed that the survival of cells injected into the hydrogels was higher than two weeks.

**Acknowledgments**

*Authors are thankful the Agency of the Slovak Academy of Sciences and the Ministry of Education for financial support in the projects No. 2/0163/15 and 2/0156/15, and the Slovak Research and Development Agency for the for financial support in the project No. APVV-14-0858.*

1. *De la Rosa V. R.* Poly(2-oxazoline)s as materials for biomedical applications // *J Mater Sci Mater Med.* 25 (2014) 1211-1225.
2. *Rossegger E., Schenk V., Wiesbrock F.* Design Strategies for Functionalized Poly(2-oxazoline)s and Derived Materials // *Polymers.* 5 (2013) 956-1011.
3. *Kronek J., Kroneková Z., Lustoň J., Paulovičová E., Paulovičová L., Mendrek B.* *In vitro* bio-immunological and cytotoxicity studies of poly(2-oxazolines) // *J Mater Sci Mater Med* 22 (2011) 1725-1734.
4. *Luxenhofer R., Sahay G., Schulz A., Alakhova D., Bronich T. K., Jordan R. Kabanov A. V.* Structure-property relationship in cytotoxicity and cell uptake of poly(2-oxazoline) amphiphiles // *J Control Rel.* 153 (2011) 73-82.
5. *Goddard P., Hutchinson L. E., Brown J., Brookman L. J.* Soluble polymeric carriers for drug delivery. Part 2. Preparation and *in vivo* behavior of N-acylethyleneimine copolymer. // *J. Control Rel.* 10 (1989), 5–16.
6. *Gaertner F. C., Luxenhofer R., Blechert B., Jordan, R., Essler M.* Synthesis, biodistribution and excretion of radiolabeled poly(2-alkyl-2-oxazoline)s // *J Control Rel.* 119 (2007) 291–300.
7. *Wiesbrock F., Kelly A. M.* Strategies for the Synthesis of Poly(2-Oxazoline)-Based Hydrogels // *Macromol Rapid Commun.* 33 (2012) 1632-1647.

## **CHITOSAN – A PROMISING WORK BENCH FOR OBTAINING DYNAMIC MATERIALS**

**L. Marin**

*Petru Poni” Institute of Macromolecular Chemistry, 41A Grigore Ghica Voda  
Alley, Iasi 700487, Romania*

[lmarin@icmpp.ro](mailto:lmarin@icmpp.ro)

Imino-chitosan biopolymers are of great interest for health care due to their promising biological properties. The obtaining and exchange processes of imines formed by chitosan polyamine and aldehydes should further be of particular interest for dynamic covalent chemistry by creating the premises for the preparation of dynamic biomaterials.

In this context, the lecture is about our achievements in the field of imino-chitosan biopolymers as pathway to functional biodynamic materials, and underlines the benefits brought by grafting imine units on chitosan backbones, with a deeper view on the advantages in using vanillin, cynamaldehyde or an aromatic aldehyde containing boronic units.

The obtained results demonstrate that chitosan polyamine is a challenging workbench toward functional biodynamic materials.

## DISENTANGLED POLYMERS AND ALL-POLYMER COMPOSITES

**A. Pawlak**

*Centre of Molecular and Macromolecular Studies, Polish Academy of Sciences,  
Sienkiewicza 112, 90-363 Lodz, Poland*

[apawlak@cbmm.lodz.pl](mailto:apawlak@cbmm.lodz.pl)

All-polymer composites, based on one or two compatible polymers, are interesting alternative for classic composites [1-2]. Their advantages are: lower specific weight, easier recycling (e.g. melting into blend), possible good adhesion between components, easier processing and forming. The negatives are: more expensive processing and needs of precise control of mixing conditions. To skip these negative aspects the new methods of preparations are developed.

The strategies for obtaining all-polymer composites are based on two main selections: one or two polymeric components and one or many steps in processing. The methods of preparation can be divided into two groups: distribution of already made polymeric fibers into matrix from other polymer [3], or blending two polymers with formation of the fibers by elongation of molten droplets of minor component [4]. The second approach was successfully applied only for some pairs of polymers: PP/PET, PE/PET, PET/PA6, PLA/PP. In most blends only some elongation of droplets was achieved.

Poly(tetrafluoroethylene) (PTFE) is an example of polymer which is hardly to process by melt blending. However, there are observations that this polymer is easy for deformation and fibrillation under the modest shear conditions when PTFE powder is mixed in solid state with a second molten polymer [5]. The positive experience with solid state transformation of PTFE particles into microfibrils motivated us for work on the obtaining of all-polymer composites based on polypropylene fibers formed during deformation. To achieve these goal, it was necessary to prepare PP able for deformation in solid state under action of low shear/elongation forces during mixing with second molten polymer. The forces should transform grains of polypropylene into micro or nanofibers. The role of molten polymer is transferring stresses from mixing device and after solidification forming a matrix of composite, containing PP fibers. Usual commercial polypropylenes are not suitable for in-situ formation of nanocomposites because they have limited ability to deformation.

Mechanical properties of polymers and their ability to plastic deformation to

## L4

large strains are controlled by macromolecular entanglements in amorphous phase, i.e. less entangled polymer may be stretched larger. The number of entanglements in semi crystalline polymer may be reduced by applying specific crystallization procedure. Three different approaches were proposed for limitation of the entanglements of macromolecules in amorphous phase of solid polymer: a) crystallization under pressure with formation of extended chains crystals (e.g. HDPE), b) crystallization during polymerization (e.g. PTFE, PE), c) crystallization from diluted solution.

The last method was attractive for us because it was applicable for wider range of polymers than other methods. This method was developed by Smith and Lemstra [6] for preparation of highly oriented and strong polyolefins filaments. When small amount of polymer is dissolved in hot solvent the number of contacts between macromolecules is low, so the chains are not entangled. During cooling of such solution is formed a gel, having structure of macromolecular network (crystals are links) with a lot of solvent inside. The disentangled state is preserved in the gel, so is possible to spun it to high strains. After drawing and removing of solvent is obtained a strong, solid filament. For example, the polyethylene gel from decalin solution was drawn 30 times, while typical ratio for melt formed PE is only 5. The filaments exhibited excellent mechanical properties, with tensile strength of 3 GPa and Young modulus of 90 GPa.

If the polymer gel is not spun but dried then is obtained a polymer powder with reduced number of entanglements, useful for preparation of all-polymer composite. It is known that in deformation of semi crystalline polymers play a role not only entanglements of amorphous network but also crystals present in structure. The stress of initiating the plastic deformation of crystals strongly depends on the temperature and in highest temperatures of solid-state stretching is only 2 MPa.

Summarizing, the new recipe for all-polymer composite is as follows: make the polymer with reduced number of entanglements and mix them with the second molten polymer in temperature just below the melting point. After some minutes of mixing the grains of first polymer should be elongated into fibers, so after cooling the composite should be ready. Some orientation of freshly formed fibers could be expected if for processing was used an extruder.

In our studies the polypropylene with reduced entanglements was prepared by dissolution 1 or 2 wt% of polymer in hot xylene, in temperature of 130 °C. Time of dissolution was 1 or 3 hrs. After this time the temperature was decreased with a rate of 15 °C/h. When the temperature reached 80 °C a gel was formed inside the flask. The solution with gel was cooled to 40 °C and the gel was filtrated and dried. In result was obtained a white powder (Fig. 1), containing reduced number of macromolecular entanglements, as confirmed by rheological studies.

The second way of preparation of the partially disentangled polypropylene was dissolution of polymer in hot oil. Using this method 2 wt% of PP was

L4

dissolved in hot mineral oil at 190 °C in time of 1 h. The solution was cooled down to 100 °C, with a rate of 30 °C/h, followed by faster cooling (approx. 50 °C/h) to temperature of 40 °C. The cloudiness of solution was observed at temperature of 100 °C, meaning the formation of gel. The solution cooled to 40 °C was poured in n-hexane, and obtained PP was precipitated, filtered, rinsed and finally dried.

The polypropylene powders were characterized using methods sensitive to entanglement degree: rheology in melt (viscosity), crystallization (growth rate), plastic deformation (stress).

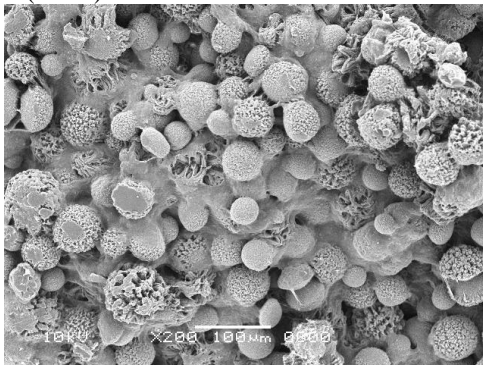


**Fig. 1.** Polypropylene powder obtained from diluted solution in xylene.

The powders were used for preparation of all-polymer composites. Polypropylene (3 or 6 wt%) was mixed with a second polymer (UHMWPE, PS, ethylene-octene copolymer EOC) in temperature higher than melting point of this polymer, but below the temperature of melting PP (i.e. 135-152 °C). The components were mixed by using Brabender W 50E measuring mixer or laboratory mini extruder EHP-5CS produced by Zamak, Poland. Plasticizing system of extruder was equipped with conical screws and return channel with a bypass valve that allowed passing the plasticizing material several times through the system.

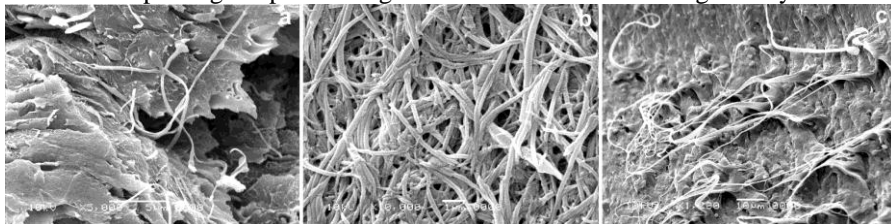


**Fig. 2.** Polypropylene fibers: dispersed in PS matrix (a); after removing PS matrix (b); dispersed in ethylene-octene elastomer matrix (c).

The shearing forces, acting in the melt, deformed PP powder particles and in result were obtained the fibers or nanofibers, dispersed inside the matrix of

## L4

second polymer, i.e. it was formed all-polymer composite. The morphologies of new nanocomposites were examined by using scanning electron microscope and examples are shown in Fig. 2

The nanofibers were successfully obtained in all compositions. The diameters of fibers were below 1  $\mu\text{m}$ , but most of them was smaller, with the size of 100-300 nm. Many fibers were circular in cross-section, but part of them was flat, tapes-like. It was difficult to judge about the length of fibers, because only part of each was visible. There were fibers which came out from the matrix and then came back to it. The comparison of effectiveness of mixer and extruder showed that the composites prepared by mixer had less uniform morphologies than composites prepared by mini extruder.

**Acknowledgments**

*The studies were financed from funds of the Polish National Science Centre on the basis of the decision number 2012/04/A/ST5/00606. The participation in Workshop was financed from statutory funds of CMMS.*

1. *Bhattacharyya, D., Fakirov S.* Synthetic Polymer-Polymer Composites, Hanser Verlag, Munich, 2012
2. *Karger-Kocsis J., Bárányi T.* Single-polymer composites (SPCs): Status and future trends, *Composites Science and Technology* 92 (2014) 77–94.
3. *Ward I.M., Hine P.J.* The science and technology of hot compaction, *Polymer* 45 (2004) 1413–1427.
4. *Denchev Z., Dencheva N.* Transforming polymer blends into composites: a pathway towards nanostructured materials, *Polym Int* 57 (2008) 11–22.
5. *Jurczuk K., Galeski A., Piorkowska E.* All-polymer nanocomposites with nanofibrillar inclusions generated in situ during compounding, *Polymer* 54 (2013) 4617-4628.
6. *Smith P., Lemstra P.J.* Ultra-drawing of high molecular weight polyethylene cast from solution, *Colloid & Polymer Sci.* 258 (1980) 891-894.

## BIOINSPIRED CRYSTAL GROWTH THROUGH POLYMERIC ADDITIVES AND TEMPLATES

**M. Mihai<sup>1</sup>, F. Doroftei<sup>1,2</sup>, B. C. Simionescu<sup>1</sup>**

<sup>1</sup>*“Petru Poni” Institute of Macromolecular Chemistry, 41A Grigore Ghica Voda  
Alley, Iasi 700487, Romania*  
[marcelas@icmpp.ro](mailto:marcelas@icmpp.ro)

<sup>2</sup>*“Babes-Bolyai” University Cluj-Napoca, 1 Mihail Kogălniceanu Str., Cluj-  
Napoca 400084, Romania*

Biominerals are everywhere in our world, including in our own bones, teeth and inner ear otoconia. Biologically regulated mineralization (biomineralization) began more than 500 million years ago in the pre-Cambrian period, and is largely responsible for the evolutionary success of the Cambrian explosion. Organisms from many different phyla evolved the ability to form about 64 different minerals known up to date [1]. The term “biomineral” refers not only to a mineral produced by organisms, but also reflects the fact that almost all of these mineralized products are composite materials of both mineral and organic components. Furthermore, being formed under controlled conditions, biomineral phases often have properties such as shape, size, crystallinity, isotopic and trace element compositions quite unlike their inorganically formed counterparts. All this complexity is reflected by the term “biomineral”.

Adapting the design concepts from nature’s ‘laboratories’ is a promising pathway to develop advanced materials, using biominerals as a wide range of examples. For instance, nature’s ability to manipulate calcium carbonate – a very simple molecule – to produce skeletal materials with considerable fracture resistance can be an inspiration for this approach. Calcium-bearing minerals comprise about 50% of known biominerals [2], most probably because calcium fulfills many fundamental functions in cellular metabolism. Calcium carbonate minerals are the most abundant biogenic minerals, both in terms of the quantities produced and their widespread distribution among many different taxa [2]. CaCO<sub>3</sub> exists as three different anhydrous polymorphs – calcite, aragonite and vaterite, all of which occur in calcified tissues. Monohydrate (monohydrocalcite), hexahydrate (ikaite) and amorphous forms of CaCO<sub>3</sub> were also identified as metastable precursor phases present during the initial stages of crystal formation [3].

The organisms strategy to control mineralization, as nature cannot

L5

manipulate parameters such as temperature or pressure as commonly done in the lab to control crystal growth, is by using organic molecules. These ones can be in the form of *insoluble organic matrices*, which generate a unique environment where crystallization occurs and can influence nucleation processes, or *soluble organic additives*, also typically present during crystal growth, which influence crystal texture and morphology.

To control the properties of crystals grown in synthetic systems a variety of strategies are commonly applied, taking biological mechanisms as an inspiration. There is a significant interest in using *soluble additives* to control crystallization [4-7]. These can vary from small molecules to large polymers, and can generate crystals with complex morphologies and with composite structures where one phase is embedded within the matrix of another, showing superior mechanical properties. Soluble additives are also believed to be the key in controlling crystal polymorphs. As an example, the influence of soluble polymeric molecules, namely the double hydrophilic block copolymer poly(*p*-hydroxystyrene-*b*-methacrylic acid), PHOS-*b*-PMAA, on the structure of CaCO<sub>3</sub> composites, as compared to bare CaCO<sub>3</sub> particles prepared in the same supersaturation conditions, was evidenced combining scanning electron microscopy and atomic force microscopy [7].

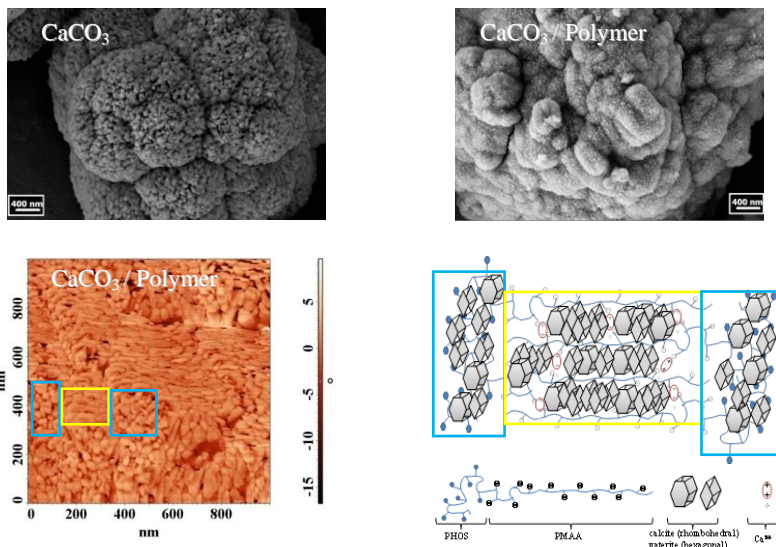


**Fig. 1.** SEM images of CaCO<sub>3</sub> and CaCO<sub>3</sub>/PHOS-*b*-PMAA 0.05 wt%, AFM phase image of sample with polymer, and schematic representation of inorganic/organic organization.

As shown by SEM images (Fig. 1), the copolymer PHOS-*b*-PMAA influences the CaCO<sub>3</sub> crystallization pathway. Thus, as compared to the typical

## L5

cauliflower shape of bare  $\text{CaCO}_3$  particles, a low amount of PHOS-*b*-PMAA (0.05 wt.%) induces the formation of smoother particles of very small grain size. The AFM phase image in Figure 1 shows some structured features:  $\text{CaCO}_3$  crystals (lighter color) seem to form elongated structures which are intercalated by the polyanion chains (darker color). At working pH (9.5) the PMAA blocks are ionized and the electrostatic repulsion between the ionic groups determines an extended conformation, whereas PHOS blocks are neutral and adopt a coiled conformation. When calcium ions are introduced into PHOS-*b*-PMAA solutions, the positive divalent calcium ions crosslink the negative ionic groups of different PMAA blocks. As shows the scheme in Figure 1, two polymeric regions can be found: one where PMAA chains are organized in crosslinked and extended conformation, and the second with intertwined coils of the PHOS blocks. Therefore,  $\text{CaCO}_3$  growth will take place as elongated structures between the crosslinked PMAA chains, and in an irregular manner between the PHOS coils.

*Insoluble organic matrices* are also extremely important in controlling the formation of biominerals. At the most fundamental level, a key feature of biological systems is that crystallization always occurs within compartments. This significantly affects the progress and outcome of reactions occurring within. A range of different model systems were used as synthetic matrix for  $\text{CaCO}_3$  crystallization [8-10]. An example is the synthesis of complex functional materials with thermo- and pH-sensitive tunable properties based on a poly(N-isopropylacrylamide-co-methacrylic acid) hydrogel and pH-sensitive and biocompatible  $\text{CaCO}_3$  [10].

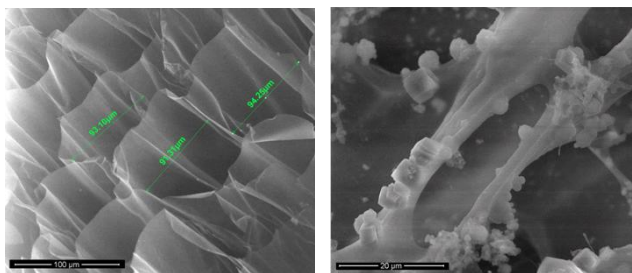


Fig. 2. SEM images of hydrogel before and after  $\text{CaCO}_3$  crystals growth.

As can be seen in Fig. 2, the hydrogel displays a regular porous structure, with pores of about 95  $\mu\text{m}$ . The presence of carboxylate groups makes the polymeric structures appropriate candidates for  $\text{CaCO}_3$  mineralization. Initially, the growth of  $\text{CaCO}_3$  on hydrogels takes place by the interaction of the acidic groups of their structure with  $\text{Ca}^{2+}$  ions, thus providing the nucleation centers upon which crystallization can occur, and then calcium carbonate crystallization takes place. As shown in Fig. 2,  $\text{CaCO}_3$  mineralization on hydrogel templates was effective,

## L5

forming a layer of inorganic material on hydrogels walls and also some CaCO<sub>3</sub> microparticles in excess. Thus, the hydrogel/CaCO<sub>3</sub> sample wall thickness is  $\sim 2.7 \pm 0.6 \mu\text{m}$ , whereas the bare hydrogel sample has a  $\sim 0.7 \pm 0.1 \mu\text{m}$  wall thickness.

Given the present state of knowledge, the prospects for finding simple, tough explanations for different effects of biomineralization mechanisms still represent challenges for further investigations. Moreover, bioinspired mineralization can transfer biomineralization principles to the synthesis of organic-inorganic materials, offering a large playground to develop future materials.

### Acknowledgments

*This work was possible due to the financial support of the Sectorial Operational Program for Human Resources Development 2007-2013, co-financed by the European Social Fund, under the project number POSDRU/159/1.5/S/132400, with the title „Young successful researchers – professional development in an international and interdisciplinary environment”.*

1. Knoll A. Biomineralization and evolutionary history // *Rev. Mineral Geochem.* 54 (2003) 329-356
2. Lowenstam H.A., Weiner S. In: *Biomineralization*, Oxford University Press, New York, 1989, pp 3-5
3. Addadi L., Raz S., Weiner S. Taking advantage of disorder: amorphous calcium carbonate and its roles in biomineralization // *Adv. Mat.* 15 (2003) 959-970
4. Colfen H., Mann S. Higher-Order Organization by Mesoscale Self-Assembly and Transformation of Hybrid Nanostructures // *Angew. Chem. Int. Ed.* 42 (2003) 2350-2365
5. Arias J. L., Fernández M. S. Polysaccharides and Proteoglycans in Calcium Carbonate-based Biomineralization // *Chem Rev.* 108 (2008) 4475-4482
6. Mihai M., Bucătariu F., Aflori M., Schwarz S. Synthesis and characterization of new CaCO<sub>3</sub> / poly(2-acrylamido-2-methylpropanesulfonic acid-co-acrylic acid) polymorphs, as templates for core/shell particles // *J. Cryst. Growth* 351 (2012) 23-31
7. Mihai M., Mountrichas G., Pispas S., Stoica I., Aflori M., Auf der Landwehr M., Neda I., Schwarz S. Calcium carbonate microparticle templates using a PHOS-b -PMAA double hydrophilic copolymer // *J. Appl. Cryst.* 46 (2013) 1455–1466
8. Zhang F-j., Yang X-g., Zhuang Y., Guo K-k., Wang M-j., Wei W-f. Crystallization of calcium carbonate in hydrogels in presence of meso-tetrakis (4-hydroxyphenyl) porphyrin // *J. Cent. South. Univ.* 19 (2012) 1802–1807
9. Mihai M., Bunia I., Doroftei F., Varganici C.-D., Simionescu B.C. Highly efficient Cu(II) sorbents obtained by CaCO<sub>3</sub> mineralization on functionalized

L5

cross-linked copolymers // Chem. – Eur. J. 21 (2015), 5220–5230

10. *Doroftei F., Mihai M., Sacarescu L., Fundueanu G., Simionescu B.C.*  
Composite materials based on poly(N-isopropylacrylamide-co-methacrylic acid) hydrogels and calcium carbonate // High. Perform. Polym. 27 (2015) 516–525

## ALL-WASTES COMPOSITES WITH INCREASED PET CONTENT

**A. Duta, C. Cazan, M. Cosnita**

*Transilvania University of Brasov, R&D Centre: Renewable Energy Systems and Recycling, 29 Eroilor Bvd., Brasov 500036 Brasov, Romania*  
[a.duta@unitbv.ro](mailto:a.duta@unitbv.ro)

Huge amounts of polymer wastes are yearly produced; a general trend towards environment protection limited the amounts of rubber and plastic wastes trashed to the landfill and supported more sustainable and feasible disposal ways. One general path is to partially recuperate the energy embedded in these products by using them as fuels in various industries (e.g. cement production); this solves the “wastes” problem but does not solve the “materials” problem, therefore recycling is more and more approached as an alternative, aiming at using these wastes as second raw materials in novel products development.

Recycling rubber(s) is well known and applied; however, recycling plastics, particularly cured plastics (as PET) represents a challenge as re-processing is no longer an option. An obvious alternative is to embed plastics in composites that can be further designed and tailored according to the application. The mechanical, thermal, chemical, etc. properties of these composites are depending on the components but mainly on the interfaces developed among these.

The interfaces in any composite are developed based on structural or at least surface charge compatibility between the components. Raw rubber and PET have a very limited compatibility (even at higher temperatures); when using waste rubber and waste PET the compatibility is more difficult to predict, as aging may significantly change the surface properties of the components and/or may differently change the bulk and surface properties [1]; as result, when using wastes, the second raw materials may end up with a variable set of properties that makes their compatibility a real issue in designing the end-product/material and its processing parameters. One solution previously proposed, is the addition of a third component supporting the interfaces formation between rubber and PET, and following the concept of “all wastes composites”, HDPE was chosen as compatibility agent. Further on, various additives can be added (as fillers) to control the interfaces and the aggregation of the components in the composites [2].

Hence, in the composites design several targets were proposed: (1) the

L6

majority components should be wastes (rubber, plastics); (2) to use PET in a large extent as being one of the most difficult to recycle polymer; (3) the type (chemical composition) and amount of additives will allow tailoring the composites according to the indoor/outdoor applications. All these targets can be met only if the composites are able to develop strong, controlled and predictable interfaces, reproducible over a rather large variety of second raw materials batches. Additionally, as these composites are obtained using wastes, the low-cost feature should be preserved (for large scale applications as in construction, roads, etc).

**1. Increasing the PET content**

Literature usually reports a maximum of 15% PET that can be dispersed into a rubber matrix without using special surface treatments that are expensive and far from being environmentally friendly (like plasma or concentrated acids).

By combining rubber, PET and HDPE, composites with much higher PET content could be obtained, through compression molding. The raw materials were scrap rubber from tires, PET and HDPE from household waste (all obtained from wastes collection companies) that were mechanically milled at grains of about 1mm. The processing temperature will influence the quality of the interface and can be responsible for oxidation reactions that can influence the surface and interfaces; in the end, the mechanical properties (stress-strain  $\sigma$  and E, compression,  $R_c$ , and impact resistance  $R_{impact}$ ) were considered as main output/optimization properties and the results in Table 1 show that the composite containing 35% of PET best meets all three properties and proved the point: PET can be embedded in high amounts in rubber matrix by using HDPE as compatibility agent, by developing good/continuous interfaces as Fig. 1a shows.

**Table 1.** Mechanical properties of the rubber-PET-HDPE composites

<b>rubber : HDPE : PET (weight)</b>	<b>T<sub>processing</sub> [°C]</b>	<b><math>\sigma</math> [N/mm<sup>2</sup>]</b>	<b>E [N/mm<sup>2</sup>]</b>	<b>R<sub>c</sub> [N/mm<sup>2</sup>]</b>	<b>R<sub>impact</sub> [kJ/m<sup>2</sup>]</b>
65 : 25 : 5	220	1,65	0,66	72,04	10,54
	240	1,20	0,68	52,07	9,51
60 : 35 : 5	220	1,34	0,41	67,78	12,39
	240	1,57	2,56	96,66	15,37
55 : 45 : 5	220	0,75	1,00	54,35	4,67
	240	1,00	1,11	50,10	6,12

When using scrap rubber from tires actually one already uses a composite, containing the rubber blend, fillers (mainly oxides but also carbon black and sulphur), traces of metals etc. As these components are proved to have a good compatibility with the matrix, the next step in designing the all-based composites was the use of small amounts of oxides, as fillers.

## 2. Tailoring the interfaces in the all-wastes composites

Adding a filler may have as primary target an increase in the mechanical strength. In the all-wastes composite case, the rational of testing and adding various oxides (in very low amounts 0.25%) was to control the aggregation of the components (around the filler) and/or to develop new interfaces; this was possible by adding the fillers as nano-sized powders (as TiO<sub>2</sub>, CaO or ZnO), [2, 3]. To preserve the “all-wastes” concept, 20µm fly ash grains were also tested.

The basic idea was to control the strength of the interfaces by controlling the macro- and micro-arrangements of the composites around the filler grains, including the nucleation/growth of the interfacial structures, thus the crystallinity. The results in Table 2 outline the mechanical properties and the crystallinity degree (obtained through XRD) and show a stiffness increase that well mirrors the increase in the crystallinity degree.

**Table 2.** Mechanical properties and crystallinity degree of the composites rubber:PET:HDPE:filler = 59.57:35:5:0.25

Filler	T <sub>processing</sub> [°C]	σ <sub>tr</sub> [N/mm <sup>2</sup> ]	E [N/mm <sup>2</sup> ]	R <sub>c</sub> [N/mm <sup>2</sup> ]	R <sub>impact</sub> [kJ/m <sup>2</sup> ]	χ <sub>c</sub> [%]
TiO <sub>2</sub>	220	1,00	10	67,23	15,10	17,6
	240	1,10	17,86	72,14	13,78	25,2
CaO	220	0,98	9,7	68,97	13,67	18,7
	240	1,12	10,73	70,41	11,42	10,5
ZnO	220	0,97	12,76	78,90	9,56	21,4
	240	0,92	20,89	82,41	10,58	23,1
Fly ash	220	1,15	13,65	79,34	10,45	25,9
	240	1,29	25,75	82,67	12,14	29,3

**Table 3.** Surface energy and roughness of the composites rubber:PET:HDPE:filler = 59.57:35:5:0.25

Filler	T <sub>processing</sub> [°C]	Θ <sub>water</sub> [°]	Eσ [mN/m]	σ <sup>d</sup> [mN/m]	σ <sup>p</sup> [mN/m]	RMS [nm]
TiO <sub>2</sub>	220	87,35	8,05	2,36	5,69	1006
	240	86,79	19,92	2,69	17,24	699
CaO	220	81,34	27,16	19,92	7,24	393
	240	84,83	25,61	17,55	8,05	245
ZnO	220	89,36	17,87	1,85	16,02	335
	240	93,39	23,13	19,45	3,68	446
Fly ash	220	84,75	26,81	23,13	3,68	399
	240	96,83	45,91	45,80	0,11	266

L6

The other mechanical properties are not actually improved by adding nano- and micro-sized fillers; however these results show that when designing the reinforced composites of this type, a compromise should be met between the macro- and the micro- effects of the fillers.

The addition of fillers has an even more significant effect on the surface. The surface energy ( $E\sigma$ ) and its polar and dispersive components ( $\sigma^d$ ,  $\sigma^p$ ) obtained based on contact angle measurements [4] and the AFM roughness (RMS) and images, Table 3 and Fig. 1 outline that the newly formed interfaces can be controlled by the size of the filler and its composition/ionic degree and these correlations will be detailed presented.

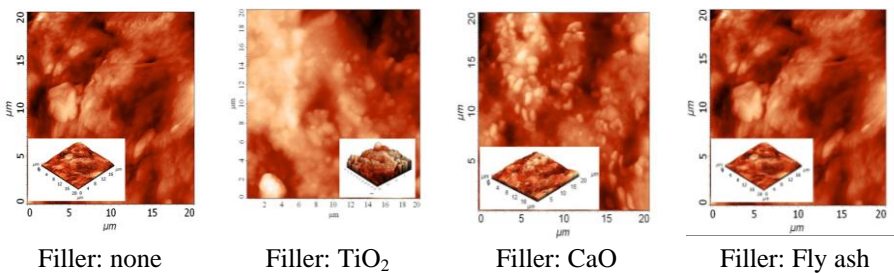


**Fig. 1** AFM Images of the all-wastes composites.

The comparative analysis can be completed by identifying the groups that are likely to be found at the interface (based on FT-IR data). Further on, the water resistance (thus the stability of the mechanical properties after long term contact with water) can differentiate the composites in terms of applications and is mainly related to the (micro)porosity of these materials that support water ad/absorption and lubrication.

1. *Awasthi K., Kulshrestha V., Avasthi D.K., Vijay Y.K.* Optical, chemical and structural modification of oxygen irradiated PET. *Radiat Meas* 45 (2010) 850-855.
2. *Vladuta C., Voinea M., Purghel E., Duta A.*, Correlations between the structure and the morphology of PET- rubber nanocomposites with different additives, *Materials Science and Engineering B*, 165-3 (2009), 221-226.
3. *Cosnita M., Cazan C., Duta A.*, Interfaces and mechanical properties of recycled rubber–polyethylene terephthalate–wood composites, *Journal of Composite Materials*, 48 (6) (2013) 683-694.
4. *Vladuta C., Andronic L., Visa M., Duta A.*, Ceramic interface properties evaluation based on contact angle measurement, *Surface & Coatings Technology* 202 (2008) 2448–2452.

# ***ORAL COMMUNICATIONS***

## **HYPOTHESES OF WELDING MECHANISMS AND NATURE OF THE WELDED JOINT OF PLASTICS**

**M.V.Iurzenko<sup>1,2</sup>**

<sup>1</sup> *Plastics Welding Department, E.O.Paton Electric Welding Institute, National Academy of Sciences of Ukraine, B.8, 11, Bozhenko Str., 03680, Kyiv-150, Ukraine*  
[iurzenko@paton.kiev.ua](mailto:iurzenko@paton.kiev.ua)

<sup>2</sup> *Institute of Macromolecular Chemistry, National Academy of Sciences of Ukraine, 48 Kharkivske Av., 02160, Kiev, Ukraine*

Construction of technological pipelines is one of the main fields of polymeric materials application in the world [1]. Among polymers used for pipes production polyethylene (PE) is one of the most commonly used [2]; this material has a perfect correlation between prices, mechanical properties and weldability, and, hence, has considerable advantage comparing with other polymers.

Pipes produced of various types of high density polyethylene (HDPE; so-called “pipe” polyethylene) are used for pipelines construction [3]. Pipes for the first technological pipelines have been produced from the raw material marked as PE-63. Later on the next brands, namely PE-80 and PE-100, have been developed and widely applied [4, 5]. Currently all these three types of polyethylene are used in pipe industry [6].

Welding is the main method of PE pipes joining for pipelines construction. As for today the following welding methods are sufficiently developed from technological point of view and are commonly used in practice: hot tool butt welding, hot tool socket welding and resistance welding [7, 8]. The last two methods require some special coupling details, such as socket and resistance fittings. Butt welding is the most simple and multipurpose method and can be used for pipes of all diameters (except the thin-wall pipes).

Performance characteristics of polyethylene pipelines are considerably dependent on the welded joint quality. As a rule the declared pipeline lifetime is at least 50 years, and all factors that could promote pipe or weld destruction are permanently investigated and can be eliminated [9]. In cases when destruction has occurred it is important to have an efficient and reliable repair technology [10]. Since pipes are produced of various types of polyethylene it is required to develop

welding technology providing reliable welds of dissimilar PE types.

All abovementioned welding methods have their own technological peculiarities and typical defects of welded joints [11]. Numerous scientific studies aim to improve hot tool butt welding method. Empiric methods are used by researchers in order to optimize main welding parameters for various technological conditions [12, 13], as well as to investigate peculiarities of various size pipes welding [14]. Mechanical and thermal properties of the pipe material also strongly affect the hot tool butt welding process [15, 16]. This should be taken into account when dissimilar types of polyethylene are welded with each other. PE-63, PE-80 and PE-100 have different technological characteristics, like, for example, shrinkage degree at cooling [17], different melt flow indexes, so special welding technology and equipment should be developed for the cases when dissimilar PE types have to be welded together.

In spite of the numerous developed technologies and wide pipes' welding practical application the detailed research of polyolefin welding nature is still not completed; mechanism of welds' formation is not explored sufficiently. Investigations of morphology, as a rule, enable to study the PE pipe macro-structure, fusion lines and heat-affected zone geometry [18, 19]. In some works the PE macromolecular structure affecting on material weldability has been investigated [20] as well as the internal deformations in PE welded joints [21], but general mechanism of welded joint formation and macromolecular structures [22, 23] in the weld are still studied insufficiently.

Hereby, there is still no complete understanding of PE and other polyolefins welded joints formation and structural peculiarities. Welding process of more complicated chemical system than polyethylene is even less explored. In this work the results of complex investigations (by means of differential scanning calorimetry, thermogravimetric and thermomechanical analysis, as well as via wide-angle X-ray scattering) of dissimilar technical PE types welds structure and their properties are presented. Basing on analysis of the results obtained some new hypothesis concerning nature and mechanism of welds' formation and polymer structuring in such welds are proposed.

### Acknowledgements

*The author would like to thank all the staff of the Plastics Welding Department of the E.O.Paton Electric Welding Institute of the NAS of Ukraine for their contribution and successful joint work on the presented subject.*

1. Bukhin VE, Fattakhov MM: Polymeric materials used for pipelines construction. *Engineering networks produced of polymeric materials* 2008, 25: 20-26. (In Russian).
2. Jeremic D: Polyethylene. *Ullmann's Encyclopedia of Industrial Chemistry* 2014, John Wiley & Sons Inc., New Jersey, USA: 1-42.

Co1

3. Editor's article: What should be known about "pipe" polyethylene. *Engineering networks produced of polymeric materials* 2002, 2: 5-9. (In Russian).
4. Ryzhov V, Kalugina E, Biserova N, Kazakov Yu: Pipe types of polyethylene. Structure and properties. *Polymeric pipes* 2011, 4: 56 – 60. (In Russian).
5. Horilovskiy N, Hvozdev I: Polyethylene pipe type PE-100. Main technical requirements and development. *Polymeric pipes* 2008, 22: 47 – 50. (In Russian).
6. Editor's article: Pipe polyethylene import market of Ukraine in 2013. *Polymeric pipes* 2013, 4 (29): 18 – 22. (In Russian).
7. Vijay K Stokes: Joining methods for plastics and plastic composites: An overview. *Polymer Engineering & Science* 1989, Vol.29, 19: 1310–1324.
8. Komarov GV: *Joints of details of polymeric materials*. Handbook. – SPb.: Profession, 2006. (In Russian).
9. Norman Brown: Intrinsic lifetime of polyethylene pipelines. *Polymer Engineering & Science* 2007, Vol.47, 4: 477–480.
10. Karandashev D: Emergency repair of polymeric pipelines. *Polymeric pipes* 2008, 4 (22): 83 – 85. (In Russian).
11. Korab NG, Mineev EA: Critical notes concerning welding methods for thermoplastic polymeric pipes. *Polimeric pipes* 2007, 1 (2): 53 – 55. (In Russian).
12. Nonhof CJ: Optimization of hot plate welding for series and mass production. *Polymer Engineering & Science* 1996, Vol.36, 9: 1184–1195.
13. Kaigorodov GK, Kargin VYu: Polyethylene pipe welded seam cooling rate affect on its strength. *Pipelines and ecology* 2001, 2: 13-14. (In Russian).
14. Hezzel J, Loogamer A, Tsunaga M: Welding of big diameter plastic pipes: characteristics and life time. *Engineering networks produced of polymeric materials* 2006, 18: 24-27. (In Russian).
15. Kimelblat VI, Volkov IV, Glukhov VV: Hot tool butt welding technology optimization. *Polymers properties consideration* 2010, 2 (28): 32 – 36. (In Russian).
16. Kimelblat VI, Volkov IV, Chuprak AI: Variations of polyethylene rheological properties as a stimulus for main hot tool butt welding parameters optimization. *Welding and diagnostics* 2012, 2: 49-52. (In Russian).
17. Mineev EA: Quality of welded joints and technological discipline. *Engineering networks produced of polymeric materials* 2006, 16: 40-41. (In Russian).
18. Vijay K: Stokes. Comparison of vibration and hot-tool thermoplastic weld morphologies. *Polymer Engineering & Science* 2003, Vol.43, 9: 1576–1602.
19. Min Nie, Qi Wang and ShiBing Bai: Morphology and property of polyethylene pipe extruded at the low mandrel rotation. *Polymer Engineering*

Co1

& Science 2010, Vol.50, 9: 1743–1750.

20. Volkov IV, Glukhov VV, Kamalov AB, Kimelblat VI: Correlation between PE-100 weldability degree and its macromolecular structure. *Kazan Technological University Messenger* 2010, 10: 600-602. (In Russian).

21. Lu Y, Shinozaki DM, Herbert S: Inhomogeneous deformation in welded high density polyethylene. *Journal of Applied Polymer Science* 2002, Vol.86, 1: 43–52.

22. Shadrin A: Martensite-Like Transformations in Welded Joints of Semicrystalline Polymers Formation. *ANTEC-92 Int. Conf. Proc.*, Detroit, USA, May 1-4, 1992, Technomic Publ., Lancaster, Penn: 1784-1787.

23. Grinyuk VD, Korab GN, Shadrin AA: Molecular mechanism of formation of welded joints in thermoplastic materials. *The Paton Welding Journal* 1992, Vol.4, 7-8: 447-451.

## **PHOTO-THERMAL ACTUATION STUDY OF ELASTOMER/CARBON NANOTUBES NANOCOMPOSITES**

**K. Czaniková<sup>1</sup>, I. Krupa<sup>1,2</sup>, M. Ilčíková<sup>1,2</sup>, J. Mosnáček<sup>1</sup>, E. Campo<sup>3</sup>,  
D. Račko<sup>1</sup>, M. Omastová<sup>1</sup>**

<sup>1</sup> *Polymer Institute, Slovak Academy of Sciences, Dúbravská cesta 9, 845 41 Bratislava 45, Slovakia*

[Kludia.Czanikova@savba.sk](mailto:Kludia.Czanikova@savba.sk)

<sup>2</sup> *Present address: Centre for Advanced Materials, Qatar University, P.O. Box 2713 Doha, Qatar*

<sup>3</sup> *School of Electrical Engineering, Bangor University, Dean Street, Bangor, LL57 1UT, Gwynedd, UK*

<sup>4</sup> *Institute of Macromolecular Chemistry, Academy of Sciences of the Czech Republic, Heyrovsky Sq. 2, 162 06 Prague, Czech Republic*

The development of new types of tactile displays based on the actuation of nanocomposite materials can aid the visually impaired [1]. In general, actuators have ability to change their dimension upon application of external stimulus (light, heat, electric voltage). Polymer/carbon nanotubes (CNTs) composites represent promising materials for designing and fabricating new stimuli responsive samples [2,3,4].

Nanocomposites based on ethylene vinyl acetate (EVA) polymeric matrices enriched by CNTs produce ensembles capable of light-induced actuation. New photo-actuating materials based on the commercial elastomer EVA and well-dispersed CNTs were developed as potential materials for the fabrication of smart actuators [5,6,7]. To improve compatibility of multi-wall CNTs (MWCNT) with EVA, the MWCNT were modified by using special synthesized compatibilizer consisting of pyrenenyl and cholesteryl groups (cholesteryl 1-pyrenecarboxylate (PyChol)). Studies showed that the presence of non-covalently bonded PyChol compatibilizer significantly improved the filler/matrix interaction leading to well dispersed MWCNT.

The contribution represents the photo-actuation testing of EVA-MWCNT nanocomposites in the form for Braille elements in response to light using a new *in situ* method of scanning electron microscopy (SEM), atomic force microscopy (AFM) and also by nanoindentation.

## Co2

The photo-actuation measurements of EVA-MWCNT nanocomposites also were carried out in the form of strips illuminated by red light emitted diode (red LED) using dynamic mechanical analysis (DMA) and dynamometer. The fully reversible photo-actuation of the nanocomposites were obtained. The dependence of the actuation stress as a function of CNTs concentration, energy and intensity of light was studied.

EVA-CNTs nanocomposites can be employed as light responsive materials to fabricate new types of photo-actuators, due to the composites exhibited high actuation stresses combined with very good long-term stability.

### **Acknowledgments**

*This work was supported in part by NOMS which is funded by the European Commission under contract no. 228916, and by project VEGA 02/0149/14.*

1. <http://www.noms-project.eu>
2. Ahir, S.V., Huang, Y.Y., Terentjev, E.M. Polymers with aligned carbon nanotubes: Active composite materials. *Polymer* 49 (2008) 3841-3854.
3. Marshall J.E., et al. Carbon-nanotube sensitized nematic elastomer composites for IR-visible photo-actuation. *Soft Matter* 8 (2012) 1570-1574.
4. Ilčíková M., et al. Tailoring of viscoelastic properties and light-induced actuation performance of triblock copolymer composites through surface modification of carbon nanotubes. *Polymer (United Kingdom)* (2015) article in press.
5. Czaniková K., et al. Photo-actuating materials based on elastomers and modified carbon nanotubes. *J of Nanophotincs* 6 (2012) 063522.
6. Czaniková K., et al. Nanocomposite photoactuators based on ethylene vinyl acetate copolymer filled with carbon nanotubes. *Sensor Actuat B-Chem* 186 (2013) 701-710.
7. Czaniková K., et al. In situ electron microscopy of Braille microsystems: photo-actuation of ethylene vinyl acetate/carbon nanotube composites. *Mater Res Express* 2 (2015) 025601.

## ***IN SITU* PHOTOGENERATION OF SILVER/GOLD NANOPARTICLES IN POLYMER TEMPLATES**

**A. Chibac, V. Melinte, T. Buruiana, E. C. Buruiana**

*“Petru Poni” Institute of Macromolecular Chemistry, 41A Grigore Ghica Voda  
Alley, Iasi 700487, Romania*  
[andreea.chibac@icmpp.ro](mailto:andreea.chibac@icmpp.ro)

In recent years, the development of hybrid polymer nanocomposites has drawn a considerable attention especially due to their potential applications in diverse industrial and biomedical fields [1]. Up to now, various inorganic nanoparticles such as metals/metal oxides, clays, carbon nanotubes, silica or hydroxyapatite have been incorporated into polymer templates leading to micro/nanofilled materials with distinctive features. Among these, silver/gold nanoparticles are extensively studied, reason for that different strategies for the achievement of Ag/Au nanoparticles have been reported. A simple and efficient method for the obtaining of hybrid composites containing *in situ* grown silver or gold nanoparticles is based on the photopolymerization of acrylic/epoxy monomers in tandem with the reduction of the metal salt by a radical arising from the photoinitiator used in the system [2].

Our study describes an interesting technique to *in situ* create noble metal nanoparticles in triazene block copolymers through the UV-triggered photodecomposition of the photolabile triazene units without the use of any conventional reducing agent. The generation of Ag/Au metal nanoparticles from noble metal precursors (1 wt% AgNO<sub>3</sub> or AuBr<sub>3</sub>) induced *via* the UV decomposition of chromophore with the formation of some radical active species was monitored in solution/thin films and the *in situ* growth of Ag/Au nanostructures into polymer matrices was proved by UV spectroscopy and TEM analysis.

### **Acknowledgements**

*This work was financially supported by CNCSIS-UEFISCDI, project number PN-II-ID-PCE-2011-3-0164 (40/5.10.2011).*

1. Paul D. R., Robeson L. M. Polymer nanotechnology: Nanocomposites, Polymer 49 (2008) 3187-3204.
2. Yagci Y., Sangermano M., Rizza G. In situ synthesis of gold-cross-linked

Co3

poly(ethylene glycol) nanocomposites by photoinduced electron transfer and free radical polymerization processes. Chem Commun 24 (2008) 2771-2773.

## **SELF-ASSEMBLED NANOPARTICLES BASED ON N-HYDROPHOBICALLY MODIFIED CHITOSAN**

**V. Balan, V. Redinciuc, L.Vereștiuc**

*Faculty of Medical Bioengineering, Gr. T. Popa University of Medicine and Pharmacy, 9-13 Kogalniceanu Street, 700454, Iasi, Romania*

[balanvera@yahoo.com](mailto:balanvera@yahoo.com)

Chitosan is a versatile biopolymer with exciting properties, such as: biocompatibility, biodegradability, antitumor activity, promoter of wound healing that recommend it for a great variety of biomedical applications [1,2]. Current evidences suggest that incorporation of hydrophobic chains into chitosan structure confers new physicochemical properties, including the ability to self-associate into different mediums and to form micelles, nanoparticles or hydrogels, with promising results as chemotherapeutic systems [3]. In this regard, the paper presents the synthesis and characterization of docetaxel-loaded nanoparticles based on N-palmitoyl chitosan (PCs) prepared through self-assembly method and evaluates their potential in biomedical applications. N-palmitoyl chitosan has been obtained through the reaction of chitosan with palmitoyl chloride; its structure has been investigated and confirmed by FT-IR and <sup>1</sup>H-NMR spectroscopy. The self-aggregation behaviour of PCs in aqueous media and its critical micelle concentration (CMC) were determined using fluorescence spectroscopy with pyrene as a fluorescent molecule. The self-assembly mechanism imply a combined effect of hydrophobic and electrostatic interactions, hydrogen bonds and van der Waals forces that take their own roles simultaneously. Docetaxel-loaded nanoparticles exhibited positive Zeta potential and a hydrodynamic diameter around 250 nm. *In vitro* drug release studies and biodegradation assays, performed in two phosphate buffered saline (PBS) mediums (pH 7.4 and 5.5) have indicated the suitability of proposed nanoparticles as drug delivery system.

### **Acknowledgments**

*This work was supported by a grant of the Romanian Ministry of Education, CNCS – UEFISCDI, project number PN-II-RU-PD-2012-3-0282.*

1. Dash, M., Chiellini, F., Ottenbrite, R.M., Chiellini, E. Chitosan-A versatile semi-synthetic polymer in biomedical applications // Progress in Polymer Science, 36, (2011) 981-1014.

Co4

2. *Kean T., Thanou M.*, Biodegradation, biodistribution and toxicity of chitosan// *Advanced Drug Delivery*, 62 (2010) 3–11.
3. *Larsson, M., Huang, W-C., Hsiao, M-H. Wang, Y-J., Nydén, M., et al.* Biomedical applications and colloidal properties of amphiphilically modified chitosan hybrids//*Progress in Polymer Science* 38 (2013) 1307–1328.

## **ELECTROCHEMICAL INVESTIGATION OF BICARBAZOLE-PYRIDINE LIGANDS**

**K. Laba<sup>1,2</sup>, P.Data<sup>1,2,3</sup>, M. Lapkowski<sup>1,2</sup>**

<sup>1</sup> *Center of Polymer and Carbon Materials, Polish Academy of Science, M. Curie-Skłodowskiej 34, 41-819 Zabrze, Poland*

[klaba@cmpw-pan.edu.pl](mailto:klaba@cmpw-pan.edu.pl)

<sup>2</sup> *Faculty of Chemistry, Silesian University of Technology, Ks. M. Strzody 9, 44-100 Gliwice, Poland*

<sup>3</sup> *Physics Department, University of Durham, South Road, Durham DH1 3LE, United Kingdom*

The main advantage of organic semiconductors over conventional conductive materials is their flexibility and wide range of optical, optoelectronic, and photo- and electroluminescent properties [1].

Within the large family of porphyrinoid systems, synthetic porphyrin analogues so-called phthalocyanines (Pcs) enjoy a privileged position. Pcs are generally difficult to dissolve in most organic solvents because of the intermolecular interaction of the Pc molecules, hence, limiting their further applications. The physicochemical properties of Pcs can be fine-tuned through synthetic manipulation for example by variation of the central metal ion, attaching various moieties to the exterior ring system or substituting the axial ligands [2, 3].

In this work, the similar compounds were investigated: pyridine substituted at 3,5-position by carbazole two different sides, the 2- and 3-positions. This molecules were proposed as axial ligands for ruthenium phthalocyanine complexes. The main aim of our project is to combine carbazole's favourable properties with very good photoinduced electron transfer and hole transport properties of metallophthalocyanines.

Carbazole and its derivatives have been known mainly due to their high hole transporting capabilities (p-type semiconductor) and strong fluorescence, as components of opto- and electroactive materials. Carbazole-based compounds show interesting electrochemical, electrochromic, light-emitting, and photorefractive properties. Their bluish photo- or electro-luminescence is a result of the large band-gap of the biphenyl unit. Moreover they exhibit high thermal and photochemical stability. These properties are especially valuable for perspective

materials, when these compounds are used as monomers in syntheses of conjugated macromolecules for optoelectronics [4,5].

Herein, we report comparison of results for bicarbazole-pyridine ligands: electrochemical (cyclic voltammetry) and *in situ* spectroelectrochemical (UV-Vis-Nir and Electron Paramagnetic Resonance).

1. *Forrest S.R., Thompson M.E.* Introduction: Organic Electronics and Optoelectronics // Chem. Rev. 107 (2007) 923-925.
2. *Nyokong T.* Effects of substituents on the photochemical and photophysical properties of main group metal phthalocyanines // Coord. Chem. Rev. 251 (2007) 1707.
3. *Arici M., Arican D., Uğur A. L., Erdoğmuş A., Koca A.* Electrochemical and spectroelectrochemical characterization of newly synthesized manganese, cobalt, iron and copper phthalocyanines // Electrochim. Acta 87 (2013) 554.
4. *Lapkowski M., Data P., Golba S., Soloduch J., Nowakowska-Oleksy A.* Unusual band-gap migration of N-alkylcarbazole-thiophene derivative // Opt. Mater. 33 (2011) 1445-1448.
5. *Data P., Pander P., Lapkowski M., Swist A., Soloduch J., Reghu R.R., Grazulevicius J.V.* Unusual properties of electropolymerized 2,7- and 3,6-carbazole derivatives // Electrochem. Acta 128 (2014) 430-438.

## **NEW RESINS FROM ALLYL-BENZOXAZINES AND BISMALIMIDES FOR OBTAINING HYBRID MATERIALS**

**O. Ursache<sup>1</sup>, C. Gaina<sup>1</sup>, V. Gaina<sup>1</sup>, F. Tanasa<sup>1</sup>, D. Ionita<sup>1</sup>, M. Iurzenko<sup>2</sup>**

<sup>1</sup> "Petru Poni" Institute of Macromolecular Chemistry, 41A Grigore Ghica Voda Alley, Iasi 700487, Romania  
[oana.buliga@icmpp.ro](mailto:oana.buliga@icmpp.ro)

<sup>2</sup>Institute of Macromolecular Chemistry of National Academy of Sciences of Ukraine, 48 Kharkivske shausse, Kyiv 02160, Ukraine

The resins and hybrid materials were synthesized by the reaction of multifunctional intermediates containing allyl, benzoxazine/benzoxazine-triethoxysilan groups with aromatic/aliphatic bismaleimides or a mixture of both type of bismaleimides. The reactions that occur during the reticulation of the multifunctional intermediates are: ene reaction (Alder-ene reaction), Diels-Alder cycloaddition reaction, Mannich reaction, hydrolysis and condensation of triethoxysilane groups. The mechanism of these reactions has been reported in our previous work [1,2].

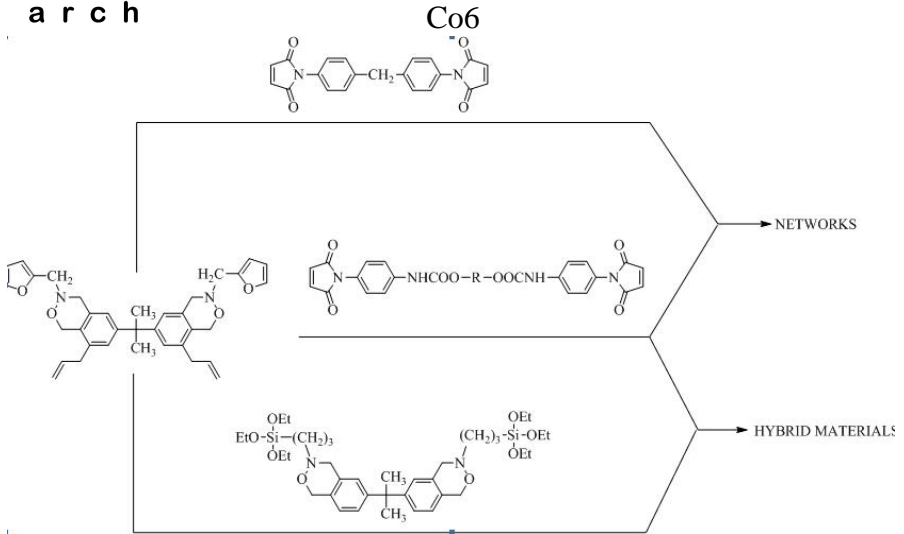
Using the reaction between the benzoxazine monomers and a mixture of aromatic and aliphatic bismaleimides, flexible benzoxazine resins with lower phase separation were obtained.

The hybrid materials were obtained by the reaction of bismaleimides with a mixture composed from a benzoxazine monomer containing allyl and furyl groups and a triethoxysilane functionalized benzoxazine monomer.

A general representation of the reaction schemes is presented below.

The structure of the compounds was confirmed by the ATR-FTIR spectroscopy. Then, the dynamo-mechanical, the dielectric and thermic properties were investigated. The morphology of the films was studied using small-angle X-ray scattering.

1. Gaina C., Ursache O., Gaina V., Musteata V. E. High performance thermosets based on multifunctional intermediates containing allyl, maleimide and benzoxazine groups // J Polym Res. 20 (2013) 263.
2. Gaina C., Ursache O., Gaina V., Varganici C. D. Poly (urethane-benzoxazine)s // J Polym Res. 21 (2014) 586.



## MICROPARTICLES OBTAINED BY THE CROSS-LINKING OF MALEIC ACID COPOLYMERS AND THEIR APPLICATION IN DYE REMOVAL

**I. Popescu, D.M. Suflet**

*“Petru Poni” Institute of Macromolecular Chemistry, 41A Grigore Ghica Voda Alley, Iasi 700487, Romania*  
[ipopescu@icmpp.ro](mailto:ipopescu@icmpp.ro)

In this work, new pH-sensitive polymeric microparticles (Figure 1) were obtained by the cross-linking of poly(N-vinyl caprolactam-co-maleic acid) (VCL-MAC). Due to the high content on carboxylic units and to the low crosslinking degree, the microparticles can retain large amount of water (200 g water/g microparticles). Their swelling was largely influenced by the pH and by the presence of cationic hydrophobic molecules.

The performance of VCL-MAC microparticles as adsorbent for cationic dyes like rhodamine 6 G (R6G) and methylene blue (MB) from aqueous solution was investigated. They proved to have high dye removal efficiency. The adsorption capacities, low at acidic media, increase with the solution pH attaining high values at pH = 10 (Figure 2).

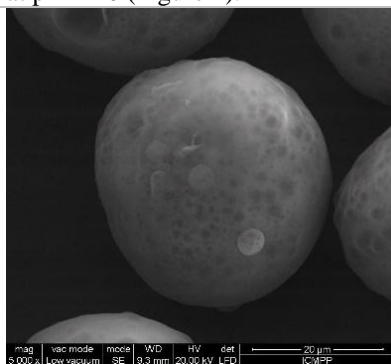


**Fig 1.** SEM pictures of VCL-MAC microparticles

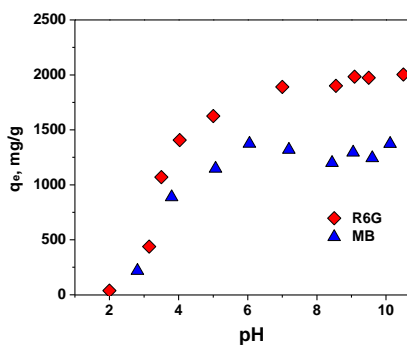


**Fig 2.** Influence of the initial pH on the dye adsorption by VCL-MAC microparticles

Co7

The equilibrium dye adsorption data were analyzed with Langmuir and Freundlich models. According to Langmuir model, the maximum adsorption capacity of VCL-MAC microparticles at pH = 10 was 2012 mg/g for R6G and 1644 mg/g for MB, values closed to those presented in the literature for hydrogels with a high content of carboxylic acid groups [6,7]. The kinetic of the dye adsorption was also study in order to obtained important information about the adsorption mechanism.

**Acknowledgements**

*This work was supported by a grant of the Romanian Ministry of Education, CNCS – UEFISCDI, project number PN-II-RU-PD-2012-3 -0059.*

1. Shukla N.B, Rattan S., Madras G. Swelling and dye-adsorption characteristics of an amphoteric superabsorbent polymer // Ind. Eng. Chem. Res. 51 (2012) 14941–14948.
2. Shukla N.B., Madras G. Kinetics of adsorption of methylene blue and rhodamine 6G on acrylic acid-based superabsorbents. // J Appl Polym Sci. 126 (2012) 463-472.

## **WASTE WOOD ROLE IN THE DESIGN OF ALL-WASTES COMPOSITES WITH RUBBER MATRIX**

**M. Cosnita, C. Cazan and A. Duta**

*Transilvania University of Brasov, RTD Dep. Renewable Energy Systems and Recycling, Eroilor 29, 500036 Brasov, Romania*

[a.duta@unitbv.ro](mailto:a.duta@unitbv.ro)

Nowadays finding solutions for the increased energy consumptions and environmental pollution represents a very topic which researchers have to face. The great development of automotives made the discharge of tire wastes to increase year by year. Tire rubber posses a set of important properties, such as impact strength, flexibility, abrasion resistance, and resistance to weathering, [1].

A new trend of sustainable development encourages to use alongside the polymers, second raw materials such as cellulose-based wastes aiming at their use as construction materials. There are some properties of cellulosic fibers, such as biodegradability, easy availability and outstanding physico-mechanical properties, which makes it proper to be used in polymeric blends, [2].

This waste in most cases is burned. Though the wood waste maybe important filler for thermoplastic composite industry. This material due to its properties and being inexpensive it is recommended for the long-term sustainability of the WPC industry, [3].

Others important wastes with desirable properties to be inserted in the rubber matrix are based on polyethylene terephthalate (PET), taking into account that the huge amounts of household waste consists mostly of polyolefin plastic (HDPE, LDPE and PP) and polyethylene terephthalate (PET), [4].

The main component of any composite system with determinant influence on the whole output properties is the coupling agent. Low molecular weight compounds are used to increase the compatibilization in such systems, but most often they are of toxic nature and are expensive. In our research paper the role of coupling agent was initially designed to be played by HDPE, but extended studies showed that sawdust compete in increasing the mechanical properties of the obtained composites.

The influence of wood waste as coupling agent in rubber-PET-wood-HDPE based composites is investigated in this work.

### Results and conclusions

The mechanical properties of any type of composites are strongly dependent on the interfacial adhesion between blended components. Often the interactions between composite components are of physical nature, but the strongest interfaces are based on chemical interactions. In previous studies we reported on the mechanical properties of rubber, PET and HDPE based composites, and the optimal properties were found for compression molding temperature of temperatures of 220, 240 and 260 °C, [5]. When adding small amount of sawdust at rubber-PET-HDPE blend, remarkable results were recorded in terms of mechanical performance, [6].

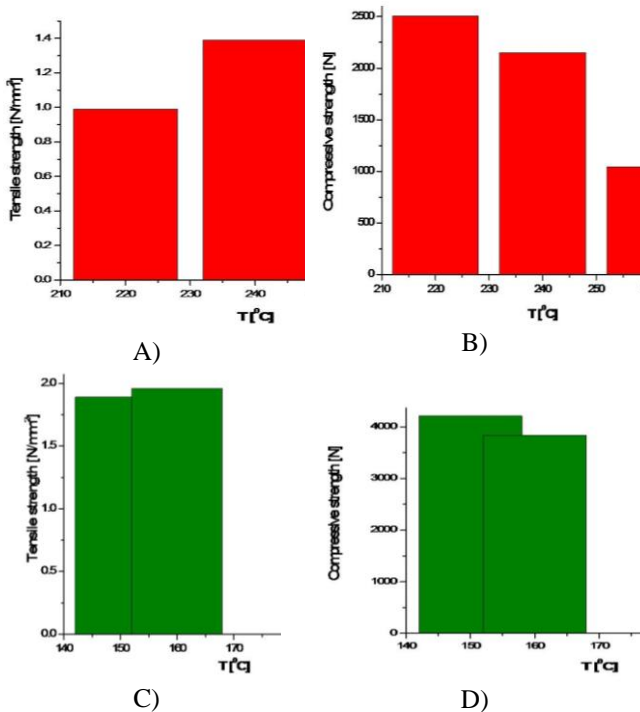


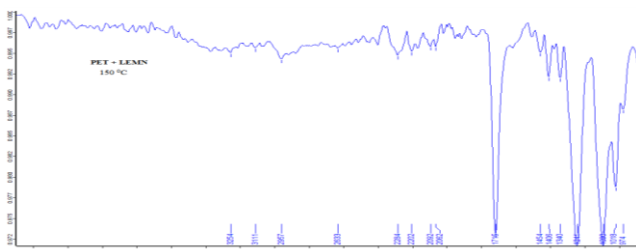
**Fig. 1.** Comparative analysis of mechanical properties of composites without wood (A, B) and with wood sawdust (C and D).

Co8

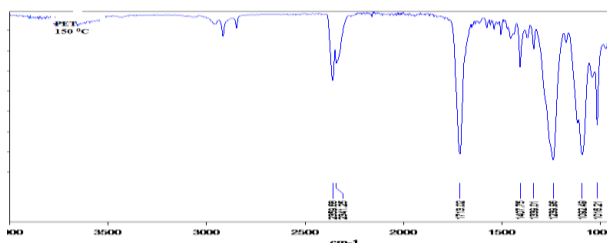
The wood sawdust addition led to important economical benefit related to decreasing the curing temperature while preserving good mechanical properties. The optimal series of temperature for composite with added wood were found for 150, 160 and 190 °C.

The mechanical tests results in terms of tensile and compression resistance of our previous composites with the composition ratio rubber, PET, HDPE = 85: 10: 5 are represented in the Fig.1 (A and B), and those of sample with added wood are found in Fig.1 (C and D), with the weight ratio rubber, PET, HDPE, wood = 80: 10: 5: 5.

There is obviously the effect of wood addition on the growth of tensile and compressive strength, Fig.1. These results are suggesting that new strong interfaces are developed when sawdust was added. These new interfaces were investigated by obtaining a composite based only on PET and wood and by characterizing them by FTIR spectroscopy. The FTIR spectra of these recorded significant changes, which are indicating that there are interactions between PET and wood, as Fig.2 shows.



A)



B)

**Fig.2.** FTIR spectra of composite based on PET and wood compared with that of PET.

The possible interaction between PET and wood can be represented as follow in Fig. 3.

Co8

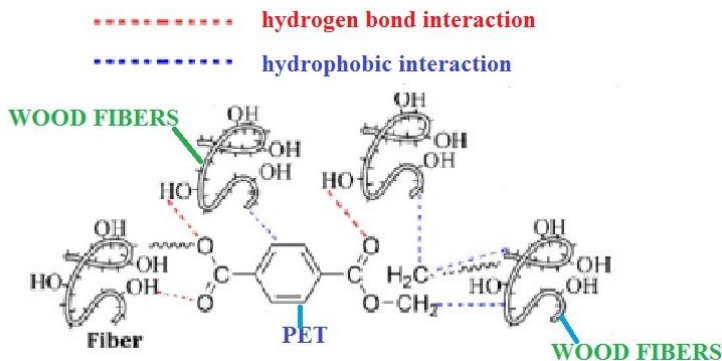


**Fig.3.** Possible interactions between PET and wood fibers.

Low cost materials based on waste of rubber, plastics and wood with good mechanical properties can be manufactured. The study reveals that wood sawdust are competing alongside HDPE for enhancing the interfacial adhesion between components of composite. Mechanical tests results recorded an improvement of performance by adding wood to rubber, PET, HDPE blend. FTIR spectra confirmed the formation of new interfaces, in which are implied PET and wood.

1. *Turgut P, Yesilata B.* Physico-mechanical and thermal performances of newly developed rubber-added bricks. *Energy and Buildings* 2008; 40:679–88.
2. *Thakur, M.K. Thakur,* Processing and characterization of naturalcellulose/thermoset polymer composites, *Carbohydr. Polym.*, 109 (2014), pp. 102–117).
3. *Nadir Ayrimis Alperen Kaymakci, Türker Güleç,* Potential use of decayed wood in production of wood plastic composite, *Industrial Crops and Products*, Volume 74, 15 November 2015, Pages 279–284.
4. *Yong Lei, Qinglin Wua., Quanguo Zhang,* Morphology and properties of microfibrillar composites based on recycled poly (ethylene terephthalate) and high density polyethylene, *Composites: Part A* 40 (2009) 904–912.
5. *Vladuta, C., Voinea, M., Purghele, E., Duta, A.,* Correlation between the structure and morphology of PET-rubber nanocomposite with different additives, *Materials Science and Engineering B* 165 (2009) 221-226.
6. *Cosnita, M., Cazan, C., Duta, A.,* Interfaces and mechanical properties recycled rubber–polyethylene terephthalate–wood composites, *Journal f Composite Materials*, (2013), DOI: 10.1177/0021998313476561.

## **EFFECT OF EPOXY AND SUCCINIC ANHYDRIDE FUNCTIONALIZED SOYBEAN OIL COATING ON WOOD RESISTANCE AGAINST PHOTODEGRADATION**

**C.-D. Varganici, D. Rosu, C.-A. Teacă, L. Rosu, R. Bodîrlău**

*Centre of Advanced Research in Bionanoconjugates and Biopolymers, "Petru Poni" Institute of Macromolecular Chemistry, 41A Grigore Ghica Voda Alley, Iasi 700487, Romania*

[varganici.cristian@icmpp.ro](mailto:varganici.cristian@icmpp.ro)

The main components of wood consist of natural macromolecules, including cellulose, hemicelluloses and lignin. Due to its exposure into the natural environment, wood undergoes photooxidation processes under the action of environmental factors. As a primary consequence, colour modifications occur at the wood surface during photooxidation. One way in preventing this unwanted aspect consists in coating the wood surface with protective layers through chemical modification. This study deals with photostability evaluation of softwood chemically modified surfaces by stages of successive treatment with succinic anhydride and epoxidized soybean oil under exposure to higher than 280 nm wavelengths. Colour and structural modifications of the materials during photooxidation phenomena were monitored as functions of irradiation dose and time. A slow increasing tendency was exhibited by chromatic coordinates values with irradiation dose and time, as compared to their initial values corresponding to unmodified wood. More intense photodegradation tendencies were exhibited by lignin. This led mainly to an increase in redness feature for the wood samples surface. The coating layer of epoxidized soybean oil was responsible for the protection of modified wood surface against photooxidation phenomena by screening effect.

### **Acknowledgements**

*Authors acknowledge the financial support of a grant of the Romanian National Authority for Scientific Research, CNCS-UEFISCDI, project number PN-II-ID-PCE-2011-3-0187.*

## Mn (II) and Zn (II) – ORGANIC FRAMEWORKS: TOWARD NEW MAGNETIC AND LUMINESCENT MATERIALS

M. F.Zaltariov, M. Cazacu, A. Vlad, S. Shova

“Petru Poni” Institute of Macromolecular Chemistry, Aleea Gr. Ghica Voda 41A,  
Iasi 700487, Romania

[zaltariov.mirela@icmpp.ro](mailto:zaltariov.mirela@icmpp.ro)

Polynuclear metal carboxylate clusters are versatile SBUs (*secondary building units*) for the synthesis of metal-organic frameworks due to their versatile binding features as well as their robustness and thermal stability. The affinity between the metal ions and carboxylate ligands determines the stability of the resulting complexes and depends on the interaction mechanism which involves the assembly processes (coordinative bonds and non-covalent interactions: H-bonds and  $\pi$ - $\pi$  stacking).

In this work two flexible carboxylic acids were reacted, in the presence of N-donor derivatives as co-ligands, with Zn (II) and Mn (II) salts or clusters. The structure of the obtained complexes was confirmed by single crystal X-ray diffraction, showing different coordination geometries of metal ions and structural motifs, in dependence on the ligand nature and reaction conditions. The presence of metal centers (Mn or Zn) confers properties of interest such as magnetism and fluorescence to the resulting structures proved by adequate measurements (fig. 1).

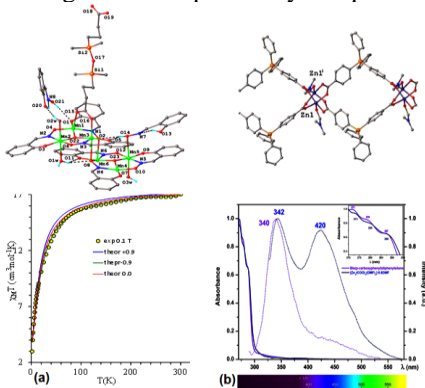


**Fig. 1.** XRD structure and magnetic susceptibility  $\chi T$  versus T plots data for Mn (II) coordination polymer (a); XRD structure and fluorescence spectrum of Zn (II) coordination polymer (b).

**Acknowledgements**

*This work was supported by a grant of the Ministry of National Education, CNCS – UEFISCDI, project number PN-II-ID-PCE-2012-4-0261 (Contract 53/02.09.2013)*

## HYDROGE PEROXIDE AS AN INITIATOR OF THE DIENE RADICAL POLYMERIZATION

**V.P.Boiko, V.K.Grishhenko**

*Institute of Macromolecular Chemistry of National Academy of Sciences of  
Ukraine, 48 Kharkivske shausse, Kyiv 02160, Ukraine*  
[boikovita@bigmir.net](mailto:boikovita@bigmir.net) /Boiko V.P

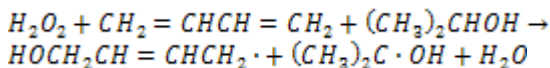
The reactive diene oligomers with terminal hydroxyl groups (HTPB, liquid rubbers) have a wide application as frost- and water-resistant products of low polarity. They mainly use for making polyurethanes by the liquid formation method.

The most economical method of HTPB synthesis is a radical polymerization with using hydrogen peroxide (HP) as an initiator. This initiator introduces into oligomer molecules required terminal hydroxyl groups. Despite the production of HTPB liquid rubbers in the industrial scale, chemistry of this process is not finally elucidated.

The main drawback is impossibility of thermal decomposition of an HP molecules on two hydroxyl radicals. The peroxide bond energy is too high to be cleaved at the temperatures of polymerization 70-150 °C. So the process does not be realized according to the accepted mechanism.

With using of labeled alcohols, we found out that the oxygen-containing alcohol radicals enter oligomer their hydroxyl groups. In case of isopropyl alcohol, these groups are tertiary ones, which have low reactivity in the urethane formation reaction and do not be determined by an acetylation reaction. So, effective functionality of an oligomer synthesized in isopropyl alcohol equal to 1.5, while in other alcohol it does to 2.

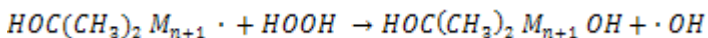
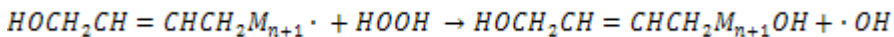
Taking into account the finding results, we proposed a new scheme of the polymerization including the decomposition of a triple complex monomer-initiator-solvent (a supramolecule), which breaks through concerted rupture of a supramolecule with forming two initiated radicals:



This conclusion was supported by thermochemical and quantum-chemical calculations.

Co11

According to this scheme, the chain termination is realized through the chain transfer onto the HP molecule. As a result, a fraction of alcohol fragments consist of one fragment on two oligomer molecules (functionality on alcohol fragments is equal to 0.5).



The results obtained permit to manage the properties of the HTPB oligodienes by virtue of a choice of solvent. The understanding the mechanism of action of HP as an initiator opens wide perspectives of its using instead expansive and dangerous initiators of (hydro)peroxide types. The high economy and ecological advantages of HP may be realized in synthesis of a range of industrial polymers.

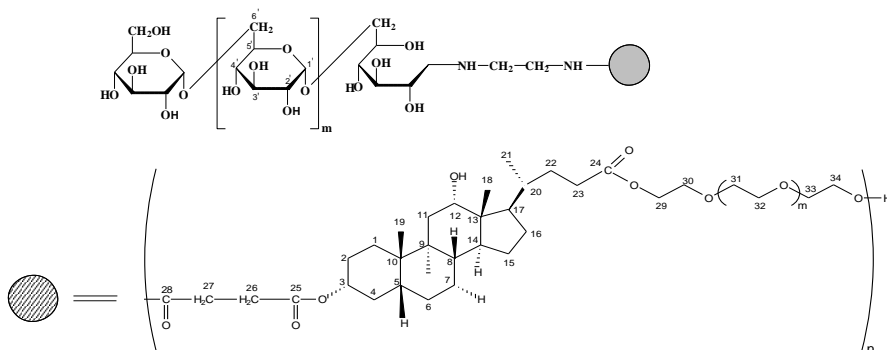
## POLYSACCHARIDE-BASED BLOCK COPOLYMERS

**Magdalena-Cristina Stanciu, Marieta Nichifor**

*“Petru Poni” Institute of Macromolecular Chemistry, 41A Grigore Ghica Voda  
Alley, Iasi 700487, Romania*

[cstanciu@icmpp.ro](mailto:cstanciu@icmpp.ro)

New biocompatible diblock copolymers based on dextran and polyesters containing deoxycholic acid were obtained and characterized by means of spectral measurements, as well as by thermal analysis and micellar characteristics in aqueous solution. The syntheses of the amphiphilic diblock copolymers were carried out in three steps. In the first step, 3 $\alpha$ -(succinoyloxy)- deoxycholic acid was obtained by esterification of the bile acid with succinic anhydride. In the second step, polyesters of 3-succinoyloxy-deoxycholic acid with different polyethyleneglycols (PEG100, PEG200, PEG400, PEG600, PEG1000) were achieved by polycondensation. In the third step, diblock copolymers (Scheme 1) were obtained by end-to-end coupling of amino terminated dextran (Dex6000, Dex11000, Dex25000) with deoxycholic acid polyesters. These biocompatible diblock copolymers can be used as nanosized matrices for drug delivery systems.



$m = 0, 2, 6, 11, 20, 34$

**Scheme 1.** Chemical structure of block copolymers.

### Acknowledgments

*This work is supported by a grant of the Romanian National Authority for Scientific Research, CNCS – UEFISCDI, project number PN-II-ID-PCE-2011-3-0622.*

## **ELECTROACTIVE STRESS SENSITIVE POLYMER COMPOSITES WITH ORIENTED STRUCTURE OF CONDUCTIVE PHASE**

**V. Levchenko<sup>1</sup>, Ye. Mamunya<sup>1</sup>, Yu. Klymenko<sup>2</sup>, I. Parashchenko<sup>1</sup>**

*<sup>1</sup>Institute of Macromolecular Chemistry of National Academy of Sciences of Ukraine, 48 Kharkivske shausse, Kyiv 02160, Ukraine.*

*[levchenko\\_v@hotmail.com](mailto:levchenko_v@hotmail.com)*

*<sup>2</sup>Institute of Space Research of National Academy of Sciences of Ukraine and National Space Agency of Ukraine, 03187, Kyiv, Ukraine*

Stress sensitive polymer materials are required in many areas of technical applications and can be widely used as the elements of electromechanical sensor devices of navigation and control (sensors of acceleration, sensors of pressure, etc.). Such materials change their resistivity under impact of applied stress. The most common type of stress sensitive material is a composite material with a non-conducting elastic polymer matrix containing conductive filler. In such composites the change of volume caused by applied external forces leads to change in electrical current that passes through the investigated composite material. Thus, the properties of stress sensitive polymer composites mostly depend on the morphology of the filler phase.

Nowadays different strategies and approaches have been used to develop stress sensitive sensors with a stable electrical response which depends on the structure changes in composite under applied force. However, all these approaches did not allow appropriate control the structure of stress-sensitive electro conductive filler channels inside the polymer matrix. This disadvantage leads to a gradual destruction of the network of conductive filler channels in the composite under loading / unloading of external force and is the reason that sensor composite materials still are not enough stable or electrically sensitive.

Therefore, the actual problem is to develop new approaches and composites effective for creation of highly stable stress sensitive materials. Recently, great interest was shown in polymer composite, in which conductive filler phase has an ordered structure, formed under the influence of a magnetic or electric fields. Oriented 1D structure of conductive phase which was obtained by treatment of the composites in a magnetic field was found to be extremely sensitive to the small values of applied stress and can be used for creation of stress sensitive polymer

composites.

The composites based on silicone polymer filled with micro-size and nano-size Ni powders were investigated. The result of the treatment of the composites in a magnetic field was the formation of anisotropic structures of nickel particles in a polymer matrix. The cyclic stresses were applied to the composites, while the deformation and electrical current were measured along the loading cycles. Apparently, formed 1D oriented structure of conductive phase was found to be different from the statistical distribution of the filler particles in the composites without the treatment in magnetic field. Composites with one-dimensional 1D structure have much lower percolation threshold than the composite with the statistical 3D distribution of the filler. Thus, composites with oriented filler structure can be attractive for use as sensor materials, because they already have high conductivity and elongated ordered structure of conductive filler that is able to not be deformed under the action of external forces.

Three types of electro-sensitive composite materials based on silicone matrix were investigated: composites filled with micron-sized nickel powder, composites filled with combination of micron- and nano-sized nickel powder and composites filled with copper particles in dendritic form.

The cyclic dependences of strain and current on the applied stress for composites filled with micron-sized nickel powder were investigated. The changes of strain and current which are passing through the sample during the applying of cyclic force were investigated as well. Each subsequent cycle of applied force led to the destruction of the orientated conductive filler structure and decreased the current pick amplitude, thus low maximal value of current for the last cycle was observed. The same effect was found for other concentrations of micron-sized nickel. Also it was observed that bigger value of applied force caused bigger changes of strain and current during the measurements. The gradual decrease of the electrical response under mechanical action can be explained by the destruction of oriented structure of the nickel particles in composite under loading/unloading of external force. Thus composites filled with micron-sized nickel powder and treated in magnetic fields cannot be used for creation of effective stress sensor.

Composite filled with a combination of micron-sized and nano-sized nickel fillers and treated in a magnetic field remained constant values of current amplitude during all steps of loading force cycles. When mixed, the nano particles have wrapped up micron particles thus prevented their sticking to each other during the deformation of the sample and thus stabilized the system. With the increase of the both fillers concentration, the signal of the current was more stable, and it was not observed any shifts of the signal amplitude (Fig.1). In order to analyze the stability of the system, 30 cycles were performed. The composite has shown stable signal even after 30 cycles. The results have shown high electrical sensibility of obtained composites with 1D structure of combined micro and nano-size fillers to the small values of applied stresses.

Co13

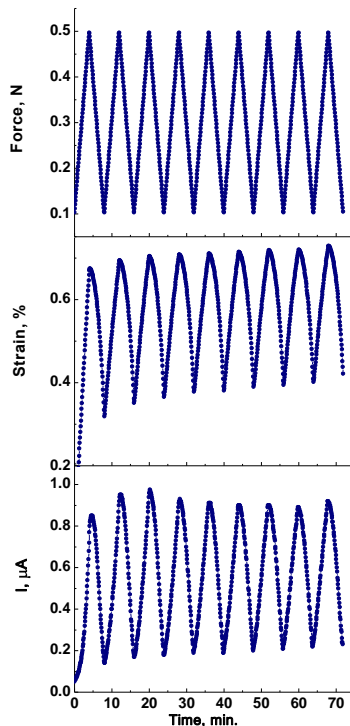


**Fig.1.** Stress sensitive silicone composite filled with a combination of micron-sized and nano-sized nickel.

For the composites with micron- sized nickel, each following cycle of applied stress led to the destruction of the conductive filler structure thus decreasing of current signal was observed. But the presence of nanoparticles in the composites increased the sensory characteristics and electrical stability of the composite material.

Composites based on silicone matrix filled with copper particles in dendritic form were investigated. In these composites micron-sized conducting copper particles are randomly distributed within a silicone matrix. Metal particles are in dendritic form and have spikes on the surface which generate high charge densities. Conduction mechanism of the composites under stress is realized through quantum mechanical tunneling of electrons via spikes. Composites characterized by high electrical sensitivity to applied pressure.

For such metal composites the shape and size of the filler particles is as important as the nature of the filler and its concentration. In particular, composite

## Co13

materials filled with conductive metal micro-particles with sharp, spiky and nanostructure formation on the surface, show a huge change in electrical conductivity in response to applied of small values of mechanical forces. Such filler morphology is responsible for strengthening the local electric field, which significantly increases the probability of tunneling through the insulating barrier between adjacent metallic particles.

The investigations of silicone/copper composite have shown that deformation properties of the composites remained constant during all loading cycles. The current amplitude is also kept constant for the cycles indicating that conductive structure is not destroyed and is resistant to external forces. Created composite with filler combination and with filler in dendritic form characterized by required elastic properties and sensitivity and may allow for the development of material suitable for practical use as sensor material for compression accelerometers.

## LASER-INDUCED SURFACE RELIEF FORMATION ON AZO-POLYMER FILMS

**A. Meshalkin<sup>1</sup>, M. Iurzenko<sup>2</sup>, S. Robu<sup>3</sup>, E. Achimova<sup>1</sup>,  
A. Prisacar<sup>1</sup>, V. Abashkin<sup>1</sup>, G. Triduh<sup>1</sup>**

<sup>1</sup>*Institute of Applied Physics of Academy of Sciences of Moldova, 5 Academiei str., Chisinau, MD2028, Moldova*  
[alexei@asm.md](mailto:alexei@asm.md)

<sup>2</sup>*Plastics Welding Department, E.O.Paton Electric Welding Institute, National Academy of Sciences of Ukraine, B.8, 11, Bozhenko Str., 03680, Kyiv-150, Ukraine*  
[iurzenko@paton.kiev.ua](mailto:iurzenko@paton.kiev.ua)

<sup>3</sup>*State University of Moldova, 60 Mateevici str., Chisinau, MD2009, Moldova*  
[s.v.robu@mail.ru](mailto:s.v.robu@mail.ru)

Carbazole-containing polymer materials attract wide interest due to their applications in optical data storage and information processing due to possessing of good photorefractive, photoconductive, and photochemical properties for hologram recording [1,2]. It was shown in [3] that holographic gratings could be obtained on carbazole materials that involves exposure of the thin film to an interference pattern. During the holographic recording two coupling gratings are formed simultaneously: 1 - phase grating, due to modulation of the refractive index and 2 - amplitude grating, resulting from the changes of absorption coefficient. The third type of holographic grating namely surface relief grating was obtained by a wet chemical process leads to film thickness changes. However, wet etching development techniques based on solvent dissolutions affect the fabrication process, leading often to a deformation of the fabricated structures and to increasing of background scattering.

Recently, new organic materials named azobenzene-containing polymers (azopolymers) have attracted much attention for the fabrication of surface structures [4]. Kim's group first showed a new possibility to direct formation of surface relief gratings (SRG) on azopolymer films without any subsequent processing steps thanks to mass transport effect under a modulated light irradiation [5]. It was reported that large surface modulations by a simple one-step process can be obtained on azo polymer films. Many theoretical models were

Co14

proposed to explain the mechanism of SRG formation but the mechanism is still not fully explained. The widely used model is the gradient force model [6]. According to this model, the resultant force can be achieved thanks to the light irradiation, which induces a trans-form  $\leftrightarrow$  cis-form photoisomerization effect in azobenzene molecules.

So the aim of our work was the synthesis and characterization of new carbazole-based azopolymer suitable for direct surface relief grating formation. The surface modulation of azopolymer film depending on the polarization of the writing beams was also considered.

Carbazole-based polymer Epoxypropylcarbazole (EPC) and azodye Disperse Orange (DO) was utilized in this study. DO was purchased as a commercial product from Sigma-Aldrich Company [18]. DO molecule was chemically attached to EPC monomer by polycondensation scheme at a temperature of 120° C for 4 hours. The molar ratio between EPC and DO was 90/10. The copolymer was purified by precipitation in hexane and then in methanol. Scheme of synthesis and chemical structure of EPC:DO is presented in Fig. 1.

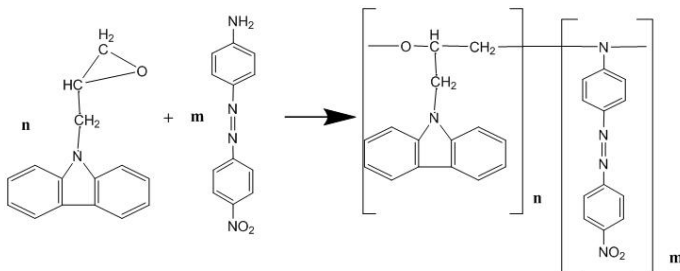


**Fig. 1.** Scheme of synthesis and chemical structure of EPC:DO.

Fourier Transform Infrared Spectroscopy (FTIR) characterization was applied for copolymer structure characterizing and identifying organic molecules. Infrared spectra of the samples were recorded with a Perkin Elmer FTIR 100 spectrophotometer (4  $\text{cm}^{-1}$  and 32 scans).

The introduction of azo group in synthesized copolymer EPC:DO was proved confirmed by the peak at 1576  $\text{cm}^{-1}$  in the IR spectrum corresponding to the N = N stretching frequency. All constituents of copolymer (monomer EPC, azodye DO and copolymer EPC:DO) were the same characterized by FTIR spectroscopy with attribution of infrared absorption bands to main functional groups.

In our study the thin polymer films were prepared from homogeneous polymer solution by spin coating procedure using programmable spin-coater “SGS

Co14

Spincoat G3P-8". Polymer thin films were prepared by spin coating of the 10 wt.% polymer solution in toluene onto glass substrate. Obtained films were dried in an oven at 60°C for 6 hours. The thickness of spin-coated films determined from the fringe pattern in the interferogram was about 270 nm. UV-Visible transmittance spectrum of the spin-coated EPC:DO thin film is shown at Fig 2.

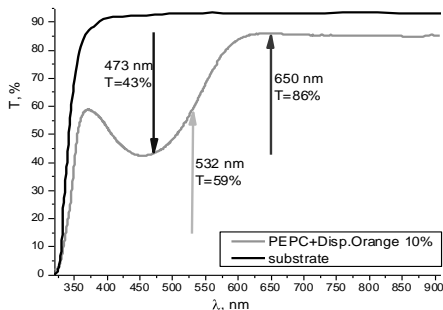


**Fig. 2.** Transmittance spectra of EPC:DO copolymer thin film and used substrate. The wavelength of used laser (532 nm), and the wavelength of 650 nm of monitoring laser during holographic recording are shown insight.

The absorption band ranges from 400 nm to 580 nm with an absorption peak at 460 nm. Therefore a green 532 nm laser is suitable for the holographic recording. The wavelength of used lasers, and the wavelength of 650 nm of monitoring laser during holographic recording are shown in Fig. 2.

Green (532 nm) DPSS laser was used for holographic recording. The polarizations of the two laser beams were controlled independently by using different wave plates (quarter-wave plate and half-wave plate). The grating period was 1 μm. In order to monitor the dynamics of grating formation, a red laser beam ( $\lambda=650$  nm, power = 1 mW) was sent into the interference area, and the first-order diffraction intensity was measured as a function of time, indicating the formation of diffraction grating.

In this work we considered three polarization configurations:

1. S:S parallel linear polarizations;
2. +45°:-45° orthogonal linear polarizations with the polarization planes oriented at an angle of 45°;
3. RC:LC right and left orthogonal circular polarizations.

For S-S polarization configuration, the polarizations are the same for both laser beams resulting in a maximal amplitude modulation (100%) of the intensity interference pattern and interference polarization keeps the same direction. For +-45 polarization configurations the interference polarization varies periodically between linear and circular forms. For the case of RC:LC polarization

configuration, the resultant polarization becomes a linear polarization with constant amplitude, but the polarization direction changes periodically in the xy-plane.

It was shown that S:S polarization configuration, providing 100% of intensity modulation, doesn't lead to grating formation. But in the case of +45° and RC:LC polarization configuration, which does not create intensity modulation, allows to obtain grating with high diffraction efficiency. So the formation of grating on azopolymer therefore depends strongly on the polarization distribution.

So we report observation of holographic surface relief gratings with relatively large amplitude on EPC:DO copolymer without any subsequent processing steps. We also found that the RC:LC polarization configuration is the best case, which allows to achieve surface relief grating with the largest amplitude about 130nm (48% of film thickness). On the other hand, the S:S polarization configuration, providing 100% of intensity modulation, doesn't lead to grating formation. The formation of surface relief grating therefore depends strongly on the polarization distribution.

We conclude that the surface relief grating formation plays a dominant role in diffraction efficiency evolution.

### **Acknowledgements**

*The authors thank Mihail Enaki and the National Center for Materials Study and Testing (Technical University of Moldova) for performing AFM measurements. The research was partially supported by the project FP7 No 609534 SECURE-R2I and FP7-INCO-2013-9-ENER2I (CEI – KEP AUSTRIA).*

1. Andries A., Abaskin V., Achimova E., Meshalkin A., Prisacar A., Sergheev S., Robu S., Vlad L.. Application of carbazole-containing polymer materials as recording media. //Phys. Status Solidi A, 208 (2011) 1837-1840.
2. Grazulevicius J. V., Strohrriegl P., Pielichowski J., Pielichowski K. Carbazole-containing polymers: synthesis, properties and applications. //Prog. Polym. Sci., 28 (2003) 1297–1353.
3. Andriesh A., Sergheev S., Triduh G., Meshalkin A.. Diffraction optical structures on the basis of chalcogenide glasses and polymers. //J. Optoelectron. Adv. M., 9 (2007) 3007-3012.
4. Won R. Azopolymer option. //Nat. Photon., 5 (2011) 649.
5. Kim D. Y., Tripathy S. K., Li L., Kumar J. Laser-induced holographic surface relief gratings on nonlinear optical polymer films. //Appl. Phys. Lett., 66 (1995) 1166–1168.
6. Kumar J., Li L., Jiang X., Kim D.Y., Lee T.S., Tripathy S.K. Gradient force: the mechanism for surface relief grating formation in azobenzene functionalized polymers. //Appl. Phys. Lett. 72 (1998) 2096–2098.

## **ELASTIC SILICONE NETWORKS WITH INCREASED PERMITTIVITY AND HIGH BREAKDOWN FIELDS FOR DIELECTRIC ELASTOMER TRANSDUCERS**

**M. Dascalu<sup>1</sup>, A. Bele<sup>1</sup>, V.E. Musteata<sup>1</sup>, M. Cazacu<sup>1</sup>, D. M. Opris<sup>2</sup>, C. Racles\*<sup>1</sup>**

<sup>1</sup>*Petru Poni Institute of Macromolecular Chemistry, Aleea Grigore Ghica Voda 41A, Iasi, 700487, Romania;*  
[raclesc@icmpp.ro](mailto:raclesc@icmpp.ro)

<sup>2</sup>*Empa, Swiss Federal Laboratories for Materials Science and Technology, Laboratory for Functional Polymers, Ueberlandstr. 129, CH-8600, Dübendorf, Switzerland*

In the actual economic and environmental context, finding new promising systems for energy harvesting or actuation is a hot topic. Electro-active polymers (EAP) represent a very attractive class of materials, being lightweight, easily processable, cost-effective and weatherproof. The relatively new concept of dielectric elastomer transducers (DET) is based on these “smart” materials, which are able to convert electrical energy to or from mechanical energy. In the first case they act as actuators, while in the second case, they are generators. Other applications of DETs include sensors and variable stiffness devices.

Silicones are, besides acrylics and polyurethanes, between the most promising materials for electromechanical transduction. However, the optimization of silicone materials for DETs has to address multiple aspects. In principle, a material should have increased dielectric permittivity, high breakdown field strength, large strains and a moderate Young modulus.

In order to increase the dielectric permittivity ( $\epsilon'$ ) polar silicones were synthesized [1], while the mechanical properties were tuned by inter-connecting or blending them with polydimethylsiloxane (PDMS) of high molecular weight. The thermal (DSC, DMA) and morphological (SEM) investigations showed the biphasic morphology of the networks. However, by appropriate control of cross-linking the macroscopic phase separation can be avoided, while by blending PDMS with preformed cross-linked polar silicone particles, further improvement of the morphology can be achieved. The dielectric, mechanical, and electromechanical properties of the thin films were investigated. Materials with good elastic properties, increased  $\epsilon'$ , high breakdown field ( $E_b$ ) and promising actuation performances were obtained [2].

Co15

1. *Racles C., Alexandru M., Bele A., Musteata V.E., Cazacu M., Opris D.M.* Chemical modification of polysiloxanes with polar pendant groups by co-hydrosilylation, RSC Adv. 4 (2014) 37620-37628.
2. *Racles C., Bele A., Dascalu M., Musteata V.E., Varganici C.D., Ionita D., Vlad S., Cazacu M., Dünki S.J., Opris D.M.* Polar-nonpolar interconnected elastic networks with increased permittivity and high breakdown fields for dielectric elastomer transducers, RSC Adv. 5 (2015) 58428-58438.

## **BIODEGRADATION OF SYSTEMS BASED ON POLY(L-LACTIC ACID) WITH TRICHODERMA VIRIDE**

**R. Lipsa<sup>1</sup>, L. Oprica<sup>2</sup>, R. N. Darie<sup>1</sup>, N. Tudorachi<sup>1</sup>, C. Vasile<sup>1</sup>**

<sup>1</sup> “Petru Poni” Institute of Macromolecular Chemistry, 41A Grigore Ghica Voda Alley, Iasi 700487, Romania  
[rlipsa@icmpp.ro](mailto:rlipsa@icmpp.ro)

<sup>2</sup> Faculty of Biology of Alexandru Ioan Cuza University, 11 Carol Boulevard, Iasi, 700506, Romania

As biomedical materials are in contact with human organs, tissues, blood or skin, the biodegradability, biocompatibility, *in vivo* stability and toxicity are very important considerations [1]. The study highlights the biodegradation of poly(L-lactic acid) (PLLA) and some PLLA systems based on components with different chemical structure, by *Trichoderma viride* fungus, in liquid medium. The PLLA and systems were obtained by melt mixing in Brabender, with mixing speed of 60 rot/min, at 175 °C for 10 minutes. After the processing step, each sample was pre-melted for 5 min and then sandwiched (in a Carver Press), under a pressure of 200 bar, to obtain plates with thickness of 1 and 4 mm, respectively. The sheets of PLLA and PLLA-based systems with thickness of 1 mm, were undergone to biodegradation tests by *Trichoderma viride* fungus, in liquid medium.

The biodegradability of the samples was evaluated by the loss in weight and the malonyldialdehyde, catalase, ATP-ase, lactatedehydrogenase and soluble protein activity, after 7 and 21 fungus inoculation days. The nonbiodegraded and biodegraded samples (after 21 inoculation days) were structurally and morphologically characterized by: FTIR-ATR and SEM. SEM micrographs revealed that the systems were biodegraded after 21 days and the biodegradation degree was influenced by the systems components. By thermal characterization (TG-DTG) it was concluded that the biodegraded PLLA and systems have lower thermal stability comparatively to the nonbiodegraded ones.

### **Acknowledgements**

*The authors are grateful for the financial support from the Romanian National Authority for Scientific Research CNCS–UEFISCDI, project: Bionanomed: Antimicrobial bionanocomposites for medical applications, Grant*

*PCCA/II, no 164/2012 and project: Interdisciplinary research on multifunctional hybrid particles for bio-requirements "INTERBIORES" PN-II-PT-PCCA-2011-3.2-0428, Grant no. 211/2012.*

1. *B. M. Holzappel, J. C. Reichert, J. T. Schantz, U. Gbureck, L. Rackwitz, U. Nöth et al.* How smart biomaterials need to be? A translational science and clinical point of view // *Adv Drug Deliv Rev.* 65(4) (2013) 581-603.

## **INFLUENCE OF THE INTERFACIAL INTERACTIONS ON THE RHEOLOGICAL PROPERTIES OF SOME NOVEL COMPATIBILIZED PP-CLAY HYBRID MATERIALS**

**M. Zanoaga, F. Tanasa**

*“Petru Poni” Institute of Macromolecular Chemistry, 41A Grigore Ghica Voda Alley, Iasi 700487, Romania*  
[zanoaga@icmpp.ro](mailto:zanoaga@icmpp.ro)

Polymer-clay nanocomposites are special hybrid materials because they allow highly dispersed distribution of fillers due to the strong interactions that occur between the matrix and clay during processing.

The classic thermodynamical studies for the reduced particle size fillers didn't predict accurately the nanofillers effect on the polymer properties. Only by using continuum mechanics [1] it was possible to substantiate that the properties of polymer nanocomposites are strongly dependent on the particular features of the nanofiller (content, aspect ratio, granulation, distribution etc.).

The highly dispersed filler distribution renders new hybrid materials improved properties as compared to initial polymers. As result, these new materials become lighter, have increased mechanical strength and scratching resistance, display flame retardancy properties, can be easily painted, and, in some cases, they can be recycled.

This study focuses on novel PP-clay nanocomposites prepared in preset ratios, by melt compounding, using an organically modified layered silicate, namely Cloisite<sup>®</sup> 20A, and MA-g-PP as compatibilizer. The compatibilizer was employed to modify the hydrophilic-hydrophobic balance which improves the interfacial interactions and leads to a better dispersion of the clay into the PP matrix. This feature was evidenced by the means of X-ray diffraction spectrometry (XRD). The thermal stability of these new materials was assessed by thermal gravimetric analysis (TGA) and their rheological behaviour was also investigated in order to assess the effect of the interfacial interactions.

1. Dill, Ellis Harold (2006). *Continuum Mechanics: Elasticity, Plasticity, Viscoelasticity*. Germany: CRC Press.

**ROOM TEMPERATURE PLD OF AL-DOPED ZNO THIN FILMS: WAXD AND SPM INVESTIGATIONS****D. Timpu, C. Ursu**

*“Petru Poni” Institute of Macromolecular Chemistry, Gr. Ghica Voda Alley, 41A, 700487, Iasi, Romania*

[dtimpu@icmpp.ro](mailto:dtimpu@icmpp.ro)

Highly oriented Al doped ZnO thin films were obtained by pulsed laser deposition (PLD) on amorphous substrate at room temperature on both crystallites orientations, i.e., in plane and out of plane c-axis orientations. Al-doped ZnO usually grows with the c-axis perpendicular on the substrate, i.e., (002) oriented films but for some particular experimental parameters we obtained (110) oriented samples. This particular growth mode enhances the quantum efficiency of the OLEDs in comparison with the usual encountered (002) growth mode where the internal electric field which come out from spontaneous and strain induced polarization affects directly the quantum efficiency. However, (110) Al-doped ZnO thin films have weaker electrical and optical properties with respect to the (002) oriented ones in order to be used as electrode for OLEDs. For this purpose, we are trying to establish the experimental growing conditions to avoid this inconvenience by systematically studying for both oriented samples the relationship between local properties such as, morphology, roughness, spreading resistance (SPM) and intrinsic material properties, i.e., crystallites dimensions and orientations, constant lattice (WAXD).

**Acknowledgments**

*This work was financially supported by the Romanian National Authority for Scientific Research, CNCS – UEFISCDI grant, project number PN-II-PT-PCCA-2013-4-1861 (contract number 272/2014).*

## SYNTHESIS AND CHARACTERIZATION OF CHALCONE-CONTAINING AROMATIC POLYAMIDES

M. Nechifor

*“Petru Poni” Institute of Macromolecular Chemistry, 41A Grigore Ghica Voda Alley, Iasi 700487, Romania*

[nechifor@icmpp.ro](mailto:nechifor@icmpp.ro)

Two novel diacid-based monomers have been synthesized by anchoring at the 5-position of the isophthalic acid ring a benzylideneacetophenone (chalcone) moiety through an amide or ester bridge. Two series of polyamides bearing chalcone side chains were prepared by direct polycondensation reaction of the aforementioned dicarboxylic acids and various aromatic diamines in *N*-methyl-2-pyrrolidinone, using triphenyl phosphite and pyridine as condensing agents. Their molecular structure and the basic properties were investigated by nuclear magnetic resonance, Fourier-transform IR and UV-Vis spectroscopy, differential scanning calorimetry, thermogravimetric analysis and wide-angle X-ray diffraction. The inherent viscosity, molecular weights measurements (by gel permeation chromatography), water uptake and solubility tests completed the research study. Introduction of the rigid and bulky chalcone units into the polymer side chains improved remarkably the solubility of the aromatic polyamides, endowed them with an amorphous nature, good thermal stability and photosensitivity. The resulting polymers were obtained in good yields, inherent viscosities varied between 0.49 and 0.86 dL/g and their relative high molecular weights conferred them film-forming properties. The polyamides underwent a photocycloaddition reaction upon UV light irradiation both in solution and film state in the absence of a photoinitiator or photosensitizer. The polymer films became insoluble in solvents as a result of the crosslinking.

## ANOMALOUS STRUCTURAL ORGANIZATION OF LITHIUM PERCHLORATE SALT IN THE ELECTROACTIVE POLYMER SYSTEMS BASED ON EPOXY RESINS

**L. K. Matkovska<sup>1,2</sup>, M. V. Iurzhenko<sup>1</sup>, Ye.P. Mamunya<sup>1</sup>, O.K. Matkovska<sup>1</sup>,  
G. Boiteux<sup>2</sup>, A. Serghei<sup>2</sup>**

<sup>1</sup>*Institute of Macromolecular Chemistry of National Academy of Sciences of Ukraine, 48 Kharkivske shausse, Kyiv 02160, Ukraine*  
[lovemk@ukr.net](mailto:lovemk@ukr.net)

<sup>2</sup>*Université de Lyon, Université Lyon 1, Ingénierie des Matériaux Polymères, UMR CNRS 5223, IMP@LYON1, France*

The paper considers thermogravimetric and thermal characteristics, structure and morphology of the electroactive polymer composite based on epoxy resins. Salt of lithium perchlorate LiClO<sub>4</sub> was dissolved in the epoxy oligomer of diglycide aliphatic ester of polyethylene glycol (DEG). These solutions were prepared with LiClO<sub>4</sub> content from 0 to 50 phr (parts per hundred) on 100 phr of DEG. Polyethylene polyamine hardener (PEPA) was used as a curing agent. DEG and PEPA contents were 90 and 10 phr, respectively, for all synthesized composites. Composites cured at 80 °C during 8 hours. Our previous investigations in [1] showed that the obtained ion-conductive polymeric material with the ionic conductivity  $\sigma' \sim 10^{-3}$  S/cm and the permittivity  $\epsilon' = 6 \cdot 10^5$  are attained for the system DEG with 20 phr of LiClO<sub>4</sub> at elevated temperatures (200 °C).

Thermogravimetric characteristics were studied by TA Instruments TGA Q50 in the temperature range from +25 to +700 °C with the heating rate of 20 °C/min. Precision of a sample weighing was 0.01%. TGA results are presented in Fig. 1. According the TGA results the weight loss at these temperatures is negligible, thus their usability at high temperatures (200 °C) is possible.

Thermal characteristics were studied by Differential Scanning Calorimetry at TA Instruments DSC Q2000 in the temperature range from -70 to +150 °C with the heating rate of 10 °C/min. The glass transition temperature ( $T_g$ ) was determined from the DSC curves at the second heating (Table 1).

Co20

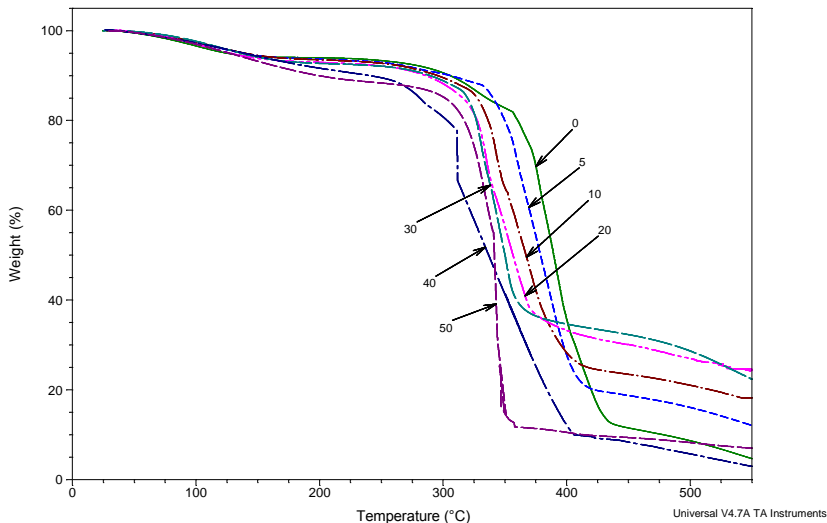


**Fig. 1.** The TGA curves of the samples with different content of LiClO<sub>4</sub>.

It is obvious that the increase of LiClO<sub>4</sub> amount in reactive mixture from 0 to 50 phr leads to the increase of glass transition temperature from -10 to 64 °C. That can be a result of electrostatic interactions between lithium cations Li<sup>+</sup> and the macromolecular chain of DEG with immediate forming of coordinative complexes, such as {ether oxygen - lithium cations - ether oxygen}, which is accompanied by the displacement of electron density of the oxygen atoms and their partial polarization. The result is a substantial reduction of segmental mobility of DEG chains within the complexes formed, which leads to a glass transition temperature rise of polymer matrix.

**Table 1.** Thermal characteristics of epoxy polymers with different content of LiClO<sub>4</sub>.

Glass temperature ( <i>T<sub>g</sub></i> ), °C	Content LiClO <sub>4</sub> , phr.									
	0	5	10	15	20	25	30	35	40	50
	-10	-1	9	18	25	33	39	55	60	64

Structural organization and features of macromolecular ordering of the synthesized polymer systems were investigated by wide-angle X-ray scattering (WAXS) using the X-ray diffractometer DRON-4.7. The investigations were carried out by automatic step scanning in the range of scattering angles ( $2\theta$ ) from 2,6 to 40 degrees, the exposure time was 5 s. The research temperature was  $T = 20 \pm 2$  °C.

Co20

The analysis of the wide-angle X-ray diffraction patterns of the systems showed that all of them are amorphous (Fig. 2). In particular, epoxy oligomer DEG that was cured with polyethylene polyamine is characterized by short-range ordering in the space translation of molecular fragments of its cross-site links. That is confirmed by presence of one diffraction peak (calculated from the angular half-width) of the diffusion type (amorphous halo), which angular position ( $2\theta_m$ ) is about 20,0 degrees.

The average value of the period ( $d$ ) of a short-range molecular ordering of DEG internodal molecular segments in a polymer volume can be calculated using Bragg equation:

$$d = \lambda(2\sin\theta_m)^{-1}$$

where  $\lambda$  - wavelength of the characteristic X-ray emission ( $\lambda = 1,54 \text{ \AA}$  for  $\text{CuK}\alpha$  emission) and it equals to  $4,44 \text{ \AA}$ .

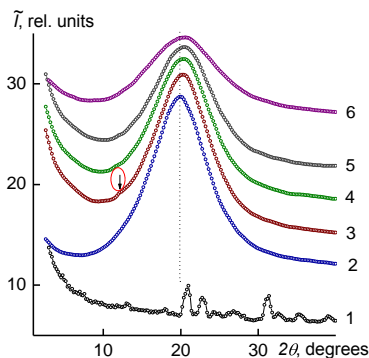


**Fig. 2.** The wide-angle X-ray diffraction patterns of a salt of lithium perchlorate  $\text{LiClO}_4$  (1) and DEG/ $\text{LiClO}_4$  systems with the salt content: 0 phr (2), 5 phr (3), 10 phr (4), 20 phr (5), 50 phr (6) at  $20 \pm 2 \text{ }^\circ\text{C}$ .

However, the introduction of the salt  $\text{LiClO}_4$  that has a crystalline structure into the epoxy resin is accompanied by changes in the diffraction pattern. This is evidenced by the presence of subtle diffraction peak of the diffuse type at  $2\theta_m \approx 12,2$  degrees on the background of the amorphous halo, which is similar to the angular position of the DEG at  $2\theta_m \approx 20,0$  degrees ( $d \approx 4,44 \text{ \AA}$ ). This diffraction peak characterizes the existence of metal-polymer complexes of the donor-acceptor type, in our case, between central ions ( $\text{Li}^+$ ) and ether oxygen of the epoxy chains in the intermolecular volume of the epoxy resin.

The gradually increasing  $\text{LiClO}_4$  content from 0 to 50 phr in the volume of epoxy resin leads to the displacement of the amorphous halo at  $2\theta_m \approx 20,0$  degrees, which characterizes the short-range order of fragments of the DEG internodal molecular segments, in the region of large scattering angles. That indicates a

tendency to decrease the Bragg distance between the molecular segments (Table 2).

**Table 2.** The Bragg distance between the molecular segments of epoxy polymers with different content of LiClO<sub>4</sub>.

Content LiClO <sub>4</sub> , phr	$2\theta_m$ , degrees	$d$ , Å
Pure LiClO <sub>4</sub> (for comparison)	20	4,44
0	20	4,44
5	20,2	4,39
10	20,4	4,35
20	20,4	4,35
50	20,4	4,3

The morphology of polymers was studied by Transmission optical microscopy at Carl Zeiss Primo Star and Reflective optical microscopy at Unicorn NJF 120A. The optical microphotos are presented in Fig. 3.

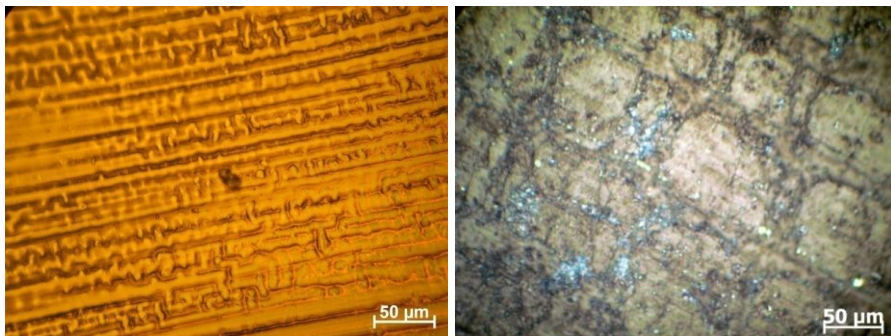


**Fig. 3.** The transmission (left) and reflective (right) optical microphotos of the DEG/LiClO<sub>4</sub> systems with the salt content of 20 phr.

The analysis of the WAXS of the investigated systems showed that all of them are amorphous except salt which has a crystalline structure. At the same time the optical microscopy shows the separated phase forming that needs more precise research.

1. Matkovska L.K., Iurzhenko M.V., Mamunya Ye.P., Matkovska O.K., Lebedev E.P., Boiteux G., Serghei A. Ion-conductive polymer system based on aliphatic epoxy resin and LiClO<sub>4</sub> // Ukr. Polym. J. 36 (2014) 361-368 (in Ukrainian).

## **EFFECT OF THE PHASE SEGREGATION ON THE PERCOLATION BEHAVIOUR IN CONDUCTIVE NANOCOMPOSITES**

**F. Tanasa<sup>1</sup>, Y. P. Mamunya<sup>2</sup>, M. Zanoaga<sup>1</sup>**

*1* “Petru Poni” Institute of Macromolecular Chemistry, 41A Grigore Ghica Voda Alley, Iasi 700487, Romania  
[ftanasa@icmpp.ro](mailto:ftanasa@icmpp.ro)

*2* Institute of Macromolecular Chemistry of National Academy of Sciences of Ukraine, 48 Kharkivske shausse, Kyiv 02160, Ukraine

Polymer composites with conductive properties arouse a great interest due to their remarkable characteristics. Considering their versatility, they have been studied of both theoretical and experimental point of view over the last decades, especially for the possibility to tune some characteristics (electric conductivity) according to specific requirements by only adjusting the content of the conductive filler.

Carbon-based fillers with conductive properties (carbon black, carbon nanotubes or nanowires, graphene, graphene oxide, etc.) are preferable because, unlike metals, they do not undergo degradation processes that may alter their conductivity. The major advantage of the conductive composites is that electrical properties are close to the fillers, while their mechanical characteristics and processing are typical for plastics. Several other advantages over the conventional conductive materials include processability, flexibility, light weight, ability to absorb mechanical shocks, low production costs.

Different morphologies can be achieved upon formulation changes, yielding in composites with superior conductivity ranging from electrostatic dissipative to highly conductive [1]. Thus, they can be used as antistatic materials and in applications such as switching devices, medical equipment, cables, transducers and gas sensors, as well as devices for electromagnetic radiation shielding and electrostatic discharge.

Conductive carbon-based fillers are able to give highly ordered distributions that lead to composites with segregated morphology. This phase segregation is characterized by ultralow values of the critical volume fraction of filler, while the electrical resistivity reaches values of  $10^{-4} \Omega \cdot \text{cm}$ .

This article presents the effect of the phase segregation on the percolation behaviour in conductive nanocomposites in comparison with random conductive composites. Factors that can influence the critical volume fraction of filler and its distribution in the matrix, such as nature of filler and matrix, processing approach and specific parameters are also reviewed, as well as some specific applications.

1. *Deng H, Lin L, Ji MZ, Zhang SM, Yang MB, Fu Q.* Progress on the morphological control of conductive network in conductive polymer composites and the use as electroactive multifunctional materials // *Prog Polym Sci* 39 (2014) 627–55.

# ***POSTERS***

## **PARTICLE SIZE EFFECT ON FUNCTIONAL PROPERTIES OF COMPOSITE MATERIALS WITH POLYMER MATRIX**

**M. Airimioaei<sup>1</sup>, V. Preutu<sup>1</sup>, R. Stanculescu<sup>1</sup>, S. Tascu<sup>2</sup>, L. Mitoseriu<sup>1</sup>**

<sup>1</sup>*Dept. of Physics, “Al. I. Cuza” University, Blv. Carol I, nr.11, 700506, Iasi, Romania*

[mirela.airimioaei@yahoo.com](mailto:mirela.airimioaei@yahoo.com)

<sup>2</sup>*Interdisciplinary Research Department – Field Science (RAMTECH), “Al. I. Cuza” University, Blv. Carol I, nr.11, 700506, Iasi, Romania*

A wide range of composite materials were being developed in the last years, but a particular attention was given to the composites that are composed of a inorganic filler and an organic polymeric matrix due to the multiple applications in different fields: medicine, biotechnology, electronic industry, etc .

The aim of this study has been to investigate the influence of the particle size of ferroelectric filler BaTiO<sub>3</sub> on the functional properties of the BaTiO<sub>3</sub>/PCL composite.

We have chosen as ferroelectric filler BaTiO<sub>3</sub> which exhibits ferroelectric properties at and above room temperature and as polymeric matrix poly-ε-caprolactone (PCL) a biocompatible, biodegradable polymer with many physicochemical properties: non-toxicity, slow degradation, and low melting point.

The xBaTiO<sub>3</sub>-(1-x)PCL (x=0, 0.02; 0.05; 0.10; 0.20) composites were prepared by solvent casting method using BaTiO<sub>3</sub> powder with different particles size. The main advantage of this method is that it involves simple equipment and low temperatures leading to composite materials with a good distribution of filler in the polymer matrix.

The composites formation and their characteristic as structure and microstructure were investigated by XRD and SEM analyses. For all the samples, the frequency dependence of dielectric properties at room temperature has been investigated and discussed in correlation with the microstructural data.

### **Acknowledgements**

*This work was financially supported by “Alexandru Ioan Cuza” University project: code GI-2014-05 in the frame of “UAIC Grants for young researcher” competition.*

## HYBRID MATERIALS BASED ON INTERPENETRATING ORGANIC-INORGANIC POLYMER NETWORKS

**N.V. Babkina, T.T. Alekseeva, T.B. Tsebrienko, N.V. Yarovaya**

*Institute of Macromolecular Chemistry of National Academy of Sciences of Ukraine, 48 Kharkivske shausse, Kyiv 02160, Ukraine*  
[nbabkina@mail.ru](mailto:nbabkina@mail.ru)

In recent years, an actual problem is obtaining new polymeric materials with the desired complex of physico-mechanical properties. This object was successfully solved by the creation of interpenetrating organic-inorganic polymer networks that combine the properties of organic and inorganic components. In addition, the intensive development of the acquired sol-gel technology, which are promising due to receive organic-inorganic materials with nanodisperse inorganic phase at the molecular level.

Hybrid organic-inorganic interpenetrating polymer networks (OI IPNs) received from cross-linked polyurethane (PU) based 2,4-2,6-toluene diisocyanate, poly(oxypropylene glycol) (POPG) and trimethylolpropane as a cross-linking agent, poly(hydroxyethyl methacrylate) (PGEMA) and poly(titanium oxide). Poly (titanium oxide) was formed *in situ* sol-gel method in the medium POPG using titanium tetra-isopropoxide (TTIP). The component ratio of PU/PGEMA in initial and organic-inorganic IPN was 70/30 wt. % and the content of TTIP was varied from 0.5 to 5.0 wt. %. The samples of initial and OI IPNs investigated by dynamic mechanical analysis, differential scanning calorimetry and thermogravimetric analysis (TGA).

Study viscoelastic and thermal properties of organic-inorganic IPNs showed that with increasing of the content poly (titanium oxide) temperature PGEMA-component glass raises, which indicates an increase in the microphase separation, which is confirmed by calculation of degree of segregation. Calculation  $M_c$  indicates the nonlinear behavior of the density of the polymer network, with the highest crosslink density have OI IPN containing 0.5 wt. % TTIP. In the study samples by TGA it shows that the introduction of an inorganic component in the polymer chain significantly increases the thermal stability of the organic-inorganic hybrid IPNs relatively initial systems.

## STUDY OF CHEMICAL MODIFICATION OF POLYAMIDE FIBERS SURFACE

**A. V. Barantsova, V. K. Grishchenko, N. A. Busko, Gudzenko N.V.,  
Z.V. Falchenko, S. N. Ostap'uk**

*Institute of Macromolecular Chemistry of National Academy of Sciences of Ukraine, 48 Kharkivske shausse, Kyiv 02160, Ukraine*

Composite polymeric materials (polymer composites) - a multi-component materials, which are the main components of the polymer base (matrix) and filler, which have a certain set of physical and mechanical properties. The combination of substances of different nature leads to the creation of a new material whose properties are quantitatively and qualitatively different from the properties of each of its components.

Significant role in shaping the properties of the composite material is interphase layer at the interface between the matrix and reinforcing phase. Interphase layer has a composition and structure, different from the composition and structure of the matrix, because in addition to the material of the matrix itself, he also includes some products that are part of a reinforcing filler. His role in shaping the properties of the polymer composite is great, but because the study and management processes of formation of the interfacial layer is of great importance. In the composites reinforced with polymer fibers, polymer matrix diffuses into the surface layers of fibers to form an intermediate interfacial layer. Thanks to the properties of the filler in the composite material properties are different from the original fiber. The strength of the reinforcing fibers can be several times greater than the strength of binding. However, to realize the benefits of reinforcing fillers to the matrix, to create a strong interaction between the matrix and fibers throughout the area of contacts. Regulation of the structure of the interphase layer is always directed at increasing the adhesive interaction at the interface and, ultimately, to improve the physical and mechanical properties of composite material.

For optimal properties of composite materials plays a significant role compatible fiber and polymer matrix, which can be obtained by chemical modification of fibers, with the aim of chemical grafting on their surface functional groups capable of reacting with reactive groups of the polymer matrix.

The modification of the surface of the polyamide fiber decreases surface

P3

tension and increases wetting angle. The influence of the modifiers on adhesion properties, which, in certain degree, determine the mechanical properties of reinforced polymer composites is difficult as the fibers have very small diameter (28-30  $\mu\text{m}$ ) and the square of adhesion contacts is small ( $\approx 10^{-2} \text{ mm}^2$ ). This will lead to a big error at measuring of force of the adhesion contact destruction. This error can grade the influence of fiber surface modification. That is why the study was carried out on the model samples.

The recycled polyamide fiber was treated by solution of the furfural in isopropanol at weight ratio 40/40 in boiling isopropanol. The unreacted furfural was washed out by isopropanol and the modified fiber was dried in vacuum. The grafting degree of the furfural to the polyamide fiber surface was determined as 2-4% by weight. The FTIR spectra of initial components and the resulting material are given in Figure 1.

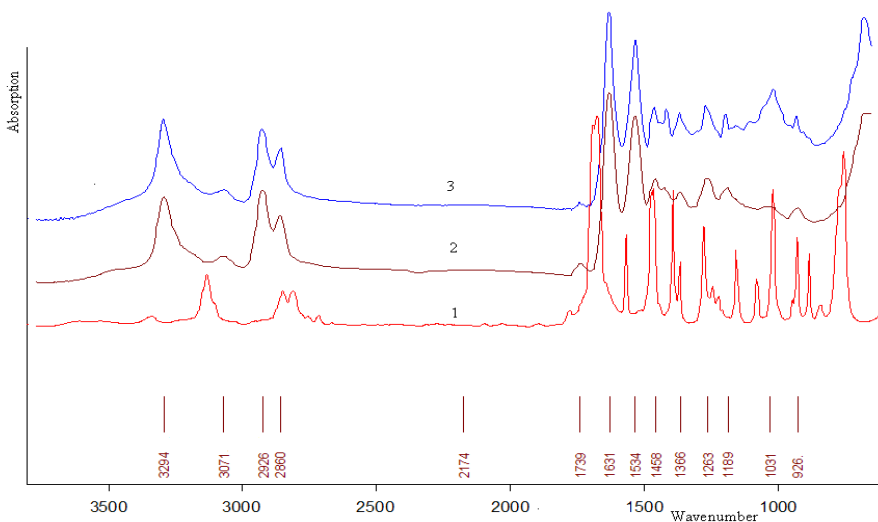
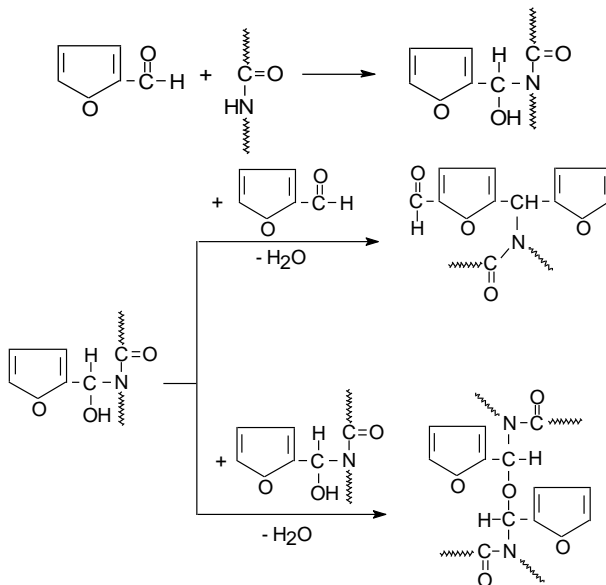


**Fig. 1.** FTIR-spectra: 1 – furfural, 2 – untreated polyamide fiber, 3- polyamide fiber modified by furfural.

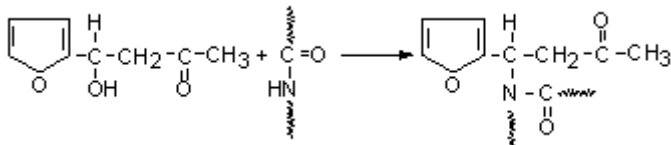
In FTIR spectrum of polyamide fiber modified by furfural we can observe (Fig. 1, curve3) changes in intensity of absorption band of CH group in the region of 1473-1388  $\text{cm}^{-1}$ . Importantly, in the spectrum the absorption bands of aldehyde group of furfural at 1692 and 1794  $\text{cm}^{-1}$  (which are present in the spectrum of furfural, curve 1) are absent. Instead of them the bands of stretching vibrations of OH-group at 3400  $\text{cm}^{-1}$  and the bands of deformation vibrations of OH-groups at 1020  $\text{cm}^{-1}$  appear, confirming formation of hydroxyl groups as a result of chemical

P3

interaction of aldehyde groups of furfural with amide groups of polyamide fiber surface according to the scheme below:



The recycled polyamide fiber was treated by the mixture of furfural with acetone (1:1) at 65°C for 50 h. The possible scheme of the chemical reaction occurred is as follows:

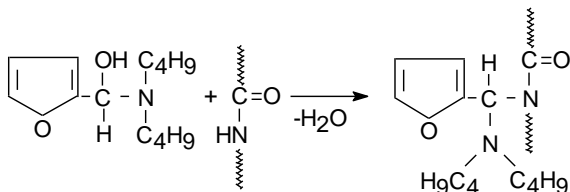


The grafting degree of the furfural in this case was determined as 2-3 wt.%. In the spectrum of polyamide fiber, modified by the mixture of furfural with acetone, the duplet of the absorption bands of aldehyde group at 1692 and 1675  $\text{cm}^{-1}$  has been replaced by the band at 1671  $\text{cm}^{-1}$  of ketone group – product of chemical interaction of furfural with acetone and by wide band in the region of 3500-3400  $\text{cm}^{-1}$  of associated OH-groups. This evidences the formation of the reaction product of furfural with acetone and its chemical grafting to the polyamide fiber surface through the reaction of the product with amide groups of the fiber.

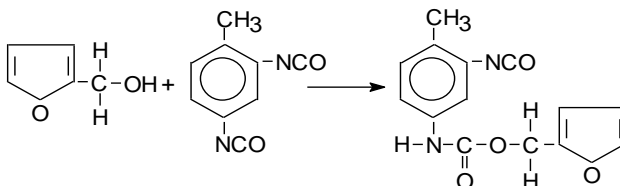
The recycled polyamide fiber was treated by the solution of the reaction product of interaction of furfural with dibutyl amine in benzene at the temperature of benzene boiling for 8 h. The ungrafted modifier was washed out from the fiber and the latter was dried in vacuum. The grafting degree for this case was

P3

determined as 2-3 wt.%. The possible scheme of chemical grafting is shown in the scheme below.



Modification of the recycled polyamide fiber by the product of interaction of furfuryl alcohol with TDI. The reaction monitoring was fulfilled by FTIR spectroscopy on decreasing of the stretching vibrations of isocyanate groups by 50 %. The reaction occurs according to the scheme:



The recycled polyamide fiber was treated by the solution of the product of interaction of furfuryl alcohol with TDI in butyl acetate at the temperature of butyl acetate boiling for 8 h at weight ratio of polyamide fiber and modifier 90:10. The modified fiber was washed out by butyl acetate and dried in vacuum. The degree of grafting of the modifier onto the fiber surface was estimated as 2-3 wt.%. In the spectrum it is seen that NCO groups of the modifier have been spent for the reaction with amide groups of the fiber. The absorption band at  $3390\text{ cm}^{-1}$  of NH of the urethane group, formed at interaction of NCO group of the modifier with amide group of the fiber, has appeared in the spectrum of the modified fiber. This and several other changes in the spectra certainly confirm the grafting of the modifier onto the fiber surface through the reaction between NCO and amide groups.

The processes of modification by reactive compounds of polyamide fiber surface have been studied. Thermal-chemical modification of surface of waste polyamide fiber by furfural, mixture of furfural and acetone, the reaction product of furfural and dibutylamine, the reaction product of furfuryl alcohol with toluene diisocyanate has been carried out. Chemical grafting of all the reactive modifiers onto the surface of PA fibers has been confirmed by the method of FTIR spectroscopy. It has been established that this method gives a noticeable effect of surface modification of fibro materials. It was proved that the use of activation of surface of polyamide fiber is perspective way.

## INFLUENCE OF THE TECHNOLOGICAL PARAMETERS OF EXTRUDER ON THE QUALITY OF POLYMER NANOCOMPOSITES

**Y. Bardadym<sup>1</sup>, E. Sporyagin<sup>2</sup>**

*<sup>1</sup>Institute of Macromolecular Chemistry of National Academy of Sciences of Ukraine, 48 Kharkivske shausse, Kyiv 02160, Ukraine  
[ferocen@i.ua](mailto:ferocen@i.ua)*

*<sup>2</sup>Dnipropetrovsk national university Oles Honchar, 72 Gagarin Avenue, Dnipropetrovsk 49010, Ukraine  
[sporiagin@rambler.ru](mailto:sporiagin@rambler.ru)*

Extrusion machines are one of the most common types of equipment used for mixing plastics and elastomers. Confusion, a process that reduces the compositional heterogeneity, is very important step in the reprocessing of polymers, whereas mechanical, physical and chemical properties as well as the appearance of products depend strongly on the composition uniformity. This stage is usually defined as a process that leads to increase in the homogeneity of multicomponent materials [1-3].

This manuscript presents a method for studying blends, in which the thickness of bands is a criterion of quality. The purpose of this investigation was to create a program to predict the quality of mixing tracks for their processing in extruders.

Model highly filled compositions based on low molecular weight rubber SKN-10Ktr and SKDM-80 were studied. Sunflower oil fatty acids, stearic and oleic acids were selected as surfactants.

**Table 1.** Structure of nanocomposition

№ composition	NaCl, mass %	SRN-10Ktr, mass %	SRDO-80, mass %	FAP-4, mass %	Surfactant, mass %	DOS, mass %
1	81,50	18,50	–	–	–	–
2	81,50	–	18,50	–	–	–
3	80,00	12,27	–	4,00	0,73	3,00
3a	83,00	12,27	–	3,00	0,73	1,00
3б	85,00	12,27	–	1,00	0,73	1,00
4	74,25	–	10,20	12,70	–	2,85
5	68,50	–	11,50	18,00	0,50	1,50

P4

Worm-disc (combined) extruder was used. Figure 1 shows a combined extruder. Its faced disc surface and body are inclined to the rotation axis normal and there is working gap between them. The minimum operating gap value is defined by the axis of rotation, constant for selected disc radius and depends on the angle values of end surfaces inclination to the axis rotation normal. Due to this structure, there is a shift of the relative movement of the melt particles from one to another strain plane. It is caused by the tension-compression strains, which are determined by changes in the working gap in one disc revolution at a constant minimum operating gap.

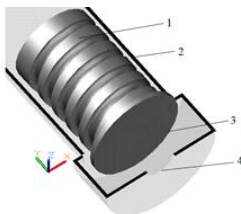


**Fig. 1.** Combined extruder: 1 – screw; 2 – body of extruder; 3 – disc; 4 – outlet.

Screw and disc rotation ( $R = 0,055$  m) was carried out using DC motor with adjustable speed in the range of  $\omega = 50-200$  rev/min. Test unit was equipped by the thermostatic cylinder system, screw, forming head with thermocouple and controlling devices for the coolant (water) temperature monitoring. Thermocouples were installed to the material cylinder for mixture temperature measuring. The forming head is provided with a pressure sensor and a thermocouple to measure the processed mixture temperature at the outlet of the cutting auger, respectively

Important component of thickness of a strip is the consistence coefficient  $K$ :

$$\tau = \eta \cdot \gamma^n$$

$$\ln \tau = \ln K + n \cdot \ln \gamma$$

Figure 2 show dependences  $\ln \tau$  from  $\ln \gamma$ .

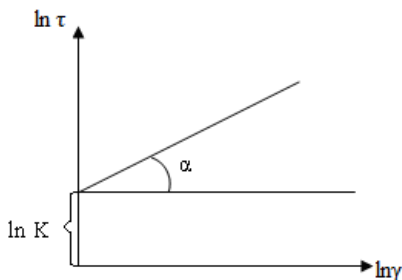


**Fig. 2.** Show dependences  $\ln \tau$  from  $\ln \gamma$ .

P4

Figure 3, 4 shows plots of dependence between the strip thickness and layer position in the gap. Curves do not take into account the stress-strain deformation at the entrance to the gap and the output, i.e., reflects only the influence of generalized deformation.

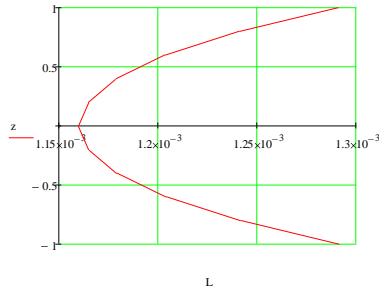


**Fig. 3.** Dependence between the layer thickness and strips position in the discs gap:  $w = 5.25 \text{ s}^{-1}$ ;  $h = 0.01 \text{ m}$ .

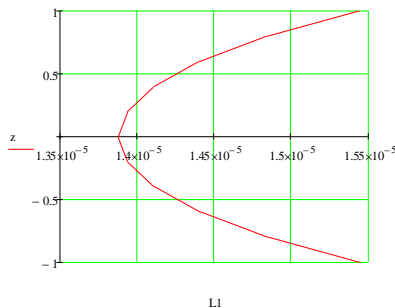


**Fig. 4.** Dependence between the layer thickness and strips position in the discs gap:  $w = 21 \text{ s}^{-1}$ ;  $h = 0.01 \text{ m}$ .

Strain-compression deformations have little influence on the mixing process at the small values of the working gap and disc speed. Thus, width of the bands is inversely proportional to the total deformation. Consequently, the larger particles and the smaller dispersed phase volume concentration, the more deformation amount required to achieve any desired final bandwidths value. Empirical regularity was obtained by Z. Tadmor during the experiments on polymer compositions mixing: good (adequate) mixing is achieved when the amount of deformation is  $18\,000 \pm 6\,000$  shift units. It corresponds to the reduction in strips width to  $10^4$  [4]. However, it should be noted that the term “adequate mixing” is defined by requirements applying to the mixture. Our results are in good agreement with Z. Tadmor and presented on Figure 3, 4.

If the smallest strip thickness is on the low speeds and small gaps, i.e. better mixing is observed at the gap center, there are two areas where the strip thickness

is the minimal (at the high speed rotation and larger gaps). Position of these regions is defined by the octahedral deformation profile  $\gamma_{okt}$ . It should be noted that the strip thickness is reduced by approximately two orders of magnitude with increasing of the disc speed rotation from 50 rpm/min to 200 rpm/min. Strip thickness is reduced by about three orders of magnitude with an increase in the gap from 0.001 to 0.003 m at the constant rotational speed ( $\omega = 21 \text{ s}^{-1}$ ) [5].

Analysis of the results shows that the mixing quality in combined extruders depends on the presence of secondary (circulation) flows in the disk area. In addition to the main melt stream extending on the spiral of Archimedes to the exit area, there will be a backflow to the disc center.

1. *Stobiac V., Heniche M., Devales C.* A mapping method based on Gaussian quadrature: Application to viscous mixing // Chem. engineer. research and design. 86 (2008) 1410.
2. *Mikulionok I. O., Radchenko L. B.* Simulation of disk extruder operation // Applied chemistry. 85 (2012) 1475.
3. *Zuilichem D. J., Kuiper E., Stolp W.* Mixing effects of constituting elements of mixing screw in single and twin screw extruders // Powder technology. 147 (1999) 147.
4. *Бардадым Ю. В., Спорягин Э. А.* Метод исследования качества энергонасыщенных композиций // Вісник Дніпропетровського університету. 21 (2013) 10 – 13.
5. *Bardadym Y., Sporyagin E.* Influence of technological parameters extruder on the quality of polymer compositions // French-Ukrainian journal of chemistry. 2 (2014) 16 – 21.

## HYBRID ORGANIC-INORGANIC COMPOSITES BASED ON CHITOSAN AND SILICA

**I. M. Bei, O. V. Slisenko, V. L. Budzinska**

*Institute of Macromolecular Chemistry of National Academy of Sciences of  
Ukraine, 48 Kharkivske shausse, Kyiv 02160, Ukraine*

[iryabei@meta.ua](mailto:iryabei@meta.ua)

In recent years the problem of environment pollution has aggravate dramatically forcing both polymer science and industry look for the renewable sources of raw materials. Among various natural polymers used for composite materials synthesis considerable attention has been given to chitosan because of its unique properties. Chitosan is the principal deacetylated derivative of chitin which is the second most important polysaccharide on earth next to cellulose and is available from waste products in the shellfish industry. Chitosan has good solubility at aqueous acidic medium and can be modified easily owing to both hydroxyl and amino groups. Thanks to its good biocompatibility, biodegradability, nontoxicity and availability chitosan has widespread applications in biomedical, food, chemical industries etc.

In this work chitosan-based nanocomposites filled with in situ condensed silica were synthesized and investigated. Chitosan was used as 2 wt.% solution in diluted acetic acid. Water solution of polysilicic acid (PSA) was used as a precursor for the silica synthesis. 3-glycidoxypropyltrimethoxysilane (GPTMS) was used for the crosslinking of chitosan. In addition thanks to its organic-inorganic nature silane acts as a coupling agent for the composite constituents. The procedure of chitosan cross-linking one can found in [1]. In brief, a certain amount of GPTMS was added to chitosan solution during vigorous stirring at 60°C. The homogenized reaction mixture was cast in a Petri dish and then heated in an oven at 60°C for 48 h. The dried films were immersed in 1N aqueous NaOH to neutralize the residual acid and then rinsed with water for several times to remove the remaining NaOH. The formed film-like samples were dried in an oven and stored in desiccators.

Chitosan nanocomposites filled with silica in situ were obtained by the same way adding inorganic precursor (water solution of polysilicic acid) into initial reactive solution. Both chitosan to GPTMS and chitosan to PSA weight ratios in

P5

final nanocomposites were varied from 2:0 to 2:2.

The cross-linking route of chitosan with GPTMS is shown in Fig.1.

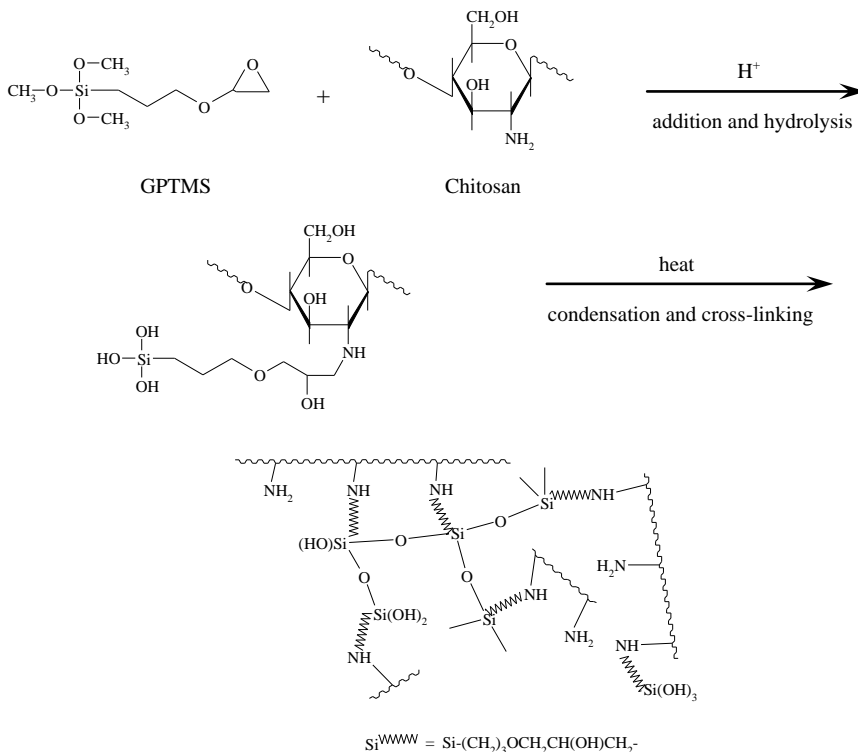


**Fig.1.** Chemical structure and reaction model for cross-linking chitosan to prepare chitosan/GPTMS hybrid matrix [2].

Chemical interaction between amino groups of polysaccharide and glycidoxy groups of GPTMS resulting in chitosan network formation was confirmed by IR-spectrometry. It was revealed intensity decreasing of absorption band of glycidoxy groups at  $910\text{ cm}^{-1}$ . Cross-linking of chitosan during composites synthesis was also confirmed by sol-gel analysis. All organic-inorganic hybrids lost their solubility in acidic media indicating hybrid chitosan/GPTMS-network formation.

Thermal properties of chitosan-based composites were studied by means of TGA under nitrogen atmosphere from room temperature up to  $700^\circ\text{C}$ . In general TGA thermograms of organic-inorganic composites are similar to the weight-loss

P5

dependence of the initial chitosan. All samples show two-steps degradation with an initial weight loss associated with water evaporation around 100°C from 6 (neat chitosan) up to 10-12% (hybrid composites). This effect could be explained by increased hydrophilicity of hybrids comparing to the neat chitosan. The main stage of degradation of neat chitosan starts from 276°C. Onset of hybrids degradation varied from 263 to 280°C and has no direct dependence on constituents' ratio. A char residue for the neat chitosan and all hybrids is around 40 – 42%.

Morphology of composites prepared was studied by means of SEM. Micrographs of two- and three-components hybrid composites are shown in Fig. 2.

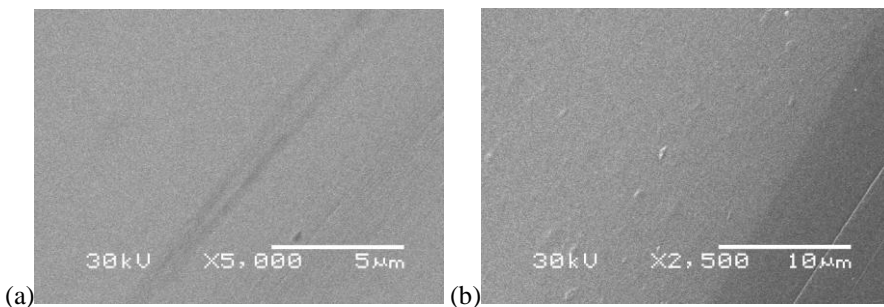


**Fig.2.** SEM micrograph of chitosan/GPTMS/PSA hybrids with components ratios 2:1:0 (a) and 2:1:2 (b).

One can see that composites obtained have homogeneous morphology with no phase separation confirming formation of organic-inorganic hybrid material. Only small amounts of condensed silica inclusions could be discerned on micrograph of the three-component composite.

1. *Shirosaki Yu., Tsuru K., Hayakawa S., Osaka A., Lopes M.A., Santos J.D., Costa M.A., Fernandes M.H.* Physical, chemical and in vitro biological profile of chitosan hybrid membrane as a function of organosiloxane concentration // *Acta Biomaterialia*. 5 (2009) 346-355.
2. *An-Chong Chao.* Preparation of porous chitosan/GPTMS hybrid membrane and its application in affinity sorption for tyrosinase purification with *Agaricus bisporus* // *J. Membrane Sci.* 311 (2008) 306–318.

## STRUCTURE AND PROPERTIES OF ORGANIC-INORGANIC COMPOSITES BASED ON INORGANIC OLIGOMER AND POLYURETANE

**V.L. Budzinska, O.V. Slisenko, I.M. Bei**

*Institute of Macromolecular Chemistry of National Academy of Sciences of Ukraine, 48 Kharkivske shausse, Kyiv 02160, Ukraine*  
[budzinska@meta.ua](mailto:budzinska@meta.ua)

The primary goal of a modern polymeric science is working out of composites with the improved operational properties. As is known, properties of composites can be regulated by carrying out of synthesis and by selection of components of reactions. At a choice of components of reactions to the foreground, there is an availability of materials and their ecological safety. So creation of organic-inorganic composites (OIC) based on a water solution on sodium of silicate and isocyanates actual sphere of last decades. These composites have found their applications as protective coatings, sealants, binders etc. Properties such OIC change depending on updating both inorganic and organic system components. Updating of an organic component gives the chance to influence formation of a polymeric organic matrix that, certainly, will be displayed on properties of final composites. Modification of composite constituents allows to control structure and properties of such materials. In this work effect of 3-(triethoxysilyl)propylamine on mechanical properties of OIC based on polyurethane (PU) and condensed sodium silicate was studied.

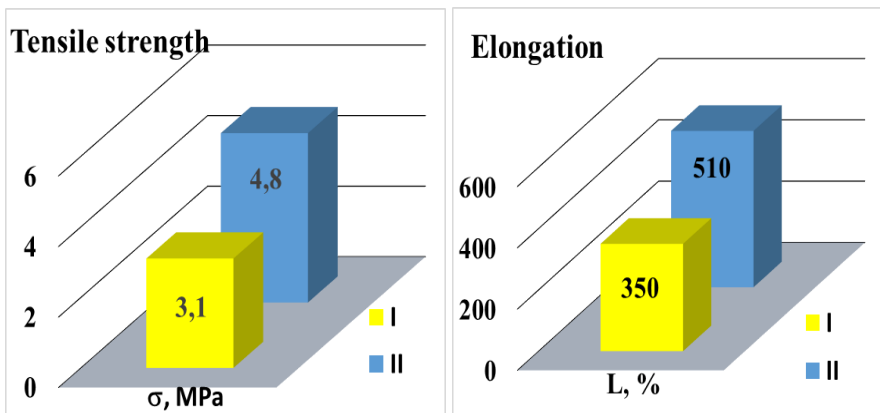
PU was synthesized from urethane oligomer based on 2,4-toluenediisocyanate and linear poly(propylene glycol) (trade mark PPG-1052) with molar ratio 2:1. NCO-groups content in urethane oligomer was 5 wt.%. Water-soluble sodium silicate ( $n\text{Na}_2\text{O} \cdot m\text{SiO}_2 \cdot w\text{H}_2\text{O}$ ,  $m:n = 3.1$ , water content – 52 wt.%) was used as inorganic precursor. Organic to inorganic constituents ratio in OIC was 60:40 wt.%. Concentration of silane coupling agent was 5 wt.%.

Mechanical properties of initial and modified PU/SiO<sub>2</sub> nanocomposites were studied. The results obtained show that OIC has increased tensile strength and elongation at break comparing to unmodified composite (Fig. 1).

The high mechanical characteristics of OIC are result of the number of parallel-competitive chemical reactions in forming composite. The first it is the reaction between -NCO groups PU and amino groups 3-(triethoxysilyl) propylamine. During formation of the organic-inorganic system, the NCO-groups

P6

of PU are concurrently spent in the reaction with water of sodium silicate to form polyurea as follows.



I – unmodified OIC; II – modified OIC

**Fig. 1** Properties of OIC based of the modified PU and sodium silicate.

The reasonable supposition is that parallel reaction between organic and inorganic constituents can path with formation of polyurethane silicates.

This could be explained by composite's structure peculiarities. The morphology of OIC prepared was studied by scanning electron microscopy. It was revealed that the presence of silane agent leads to the size decreasing of silicate particles (Fig.2) formed in situ.

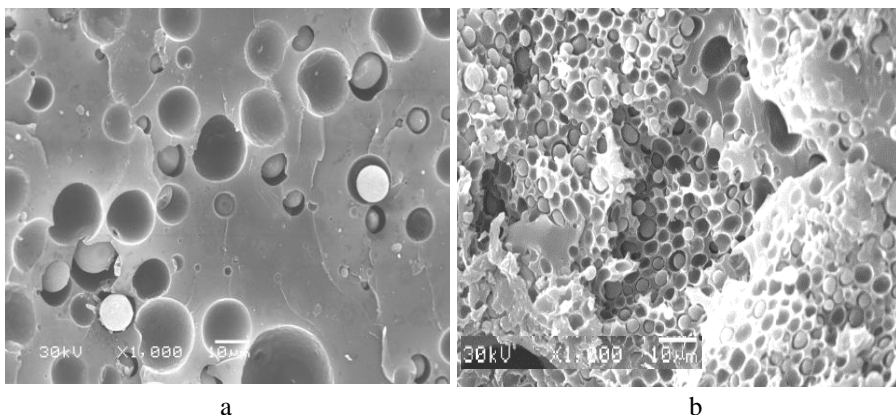


**Fig. 2.** SEM images of (a) OIC unmodified PU and (b) OIC modified PU.

## P6

This effect provides decreasing of heterogeneity and formation of compact structure of OIC. Introduction 3-(triethoxysilyl)propylamine in system OIC leads to reduction of the sizes of particles of silicate, which are formed in such systems in situ. Reduction of the size of particles of silicate leads to increase in the area of contact of two phases (organic and inorganic), that subsequently gives the chance to receive structure that is more compact. Such phenomena result in improved mechanical properties of silane-containing OIC comparing to unmodified composite.

Created OIC based on modified PU and condensed sodium silicate by fast time of formation of a composite that is important at use of such systems as protective compositions and heretics for concrete structures, waterproofing of concrete collectors and pipes also are characterised.

## PROPERTIES OF BLOCK COPOLYMERS OBTAINED ON THE BASE OF OLIGOMER INITIATOR AND MONOMERS OF PYROLYSIS FRACTION OF C<sub>9</sub> PETROLEUM PRODUCTS

**N. A. Busko, V. K. Grishchenko, A. V. Barantsova, Ya.V., Kochetova,  
U.A. Silchenko, N.V.Gudzenko**

*Institute of Macromolecular Chemistry of National Academy of Sciences of Ukraine, 48 Kharkivske shausse, Kyiv 02160, Ukraine*

In the last decades vegetable oils get considerable interest in polymeric chemistry as initial raw materials for synthesis of polymeric materials. Investigations on modification of vegetable oils have allowed to synthesize new reactive oligomers (RO), which are used as extension agents and block copolymers (BCP).

The perspective method of obtaining copolymers and block copolymers on the basis of vegetable oils is preliminary synthesis of oligomer azoinitiator (OAI). This method not only is directly incorporated a well-characterized OAI block into the BCP chain, but blocks, which can be prepared by different routes (i.e., either polymerization or polycondensation). At first, low-molecular azoinitiator with end functional groups interacts with vegetable oil, and then thermal decomposition of azo-groups in the vinyl monomer presence initiates formation of triglyceride-vinyl copolymer by radical polymerization.

Development of new technologies of synthesis of hydrocarbon (petropolymeric) resins (PPR) by oligomerization of vinyl-containing monomers of pyrolysis fractions of the oil products forming as the waste of ethylene manufacturing is an actual problem. This problem is connected not only the solution of ecological problems of recycling the waste of petrochemical manufactures, but ones of replacement of polymers of natural origin which are used in the food-processing industry on synthetic products in manufacture of paint and varnish materials, replacement of rosin and softeners in paper manufacture, industrial rubber goods and tire rubbers. The basic lack of PPR is their enhanced fragility that causes low elasticity of coverings on their base. In this connection, vegetable oils are added to PPR. It is caused by high plasticizing ability of oils and propensity of vegetable oils to oxidizing polymerization in films. For improvement of compatibility of PPR with oils, it is expedient to add to them modified by oils

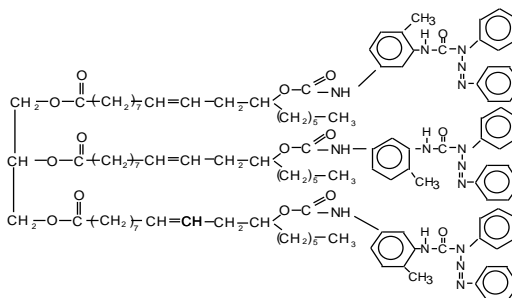
P7

PPR or block copolymers that will promote improvement of physical-mechanical, protective and decorative properties of coverings. Using of PPR in paint and varnish industry provides fast drying of coverings, excellent water, oil and chemical resistance.

The purpose of the given work is study of synthesis of block copolymers (BCP) by method of radical polymerization, initiated by oligomer azoinitiators on the base of vegetable oil, and characterization of their physical-chemical properties.

In our works [1-3] oligomeric azo- and poliazoinitiator (OAI) are synthesized on a basis macrodiisocyanates and azo-compounds with end functional groups were used for both thermal- and photo-initiation of vinyl and diene monomer polymerization.

The method of synthesis of oligomer azoinitiator of castor oil (OAICO) was developed on the base of monomer azoinitiator diazoaminobenzol (DAAB) and triisocyanate of castor oil (TICO) at molar ratio of TICO:DAAB=1:3 the OAICO of the structure:



The reaction of interaction of isocyanate groups TICO with amine groups DAAB has been studied by method of FTIR-spectroscopy on the IR-spectrometer Tensor 37 (Bruker).

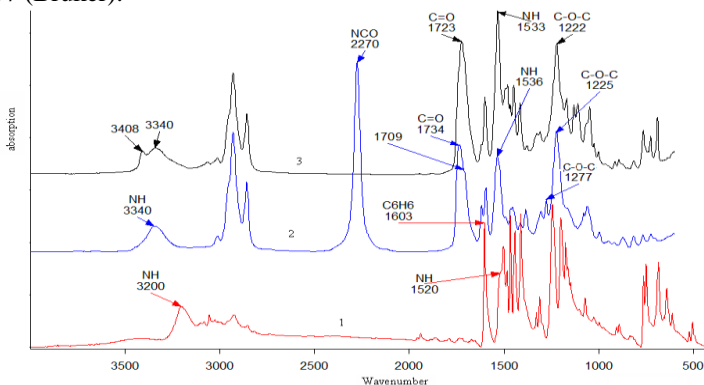


Fig. 1. IR spectra of DAAB (1), TICO (2), oligomer azoinitiator of castor oil (3).

On the base of synthesized oligomer azoinitiator of castor oil and monomers of the C<sub>9</sub> pyrolysis fraction of petroleum products or styrene, block copolymers of type ABA (A – block of castor oil, B – block of oligostyrene or fraction C<sub>9</sub>) were synthesized by method of thermoinitiated radical polymerization at temperature 130°C during 10 hours. Kinetic studies of synthesis of BCP were conducted by method of differential calorimetry on the calorimeter DAK1-1A. The structure of the new block copolymers was investigated by the means of FTIR- spectroscopy.

Molecular-weight characteristics of TICO, petrol-polymer resin, received on the monomer initiator DAAB, oligostyrene (OSt) castor oil-oligostyrene (BCP CO-St) and castor oil- petrol-polymer (BCP CO-C<sub>9</sub>) of synthesized block copolymers were studied by the method of exclusion chromatography on the chromatograph Du Pont LC System 8800 with bimodal exclusion columns Zorbax. The resulted viscosity has been calculated for synthesized BCP, TICO and petrol-polymer resins, received on the monomer initiator DAAB for what relative viscosities have been defined at use of Ubbelohde type viscometer at temperature 25°C (Table 1). The calculated specific viscosities change similarly to the molecular masses, measured by the method of chromatography.

**Table 1.** Molar weight characteristics of BCPs.

Samples	M <sub>n</sub>	M <sub>w</sub>	M <sub>z</sub>	M <sub>w</sub> /M <sub>n</sub>	P (M <sub>w</sub> ) hm/lm, (%)	specific viscosity [η]
OSt	8000	10000	12000	1,23	100	-
TICO	3000	7000	23000	2,21	29/71	0,045
PPR	22000	48000	112000	2,22	19/81	0,052
BCP CO-C <sub>9</sub>	35000	130000	341000	3,71	50/50	0,084
BCP CO-St	81000	163000	253000	2,02	86/14	0,148
P (M <sub>w</sub> ) percentage ratios of fractions of the polymer, calculated on the integrated area of high-molecular and low-molecular peaks of a curve MMW; hm – high-molecular weight fraction; lm- low-molecular weight fraction.						

Thermal behaviour of the new block copolymers was evaluated by differential scanning calorimetry (DSC), with respect to relaxation transitions in the soft (castor oil) and the hard (C<sub>9</sub> or St) blocks of the type ABA. The experimental data for heat capacity and glass transition temperatures are summarized in Table 2 and thermograms corresponding to block copolymers ABA are presented in Figure 2.

It was shown that studied BCPs are a typical two-phase polymeric systems with two glass temperatures (T<sub>g</sub>) with a formed interphase field.

P7

**Table 2.** Thermodynamic characteristics of BCPs

Samples	T <sub>g,1</sub> , K	ΔC <sub>p,1</sub> , J/(g·K)	T <sub>g,2</sub> , K	ΔC <sub>p,2</sub> , J/(g·K)
TICO	222	0.36		
PPR	272	0.34		
St			334	0.54
BCP CO-St	230	0.21	311	0.32
BCP CO-C <sub>9</sub>	234	0.29	263	0.35

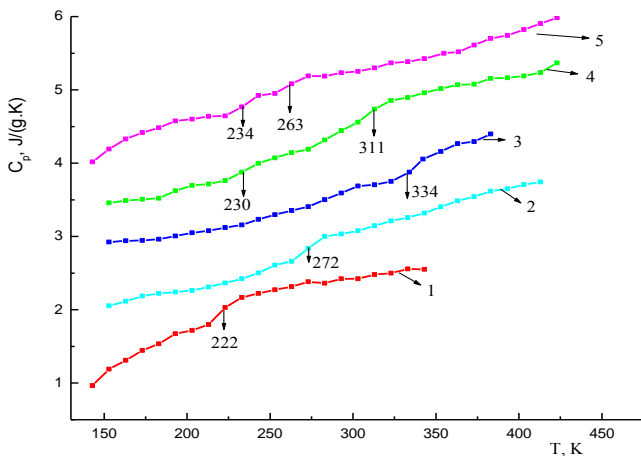


**Fig. 2.** Temperature dependences of heat capacity triisocyanate of castor oil (TICO) (1); petrol-polymer resin, received on the monomer initiator DAAB (2); OSt (3); BCP CO-St (4); BCP CO-C<sub>9</sub> (5). Beginning at curve 3, all the subsequent ones are displaced relative to the ordinate axis 0.5.

1. Busko N. A., Grishchenko V. K., Kochetov D. P. (1993) Photoinitiated radical polymerization of urethane-containing copolymer. *Teor. Eksper. Khim.*, Vol. 29, pp. 539-543.
2. Busko N. A., Grishchenko V. K., Shtompel V. I., Babkina N. V., Rosovitski V. F., Privalko V. P. (2001) Phase morphology and dynamic mechanical properties of model polyblock copolymers prepared from reactive. *Polymers & Polymer Composites*, Vol. 9, No 8, pp. 509-513.
3. Busko N. A., Barantsova A., Babkina N. V., Privalko E. P., Grishchenko V. K. (2004) Synthesis and properties of block copolymers on the base of oligomeric polyazoinitiators and butylmethacrylate, *Polymer journal*, Vol. XXVI, No 2, pp. 78-82.

## **DESIGN AND PROPERTIES CONTROL IN OMPOSITE MATERIALS BASED ON RECYCLED RUBBER, PET, PVC and HDPE**

**C. Cazan, M. Cosnita, A. Duta**

*Transilvania University of Brasov, Centre Product Design for Sustainable Development, Eroilor 29, 500036 Brasov, Romania*

Composite materials were developed by optimizing the composition parameters (filler, percent of filler) and the technological parameters (compression molding time, the temperature range, duration, pressure, and speed of injection). The interface properties optimization were done by using an additive (HDPE) to make the matrix (tire rubber) compatible with the fillers (PET and/or PVC). Correlations microstructure - interface properties are developed, as an essential step in the design of multifunctional composites. The interface and mechanical properties were evaluated using integrated characterization techniques for: composition (FTIR spectroscopy), morphology (AFM), surface energy (contact angle measurements), crystalline structure (XRD), mechanical strength (tensile strength, compression, impact); mechanical characterization allowed comparing the synergetic effects of polymer-polymer composites and the influence of the processing parameters on the fracture behavior.

Since injection molding has been a successful method for mass production of glass fiber-reinforced plastics, it is of great interest to optimize this process for the production of composites based on wastes: tire rubber and plastic materials. The injection used a standard mold for developing samples to conduct tensile tests, compression tests and impact tests. The results allowed to optimize the processing parameters for each composition: injection speed, injection pressure, injected dose, injection temperature and velocity.

**Table 1.** The samples composition

<b>Samples cod</b>	<b>rubber (%)</b>	<b>PET (%)</b>	<b>PVC (%)</b>	<b>HDPE (%)</b>
<b>1</b>	50	45	-	5
<b>2</b>	45	45	5	5
<b>3</b>	45	35	15	5
<b>4</b>	45	25	25	5
<b>5</b>	45	15	35	5
<b>6</b>	45	10	40	5
<b>7</b>	50	-	45	5

The compositions of the wastes-based composites in injection moulding are presented in Table 1, while the processing parameters that were varied during injection are included in Table 2.

**Table 2.** The processing parameters

Code	T 1 (°C)	T2 (°C)	T 3 (°C)	T4 (°C)	V <sub>d</sub> (cc)	P (bar)	Velocity V <sub>1</sub> , V <sub>2</sub> , V <sub>3</sub>
1a	195	205	205	210	64	175	15%;13%;12%; 12mm;10mm
2a	195	205	205	210	64	175	15%;13%; <b>10%</b> ; 12mm;10mm
2b	195	205	205	210	64	<b>150</b>	15%;13%;10%; 12mm;10mm
3a	195	205	205	210	<b>63</b>	175	15%; 13%; 10%; 12mm;10mm
3b	195	205	205	210	63	<b>150</b>	15%; 13%; 10%; 12mm;10mm
3c	195	205	205	210	63	<b>125</b>	15%; 13%; 10%; 12mm;10mm
4a	195	205	205	210	<b>62</b>	175	15%; 13%; 10%; 12mm;10mm
4b	<b>200</b>	<b>210</b>	<b>210</b>	<b>220</b>	62	175	15%; 13%; 10%; 12mm;10mm
5a	<b>205</b>	210	210	<b>215</b>	<b>60</b>	175	15%; 13%; 10%; 12mm;10mm
6a	200	210	210	<b>215</b>	<b>58</b>	175	15%; 13%; 10%; 12mm;10mm
6b	200	210	210	215	58	175	15%; 13%; 10%; <b>20mm;15mm</b>
6c	200	210	210	215	58	175	15%; 13%; 10%; <b>35mm;20mm</b>

After analysing all the data (Table 3) obtained during the experiments, it can be concluded that no significant differences in the mechanical properties are registered when the injection parameters are varied for the same type of composite material, except a slight in the tensile strength with the decrease in the injection pressure for composite 3, while an increase of the injection temperature led to an increase in the compression strength for composite 4. The reason for the small differences between the composites created with different injection parameters is

the small steps in which the parameters were varied. If the injection parameters would be changed more drastically, larger differences could become clearer.

**Table 3.** The mechanical properties for the rubber :HDPE :PET :PVC composites

Code	R <sub>tr.</sub> (N/mm <sup>2</sup> )	E (N/mm <sup>2</sup> )	R <sub>compr.</sub> (N/mm <sup>2</sup> )	E <sub>Charpy</sub> (kJ/m <sup>2</sup> )	E <sub>Izod</sub> (kJ/m <sup>2</sup> )
1a	12,09	320,0	75,66	57,11	3,35
2a	13,79	805,5	78,71	21,60	4,20
2b	8,42	407,0	57,73	59,08	2,87
3a	5,64	638,5	36,30	27,99	2,05
3b	3,86	284,9	37,59	35,33	3,23
3c	6,51	515,6	35,76	25,60	2,64
4a	4,4	180,1	22,35	33,21	2,99
4b	3,64	364,8	34,28	31,45	2,05
5a	4,43	254,4	31,17	36,05	2,52
6a	5,22	386,3	35,75	33,91	2,75
6b	5,02	621,1	27,07	29,36	3,11
6c	4,66	383,6	28,09	34,62	2,75

In order to elucidate what chemical and/or physical interaction took place between composite components during blend curing, FTIR spectra analysis were performed for the composite with the highest dimensional stability and the data show that more bands are formed, indicating new chemical interaction between polymeric composite components (PVC, HDPE and rubber). These results are supporting the mechanical tests results. Considering the FTIR analysis and contact angle measurements, it may be conclude again that new interfaces between the components of composites are formed.

**Table 4.** Contact angle, surface energy ( $\sigma_{sv}$ ) and its polar ( $\sigma^p_{sv}$ ) and dispersive ( $\sigma^d_{sv}$ ) components for the samples 2b and 3b

Samples cod	$\Theta_{water}$	$\Theta_{salt}$	$\sigma_{sv}$ [mN/m]	$\sigma^d_{sv}$ [mN/m]	$\sigma^p_{sv}$ [mN/m]
2b	86,3	70,2	23,46	17,87	5,59
3b	82,4	72,8	38,45	27,47	10,58

For the 3b sample the lowest surface energies of 27.47 mN/m were registered as result of a compact structure, in good agreement with mechanical test results (mainly in terms of compression resistance). From the results of the contact angle measurements one can observe the decrease in the surface energy value after

long term water immersion, recorded for the composites thermally treated at composite type 3. This result is in good agreement with mechanical tests result, which showed an increase in compression strength of this composite, proving that more compact interfaces are developed.

Results obtained from contact angle measurements, support the assumptions of the changes in the morphological properties. When the functionalized PVC were used for obtain the rubber-PVC-HDPE composites, the dispersed particles were reduced and the interfacial adhesion of the phases has been improved. Therefore, the compatibilized blend clearly revealed a finer phase dispersion and smaller domain size in SEM micrographs, and composites 2b and 3b confirm a better interfacial adhesion and finer particle morphology than another composites.



**Fig. 1** SEM image of sample 2b

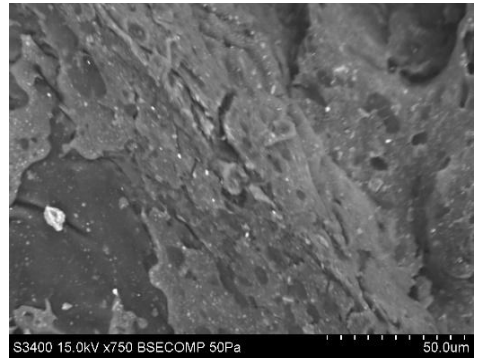


**Fig. 2** SEM image of sample 3b

In the scanning electron microscopy images of the fractured surface (Figs. 1 and 2), more phases and voids are outlined, occurred after the failure of the sample at tensile test. This homogeneous and dense structure is confirmed by contact angle measurements. It can be distinguished phases and interfaces achieved between composite components. The areas wide open / dark colour represent a mixture of homogeneous / less homogeneous interface between rubber and HDPE.

When different composites are compared to each other, it can easily be seen that increasing amounts of HDPE and PVC in the composite have a positive influence on all the mechanical properties. The composites 2b and 3b showed the most promising set of properties to be used as construction materials, also proving very good stability after long term water immersion, thus these could be used as water-proof foils, bricks, etc.

**Acknowledgements**

*This paper is supported by the Sectoral Operational Programme Human Resources Development (SOP HRD), financed from the European Social Fund and by the Romanian Government under the project number POSDRU/159/1.5/S/134378.*

**SHEDDING LIGHT UPON THE INFLUENCE OF  
CONFORMATIONS AND MICROSTRUCTURE ON THE  
PHOTOPHYSICAL PROPERTIES OF CONJUGATED  
POLYMERS: CASE STUDY ON FLUORENE-VINYLENE  
ALTERNATING COPOLYMERS IN “HAIRY-ROD”  
ARCHITECTURE**

**I. Cianga<sup>1,2</sup>, D. Göen Çolak<sup>2</sup>, L. Cianga<sup>1</sup>, E.- G. Hitruc<sup>1</sup>, Y. Yagci<sup>2,3</sup>**

*1 “Petru Poni” Institute of Macromolecular Chemistry, 41A Grigore Ghica Voda Alley, Iasi 700487, Romania*  
[ioanc@icmpp.ro](mailto:ioanc@icmpp.ro)

*2 Department of Chemistry, Faculty of Science and Letters, Istanbul Technical University, 34469, Istanbul, Turkey*

*3 Center of Excellence for Advanced Materials Research (CEAMR) and Chemistry Department, Faculty of Science, King Abdulaziz University, P.O. Box 80203, Jeddah, 21589, Saudi Arabia*

Conjugated polymers (CPs), one of the most fascinating examples of specialty soft materials, have undergone an unprecedented pace of development in the last four decades. Their applications, such as light-emitting devices (LED) and displays, photovoltaics and organic field effect transistors (OFET), electrochromic devices (ECD) or sensors and actuators, rely on their conductivity, photo- or electroluminescence, light-induced charge generation and non-linear optical behavior [1]. It is also noteworthy that research on CPs for biomedical applications expanded greatly in the 1980s and, since then, their useful properties were exploited in order to obtain advanced materials for biomedical applications like regenerative medicine [2,3] or diagnosis and therapy [4-7].

Concerning the CPs biomedical application, there is a shift from the use of organic electronic coatings to the use of organic electronic devices both *in vitro* and *in vivo* that positively impacts the worldwide individuals quality of life. The new rising field of organic bioelectronics attracts great scientific interest [8]. As one of the main objectives is to develop low cost and flexible electronic

components in large-scale, at the core of the structure–property relation research is the need to improve the performance of electronic devices based on CPs.

Understanding the role that morphology plays in the electronic properties and long-term stability of these devices concomitantly with the identification of a proper synthetic strategy, allowing the conformation chains modification in a controllable and systematic manner, are critical for creating better materials.

The physical and electronic properties of CPs are very sensitive toward the conformation adopted by the polymer chain in a given solvent. Some experimental evidences suggest that the “memory” of the solution phase is retained in thin films through solution processing. On the other hand it has been proven that, efficient and rapid migration of excitation and charges through CPs material could be reached by films having ordered structures from the nano- to macroscale.

The molecular self-assembly (SA) in solution or in melt, is an elegant path to achieve reproducible materials structuring at the nanometer scale. The complex attractive and repulsive interactions required for SA of structures composed of different building blocks need to be already encoded in the basic units. To design and build macromolecules capable of forming a desired superstructure by SA, manipulating elemental monomer units through “bottom-up” strategy is a today important aspect in the CPs field. [1]

Excepting the fact that CPs are sensitive at almost all the external stimulus (electric, photo, electromagnetic, mechanic, electromechanic, etc.), their organizing capability through self-assembling mediated by non-covalent interactions ( $\pi$ - $\pi$  staking, electrostatic, van der Waals, hydrophobic, hydrogen bonding) is notorious and could be usefully directed by their covalent linking with coil-like polymers [1].

The resulting *rod-coil* copolymers, due to the anisotropic molecular shape and orientational organization imparted by the stiff rod-like conformation of the conjugated blocks, give a plethora of different morphologies in solid and solvent-dispersed states even at low molecular weights [4].

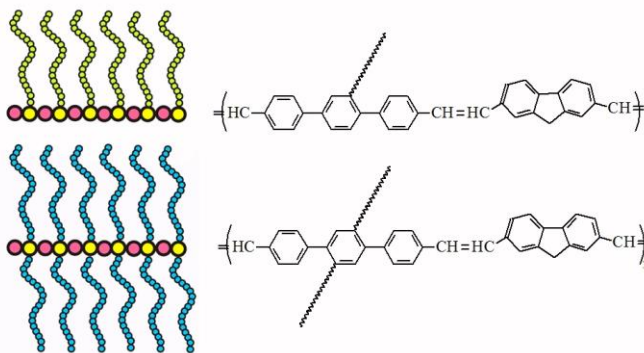


**Fig. 1.** “Hairy-Rod” models and the molecular formula of the reported copolymers.

Both supramolecular shapes of the formed aggregates as well as their stability can be manipulated by the variation of macromolecular architecture. In this context conjugated rod-coil copolymers in “hairy-rod” architecture [1], become an exciting research field for the new materials with unexpected properties otherwise impossible to be obtained by the polymers with common topology. Although they have similar propensity for SA as their linear rod-coil block-copolymer analogs, nevertheless the morphology and the properties of “hairy-rods” are significantly better when used for electronic devices, as recently reported [9].

Based on our own previous experience, in the present approach we focused on *the materials design strategy* toward the new conjugated polymers having “hairy-rod” topology (Figure 1), by engineering both main and side chains.

The “*macromonomer technique*” was chosen for the synthesis of new copolymers, due to its advantages related to well-defined grafting density and side-chain length, defect-free polymer structures and ease of access in copolymer synthesis [4]. As conjugated, rigid main chains we drive our attention toward poly(fluorenylene vinylene)s (PFVs) which, having similar structures to PPVs, combines the structural characteristics of PPVs with those of polyfluorenes, and show higher thermal stability and photoluminescence quantum yields.

The Wittig polycondensation was chosen due to the fact of being a suitable route for the synthesis of well-defined strictly alternating copolymers. *p*-Terphenyl is a chemically, electrochemically and photochemically stable light-emitting chromophore. It is also a well-known mesogene, which has been widely used to generate liquid crystals with high birefringence.

Oligostyrenic, oligo- $\epsilon$ -caprolactonic and PEG 2000 side chains were used in the synthesis of “T”-shaped or “cross-shaped” *p*-terphenyl macromonomers that were subsequently conducted to amphiphilic, amphipolar or low mixing entropy materials.

**Targeted goals of the present research are as follow:**

(i)- Self-assembling in solution of the synthesized alternating copolymers in various solvents; modifying their selectivity in relation to the main or side chain by direct dissolution method;

(ii)- Size and shape characterizations of the formed colloidal assemblies by integrated methods (<sup>1</sup>H-NMR, dynamic light scattering-DLS- and atomic force microscopy-AFM);

(iii)- Obtaining thin films by drop-casting method on the supports with different surface energy (mica and HOPG), morphology characterization and the assessment of the influence of surface character on the morphological transition during the film forming;

(iv)- Studying the photophysical properties of the synthesized materials in solution and film in order to establish how the peculiar structural characteristics as well as their processing are decisive factors in manipulating chain conformations and morphology that directly impact the properties;

**The results of our investigation demonstrated** that the conjugated chain conformation as well as the self-assembling properties and film morphologies can be manipulated by chemical changes (the nature, number of the side chains) and also by processing (solvent- or surface-induced changes). Best to the our knowledge our studies on the new obtained structures revealed for the first time:

- Foldamers forming from oligomers of PPV type, totally water self-dispersible with promising applications in both bio- or optoelectronic devices;
- Vesicle forming from conjugated polymers “hairy-rods” in backbone – selective solvent;

### **Acknowledgements**

*One of the authors (I.C.) acknowledges the financial support given by The Scientific and Technological Research Council of Turkey (TÜBİTAK) through a fellowship.*

1. Cianga I., Yagci Y. // Prog Polym Sci. 29 (2004) 387-399.
2. Bendrea A.-D., Cianga L., Cianga I., // J Biomat Appl. 26 (2011), 3-85.
3. Bendrea A.-D, Fabregat G., Torras J., Maione S., Cianga L., del Valle L. J, Cianga I., Aleman C., // J. Mater.Chem B, 1, (2013), 4135-4145.
4. Cianga L., Bendrea A.-D., Fifere N., Nita L.-E., Doroftei F., Ag D., Selecı M., Timur S., Cianga I., // RSC Adv. 4, (2014), 56385-56405.
5. Ag D., Selecı M., Bongartz R., Can M., Yurteri S., Cianga I., Stahl F., Timur S., Scheper T., Yagci Y., // Biomacromolecules 14 (2013), 3532-3541.
6. Yuksel M., Colak D.G., Akin M., Cianga I., Kukut M., Ilker Medine E., Can, M., Sakarya, S., Unak, P., Timur, S., Yagci, Y. // Biomacromolecules 13 (2012), 2680-2691.
7. Colak D. G., Ciang, I., Demirkol D.O., Kozgus O., Medine E. I., Sakarya S., Unak P., Timur S., Yagci Y. // J. Mater. Chem. 22 (2012), 9293-9300.
8. Rivnay J., Owens R.M., Malliaras G.G. // Chem. Mater., 26, (2014), 679–685.
9. Kim H. J., Kim J.-H., Ryu J.-H, Kim Y., Kang H., Lee W. B., Kim T.-S., Kim B.J. // ACS Nano, 8, (2014), 10461-10470.

**FROM FUNCTIONALITY TO FUNCTION WITH  
CONDUCTING POLYMERS: CARBOXYL, SCHIFF BASE  
AND TERTHIOPHENE-CONTAINING RANDOM  
COPOLYMERS AS PROSPECTIVE BIOMATERIALS**

**L. Cianga<sup>1</sup>, M. M. Pérez-Madrigal<sup>2,3</sup>, L. J. del Valle<sup>2</sup>, I. Cianga<sup>1</sup>,  
C. Alemán<sup>2,3</sup>**

*<sup>1</sup> “Petru Poni” Institute of Macromolecular Chemistry, 41A Grigore Ghica Voda  
Alley, Iasi 700487, Romania  
[lciana@icmpp.ro](mailto:lciana@icmpp.ro)*

*<sup>2</sup> Departament d'Enginyeria Química, ETSIEB, Universitat Politècnica de  
Catalunya, Barcelona, E- 08028, Spain*

*<sup>3</sup> Center for Research in Nanoengineering, Universitat Politècnica de Catalunya,  
Barcelona, E- 08028, Spain*

An interesting sociological aspect of the research on conducting conjugated polymers (CPs) has been the evolving target for technological applications, and hence emphasis on peculiar physical properties, that has motivated the research in the ensuing almost 40 years.

Driven by the possibility of mass-producing cheap and sustainable electronic devices, the interdisciplinary emerging field of “polymer electronics” (organic/plastic electronics) rise based on  $\pi$ -conjugated molecules with increasingly complex structures [1]. Recently brought to market Sony’s OLED televisions, as well as Samsung Impression cell phone near to the first general illumination OLED panels (Philips Lumiblade and Osram ORBEOS) are successful commercial examples of CPs applications.

On the other hand, integration of CPs was also considered in the field of the biomaterials, tailoring them into more intelligent and advanced ones. Freedom in chemical modification, ease of processing on flexible substrates, soft mechanical properties and, most important, combined ionic and electronic conductivity and capability to operate in hydrated state make CPs uniquely suited for interfacing

with biological systems [2].

Placed at the convergence between organic electronics and biology, the new rising field of organic bioelectronics attracts great scientific interest [1] and it is naturally developing taking the CPs' above mentioned advantages.

Already known as a viable alternative for tissue engineering [3], the use of CPs in new bioelectronic devices is expected to provides conformal, highly-compliant, functional human-machine interfaces for this application.

These targets fuel the research interest in the synthesis of new CPs as suitable materials for such applications. It is also the case of the present study that reports about electroactivity and bioactivity of random copolymers films, P(AzbT-co-Th<sub>3</sub>), obtained by electrochemical copolymerization between 2,2':5',2''-terthiophene (Th<sub>3</sub>) with a new reported bis-thienyl type monomer (AzbT), containing preformed azomethine likages and a carboxyl functional group as is presented in Figure 1.

As electrochemical method, chronoamperometry was applied for synthesis, using acetonitrile and tetrabutylammonium tetrafluoroborate (TBATFB) as the solvent and the dopant agent, respectively [4].

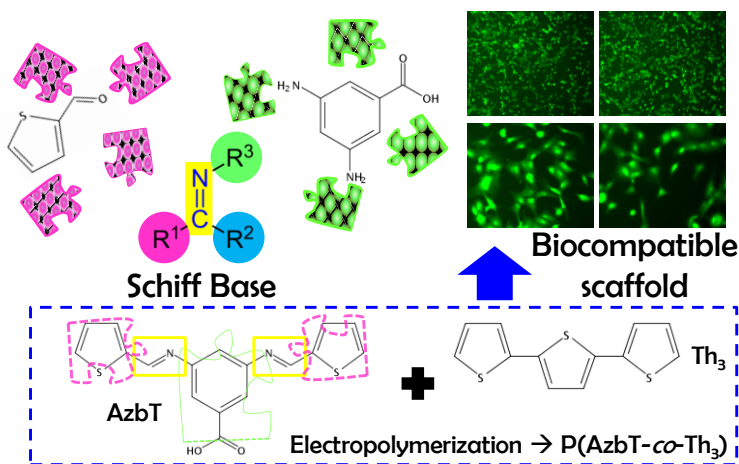


**Fig. 1.** Suggestive representation of the comonomers structure used for the synthesis of copolymers and optical images of biocompatible scaffolds.

The structure of the new monomer AzbT was spectroscopically proved (NMR and IR), while the copolymers film composition was assessed by XPS and IR analyses.

The electroactivity (charge storage ability) and electrostability (loss of electroactivity with consecutive oxidation-reduction cycles) of PTh<sub>3</sub> and P(AzbT-

## P10

*co*-Th3) films were determined by cyclic voltammetry (CV) assays, while optical properties of P(AzbT-*co*-Th3) films deposited onto ITO were recorded between 300 and 800 nm in the absorbance mode by UV-vis spectroscopy. Thickness, morphology and topography of the obtained films were evaluated as well by specific methods (profilometry, SEM and AFM microscopy).

The study results revealed that, in spite of the easiness of its obtainment, the AzbT's structural peculiarities are responsible for both the impossibility of its electrochemical homopolymerization and the concomitant and complex phenomena that take place in the reaction medium when its copolymerization with Th3 was applied. Thus, due to the presence of the ionizable carboxyl function, AzbT can work as both comonomer and dopant, the resulting copolymers belonging to the so-called "*self- or autodoping polymers*". The amount of Th<sub>3</sub> in the reaction medium shifts the equilibrium between the two forms of AzbT and consequently dictates the final properties of the obtained materials.

The potential application of P(AzbT-co-Th3) films as bioactive substrates has been evaluated using human osteosarcoma and monkey kidney epithelial cell lines (MG-63 and Vero, respectively). The film of 80 : 20P(AzbT-co-Th3) copolymer promotes cellular viability, most probably due to the presence of the carboxyl groups. More specifically, we hypothesize that such a favorable response is essentially due to the recognition of fibronectin and integrins from cells by the imine and carboxylate groups of AzbT units.

If the antibacterial activity is *a priori* taken into account due to the presence of the Schiff base functionalities in its structure, the obtained materials should be considered as a suitable bioactive platform for advanced biomedical applications in which optical properties similar to those displayed by semiconducting polythiophene derivatives are required.

1. de Mello J., Anthony J., Lee S. // ChemPhysChem. 15, (2015) 1099-1100.
2. Guo B., Glava L., Albersson A.-C. // Prog. Polym. Sci.38 (2013) 1263-1286.
3. Bendrea A.-D., Cianga L., Cianga I., // J Biomat Appl. 26 (2011), 3-85.
4. Perez-Madrigal M.M., Cianga L., del Valle L.J., Cianga I., Aleman C. // Polym. Chem., 6, (2015), 4319-4335.

## STRUCTURING, THERMOMECHANICAL AND ELECTRICAL PROPERTIES OF NANOCOMPOSITES BASED ON PECTIN, POLYETHYLENIMINE AND Cu/Cu<sub>2</sub>O CORE-SHELL NANOPARTICLES

**V.L. Demchenko, S.V. Riabov, V.I. Shtompel**

*Institute of Macromolecular Chemistry of National Academy of Sciences of Ukraine, 48 Kharkivske shausse, Kyiv 02160, Ukraine*  
[dvaleriy@ukr.net](mailto:dvaleriy@ukr.net)

In the last decade, considerable attention is paid to the scientific researches dealing with polymer nanocomposites, filled with nanoparticles of different metals or metal oxides [1]. Metallo-containing compounds can provide polymer materials with special optical, electrical, magnetic, and mechanical properties as well as catalytic activity [2]. The capability of functional groups on polyelectrolytes to bind metal ions offers a possibility for their application as sorbing agents, ion-exchange materials, components of selective membranes, or as precursors for preparation of polymer–inorganic hybrids via reduction or precipitation of metal ions [3]. Polymer–inorganic nanocomposites are important candidates for construction of photonic devices, band-pass filters, components of nonlinear optical systems, optical limiters, elements of microcircuit chips, etc. Polyelectrolyte-based materials, including ultrafine particles of silver and noble metals, exhibit antibacterial properties and are therefore promising for application in medicine [4].

The aim of this study is to investigate the features of the structuring, thermomechanical and electrical properties of the nanocomposites obtained via the chemical reduction of Cu<sup>2+</sup> cations in the ternary polyelectrolyte-metal complexes (TPMC) based on oppositely charged polyelectrolytes (pectin, polyethyleneimine) and salt CuSO<sub>4</sub>.

The stoichiometric polyelectrolyte complex (PEC), which is formed by equimolar amounts of the anionic and cationic polyelectrolytes, is characterized by short-range ordering during translation of fragments of oppositely charged polyelectrolyte macromolecular chains in space. This circumstance is indicated by the appearance of one diffuse diffraction maximum with  $2\theta_m \sim 20.8^\circ$  on the X-ray diffractogram of the PEC sample (see Fig. 1, curve 1). The average value of the

P11

period of short-range ordering of fragments of complementary macromolecular chains of oppositely charged polyelectrolytes in the PEC (the Bragg distance between the macromolecule chains of anionic and cationic polyelectrolytes in the PEC) is 4.3 Å.

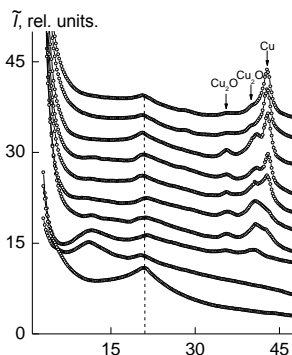


**Fig. 1.** Wide-angle X-ray diffractograms of (1) the PEC; (2) the TPMC; and (3–10) the PEC–Cu<sub>2</sub>O nanocomposites obtained via the chemical reduction of Cu<sup>2+</sup> cations in the TPMC at molar ratios of [BH<sub>4</sub><sup>-</sup>] : [Cu<sup>2+</sup>] = (3) 0.5, (4) 1, (5) 2, (6) 3, (7) 4, (8) 5, (9) 6, and (10) 10.

However, the sorption of CuSO<sub>4</sub> by the initial PEC sample and formation of the PEC–Cu<sup>2+</sup> TPMC is accompanied by a change in the diffractogram. This result is indicated by the appearance of an intense diffuse diffraction maximum at  $2\theta_m \sim 11.2^\circ$  (curve 2) in the presence of a low-intensity amorphous halo, which, unlike that for the initial PEC, has an angular position at  $2\theta_m \sim 20.4^\circ$  ( $d \sim 4.4$  Å). This diffraction maximum, according to [5], characterizes the existence of polyelectrolyte-metal complexes between the central ions (Cu<sup>2+</sup>) and ligands, whose role is likely to be played by the nitrogen atoms of the amino groups of PEI and by the carbonyl oxygen atoms of the anionic polyelectrolyte. With the use of the angular position of this diffraction peak on the X-ray diffractogram of the TPMC, average Bragg distance  $d$  between the macromolecule chains of polyelectrolytes coordinated with Cu<sup>2+</sup> cations is found to be 7.9 Å.

During investigation of the sorption characteristics of PEC films it was found that the PEC has a high sorption capacity  $A = 2.9$  mmol/g with respect to Cu<sup>2+</sup> cations.

After the chemical reduction of Cu<sup>2+</sup> cations with the use of sodium borohydride (molar ratio [BH<sub>4</sub><sup>-</sup>] : [Cu<sup>2+</sup>] = 0.5–10) in the TPMC bulk, the X-ray diffractograms of nanocomposites show a gradual transition from nanocomposites based on PEC and Cu<sub>2</sub>O nanoparticles to the nanocomposites based on PEC and Cu/Cu<sub>2</sub>O core-shell nanoparticles, when the amount of the reducing agent is increased (curve 3–10). At the same time, one can observe a significant decrease in the intensity of the diffraction peak, characterizing the existence of polyelectrolyte-metal complexes at  $2\theta_m \sim 11.2^\circ$ , and two diffraction peaks also appeared at  $2\theta_m \sim$

P11

35.6° and 40.8°, confirming the formation of Cu<sub>2</sub>O nanoparticles, and additional two diffraction peaks emerged at  $2\theta_m \sim 42.8^\circ$  and  $49.6^\circ$ , relating to the metallic copper's phase structure of Cu/Cu<sub>2</sub>O nanoparticles in the PEC bulk [6]. Also, according to wide-angle X-ray diffraction it may be concluded that the molar ratio  $\text{BH}_4^- : \text{Cu}^{2+} = 6$  is optimum for the formation of PEC–Cu/Cu<sub>2</sub>O nanocomposites, when the full structural appearance of the metal Cu phase is observed.

The conversion of PEC–Cu<sup>2+</sup> ternary metal-polyelectrolyte complexes into nanocomposites containing Cu/Cu<sub>2</sub>O nanoparticles is confirmed by transmission electron microscopy (see Fig. 2), and the average size of the Cu/Cu<sub>2</sub>O nanoparticles in nanocomposites is 10 nm. Analysis of the micrographs showed that the nanoparticles are statistically distributed in the PEC.

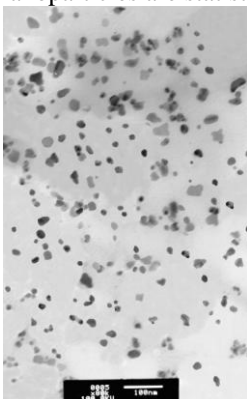


**Fig. 2.** TEM micrograph of the PEC–Cu/Cu<sub>2</sub>O nanocomposite obtained via the chemical reduction of Cu<sup>2+</sup> cations in the TPMC at a molar ratio  $[\text{BH}_4^-] : [\text{Cu}^{2+}] = 6$ .

Analysis of the thermomechanical curve of the initial PEC (see Fig. 3, curve 1) demonstrated that temperature transitions that are associated with the temperatures of the glass transition and flow occur in the temperature ranges 25–145°C and 265–350°C, respectively.

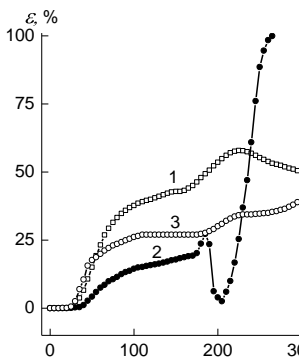


**Fig. 3.** Thermomechanical curves of (1) the PEC, (2) the TPMC, and (3) the PEC–Cu/Cu<sub>2</sub>O nanocomposite obtained via the chemical reduction of Cu<sup>2+</sup> cations in the TPMC at a molar ratio  $[\text{BH}_4^-] : [\text{Cu}^{2+}] = 6$ .

Furthermore, in the range of temperatures 80–245°C, there is a temperature transition that is due to the melting of the crystallites in the PEC that are related to anionic polyelectrolytes. However, the introduction of CuSO<sub>4</sub> into the initial PEC, which causes the TPMC formation, is accompanied by the appearance of a temperature transition at 205°C on the thermomechanical curve, a phenomenon that is due to the melting of CuSO<sub>4</sub> in the PEC. This leads to the transition of the polymer to the viscous-flow state (curve 2). Analysis of the thermomechanical curves of the PEC, the TPMC, and PEC–Cu/Cu<sub>2</sub>O nanocomposite shows that, during the transition from the PEC to the TPMC, glass-transition temperature  $T_g$  increases, and during the transition from the TPMC to the PEC–Cu/Cu<sub>2</sub>O nanocomposite,  $T_g$  significantly decreases. Simultaneously with the decrease in  $T_g$ , a decrease in transition temperature in the viscous-flow state,  $T_f$ , occurs in the following series:  $T_{f(PEC)} > T_{f(PEC-Cu/Cu_2O)} > T_{f(TPMC)}$ .

Studying of the frequency dependence of the real part of the samples' complex conductivity  $\sigma_{ac}(f)$  revealed that the PEC and TPMC exhibit dielectric properties, nanocomposite PEC–Cu/Cu<sub>2</sub>O has the properties intrinsic to insulator–semiconductor (Fig. 4). It was found that the transition from PEC and TPMC to nanocomposites PEC–Cu/Cu<sub>2</sub>O resulted in the enhancing of  $\sigma_{ac}(f)$  magnitude in the range of two orders.

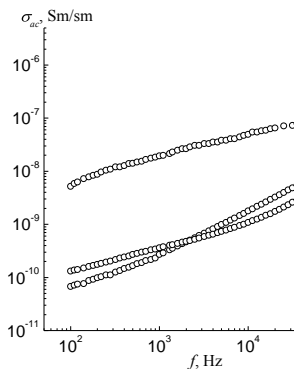


**Fig. 4.** The frequency dependence of the real part of the complex conductivity  $\sigma_{ac}(f)$  at  $T = 20 \pm 2$  °C of (1) the PEC, (2) the TPMC, and (3) the PEC–Cu/Cu<sub>2</sub>O nanocomposite obtained via the chemical reduction of Cu<sup>2+</sup> cations in the TPMC at a molar ratio  $[BH_4^-] : [Cu^{2+}] = 6$  (3).

1. Nicolais L. Metal–Polymer Nanocomposites (2005) New York: Wiley.
2. Yan Y., Huang J. Hierarchical assemblies of coordination supramolecules // *Coord. Chem. Rev.* 254 (2010) 1072-1080.
3. Bruening M.L., Dotzauer D.M., Jain P., Ouyang L., Baker G.L. Creation of functional membranes using polyelectrolyte multilayers and polymer brushes // *Langmuir* 24 (2008) 7663-7673.
4. Nicolais L., Carotenuto G. (ed.) Metal-polymer nanocomposites (2005) John Wiley & Sons.

P11

5. *Shtompel' V.I., Kercha Yu.Yu.* Structure of Linear Polyurethanes (2008) Naukova dumka, Kiev [in Russian].
6. *Kou T., Jin C., Zhang C., Sun J., Zhang Z.* Nanoporous core-shell Cu@Cu<sub>2</sub>O nanocomposites with superior photocatalytic properties towards the degradation of methyl orange // RSC Adv. 2 (2012) 12636-12643.

## THE INFLUENCE OF STRUCTURE AND FUNCTIONALITY OF CAPROLACTAM BLOCKED ISOCYANATES ON THEIR THERMAL PROPERTIES

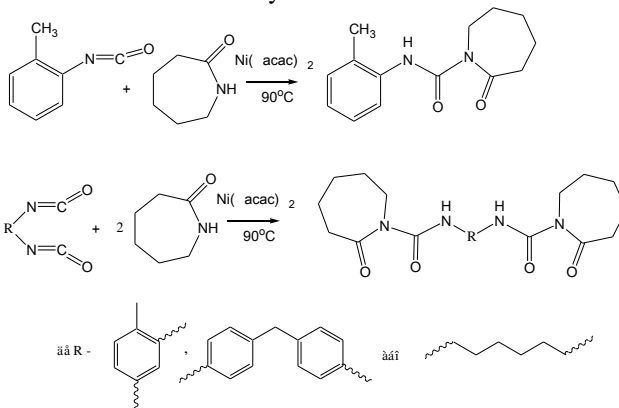
**K. S. Didenko, N. V. Kozak, T. V. Dmytriieva, H. M. Nesterenko,  
V.I. Bortnytskyi, N.I. Stepanenko, V.V. Klepko**

*Institute of Macromolecular Chemistry of National Academy of Sciences of Ukraine, 48 Kharkivske shausse, Kyiv 02160, Ukraine*  
[didenko.katherina@gmail.com](mailto:didenko.katherina@gmail.com)

Latent (or blocked) isocyanates (BIC) are compounds that can release free reactive isocyanate groups at a distinct temperature. The BIC thermal dissociation temperature depends on structure of isocyanate (IC) and blocking agent, medium (solvent) and catalyst [1,2]. Moreover, IC functionality and structure (aromatic or aliphatic) has a significant impact on process of BIC thermal dissociation [3,4].

Hence, the aim of our research was to investigate the influence of structure and functionality of  $\epsilon$ -caprolactam (CL) blocked isocyanates (o-tolyl isocyanate (o-TICb), toluene diisocyanate (TDIb), methylene diphenyl isocyanate (MDIb) and hexamethylene diisocyanate (HDIb)) on their thermal properties, particularly on thermal dissociation temperature.

Scheme below illustrates the synthesis of CL blocked IC:



The reaction was carried out at  $90^\circ\text{C}$  for 4 hours. Reactant contents used-for BICs synthesis are listed in table 1.

**Table 1** The content of reactants for BIC synthesis

BIC	IC	CL	Ni(acac) <sub>2</sub>
o-TICb	1	1	0,03
TDIb	0,7	1	0,01
MDIb	1	1	0,01
HDIb	0,7	1	0,01

The blocked isocyanates thermal characteristics and thermal dissociation temperature ( $T_d$ ) of are shown in table 2.

**Table 2** The characteristics of CL blocked IC

BIC	Form	Yield, %	$T_d$ , °C	$T_{melt}$ , °C
o-TICb	light-yellow powder	91	100-110	76-78
TDIb	white powder	88	120-130	72-74
MDIb	white powder	85	150-160	148-150
HDIb	light-grey powder	66	110-120	57-60

The reaction was controlled by FTIR spectroscopy. FTIR spectra were recorded on the TENSOR 37 spectrometer (Bruker) in the frequency region of 4000 – 400  $\text{cm}^{-1}$ .

Thermal properties, particularly thermal dissociation temperature, were investigated by thermogravimetric analysis (TGA) and pyrolysis mass-spectrometry (MS). TGA was performed with a TGA analyzer (Derivatograph Q–1500D system F.Paulik, J.Paulik, L.Erdey). In the analysis, 50 mg of sample was heated from room temperature to 700°C with a 10°C·min<sup>-1</sup> heating rate.

The MS-instrument that consists of liner pyrolysis cell (temperature range 25 – 400°C) and mass-spectrometer MX–1321 allowing determination of the components of gas mixture in the mass number region of 1-4000, was used for investigation of initial isocyanates and caprolactam blocked ones.

From the FTIR spectroscopic analysis, all BIC spectra are similar and does not show intensive NCO absorption peak at 2275  $\text{cm}^{-1}$ . Characteristic bands at 1705, 1535 and 1395  $\text{cm}^{-1}$  (amide I, II and III, respectively) are observed. It ought to be noted that BIC-spectra have two amide I bands: 1705  $\text{cm}^{-1}$  corresponds to formation of amide bond during reaction of IC and CL whereas 1655  $\text{cm}^{-1}$  is amide I band presented in CL spectra. FTIR spectra confirm the formation of new bond in BIC: o-TICb, TDIb, DFMDIb and HMDIb.

According to TGA data the thermoxydative destruction character of BIC in the temperature range of 110 – 335°C depends on structure and functionality of IC. The  $T_d$  was defined as the temperature of endothermic region in DTA curve where the weight losses at TG curve begins. Table 2 represents  $T_d$  temperatures.

The o-TIC degraded in a single step, while for the blocked diisocyanates the

degradation process exhibited two stages.

Thermal dissociation of BIC can pass not only through the formation of NCO-groups. Thus, the identification of products of BIC thermal decomposition is important factor for prediction of the main reaction possibility.

The identification of BIC thermal decomposition products was carried out by using mass-spectra of their pyrolysis decomposition at appropriate temperature range to BIC thermal dissociation temperature.

Pyrolysis of BIC occurred in several stages. The temperature range of first stage corresponds to BIC thermal dissociation process. Pyrolysis decomposition of o-TICb goes through the 3 stages: 100-155°C, 155-210°C, and 210-340°C. The main decomposition ion fragments at 100°C are fragments of mass number 113 and 133 that correspond to molecular mass of CL and o-TIC, respectively. The molecular ion of o-TICb (mass number is 246) is also present. Such fragments are present in mass-spectrum also at higher temperatures. With temperature increasing the content of o-TICb molecular ion decreases and it does not observed at 300°C.

In contrast to blocked monoisocyanate, pyrolysis decomposition of blocked diisocyanates passes in two stages. The characteristic ion current vs temperature dependence and corresponding mass-spectra are illustrated in fig. 1a and 1b, respectively.

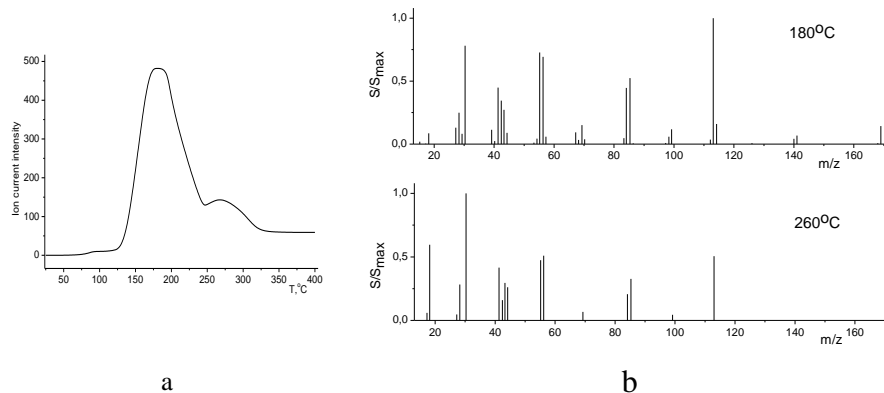


**Fig. 1.** The temperature dependence of ion current intensity (a) and mass-spectra of HDIb at various temperatures (b).

The temperature decomposition of TDIb occurs in the ranges of 135-250°C and 250-320°C. At 140°C the main ion fragments of mass number 113 and 174, agreed with molecular mass of CL and TDI, in proportion of 2:1 are occurred. The presence of fragment with mass number 287 corresponding to blocked TDI by one NCO-group together with CL and TDI fragments refer to continuing the deblocking process.

Decomposition stages of MDIb reside in the temperature region of 235-300°C and 235-300°C. The main pyrolysis decomposition fragments at 160°C are 113 and 250 in the ratio of 2:1 that agreed with molecular mass of CL and MDI, respectively. At the higher temperature the diisocyanate fragment is absent.

HDib pyrolysis decomposition occurs in temperature range 135-250°C and 250-300°C. The main pyrolysis decomposition fragments at 180°C are 113 and 169 that correspond to molecular mass of CL and HDI, respectively. The ion fragment of diisocyanate is absent at the higher temperature.

From obtained data it was concluded—that not only the number of NCO-groups but also their position in molecule has an influence on thermal dissociation of BIC. Deblocking reaction of MDIb and HDIb occurs simultaneously by two NCO-groups, whereas it is seen from TDib mass-spectra that its pyrolysis occurs with releasing of only one isocyanate group. Opposed to MDIb, isocyanate groups of TDib are located in the same benzene ring. Thus, deblocking of one NCO-group TDib can inhibit the release of another NCO-group. Such behavior can be explained in terms of different reactivity of TDI isocyanate groups [4,5].

Thus, the investigation of thermal properties of caprolactam blocked mono-(o-TICb) and bifunctional isocyanates (TDib, MDIb and HDIb) demonstrates that thermal dissociation temperature depends on the structure and functionality of IC. Moreover, it was found that  $\pi$ -conjunction of aromatic ring with p-orbital of nitrogen atoms can influence the dissociation order of blocked NCO-groups located in the same benzene ring.

1. *Wicks D.A. Wicks Z.W. Blocked Isocyanates III: Part A. Mechanisms and Chemistry // Prog. in Org. Coatings. 36 (1999) 148-172.*
2. *Delebecq E., Pascault J.-P., Boutevin B., and Ganachaud F. On the Versatility of Urethane/Urea Bonds: Reversibility, Blocked Isocyanate, and Non-isocyanate Polyurethane // Chem. Rev. 113 (2013) 80 – 118.*
3. *Jung Min Lee, Sankaraiah Subramani, Young Soo Lee, and Jung Hyun Kim Thermal Decomposition Behavior of Blocked Diisocyanates Derived from Mixture of Blocking Agents // Macromol. Research. 13 (2005) 427-434.*
4. *Gedan-Smolka M., Haubler L., Fischer D. Thermal deblocking of masked low molecular isocyanates I. Aliphatic isocyanates // Thermochemica Acta 351 (2000) 95-105.*
5. *Saunders J.H., Frisch K.C. Polyurethanes Chemistry and Technology. Part I. Chemistry // New York: Interscience Pub. (1962) 368.*

## **POLYCYCLOTRIMERIZATION OF BISPHENOL E DICYANATE ESTER CATALYSED BY IONIC LIQUID**

**A. M. Fainleib<sup>1</sup>, A. V. Vashchuk<sup>1</sup>, O. M. Starostenko<sup>1</sup>, O. P. Grigoryeva<sup>1</sup>,  
S. P. Rogalsky<sup>2</sup>, D. Grande<sup>3</sup>**

<sup>1</sup>*Institute of Macromolecular Chemistry of National Academy of Sciences of Ukraine, 48 Kharkivske shose, Kyiv 02160, Ukraine*

[fainleib@i.ua](mailto:fainleib@i.ua)

<sup>2</sup>*Institute of Bioorganic Chemistry and Petrochemistry of National Academy of Sciences of Ukraine, 50 Kharkivske shose, Kyiv 02160, Ukraine*

[rogalsky@ukr.net](mailto:rogalsky@ukr.net)

<sup>3</sup>*Institut de Chimie et des Matériaux Paris-Est, UMR 7182 CNRS – Université Paris-Est Créteil Val-de-Marne, 2, rue Henri Dunant, 94320 Thiais, France*

[grande@icmpe.cnrs.fr](mailto:grande@icmpe.cnrs.fr)

### **INTRODUCTION**

Last years the considerable interest has grown to ionic liquids. Their advantages over other organic solvents are in unique physical and chemical properties such as low melting temperature, incombustibility, ecological, electrochemical and high temperature stability. Ionic liquids are progressively used as solvents and substances with catalytic properties [1-2]. The structure of such catalytic systems allows easier separation, recovery and recycling of the catalyst from the reaction mixtures. This combination of properties makes ionic liquids excellent candidates for accelerating the polycyclotrimerization of cyanate ester resins (CER), which is usually carried out at relatively high temperatures.

Cure kinetics of the neat cyanate ester resins is extensively available in literature [3]. For the best of our knowledge the catalytic effect of ionic liquids on the cure kinetics of CER has not been reported yet. Therefore, the idea of this work was to verify if there is any acceleration effect at polymerization of cyanate ester monomer in the presence of ionic liquid.

### **RESULTS AND DISCUSSION**

In the current work we investigated an influence of 1-octyl-3-

P13

methylimidazolium tetrafluoroborate ([OMIm][BF<sub>4</sub>]) ionic liquid on curing behavior of dicyanate ester of bisphenol E (DCBE). The chemical formula of DCBE and [OMIm][BF<sub>4</sub>] are presented in Figure 1. The kinetic peculiarities of polycyclotrimerization of DCBE as well in the presence of [OMIm][BF<sub>4</sub>] was investigated using FTIR analysis.

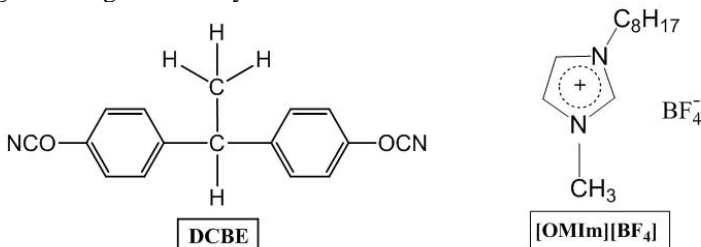


**Fig.1.** Chemical structures of the DCBE and [OMIm][BF<sub>4</sub>].

Figure 2 shows the change in FTIR spectra after heating at 150°C for 6 hours for neat DCBE and DCBE/[OMIm][BF<sub>4</sub>] blends with varying content of the latter. As an internal standard the band at 1501 cm<sup>-1</sup> of the benzene ring backbone stretching vibrations was used. It is seen that at polycyclotrimerization of DCBE an intensity of the peaks of cyanate groups at 2266-2235 cm<sup>-1</sup> decreases and the new bands appear at 1563 and 1366 cm<sup>-1</sup> corresponding to C=N-C groups (triazine cycle) and N-C-O groups (cyanurate cycle).

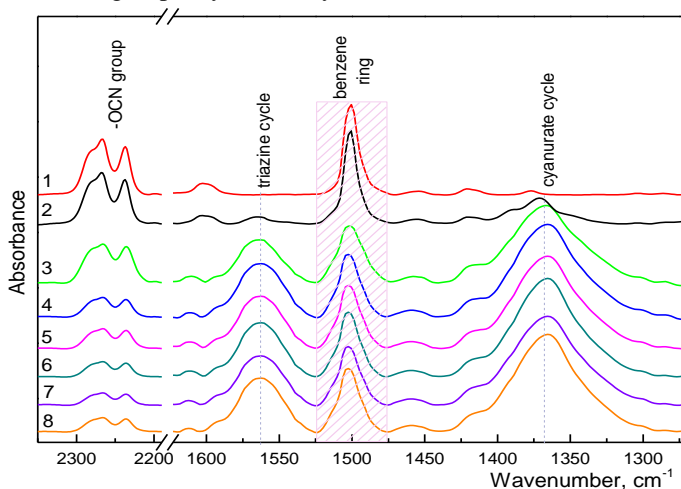


**Fig.2.** FTIR spectra of uncured DCBE (1) and DCBE/[OMIm][BF<sub>4</sub>] blends cured at 150 °C for 6 hours with different [OMIm][BF<sub>4</sub>] content, wt.%: 0 (2), 0.5 (3), 1.0 (4), 2.0 (5), 3.0 (6), 4.0 (7), 5.0 (8).

P13

The conversion of DCBE was calculated using Equation (1):

$$\alpha_{(t)} = 1 - \frac{A_{(t)2266-2235}/A_{(0)2266-2235}}{A_{(t)1501}/A_{(0)1501}} \times 100\% \quad (1)$$

where  $A_{(t)2266-2235}$  is the area under absorbance peak of  $-\text{OCN}$  group of DCBE at time (t);  $A_{(t)1501}$  is the area under absorbance peak of benzene ring backbone stretching vibrations at time (t);  $A_{(0)}$  is the area under absorbance peak of corresponding group in the FTIR spectra of the initial DCBE monomer.

The values of conversion obtained for the each blend applying equation 1 versus  $[\text{OMIm}][\text{BF}_4]$  content are plotted in Figure 3. The FTIR data evidence the acceleration effect of the ionic liquid used on kinetics of the early stages of DCBE polymerization at 150 °C. Moreover, catalytic effect is already noticeable at the lowest concentration (0.5 wt.%) of  $[\text{OMIm}][\text{BF}_4]$  checked.

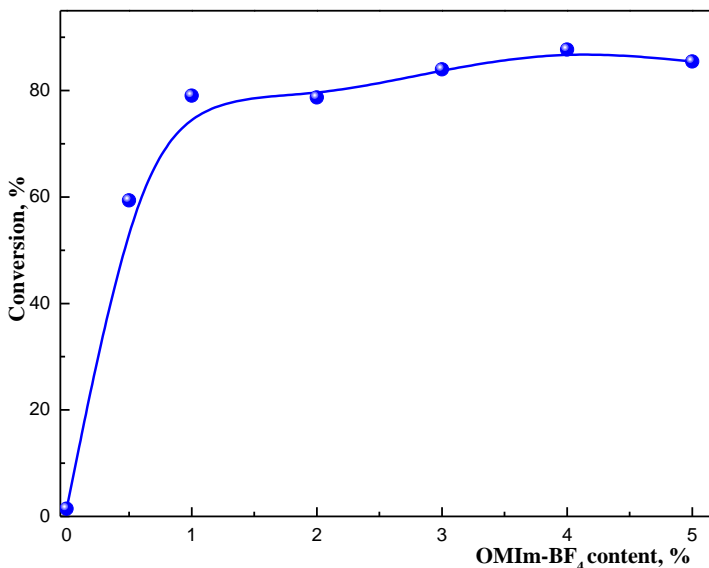


**Fig. 3.** Conversion of  $-\text{OCN}$  groups of DCBE versus  $[\text{OMIm}][\text{BF}_4]$  content.

It is known [4] that Lewis acids such as  $\text{TiCl}_4$  are used as catalyze polycyclotrimerization of CERs. The mechanism of the catalytic effect was investigated in some publications, for example [4]. Taking into account that fragment  $[\text{BF}_4]^-$  is similar to  $\text{TiCl}_4$ , we have suggested the mechanism of polycyclotrimerization of DCBE in the presence of the ionic liquid (Fig.4). The  $[\text{BF}_4]^-$  catalyzed polycyclotrimerisation of DCBE is possible via formation of  $\text{OCN}^{\delta+} \cdots [\text{BF}_4]^{-\delta-}$  complex.

P13

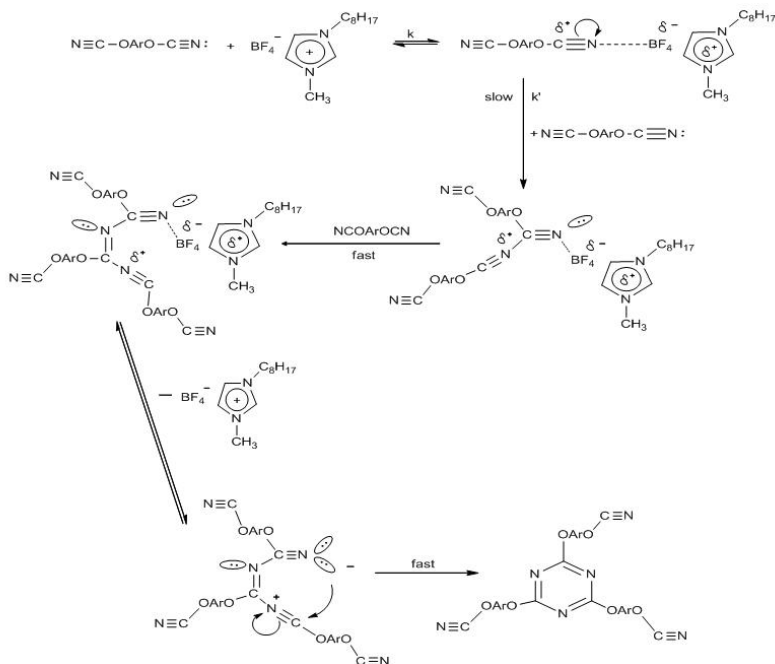


**Fig.4.** The mechanism for the [OMIm][BF<sub>4</sub>] catalyzed polycyclotrimerization of CER.

## CONCLUSIONS

The incorporation of [OMIm][BF<sub>4</sub>] ionic liquid has shown the catalytic effect on the curing reaction of bisphenol E dicyanate ester. The mechanism of the catalysis has been suggested.

### Acknowledgements

*The authors are gratefully acknowledged for partial financial support of the work to the NAS of Ukraine and CNRS of France (project N26199).*

1. Wang Y., Li H., Wang C., Jiang H. Ionic liquids as catalytic green solvents for cracking reactions. // Chem. Commun. (2004) 1938 -1939
2. Olivier-Bourbigou H., Magna L., Morvan D. Ionic liquids and catalysis: Recent progress from knowledge to applications. // Appl. Catal., A-GEN (2010) 1-56
3. Hamerton, I. Chemistry and Technology of Cyanate Ester Resins. // Ed. Blackie Academic and Professional (1994) 1–6.
4. Cunningham I., Brownhill A., Hamerton I., Howlin B. Kinetics and mechanism of the titanium tetrachloride-catalysed cyclotrimerisation of aryl cyanates. // J.Chem. Soc. Perkin Trans. 2 (1994) 1937-1943.



thermal analysis.

The thermostability has been estimated by the temperature  $T_p$  polymer beginning schedule when starting the weight loss and temperatures  $T_{10}$ ,  $T_{20}$ ,  $T_{50}$ , when there is a loss of 10, 20 and 50% of the mass of the sample in research under the same conditions.

Outlines all curves "weight loss - temperature" PITE similar, that expansion is uniform (like the mechanism and nature of destruction), in addition, such a character curves indicates the complexity of the processes thermooxidative destruction under dynamic heating samples in the atmosphere air. The studies have been shown that PITE is heat resistant compounds.

**Table 1.** Chemical resistance of polyionens based on tetrahydro-1,4-oksazyn and epoxidized derivatives of 1,2-epoxy-4,7-dioksononen-8

Compound	$T_{10}$ , °C	$T_{20}$ , °C	$T_{30}$ , °C	$T_{50}$ , °C	$T_b$ , °C	$T_e$ , °C	Balance at 350°C, %	The activation energy in the temperature range, kJ/mol			
								$\frac{0,764}{65+150}$	$\frac{0,385}{150+215}$	$\frac{1,673}{215+315}$	$\frac{7,178}{315+430}$
PI-1-1	51	54	98	199	53	300	11	$\frac{0,523}{75+150}$	$\frac{3,416}{150+240}$	$\frac{21117}{250+325}$	$\frac{12,824}{325+520}$
PI-1-2	75	110	180	230	75	300	7	$\frac{0,208}{31+105}$	$\frac{4,255}{105+177}$	$\frac{9,722}{177+260}$	$\frac{6,832}{260+525}$

*Note:*  $T_{10}$ ,  $T_{20}$ ,  $T_{30}$ ,  $T_{50}$  - temperature 10, 20, 30, 50% weight loss, respectively;  $T_b$  - beginning autocatalytic process of destruction;  $T_e$  - end process autocatalytic degradation.

In the temperature range 25-50°C observed small weight loss (7-15%) samples PITE, which is probably due to loss of moisture.

And then, at higher temperatures to 100-300°C, there avtocalitical progress of the destruction. In this temperature range the difference in the behavior is best expressed of the studied PITE. Thus, on the table 1 shows that 20% -the weight loss: for PI-1-1 occurs at 54°C; for PI-1-2 - at 110°C; for PI-2-2 - at 90°C; 50% -the weight loss: PI-1-1 occurs at 199°C; PI-1-2 at 230°C; PI-2-2 at 158°C.

At temperatures above 300°C (PI-1-1 and PI-1-2) 500°S (PI-2-2); weight loss slows down and does not change, that the destruction process is terminated. Thus, the final stage of thermooxidative destruction observed the behavior is identical for all investigated PITE.

P14

According to thermographic analysis IPPITE characterized by thermal stability up to 50<sup>0</sup>C (PI-1-1 and PI-2-2); 75<sup>0</sup>S (PI-1-2). It should be noted that PITE PI-1-2 is most resistant to thermooxidative degradation.

Almost the same pattern for PITE observed with autocatalytic decomposition. At the final stage of thermooxidative destruction PITE not fully decompose - form a mass balance.

We also investigated the specific ionic conductivity and molar new PITE. Analysis of the results of ionic conductivity at 25<sup>0</sup>C of new PITE showed that PITE have high ( $10^{-2}$ - $10^{-4}$  Cm<sup>2</sup>cm<sup>-1</sup>) and the specific molar ionic conductivity (Fig. 1, 2). The influence of external factors and structural properties of new PITE on their ionic conductivity. It has established that with increasing temperature ionic conductivity relative new PITE increases corresponding to the Arrhenius equation. The influence of cationic nature, the distance between the quaternary nitrogen atoms in the macromolecule, functional groups in the radical cation and symmetry in the cation radical new PITE on their ionic conductivity.

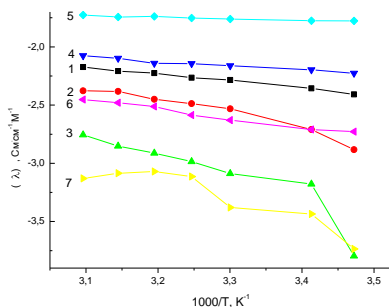


**Fig. 1.** Temperature (1000/T) dependence of ion conductivity ( $\log \sigma$ ) polyionens: 1 – PI-1-1; 2 – PI-1-2; 3 – PI-1-3; 4 – PI-1-4; 5 – PI-2-2; 6 – PI-3-3; 7 – PI-4-4.

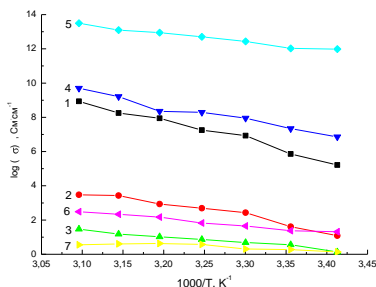


**Fig. 2.** Arrhenius curves molar ionic conductivity ( $\lambda$ ) polyionens: 1 – PI-1-1; 2 – PI-1-2; 3 – PI-1-3; 4 – PI-1-4; 5 – PI-2-2; 6 – PI-3-3; 7 – PI-4-4.

PITE are low-temperature ionic liquids of new type, capable of operating in temperatures ranging from 15-55<sup>0</sup>C with high ionic conductivity due to the structure of their cationic parts.

So, investigated new PITE can be recommended for use as a component of liquid and polymeric electrolytes for electrochemical devices of a new type (in lithium batteries, capacitors, solar batteries, etc.).

1. *Burmistr M.V., Burmistr E.M.* Alkylaromatic polyionenes. - Dnepropetrovsk: USUCT, 2005. - 131 p.
2. *Sverdlikovskaya O.S., Burmistr M.V., Fedenko O.A.* Polyionenes based on derivatives of oxirane compounds and morpholine / Abstracts of X International Scientific and Practical Conference "TRANS-MECH-ART-CHEM", 27-28 May 2014, Moscow, Russia. - P. 34-36.
3. *Wolfson, N.S.* Preparative organic chemistry [Text] / Ed. NS Wolfson - M.: Chemistry, 1964. – 908 p.

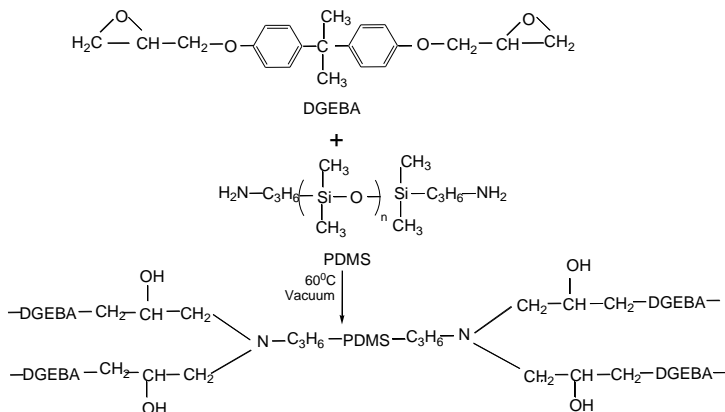


### Characterization

IR spectra were registered on a FTS 40A Bio-Rad spectrometer at room temperature on KBr pellets. Scanning electron microscopy images were obtained on a Quanta 200 ESEM microscope operating at 30 kV with secondary electrons. The mechanical properties were measured on an Instron testing machine, model 4411. The tensile strength was determined at 10 mm/min. rate.

### RESULTS AND DISCUSSIONS

Siloxane modified epoxy resins were prepared according to Scheme 1, by reacting the ROPOXID/e-DS/e-PDMS/a-PDMS (30/1/1/1 weight ratio) mixture at 60 °C, under vacuum for 6 h. Then POLYA or DETA curing agents were added in a 10/1 mixture/curing agent weight ratio and the resulted viscous products were cast in films of about 1 mm width. The films were left to cure at room temperature for 24 h to obtain the RESINS I and II samples, respectively. The film samples were further submitted to aging experiment and their properties were analysed before and after aging.



**Scheme 1.** General pathway toward siloxane-modified epoxy resins.

The aging under simultaneous heating and UV irradiation was followed by investigating the structural and surface morphology modifications through IR spectroscopy and SEM, respectively, and by measuring the mechanical properties.

IR spectra of both REFERENCE and RESIN samples before and after aging experiments (not shown) indicate important modifications in the regions of aromatic bands (1400-1650 cm<sup>-1</sup>) a prove of chain decomposition involving arylene moieties. This observation was proved by EDX analysis (Table 1) where for RESIN samples and increase of silicon and nitrogen and a decrease of carbon contents were registered.

**Table 1.** EDX determined compositions for siloxane-modified epoxy resins

Element Wt %	RESIN I	RESIN I-600	RESIN II	RESIN II-600
C	81.02	78.76	76.96	75.80
N	3.09	4.60	1.92	2.26
O	13.96	14.73	15.33	16.43
Si	1.93	1.91	5.64	5.61

### Mechanical properties

The mechanical properties were measured for both original and aged resin samples for 600 h (Table 2). As expected, the siloxane-modified epoxy resins showed lower Young modulus as compared to the REFERENCE sample. As one may see from the data presented in Table 2, all studied samples presented an increase in stiffness after aging. While the non modified epoxy resin keeps its tensile strength and manifests a reduction of the elongation after the aging treatment, the siloxane-modified resins showed different behavior, depending on the nature of the curing agent. A small improvement of the tensile strength was registered for RESIN I cured with POLYA, whereas RESIN II (curing agent, DETA) has an opposite behavior. Both modified resins get a higher modulus and a lower elongation to break after aging.

**Table 2.** Mechanical properties of epoxy resins before and after aging treatment

Samples*	Young's modulus MPa	Tensile strength MPa	Elongation to break mm
REFERENCE	1351.63	25.32	1.16
REFERENCE-600	2492.87	25.62	0.62
RESIN I	1256.32	20.05	0.81
RESIN I -600	2213.34	21.96	0.60
RESIN II	1288.12	26.65	0.75
RESIN II-600	2212.97	18.1	0.56

\* REFERENCE and REFERENCE-600 are epoxy resins prepared by curing ROPOXID with DETA, before and after aging treatment, respectively; RESIN I and II are the siloxane-modified epoxy resins before aging treatment; RESIN I-600 and II-600 are the siloxane-modified epoxy resins after aging treatment

### Conclusions

Siloxane-modified epoxy resins revealed good mechanical properties before and after aging treatment, being suitable materials for self-healing of epoxy composites.

### Acknowledgements

*The authors acknowledge the grant of the Romanian Ministry of Education, UEFISCDI, contract PNII-59/2014 for the financial support.*

1. *Yin T., Rong M.Z., Wu J.S., Chen H.B., Zhang M.Q.* Healing of impact damage in woven glass fabric reinforced epoxy composites// *Composites A39* (2008) 1479–87.
2. *Keller M.W., White S.R., Sottos N.R.* A self-healing poly(dimethyl siloxane) elastomer// *Adv. Funct. Mater.* 17 (2007) 2399–404.
3. *Cho S.H., White S.R., Braun P.V.* Self-healing polymer coatings// *Adv. Mater.* 21 (2009) 645–49.
4. *Beiermann B.A., Keller M.W., Sottos N.R.* Self-healing flexible laminates for resealing of puncture damage// *Smart Mater. Struct.* 18 (2009) 085001.
5. *Trask R., Bond I.* Biomimetic self-healing of advanced composite structures using hollow glass fibres// *Smart Mater. Struct.* 15 (2006) 704–10.
6. *Williams H.R., Trask R.S., Knights A.C., Williams E.R., Bond I.P.* Biomimetic reliability strategies for self-healing vascular networks in engineering materials// *J. R. Soc. Interface* 5 (2008) 735–47.
7. *Lorente S., Bejan A.* Vascularized smart materials: designed porous media for self-healing and self-cooling// *J. Porous Media* 12 (2009) 1–18.
8. *Arag 'on A.M., Wayer J.K., Geubelle P.H., Goldberg D.E., White S.R.* Design of microvascular flow networks using multi-objective genetic algorithms// *Comput. Methods Appl. Mech. Eng.* 197 (2008) 4399-410.
9. *Hansen C.J., Wu W., Toohey K.S., Sottos N.R., White S.R., Lewis J.A.* Self-healing materials with interpenetrating microvascular networks// *Adv. Mater.* 21 (2009) 4143–47.
10. *Tuncaboylu D.C., Sari M., Oppermann W., Okay O.* Tough and self-healing hydrogels formed via hydrophobic interactions// *Macromolecules* 44 (2011) 4997-5005.
11. *Lv L.-P., Zhao Y., Vilbrandt N., Gallei M., Vimalanandan A., Rohwerder M., Landfester K., Crespy D.* Redox responsive release of hydrophobic self-healing agents from polyaniline capsules. *J. Am. Chem. Soc.* 135 (2013) 14198-205.
12. *Zhang Z.P., Rong M.Z., Zhang M.Q., Yuan C.E.* Alkoxyamine with reduced homolysis temperature and its application in repeated autonomous self-healing of stiff polymers// *Polymer Chemistry* 4 (2013) 4648-54.
13. *Liu Y.-L., Chuo T.-W.* Self-healing polymers based on thermally reversible Diels–Alder chemistry// *Polymer Chemistry* 4 (2013) 2194-205.
14. *Oehlenschlaeger K.K., Mueller J.O., Josef Brandt, Hilf S., Lederer A., Wilhelm M., Graf R., Coote M.L., Schmidt F.G., Barner-Kowolli C.* Adaptable hetero Diels–Alder networks for fast self-healing under mild conditions// *Adv. Mater.* 26 (2014) 3561-6.

## NEW POLYURETHANE ACRYLATE/ORGANOCLAY NANOCOMPOSITES

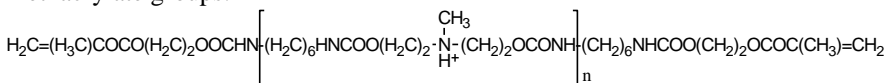
**A. N. Gonchar, Yu. V. Savelyev, T.V. Travinskaya**

*Institute of Macromolecular Chemistry, Natl. Acad. of Sci. of Ukraine.  
Kharkovskoe shosse 48, 02160, Kiev, Ukraine.*

[lexgon@ukr.net](mailto:lexgon@ukr.net)

An actual trend in the field of surface modification is the creating of new nanofillers for improvement strength and barrier properties of based materials. Natural inorganic structures such as montmorillonite (MMT) are commonly used to produce polymer nanocomposites. Surface modification of MMT nanoparticles by chemical adsorption of organic cations has opened the opportunities for compatibility of silicate nanoparticles with polymer.

In order to create polymer nanocomposites with high performance properties on the basis of polyurethane acrylates the method of montmorillonite modification with a new modifier oligourethane methacrylate ammonium chloride (OUMAAC) has been developed. Synthesized new modifier comprises both urethane and reactive methacrylate groups.



$n=1,8$

Intercalation of modifier into the interlayer space of MMT was confirmed by X-ray analysis; the content of organic component in the MMT modified with OUMAAC (MMT/M) was determined by thermogravimetric analysis. The new modifier – OUMAAC provides high affinity of MMT/M with polymer matrix due to the possibility of physical and chemical bonds formation. The physic-mechanical tests of the polymer nanocomposite with MMT/M concentration of about 3% have shown the strength increase in almost 3 times as compared to polyurethane acrylate matrix. Study of vapor permeability and water absorption of nanocomposites based on polyurethane acrylate and MMT modified with OUMAAC has shown the improved in 2.23 times gas barrier properties as compared to the original matrix.

New method of MMT modification is universal and can be applied to MMT of various origins (deposits).

## **NANOSTRUCTURED ORGANIC-INORGANIC COMPOSITES WITH INCREASED ADHESION**

**L.A.Gorbach, O.O.Brovko, O.D.Lutsyk, M.G.Tkalich**

<sup>1</sup>*Institute of Macromolecular Chemistry, National Academy of Sciences of Ukraine,  
48 Kharkivs'ke shose, 02160 Kyiv, Ukraine*  
[gorbachla@bigmir.net](mailto:gorbachla@bigmir.net)

Today nanostructured organic-inorganic (NOI) composites attracted a great attention of scientists, researchers, first of all as the basis for the creation of new structural materials with unique properties which may be used in modern technology, especially aviation, space rocket, as well as mass media devices.

The formulation and technology of obtaining of nanostructured adhesives based on of epoxy resins and methacrylic oligomers with the use of interpenetrating polymer networks (IPN) method has been developed. Silanes with epoxy and amino groups were served as silicon comprising derivative.

A series of simultaneous IPN with different components' ratio and silicon comprising derivative have been obtained. For comparison the NOI IPN both with silicon comprising component and without it has been synthesized.

Viscoelastic properties of simultaneous NOI IPN based on epoxide, dimethacrylate and functionalized tetrametoxysilane with different components' ratio and silicon comprising derivative have been studied using dynamic mechanical analyzer TA Instruments Q800 in the temperature range of -100 to 250 °C with the heating rate of 3<sup>o</sup> / min, at a frequency of 10 Hz in the stretching mode.

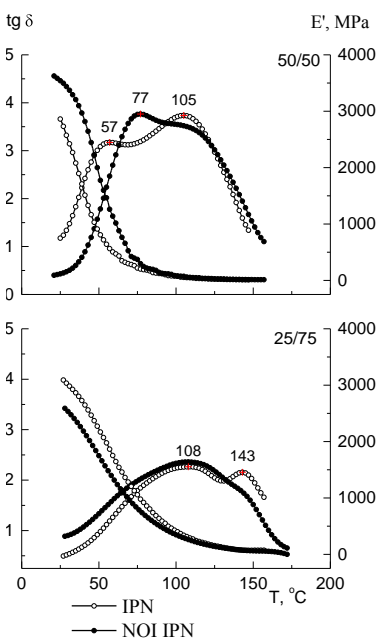
It has been shown that for NOI IPN with the built-in into the epoxy network's structure of silicon comprising component, regardless of a composition the closeness of glass transition temperatures of acrylate and epoxy networks has been observed. That suggests the reduction of microphase separation in the system.

The character of elastic modulus of and loss tangent of epoxy and acrylate networks are essentially differed; both networks have their fixed glass transition temperatures. It should be noted the gradual reduction of elastic modulus of acrylate network that accompanies its transition from glassy to the viscoelastic state in a wide temperature range from 100 to 250°C. Contrary, the sharp reduction of elastic modulus in the temperature range of 50 to 100°C has been observed for epoxy networks in the transition region. The intensity of epoxide transition

calculated in accordance with loss tangent, is in ten times higher than that of acrylate network. The calculated  $M_c$  values amount 400 and 286 for epoxy and acrylate networks, correspondingly.

The increase of elastic modulus in the temperature range corresponding to the glassy state of the system has occurred for the IPN with the component ratio of 50/50.

Silicon comprising fragments (as structural epoxy modifiers) significantly influence on NOI IPN microphase structure, namely promote the reduction of microphase separation and result in obtaining compositions with a high modulus of elasticity. Introduction of silicon comprising compounds into the polymer part of NOI IPN essentially improve their adhesion properties. The strength of adhesive line was tested on steel mushrooms, when gluing carbon fiber with titanium foil.



The obtained dependence has an extreme character. The maximal value (50 MPa) has the NOI IPN containing 1 wt% of silicon component.

It has been proved that the adhesive strength of NOI IPN modified with silanes with amino group increases significantly and substantially higher than that of modified with silane with epoxy group. The modification of epoxy adhesive materials with silane comprising compounds on micro- and macro- levels can improve the technical adhesive properties both when gluing a metals (steel, aluminum alloys, titanium, etc.) and other materials of different nature (fiberglass and carbon plastics).

The use of new environmentally friendly technologies will significantly reduce or completely eliminate the use of toxic solvents and hardener. This in turn will contribute to reduce the cost of

adhesive systems. Domestic polymer materials can compete with well-known foreign companies.

## PRODUCING OF POLYMERIC MATERIALS BASED ON REACTIVE FUNCTIONAL OLIGOMERS

**N.V. Gudzenko, A.S. Bubnova, A.V. Barantsova, N.A. Busko,  
V.K. Grishchenko**

*Institute of Macromolecular Chemistry of National Academy of Sciences of  
Ukraine, 48 Kharkivske shausse, Kyiv 02160, Ukraine*

At present, significant progress has been research on the synthesis of polymeric materials based on reactive oligomers with terminal functional groups. The changing nature of the functional groups in these oligomers can vary their physicochemical properties and, therefore, extends the possibilities of their use in various industries. Were carried out to develop methods for the synthesis of oligomers with terminal functional groups (amide, hydroxyl, epoxy, urethane, acrylate) [1-3]. As the monomers used isoprene, styrene, acrylate, aliphatic isocyanates and polyols nature. Synthesis oligodiene / oligovinyl with terminal amide and hydroxyl groups were carried out in methanol by free radical polymerization initiation 2.2 azo-bis-isobutiroamide [4]. Product yield was 25-80%, depending on the nature of the initial monomer.

By physical modification of alkyd resins functionalized oligomers of these formulations have been developed polymeric film-forming materials (PPM). It is proved that the increase in rates of adhesion and impact strength with the introduction of the MRP is 3-5% (by weight) of modifying-oligomers in the alkyd resin.

Products based on them are characterized by adhesion to the surfaces of various materials, high dielectric properties, hardness and resistance to corrosion and water, as well as a sharp change in temperature. Also, was a conducted study on the synthesis and modification of photopolymeric composite materials for protective decorative coatings, informational images in printing and microelectronics. As part of this work, was carried out research to develop of methods for producing photosensitive composite materials based on oligouretanacrylate / oligoetheracrylate oligomers (photofragment initiators). The synthesis of aliphatic oligoetheracrylate oligomers was conducted by reactions between isophorone diisocyanate, trimethylolpropane, and monometacrylate ether glycol, with specific working parameters and process conditions. The modifier based on organosilicon oligomers was designed, which improves the protective properties of polymeric materials [5].

P18

Have been received modified polymeric film-forming alkyd materials with high protective properties by interaction alkyd resin (varnish PF-060) and synthesized functional oligomers with amide groups. It is proved, that at presence in structure alkyd 5 % oligomers result in substantial increase of parameters of durability at impact, elasticity and adhesion to a metal surface.

**Table. 1.** Comparative physicochemical parameters of the synthesized polymeric film-forming material and industrial analogue PF-060

Parameter	Industrial analogues PF-060	Polymeric film-forming materials
Drying time of film to degree 3, at 20+5 °C, hour	27	24
Hardness, point	0.38	0.43
Adhesion, (Method of trellised cuts), point	2	1
Shock strength, κGs	20	50
Elasticity, mm	1	1
Tg, °C	18.94	13.30
ΔCp, Jg/K*grad	0.270	0.296

It was determined that obtained materials are significantly better than industrial analogues by their physical chemical and protective properties, especially anticorrosion stability. So, these materials can be recommended for using as protective coatings for energy and chemical equipment, autoindustries and the objects of domestic facilities.

The photopolymer compositions consist of oligomers: oligourethanacrylate OUA-ISF, oligoetheracrylate TGM-3 (active solvent) and photoinitiator mixture Darocur 1173 and Lucirin TPO-L, also aminoglycidylmethacrylate. Elasticity (mm) is estimated by method of bending coatings around of metal cylinders of different diameters. Conditional hardness of coatings is determined by the method using standard of pencils of varying hardness, with control resistance of surface to scratching (method complies with DIN, Germany). Adhesion was assessed in points per GOST 15140 method lattice cuts (1 point corresponds to the high of adhesion strength, 2.3 points - decreasing adhesion, 4 points – low adhesion with the complete destruction of the coating).

In Table 2 are shown the effect of modifier based on silicon-organic oligomers on physical and mechanical properties of the compositions and coatings.

**Table 2.** - Effect of modifier on the properties of the material

Amount MD, mas. %	Exponenti al,sec.	Hardness, point	Elasticity, mm	Adhesion, point
0	5	13	3	3
3	5	13	2	1
5	5	15	1	1
7	5	15	1	1
10	15	12	3	2
15	30	9	5	2

According to the research the optimal number of silicon-organic oligomer in the FPC is 5-7 wt. %. Increasing modifier content leads to deterioration of material properties - increasing exposure time, reducing of the hardness and elasticity of the polymer film, a violation of adhesion strength. Such changes are caused the structural transformations of the polymer network and increasing degree of heterogeneity.

Thus, the inclusion in the base polymer matrix a structural fragment of functional oligomers (various amounts) forms systems with new desired properties. Found a significant increase in sensitivity of the compositions, degree of the structure-forming (estimated by determining the hardness), a significant improvement in adhesion to the base of the application layer. This allows you to create new composite materials with controllable properties and to extend the capabilities of these materials for application in instrument manufacture, microelectronics as a protective coating of printed circuit boards and chips in the printing industry in the manufacture of label production, packaging, securities.

1. *B. Pabin-Szafko, E. Wisniewska, Z. Czech* Selected radical azoinitiators in the synthesis of solvent-borne acrylic pressure-sensitive // *Adhesives.-Chemistry & Chemical Technology*. 3 №.2 (2009).
2. *B. Yameen, M. Ali, M. Alvarez, R. Neumann, W. Ensinger, W. Knoll and O. Azzaroni* A facile route for the preparation of azide-terminated polymers. "Clicking" polyelectrolyte brushes on planar surfaces and nanochannels // *Polym. Chem.* 1 (2010) 183–192.
3. Synthesis of telechelics with furanyl end-groups by radical polymerisation with azo-initiators and network formation with unsaturated polyesters via *Diels-Alder additions* *Dirk Edelmann, Helmut Ritter* // *Makromolekulare Chemie*. 194 (1993) 1183–1195.
4. Патент на корисну модель UA 47180 U МПК(2009) C07CF 25.01.2010, Бюл.№2 Амід 2,2'-азо-біс-ізомаляної кислоти як ініціатор радикальної полімеризації дієнових і вінілових мономерів // *Грищенко В. К., Гудзенко Н. В., Баранцова А.В., Бусько Н. А.*

5. *Hiroshi Morita*. The Photopolymer Science and Technology Award //  
Journal of Photopolymer Science and Technology. 14 №.1 (2001) 3-5.

## REACTIVE PROTIC OLIGOMERIC IONIC LIQUIDS

**M.A. Gumenna, A.V. Strytsky, N.S. Klymenko, S.I. Lobok, S.M. Ostapyuk,  
A.A. Fomenko, V.V. Klepko, V.V. Davydenko, V.V. Shevchenko**

*Institute of Macromolecular Chemistry of National Academy of Sciences of  
Ukraine, 48 Kharkivske shausse, Kyiv 02160, Ukraine*

[Mary-G@ukr.net](mailto:Mary-G@ukr.net)

Oligomeric ionic liquids (OILs) can be considered as an individual type of ionic liquids (ILs) that combine the properties of ionic liquids with the classic features of the oligomeric state of matter. The unique properties of these compounds are defined by the ability to self-organization, the vast possibilities of varying molecular architecture and the great influence of nature of terminal groups on their properties. Similarly to traditional ILs, OILs can be classified as protic or aprotic; while in analogy to the polymer ILs they can be also divided into anionic or cationic ones. As usual OILs based on oligo(ethylene oxide)s are used as ion-conducting media for lithium power sources. The introduction of reactive groups into OILs opens new possibilities to construction of block polymeric analogs of ionic liquids with the prospect of their practical use in various fields.

The purpose of this research is the synthesis of reactive protic oligomeric ionic liquids - oligo(ethylene oxide)s containing imidazolium terminal groups.

The conditions of the oligomers synthesis were investigated for a model reaction of butyl glycidyl ether with an excess of 1-(3-aminopropyl) imidazole. The two types of basic centers in formed compounds (secondary amine and imidazole) were full or partially (50%) neutralized by the ethanesulfonic acid (Fig.1).

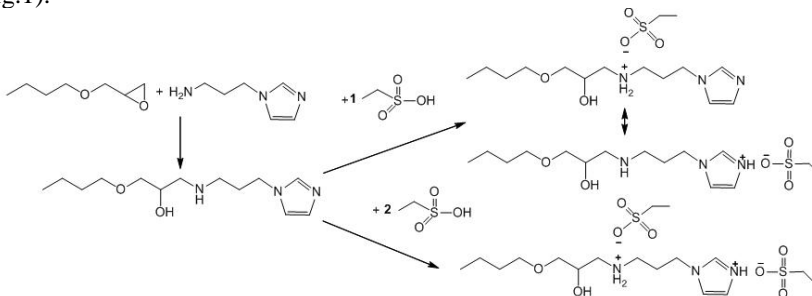


**Fig.1.** Scheme for obtaining the model reactive ionic liquids.

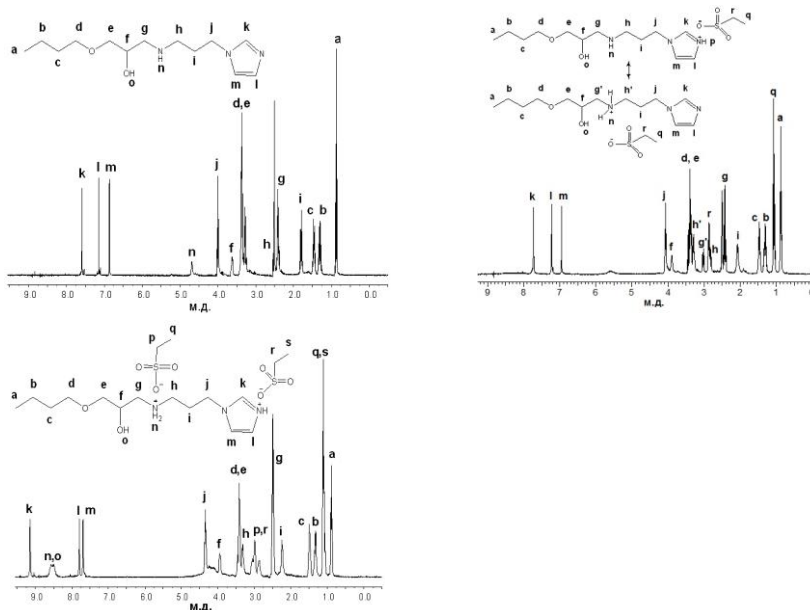


**Fig.2.**  $^1\text{H}$  NMR ( $\text{DMSO} - \text{d}_6$ ) spectra of model reactive ionic liquids.

It was indicated that in case of partial neutralization in the obtained  $^1\text{H}$  NMR spectra (Fig.2) there are the signals typical for compounds containing positive charged imidazolium and quaternary ammonium groups. Furthermore, the spectrum contains a broad peak in the region 5.4-5.8 ppm corresponding to mobile protons involved in rapid exchange between the basic centers in spite of their different strength (pKa of conjugate acid di-n-butyl amine  $\sim 11$ , N-methylimidazole  $\sim 7$ ).

Protic oligomeric reactive ionic liquids were synthesized by the reaction of diglycidyl ether of oligo(ethylene oxide diols) (MM 1000) with a twofold molar excess of 1- (3- aminopropyl) imidazole followed by partial (50 %) and complete neutralization of the basic centers by ethanesulphonic acid (Fig.3). Obtained OIL with hydroxyl groups are viscous liquids, soluble in polar solvents. By the method of  $^1\text{H}$  NMR spectroscopy it was found that the features of neutralization in the preparation of the model ionic liquids and OILs are similar.

P19

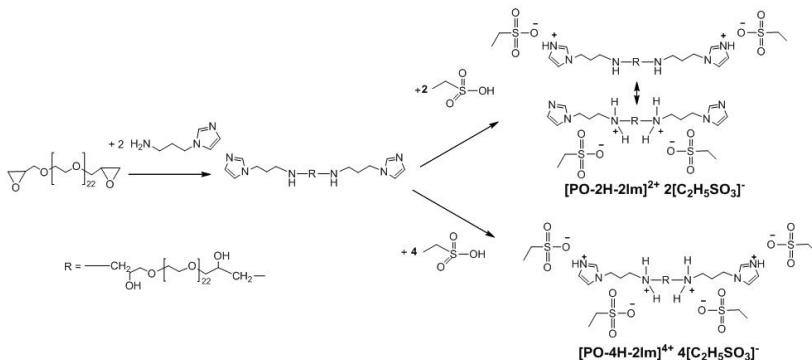


Fig.3. Scheme for obtaining the reactive OILs.

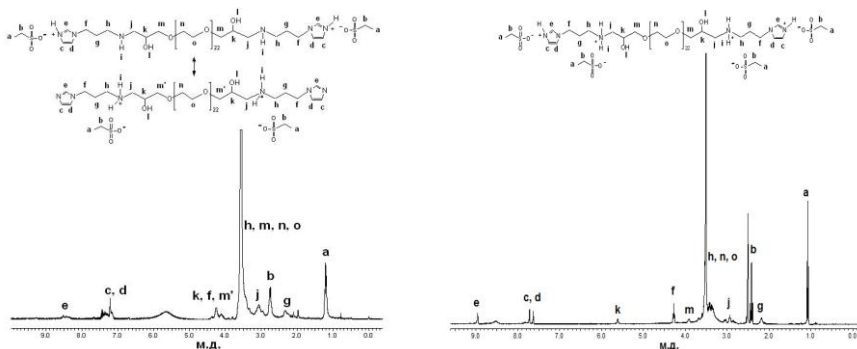


Fig.4. <sup>1</sup>H NMR (DMSO - d<sub>6</sub>) spectra of reactive OILs.

According to DSC (Fig.5), the resulting compounds contain both amorphous (glass transition temperature  $-42 \div -43^\circ\text{C}$ ) and a crystal (melting point  $30-32^\circ\text{C}$ ) phase. They are thermally stable up to  $280^\circ\text{C}$ .

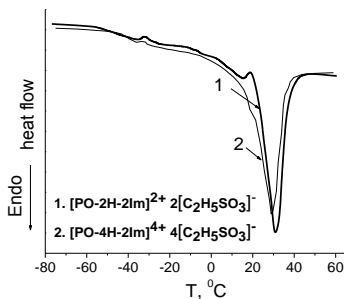
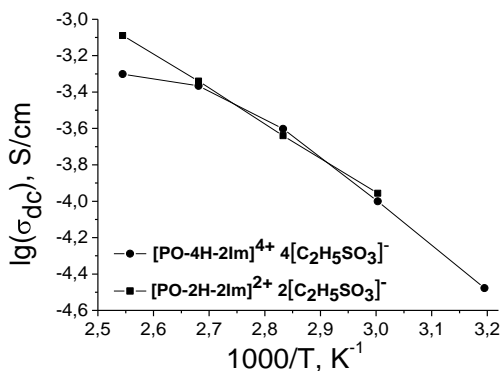


Fig.5. Temperature dependence of heat flow of reactive OILs.

P19

Conductivity of OILs (defined by dielectric relaxation spectroscopy at 40-120 °C under anhydrous conditions) range from  $3,33 \cdot 10^{-5}$  to  $8,14 \cdot 10^{-4}$  S/cm (Fig.6). These compounds are characterized by similar values of conductivity in spite of different content of ionic groups. Apparently, this is explained by the contribution of the rapid exchange of mobile protons between the basic centers to conductivity of the ionic liquid containing 50% cationic groups.



**Fig.6.** Temperature dependence of ion conductivity of reactive OILs.

In this work it were developed the methods of synthesis of low molecular weight cationic proton ionic liquids, as well as oligomeric ionic liquids - oligo(ethylene oxide)s terminated with imidazolium groups which contains basic centres partially (50%) and completely neutralized by ethanesulfonic acid. The compounds were studied by IR and <sup>1</sup>H NMR spectroscopy. The relationship between the degree of neutralization and the level of conductivity of ionic liquids oligomer was established. The synthesized compounds are of interest for use as a polyelectrolyte for fuel cell operated under anhydrous conditions at a temperature above 100 °C.

## CHEMICAL STRUCTURE AND THERMAL PROPERTIES OF ENVIRONMENTALLY FRIENDLY PHB/NR FILM MATERIALS

**K. Gusakova, O. Grigoryeva, O. Starostenko, A. Fainleib**

*Institute of Macromolecular Chemistry of National Academy of Sciences of Ukraine, 48 Kharkivske shose, Kyiv 02160, Ukraine*  
[polymernano@ukr.net](mailto:polymernano@ukr.net)

Nowadays accumulation of millions of tons of non-biodegradable polymer wastes (plastic, rubbers, etc.) causes an irreparable harm to the global ecosystem and environment. Their recycling requires significant investments and elimination by combustion leads to uncontrollable strengthening of greenhouse effect [1]. Microbial polyhydroxybutyrate (PHB) and copolymers thereof representing a family of natural polyesters and combining an excellent antioxidant and optical characteristics with an exhaustive biodegradability under natural environmental conditions is one of the most perspective alternatives [2]. However, a certain rigidity and brittleness of the initial PHB stipulates the necessity of their modification by polymers and/or plasticizers, e.g. natural rubber (NR). Considering the apparent advantages in physical-chemical performances of the vulcanized NR versus uncured analogues, the present study was focused on generation and investigation of environmentally friendly PHB-based film materials reinforced with *in situ* vulcanized NR.

PHB/NR<sub>DCP</sub> film samples (thickness up to 300  $\mu\text{m}$ ) comprising 10-30 wt.% NR have been synthesized. Poly-3-hydroxybutyrate, PHB, was purchased from "Biomer" (Germany). Natural rubber, NR, with molecular weight of  $M_n \sim 1,0 \times 10^6$  was kindly supplied by "Brasilstex Industria e Comercio Borrachas Ltd" (Brazil). Dicumylperoxide (DCP) and chloroform were from "Sigma-Aldrich". PHB/NR blends (in different ratio) were prepared by mixing of 5% solutions of PHB and NR in chloroform. After that, 1.5 phr of DCP as a vulcanizing agent was added. The gradual removal of the solvent was reached through subsequent heating of the resulting solution from 100 to 170°C for  $\sim 45$  min. Finally, an isothermal curing at  $T = 170^\circ\text{C}$  for 30 min was fulfilled. The resulting PHB/NR<sub>DCP</sub> composition was cooled up to room temperature. In sake of comparison the samples of individual PHB and NR film materials comprising 1.5 wt.% of DCP were also prepared at the same curing conditions.

Fourier transform IR (FTIR) spectra were recorded on a Bruker Tensor 37 DTGS spectrometer between 4000 and 700  $\text{cm}^{-1}$ . Thermal properties of the all samples obtained were investigated via Differential Scanning Calorimetry (DSC) measurements performed by using "TA Instruments DSC Q2000" through a single heating from -80 to 250°C at 20°C  $\text{min}^{-1}$ . Glass transition and melting temperatures were calculated by using TA Universal Analysis v.4.5 software.

The comparative analysis of the FTIR data for PHB film materials before and after treatment (PHB and PHB<sub>DCP</sub> samples, respectively) has shown the distinct changes in intensities and shapes of the main characteristic absorption bands corresponding to C-H stretching (at  $\sim 3150\text{-}2800 \text{ cm}^{-1}$ ) and to C=O stretching (at  $\sim 1780\text{-}1600 \text{ cm}^{-1}$ ) together with C–O–C asymmetric (at  $\sim 1320\text{-}1200 \text{ cm}^{-1}$ ) vibrations reflecting the rearrangement of crystalline and amorphous microphases in the PHB<sub>DCP</sub> sample. The calculations of the crystallinity indices according to [3] allowed concluding a significant reduction of the crystallinity degree of the treated PHB matrix due to the interaction between PHB and DCP free radicals formed via thermal decomposition of peroxide. According to [3] an assumption of generation of branched and/or cross-linked PHB fragments was also made.

The FTIR results for the initial and treated NR film samples have indicated of at least partial NR vulcanization resulting in generation of the cross-linked NR structure with preferably saturated bonds. The confirmation was found from a certain shift of the maximum corresponding to stretching vibrations of –C=C– groups (in frequency range from 1600 to 1700  $\text{cm}^{-1}$ ) to higher wavenumbers with significant increase in the intensity of absorption bands with maxima at 1126 and 1037  $\text{cm}^{-1}$  corresponding to C–C stretching. Noteworthy evidence was also noticed in the manifestative disappearance of the peak at 804  $\text{cm}^{-1}$  indicating the out-of-plane vibrations of CH double bonds conjugated with diene C=C groups.

The FTIR spectra of the PHB/NR<sub>DCP</sub> compositions represented itself as cumulative chemical structures of both the individual PHB<sub>DCP</sub> and NR<sub>DCP</sub> samples (Fig.1). The increase of the initial NR content caused the growth of the intensity of stretching and deformation vibrations of C-H bonds (at around  $\sim 2800\text{-}3060 \text{ cm}^{-1}$ ,  $\sim 1500\text{-}1340 \text{ cm}^{-1}$  and  $\sim 900\text{-}750 \text{ cm}^{-1}$ ). Along with that, obvious variations were observed in shape and intensity of the absorption bands corresponding to the characteristic C=O stretching (sharp maxima at 1718-1740  $\text{cm}^{-1}$ ) and C-O-C groups (doublet with maxima at  $\sim 1275\text{-}1260 \text{ cm}^{-1}$ ) vibrations reflecting the redistribution between the amorphous and the crystalline microphases of PHB matrix along with formation of the vulcanized NR in all the samples investigated.

To confirm the conclusions made and to determine thermal properties of the PHB/NR<sub>DCP</sub> film materials obtained depending on the composition, the DSC investigations were carried out (Fig.2). The DSC analysis have shown the presence of endothermic transition in temperature range around  $T \sim 0\text{-}10 \text{ }^\circ\text{C}$  associated with devitrification of PHB macromolecules for all the investigated PHB-containing

P20

samples. However, the values of glass transition temperature,  $T_g$ , increased from  $\sim 3,3$  °C for the neat PHB sample up to  $\sim 4,5$  °C for the PHB<sub>DCP</sub> sample. Thus, the formation of at least partially cross-linked PHB matrix can be concluded.

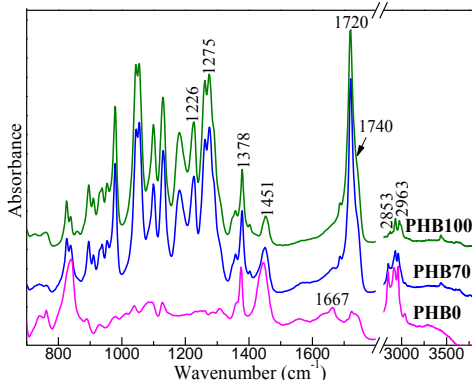


Fig. 1. Typical FTIR spectra of the samples studied.

Moreover, several additional endo- and exothermic transitions at  $T \sim 107$ - $167$  °C associated with thermal decomposition of unreacted DCP and possible partial branching of PHB macromolecules were also observed for all the PHB<sub>DCP</sub>-based compositions. As a result, the melting temperature,  $T_m$ , decreased from  $177,9$  °C for the non-treated PHB film to  $173,6$  °C for the PHB<sub>DCP</sub> sample. Additionally, the reduction of enthalpy of fusion,  $\Delta H_m$ , on the DSC thermogram of the latter was

also established. Thus, one can suppose the formation of disordered crystalline microphases with lower crystallinity degree due to partial cross-linking and/or branching of PHB macromolecules.

The DSC thermograms of the individual initial and vulcanized NR in temperature range from  $-70$  to  $-40$  °C have shown a slight shift of the  $T_g$  value from  $-62$  °C for the neat NR to  $-65$  °C for the NR<sub>DCP</sub> sample. Moreover, the occurrence of additional glass transition process with maximum at  $T_{g2} \approx -48$  °C in the latter was also observed. One can suggest the formation of chemically cross-linked macromolecular fragments possessing additional glass transition ( $T_{g2}$ ) at higher temperature after peroxide vulcanization.

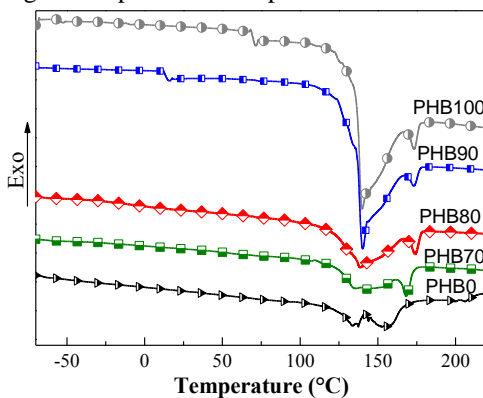


Fig.2. DSC thermograms of PHB/NR<sub>DCP</sub> samples investigated.

DSC investigations of thermal properties of PHB/NR<sub>DCP</sub> samples have also shown the occurrence of several partially overlapping endo/exothermic transitions in the temperature range from  $\sim 110$  to  $175$  °C that could be attributed to possible branching of PHB macromolecules and decomposition of unreacted DCP with the appearance of free cumyloxy-radicals as well as to the post-vulcanization of NR component during DSC measurements (Fig. 2) [4]. It was also found that

crystallization of PHB-matrix was not impeded by post-vulcanization process of NR due to improving in microphase separation between crystalline and amorphous microphases in the samples. However, the increase of initial NR content in the PHB/NR<sub>DCP</sub> compositions promoted decreasing  $T_m$  values from  $\approx 174$  °C (for the PHB-based samples containing 10 and 20 wt.% of NR) to  $T_m \approx 169$  °C (for PHB/NR<sub>DCP</sub> = 70/30 wt.%), indicating disordering crystalline PHB microphase and, generation of more defective and smaller crystallites in the PHB matrix due to partial crosslinking (or branching) of PHB macromolecules caused by their chemical interactions with DCP radicals. Noteworthy that significant inhibition of segmental mobility of macromolecules in glass transition regions of both the NR and PHB components was also noticed. This is explained by the partial crosslinking and/or branching of PHB and NR including possible intercrosslinking with formation of PHB/NR co-network.

1. *Nkwachukwu O. I., Chima C. H., Ikenna A. O., Albert L.* Focus on potential environmental issues on plastic world towards a sustainable plastic recycling in developing countries // *Int J Industrial Chem* 4 (2013) 34-47.
2. *Bugnicourt E., Cinelli P., Lazzeri A., Alvarez V.* Polyhydroxyalkanoate (PHA): Review of synthesis, characteristics, processing and potential applications in packaging // *eXPRESS Polym Lett* 8 (2014) 791-808.
3. *Wei L., McDonald A.G.* Peroxide induced cross-linking by reactive melt processing of two biopolyesters: poly(3-hydroxybutyrate) and poly(L-lactic acid) to improve their melting processability // *J Appl Polym Sci* (2015) app. 41724.
4. *Kruželák J., Sýkora R., Hudec I.* Peroxide vulcanization of natural rubber. Part I: effect of temperature and peroxide concentration // *J Polym Eng* 34 (2014) 617-624.

## EFFECT OF NANOCCLAY MODIFICATION ON STRUCTURE AND THERMAL PROPERTIES OF NANOCOMPOSITES BASED ON CYANATE ESTER RESINS

**K. Gusakova<sup>1</sup>, A. Fainleib<sup>1</sup>, N. Lavrenyuk<sup>1</sup>, D. Timpu<sup>2</sup>**

<sup>1</sup>*Institute of Macromolecular Chemistry of National Academy of Sciences of Ukraine, 48 Kharkivske shose, Kyiv 02160, Ukraine*  
[polymernano@ukr.net](mailto:polymernano@ukr.net)

<sup>2</sup>*“Petru Poni” Institute of Macromolecular Chemistry, 41A Grigore Ghica Voda Alley, Iasi 700487, Romania*

High-performance Cyanate Ester Resins (CER) represent a family of thermosetting polymers possessing excellent thermal and chemical stability combined with high adhesion, remarkable optical and dielectric characteristics etc. Obvious disadvantage of high-densely crosslinked CERs appears in a certain brittleness materials thereof [1]. As known, the improvement of mechanical properties while maintaining CER intrinsic characteristics can be achieved through the creation of CER-based nanocomposites comprising layered silicates. At that either intercalated and/or exfoliated structure of the CER nanocomposite is generated [2]. The better results are reached when organo-modified nanofillers are used. Recently [3, 4] we have investigated chemical structure of CER nanocomposites filled with different amino-modified montmorillonites using FTIR spectroscopy technique. The occurrence of chemical interaction between the amino-groups of the functionalized clay with the reactive OCN groups of the CER monomer resulting in acceleration of CER network formation and chemical grafting of the reactive nanofiller to the final CER matrix were established [3, 4].

The present work was focused on the investigation of the effect of different amino-functionalized montmorillonites (amino-MMT) on structural peculiarities and thermal behavior of the CER-based nanocomposites.

1,1'-bis(4-cyanatophenyl) ethane under the trade name Primaset LECy from “Lonza” (Switzerland) as CER monomer was used. Three types of commercially available amino-modified nanoclays under trade name Nanomer® I.28E, I.30E and I.31PS from Nanocor® Inc. as nanofillers were applied. Synthesis of the nanocomposites was fulfilled by dispersing 5 wt % of nanofiller in liquid CER monomer using magnetic stirrer with stirring rate ~ 1300 rpm at 165°C for 30-95 min (depending on the clay used) followed by thermal curing of CER monomer/nanoclay compositions as follows: 150°C – 5h, 180°C – 3h, 210°C – 1h.

X-Ray Diffraction (XRD) measurements were performed on a Diffractometer Bruker D8 ADVANCE using Bragg-Brentano parafocusing goniometer, in the range of diffraction angles  $2\theta$  from  $0.7^\circ$  to  $40^\circ$  with a step size of  $0.01^\circ$  at a room temperature. Scans were recorded in step mode by using the Ni-filtered Cu-K $\alpha$  radiation (wavelength  $\lambda = 0.1541$  nm). The working conditions were 36 kV and 30 mA tube power.

DSC measurements were carried out with a TA Instruments DSC Q2000 calorimeter under nitrogen atmosphere. Samples with masses of  $\sim 10$  mg were first heated from 40 to  $300^\circ\text{C}$ , and cooled back. A second scan was performed under the same conditions. The main glass transition characteristics were measured in a second run and calculated using TA Universal Analysis v.4.5 software.

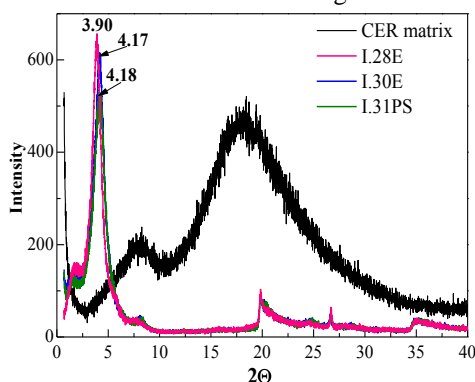


**Fig.1.** XRD patterns for the neat CER matrix and the nanoclays under investigation.

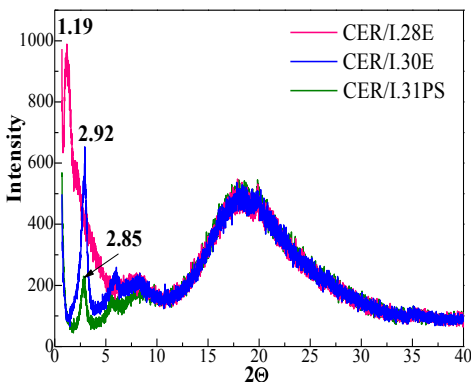
from  $\sim 2.11$ - $2.12$  for I.31PS and I.30E samples, respectively, to  $\sim 2.26$  nm for I.28E nanoclay. Thus, the interlayer spacing strongly depended on the type of the amino-modifier used as expected. Along with that, the I.28E sample was also characterized by the peak of the highest intensity whereas the I.31PS clay possessed the lowest reflection.

Figure 2 represents the XRD patterns for the CER/amino-clay nanocomposites synthesized. Comparative analysis of the XRD data obtained for the CER/amino-clay nanocomposites and for the individual components has shown decreasing intensity of the nanoclay diffraction peak along with significant shift of the maxima to lower  $2\theta$  values depending on the amino-modified nanofiller used.

The smallest shift of diffraction peak from  $2\theta = 4.17^\circ$  (the for the initial I.30E) to  $2\theta = 2.92^\circ$  (for the nanocomposite) was established for the CER/I.30E sample. Therefore, the increase of interlayer spacing from  $\sim 2.12$  nm (for the initial nanoclay) to  $\sim 3.03$  nm (for the nanocomposite) can be concluded. The CER/I.31PS nanocomposite was characterized by higher final value of interlayer spacing at  $2\theta \approx 2.85^\circ$  ( $\sim 3.09$  nm). The largest shift of diffraction angle

XRD pattern of the neat CER matrix (Fig.1) have shown the presence of amorphous halo with two maxima at around  $2\theta \approx 8.03^\circ$  and  $2\theta \approx 18.20^\circ$ . In turn, for the highly crystalline nanoclays studied, strong diffraction peaks at  $2\theta = 3.90^\circ$  (for I.28E),  $2\theta = 4.17^\circ$  (for I.30E) and  $2\theta = 4.18^\circ$  (for I.31PS) corresponding to the diffraction of atomic layers of the crystal lattices were noticed (Fig.1). According to the Bragg's law, the interlayer spacing in the initial nanoclays investigated was varied

( $\Delta 2\theta \approx 2.71^\circ$ ) as compared to the initial nanoclay was observed for the CER/I.28E nanocomposite indicating the extension of the distance between the layers from



**Fig.2.** XRD patterns for the CER/nanoclay nanocomposites synthesized. Amount of nanofiller was 5 wt.%

2.26 to 7.42 nm.

Therefore one can conclude that in all the cases at least intercalated structure was formed. However, the intercalation degree in the CER/I.28E nanocomposite was found to be the highest whereas penetration of CER into the galleries of I.30E was the lowest among all the CER nanocomposites studied. This fact can be explained by the different amount of the reactive groups of the clay modifier and their reactivity toward the cyanate groups of the CER matrix.

Recently [4] we have shown that chemical grafting of amino-MMT to CER network improves dispersing nanofiller in the matrix. Moreover, comparing the intensity of the peaks corresponding to the nanoclay galleries in all the nanocomposites studied, one can assume the occurrence of partial exfoliation. At that, the exfoliation degree seems to be the highest in the case of CER/I.31PS and CER/I.28E nanocomposites whereas I.30E was worse distributed in the matrix.

The effect of the nanoclay modifier used and the structural characteristics of the CER-based nanocomposites produced on thermal properties of the latters were evaluated by means of DSC technique. The results are summarized in Table 1.

**Table 1.** Thermal properties of the CER-based samples under investigation

Sample	$T_{g \text{ onset}}$ (°C)	$T_{g \text{ end}}$ (°C)	$\Delta T_g$ (°C)	$T_g$ (°C)	$\Delta C_p$ ( $J g^{-1} \text{ } ^\circ C^{-1}$ )
CER	211	230	19	221	0,138
CER/I.28E	226	262	36	246	0,318
CER/I.30E	215	238	23	226	0,280
CER/I.31PS	204	236	32	223	0,292

One can see that the presence of the nanoclays in the CER matrix results in improvement of the main thermal properties of the nanocomposites investigated regardless the modifier used. However, the growth of the values of glass transition temperature interval ( $\Delta T_g$ ) and heat capacity jump ( $\Delta C_p$ ) in all the cases allows concluding generation of a nanoheterogeneous structure in the composites as

compared to the individual CER matrix. At that, the heterogeneity degree strongly depended on the type of nanoclay modifier used. The largest differences in  $\Delta T_g$  and  $\Delta C_p$  values as compared to the neat CER were found for the CER/I.28E nanocomposite, whereas the lowest ones were established for CER/I.30E sample (see Table 1). Noteworthy, that glass transition process in the CER/I.31PS nanocomposite occurred at the lowest temperature of glass transition onset  $T_{g \text{ onset}} \approx 204$  °C that was even lower by  $\sim 6^\circ\text{C}$  than that for the neat CER matrix. It can be explained by formation of the defected CER matrix at using this nanofiller due to character and intensity of the chemical interaction between the components.

Thus, the chemical dispersing of amino-functionalized MMT in the CER matrix is effective and both the chemical grafting of the modifier into the CER network structure and the nanoheterogeneity appeared provide improvement of thermal behavior of CER/nanoclay nanocomposites obtained depending on amount and reactivity of the amino groups of the nanoclay modifier used.

1. Chemistry and technology of cyanate ester resins / [ed. I. Hamerton] – Glasgow : Chapman & Hall, 1994. – 359 p.
2. Ganguli S, Dean D, Jordan K, Price G, Vai R. Mechanical properties of intercalated cyanate ester-layered silicate nanocomposites // Polymer 44 (2003) 1315–19.
3. Gusakova K, Fainleib A, Grigoryeva O, Youssef B, Saiter J-M. Reactive dispersing and catalytic effect of amino-functionalized MMT in cyanate ester resins.[abstract] Rouen Symposium on Advanced Materials, Rouen-France, June 2013, Abstract book, p 49.
4. Bershtein V, Fainleib A, Egorova L, Gusakova K, Grigoryeva O, Kirilenko D, Konnikov S, Ryzhov V, Yakushev P and Lavrenyuk N. The impact of ultra-low amounts of amino-modified MMT on dynamics and properties of densely cross-linked cyanate ester resins // Nanoscale Res Lett 10 (2015) 165.

## THE INFLUENCE OF FULLERENE CONCENTRATION ON MORPHOLOGY AND OPTICAL PROPERTIES OF P3HT/PCBM THIN FILMS

**B. Hajduk, J. Jurusik, H. Bednarski, B. Jarzabek**

*Centre of Polymer and Carbon Materials of the Polish Academy of Sciences*

In this work we have investigated the optical properties and morphology of P3HT/PCBM thin films [1,2]. The films were deposited onto quartz substrates and studied with the spectroscopic ellipsometer working in transmission mode and with the atomic force microscope. The P3HT (poly (3-hexylthiophene) and PCBM (phenyl-C61-butyric acid methyl ester) were used in different weight portions and the solution percentage concentration in chlorobenzene was constant.

The determined value of the surface roughness coefficients for pure P3HT thin film was relatively large (12.96) and significantly lower for pure PCBM (0.90). Whereas, the roughness coefficients obtained for P3HT/PCBM thin films were in the narrow range (0.71 to 1.96) depending on the P3HT/PCBM percent ratio.

The optical transmission spectra measured on prepared films were converted to absorption. The absorption spectrum of pure P3HT thin film showed one strong absorption band with the maximum placed at about 2.25 eV, while in the spectrum of pure PCBM one can observe two strong bands with the maxima placed at about 3.6 and 4.4 eV. All these bands are visible in absorption spectra of P3HT-PCBM thin films. Moreover, the intensities of these bands are strongly dependent on percentage concentration of the P3HT/PCBM thin films. Additionally, the refractive index and the extinction coefficients of all of the studied samples were determined and correlated with the thin films composition.

1. *Chetan Kamble, D.R. Mehta* Organic Solar Technique using P3HT and PCBM as Promising Materials // International Journal of Engineering Research and Applications 3/1 (2013) 2024-2028
2. *Balderrama V.S., Estrada M., Cerdeira A., Soto-Cruz B.S., Marsal L.F., Pallares J., Nolasco J.C., Iniguez B., Palomares E., Albero J.* Influence of P3HT:PCBM blend preparation on the active layer morphology and cell degradation // Microelectronics Reliability 51 (2011) 597-601

(\* This work has been supported by the NCN grant (Poland) No. UMO-2013/09/B/ST8/01629.

## THE SPECTROSCOPIC ELLIPSOMETRY STUDY OF THIN FILMS OF POLYAZOMETHINE WITH OXYGEN

B. Hajduk<sup>a</sup>, H. Bednarski<sup>a</sup>, B. Jarzabek<sup>a</sup>, S. Kotowicz<sup>a</sup>, V. Cozan<sup>b</sup>, M. Bruma<sup>b</sup>

<sup>a</sup> Centre of Polymer and Carbon Materials of the Polish Academy of Sciences, 34 Marie Curie-Skłodowska str, 41-819 Zabrze, Poland

<sup>b</sup> Institute of Macromolecular Chemistry "Petru Poni", Aleea Grigore Ghica Voda, No. 41A, 700487 Iasi, Romania

In this work we have presented the properties of poly(1-(4-methylenephenoxy-1)phenylene-4-methylene-1,4-phenylnitrylomethylene) [1] PPI2 thin films using the spectroscopic ellipsometry. Thin films were deposited onto microscopic glass substrates via low-temperature chemical vapour deposition (LCVD) by polycondensation of monomers. The paraphenylenediamine (PPDA) was purchased from SIGMA-Aldrich and the 4,4'-oxydibenzaldehyde (PPDA) was synthesized in the Institute of Macromolecular Chemistry of Romanian Academy of Sciences in Iasi, Romania. The 3D and 2D thickness distribution maps were performed with ellipsometer mapping mode, where the surface was scanned point after point using microspots, where the diameter of every measured point was at about 200 μm. The thickness of every layer was checked in 168 points.

Obtained results showed that thin films are growing in conoidal way and average value of growing rate is included in range 1.4–1.8 nm/s. The theoretical model used for determining the thickness and optical coefficients was considering the glass substrate and polyazomethine layer. The PPI2 polyazomethine layer has been fitted with three Tauc-Lorentz oscillators and the glass substrate has been fitted with Cauchy layer. Obtained results showed that refractive index of polyazomethine is near to 1.6 for 630 nm wavelength and the extinction coefficient is near to 0.05 for the same wavelength.

1. B. Hajduk, J. Wieszka, V. Cozan, B. Kaczmarczyk, B. Jarzabek, M. Domański „Optical properties of polyazomethine with oxygen atom in the backbone”, Archives of Materials Science and Engineering, Vol.32/2 (2008) 85-88.

(\*) This work has been supported by the NCN grant (Poland) No. UMO-2013/09/B/ST8/01629.

## THE IMPACT OF IMMEDIATE ENVIRONMENT ON THE PHOTOPHYSICAL PROPERTIES OF A POLYMER CONTAINING BISPHENOL A AND 1,3,4-OXADIAZOLE MOIETIES

**M. Homocianu, A. Airinei, P.P. Dorneanu, A.M. Ipate, C. Hamciuc**

*“Petru Poni” Institute of Macromolecular Chemistry, 41A Grigore Ghica Voda  
Alley, Iasi 700487, Romania*

[michalupu@yahoo.co.uk](mailto:michalupu@yahoo.co.uk)

The presence of bisphenol A (BPA) in the many consumer products (toys, drinking containers, eye glass lenses, baby bottles and medical equipments etc.) [1], and risk of human exposure to BPA [2], as well as the small number of studies from literature regarding the photophysical behavior of bisphenol A derivatives in different conditions of medium motivated the study performed by the authors of this paper. Other aspects that justify these studies were the presence of some nanoparticles in many food products [3] and the advantage of microheterogeneous environment (a mixture of solvents) to choose the suitable solvents and ratios, thus creating a new system more environmental friendly.

Thus, this article presents the photophysical behavior of a polymer containing bisphenol A and 1,3,4-oxadiazole moieties in different conditions of medium (various pure solvents, microheterogeneous environment (mixture of solvents) and in presence of some metal oxide nanoparticles).

Influence of the medium characteristics on photophysical behavior was examined by multiple parametric regression analysis in terms of solvent parameters of the two new solvent scales (Catalan and Laurence) [4,5]. The polarity parameters of solvents were found as the most important factor determining the photobehavior in ground state, while acidity was found to be the dominant factor for the excited state.

Changes induced in the spectral characteristics of fluorophore molecules were studied in chloroform solution in the presence of various amount of SnO<sub>2</sub> and NiO oxide nanoparticles. The fluorescence band of investigated polymer gradually decreased intensity with increase of both SnO<sub>2</sub> and NiO oxide nanoparticle concentrations. The NiO nanoparticles have a lower quenching efficiency for emission of this compound.

Generally, photophysical properties of fluorescent molecules are affected in a microheterogeneous environment. The binary mixtures of solvents have drawn attention because of their diverse applications, such as cryoprotecting agents and in investigations of the photochemical and biological process. Binary mixtures of methanol and chloroform presents the advantage that it's complete miscibility in all ratios [6]. The emission intensity of studied compound was sensitive to the compositions of the microheterogeneous media (involving different chloroform-methanol ratios). The preferential solvation of studied polymer in chloroform-methanol solvent mixtures indicate that this polymer is preferentially solvated by methanol.

1. *Liao C., Kannan K.* Widespread occurrence of bisphenol A in paper and paper products: Implications for human exposure. *Environ Sci Technol.* 45 (2011) 9372–9379.
2. *Wilson N. K., Chuang J. C., Morgan M. K., Lordo R. A., Sheldon L. S.* An observational study of the potential exposures of preschool children to pentachlorophenol, Bisphenol A, and nonylphenol at home and daycare. *Environ Res.* 103 (2007) 9-20.
3. *Hannon J. C., Kerry J., Cruz-Romero M., Morris M., Cummins E.* Advances and challenges for the use of engineered nanoparticles in food contact materials. *Trends Food Sci Technol.* 43 (2015) 43–62.
4. *Catalan J.,* Toward generalized treatment of the solvent effect based on four empirical scales: dipolarity (SdP, a New Scale), polarizability (SP), acidity (SA), and basicity (SB) of the medium. *J Phys Chem B.* 17 (2009) 5951-5960.
5. *Laurence C., Legros J., Chantzis A., Planchat A., Jacquemin D.* A database of dispersion-induction DI, electrostatic ES, and hydrogen bonding  $\alpha_1$  and  $\beta_1$  solvent parameters and some applications to the multiparameter correlation analysis of solvent effects. *J Phys Chem B.* 119 (2015) 3174–3184.
6. *Gratias R. Kessler H.,* Molecular-dynamics study on microheterogeneity and preferential solvation in methanol chloroform mixtures. *J Phys Chem B.* 102 (1998) 2027–2031.

## POLYSACCHARIDE COMPOSITES FOR FUEL CELL APPLICATION

T. Yemel'yanova<sup>1</sup>, Ie. Lobko<sup>1</sup> M. Vorokhta<sup>2</sup>, A. Hubina<sup>1</sup>

<sup>1</sup> *Institute of Macromolecular Chemistry of National Academy of Sciences of Ukraine, 48 Kharkivske shausse, Kyiv 02160, Ukraine*

[zurako@ukr.net](mailto:zurako@ukr.net)

<sup>2</sup> *Charles University, Surface Physics Group, V Holešovičkách 747/2, CZ-180 00 Praha 8 – Libeň, Praha, Czech Republic*

Proton exchange membrane (PEM) is a principal component in a proton conductive fuel cell. In recent years a diverse number of sulfonated synthetic polymers was developed to serve as PEM. Using the renewable “green” polymers such as polysaccharides as potential base for fuel cell application is one of the prospective trends in current research. To date a number of chitosan and cellulose derivatives are described in literature as prospective materials for PEM. But still the development of new solid and gel electrolytes based on the “green” polymers are of great importance in actual polymer science

This research concerns development of PEM on the base of microbial polysaccharide xanthan. In current research two approaches for introducing PVA into xanthan-PVS composite were used. The conditions for gel formation of xanthan/PVA blends were determined to obtain membrane-like films.

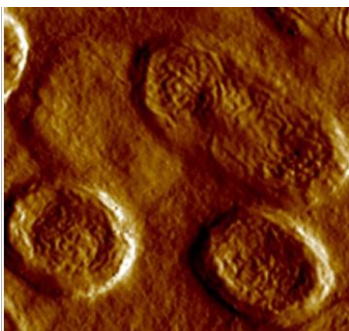


**Fig. 1.** The surface organization of 10:1 xanthan/PVA film.

The optimal conditions for film-casting were achieved for low concentrations of xanthan/PVA blends in ratios 10:1. Obtained films were investigated via SEM, AFM, DSC and used as PEM in Fuel Cell Test Station.

## WELDING AND WELDED JOINTS OF THE HEAT-RESISTANT PLASTICS

**M.V. Iurzenko<sup>1,2\*</sup>, V.L. Demchenko<sup>1,2</sup>, M.G. Korab<sup>1</sup>, A.M. Galchun<sup>1</sup>,  
V.Yu.Kondratenko<sup>1</sup>, V.V. Anistratenko<sup>1</sup>, S.M. Dyachenko<sup>1</sup>, M.G. Menzheres<sup>1</sup>**

<sup>1</sup> *Plastics Welding Department, E.O.Paton Electric Welding Institute, National Academy of Sciences of Ukraine, B.8, 11, Bozhenko Str., 03680, Kyiv-150, Ukraine*  
[iurzenko@paton.kiev.ua](mailto:iurzenko@paton.kiev.ua)

<sup>2</sup> *Institute of Macromolecular Chemistry, National Academy of Sciences of Ukraine, 48 Kharkivske Av., 02160, Kiev, Ukraine*

Nowadays the requirements for durability, strength, heat-resistance of industrial plastic products for oil and gas, aerospace and other industries are constantly increasing. In recent years, new high-performance polymeric materials, such as polyetherimides (PEI) and polyetheretherketones (PEEK), have already become competitors to metals, ensuring long-term reliability, heat, thermal, chemical and radiation resistance in difficult operating conditions of specific constructions. These polymers are used in a pure form as well as a matrix for various composite materials. At the same time manufacture of many products needs joining of polymeric parts, so the development of efficient technologies of such heat-resistant polymers welding is actual.

In the present work welding of Zedex plastics, namely ZX – 410 based on polyetherimide and ZX – 324 based on polyetheretherketone, were conducted by three traditional methods, namely welding with the heated tool (Fig. 1, Fig 2.), thermistor (Fig. 3, Fig. 4) and ultrasonic (Fig. 5, Fig. 6) welding.

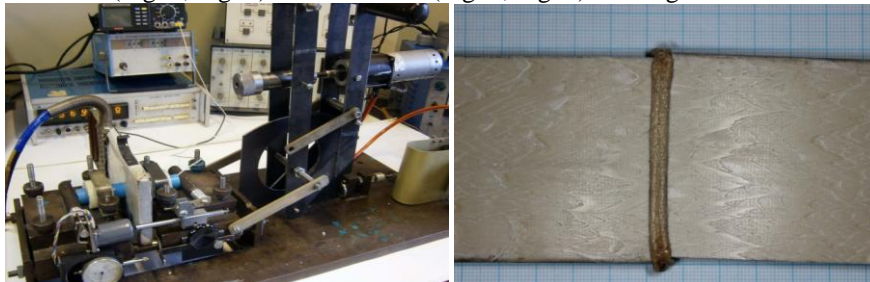


**Fig. 1.** The experimental equipment for butt fusion welding with the heated tool and the welded joint of the PEI plates, obtained using the heated tool butt welding.

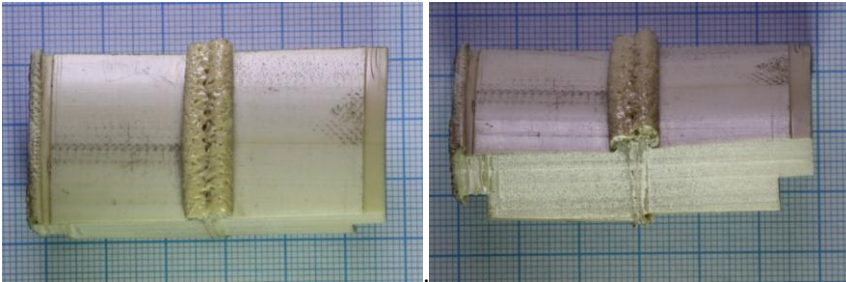


**Fig. 2.** The welded joint of the PEI pipes, obtained using the heated tool butt welding.

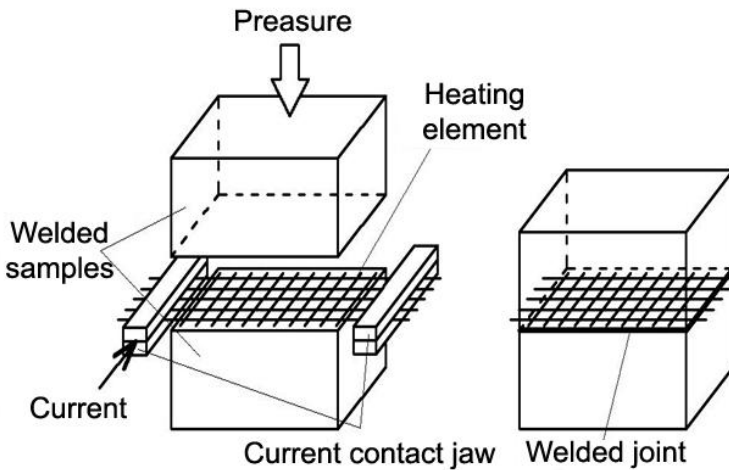


**Fig. 3.** The principal scheme of the thermistor welding.

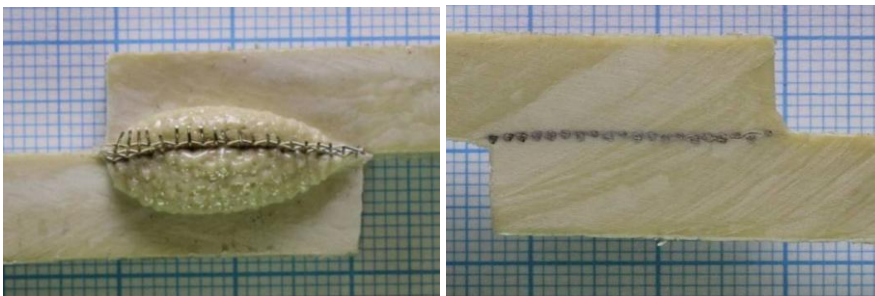


**Fig. 4.** The outward view and the cross-section of the lap thermistor weld of the PEI plates.

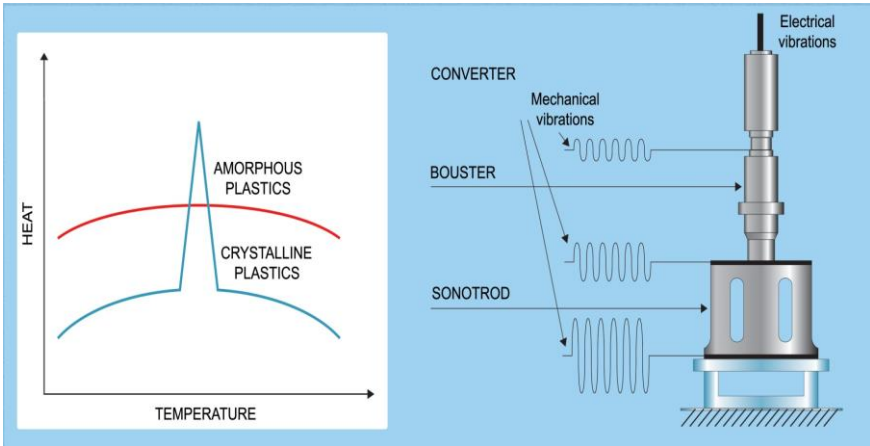


Fig. 5. The principal scheme of the ultrasonic welding.

*PEI*

*PEEK*

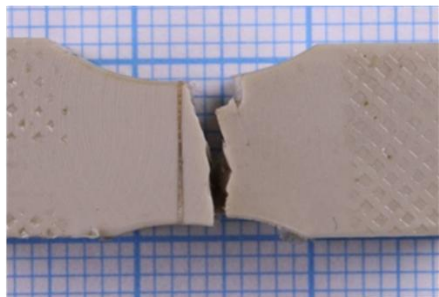
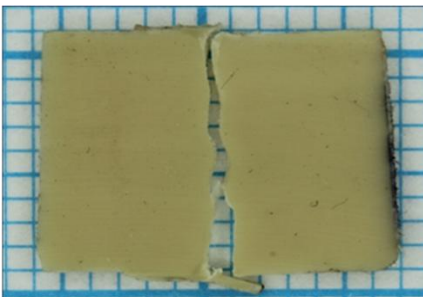
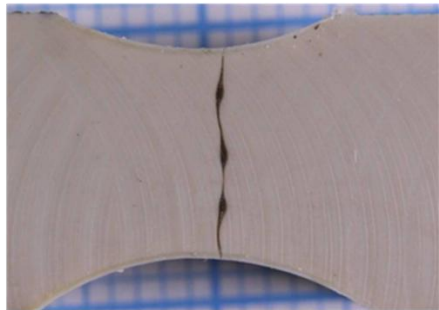
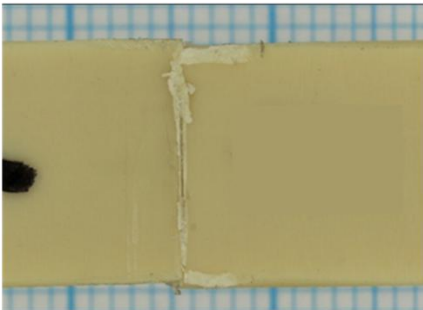
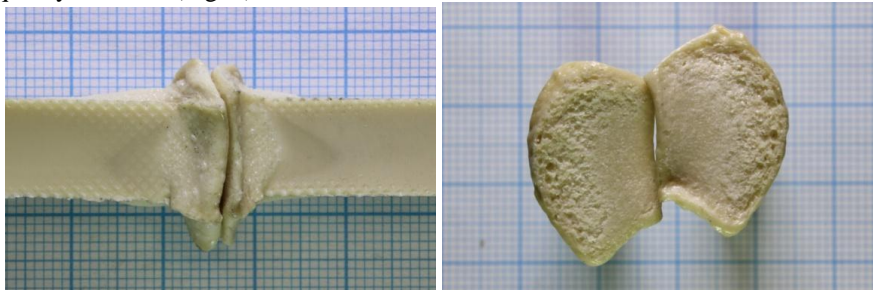


Fig. 6. The welded joints of the PEI and PEEK samples and their deconstruction at mechanical tests.

It was revealed that materials melts are prone to cavitation that degrades the quality of welds (Fig. 7).



**Fig. 7.** The general view and character of the welded joint destruction of the PEI plates, obtained using butt welding with the heated tool.

For the best understanding of the welding processes [1] and development of the efficient welding technology the structural features of the welded joints were studied by optical (TOM and POM) and electron microscopy (TEM and SEM), wide-angle (WAXS, Fig. 8) and small-angle (SAXS) X-ray spectroscopy.

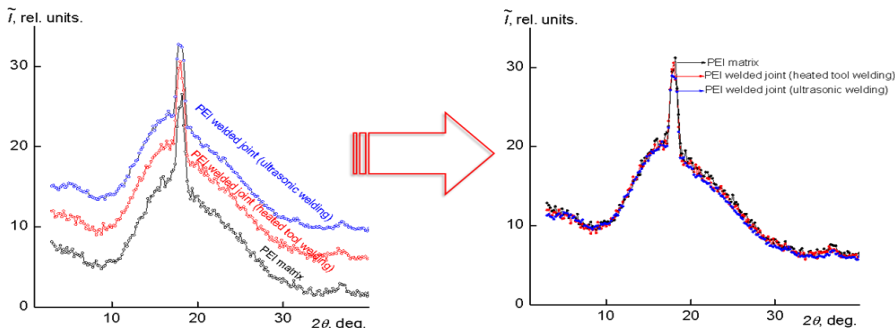


**Fig. 8.** The WAXS spectra of the PEI welded joints.

As the result it was found that the strongest joints were formed by welding at "soft" modes. The mechanical strength of joints at break has been received about 86% comparing to the mechanical strength of the basic material at optimal mode of butt welding and 100% at optimal mode of overlapping welding, which are the maximum level reached in the world (according to the literature) by similar types of welding for these materials.

- Galchun A., Korab N., Kondratenko V., Demchenko V., Shadrin A., Anistratenko V., Iurzhenko M. Nanostructurization and thermal properties of polyethylenes' welds // *Nanoscale Research Letters*, 10 (2015), P. 138-149.

## **FEATURES AND BEHAVIOR OF PLASTICS AT LASER IRRADIATION WELDING**

**M.V.Iurzhenko<sup>1,2</sup>, O.O.Tarasenko<sup>1</sup>, V.L.Demchenko<sup>1,2</sup>, A.O.Shadrin<sup>1</sup>,  
A.M.Palagesha<sup>1</sup>, O.V.Fedoseeva<sup>1</sup>, M.G.Menzheres<sup>1</sup>, A.Meshalkin<sup>3</sup>**

<sup>1</sup> *Plastics Welding Department, E.O.Paton Electric Welding Institute, National Academy of Sciences of Ukraine, B.8, 11, Bozhenko Str., 03680, Kyiv-150, Ukraine*  
[iurzhenko@paton.kiev.ua](mailto:iurzhenko@paton.kiev.ua)

<sup>2</sup> *Institute of Macromolecular Chemistry, National Academy of Sciences of Ukraine, 48 Kharkivske Av., 02160, Kiev, Ukraine*

<sup>3</sup> *Institute of Applied Physics of Academy of Sciences of Moldova, 5 Academiei str., Chisinau, MD2028, Moldova*  
[alexei@asm.md](mailto:alexei@asm.md)

Among the classical welding methods, laser welding has recently become an interesting alternative and offers a number of advantages. This method is characterized by improved optical properties, small heat affected zone, miniaturization, less thermal, mechanical or electrical load upon the product, less flash or no flash at all, feasibility of 3D weld geometries etc. Also in some cases it allows to weld dissimilar polymers, which cannot be welded by other methods.

There are two kinds of laser welding: overlap (transmission) welding and butt welding. Today the most commonly used is transmission welding. In this method the first material is transparent and the second is absorbing of the laser irradiation. Laser beam penetrates through the first polymer (upper) and it is absorbed by the second (lower) one. The result and process depend on the type of polymers and lasers. The major benefits of the transmission laser welding technique can be summarized as: weld high quality seam, no direct contact with the welding tool, flexible configurations of joint, controlled and localized energy input, high strengths of joint, minimal thermal motion and deformation. In process of the butt welding, laser beam focuses at the junction of two semi-transparent materials. The result and quality of junction depends on optical properties of plastics to be joined, their thickness and thermal properties.

## P27

There are no researches in Ukraine of plastics laser welding, and it is very vivid nowadays. The main areas of progress and plastics laser welding researches can be the following: multilayer film welding (triple layer joining), influence of different laser irradiations on different plastics, welding of high-temperature thermoplastics, technological features in welding of plastics.

In this work we present the results of investigations of laser irradiation influence of different lasers on engineering plastics like high density polyethylene, namely PE-100, PE-400, PP, PEEK and PEI plastics. CO<sub>2</sub>, Nd:YAG and fiber lasers were used. This made it possible to investigate the effect of different wavelengths on each polymer. After lasers' processing the microscopic analysis of morphological changes in these plastics have been performed.

## ANNEALING EFFECT ON THE ABSORBANCE SPECTRA OF POLYMER THIN FILMS

**B. Jarzabek<sup>1</sup>, I. Sava<sup>2</sup>, M-D. Damaceanu<sup>2</sup>, R-D. Rusu<sup>2</sup>, B. Hajduk<sup>1</sup>, M. Bruma<sup>2</sup>**

<sup>1</sup> Centre of Polymer and Carbon Materials Polish Academy of Sciences,  
34 M. Curie-Sklodowska Str., 41-819 Zabrze, Poland  
[bozena.jarzabek@cmpw-pan.edu.pl](mailto:bozena.jarzabek@cmpw-pan.edu.pl) (corresponding author)  
[barbara.hajduk@cmpw-pan.edu.pl](mailto:barbara.hajduk@cmpw-pan.edu.pl) (presenting author)

<sup>2</sup> “Petru Poni” Institute of Macromolecular Chemistry, Aleea Grigore Ghica Voda  
41A, Iasi -700487, Romania

Polymer thin films, as a parts of optoelectronic and photovoltaic devices, are exposed to the effect of high temperature (up to 180°C) so these polymer films are required to be both time- and thermo-stable. Good candidates for these applications seem to be different derivatives of polyimides and polyoxydiazoles because of their high thermal stability and good photo-optical and electrochemical properties. The study of optical absorbance during *in situ* heat treatment of films is a simple, new method to investigate thermal stability and to observe the changes of polymer chain conformation and conjugation during annealing process.

This work presents temperature dependences (up to 250-350°C) of absorbance spectra for thin films of aromatic polyimides containing side-substituted azobenzene groups, copolyimides containing oxadiazole and perylene units and for thin films of copoloyoxydiazoles. Generally the obtained results confirm good thermal stability of these polymer films. Some slight changes of absorption spectra, connected with the thermal structural disorder, have been discussed, being dependent on the polymer chain structure. For all the studied polymer films conjugation is preserved at high temperatures (energy gap is invariable), what is particularly important in applications as advanced materials.

## SYNTHESIS AND CHARACTERIZATION OF FLUORINATED POLY(AZOMETHINE)S FROM NEW CORE-PERFLUORINATED AZOMETHINE-CONTAINING MONOMERS

**Ya.L. Kobzar, I.M. Tkachenko, O.V. Shekera, V.V. Shevchenko**

*Institute of Macromolecular Chemistry of National Academy of Sciences of Ukraine, 48 Kharkivske shausse, Kyiv 02160, Ukraine*  
[varoslav\\_kobzar@mail.ru](mailto:varoslav_kobzar@mail.ru)

Polyazomethines (PAMs) or polymeric Schiff bases are an interesting class of polymers and show various excellent properties such as good thermal and environmental stability, mechanical strength, nonlinear optical, and semiconducting electrical properties under doping. They often display liquid crystalline (LC) behavior at room temperature as well as ability to form chelates with metals [1, 2]. As a consequence, PAMs have a potential for numerous application in electronics, optoelectronics, photonics and sensors [2].

PAMs can be synthesized in a traditional approach (also known as polyazomethine route) by a reaction of dialdehydes with diamines [3]. On the other hand, PAMs can be obtained by an alternative route that consists in using of azomethine-containing compounds (like bis-diols, bis-phenols, etc.) [4]. Unfortunately, the majority produced polymers are characterized by limited solubility in the most of common organic solvents [3]. The growing macromolecular chains of PAMs precipitate from the solution during the polycondensation reaction. Moreover, high melting temperatures of the PAMs make them intractable for processing by other conventional techniques. One of possible ways for solving the aforementioned problem consists in reducing density packing of their polymer chains.

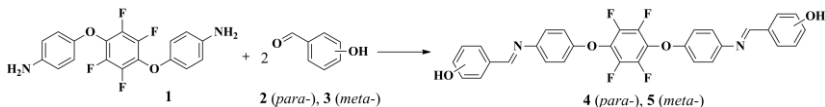
It is generally recognized that the presence of alkyl chains and isomeric fragments in a polymer backbone imparts higher segmental mobility to the polymers and so simultaneously enhances their solubility and reduces their glass transition temperatures [5]. Additionally, the incorporation of the aliphatic moieties, flexible ether linkages and isomeric fragments into the polymer chains of PAMs is sufficient to induce LC properties to such macromolecular compounds [3].

On the other hand, it is known that introduction of fluorine atoms into polymers' structure enhances their thermal stability and chemical resistance, as

well as allows reduction the polymers' dielectric constant, the refractive index, optical losses at the same time improving their ability to form LC phases [6]. It is interesting to note that such fluorinated liquid crystals have good stability, high voltage holding ratio and specific resistance. Moreover, they are characterized with low threshold switching voltage ( $V_{th}$ ) and small temperature coefficient of  $V_{th}$ , and are, therefore, widely used now in LC displays [6].

The aim of this study was in the synthesis of new isomeric core-perfluorinated azomethine-containing monomers and PAMs with aliphatic spacers different lengths in the main chain based on them.

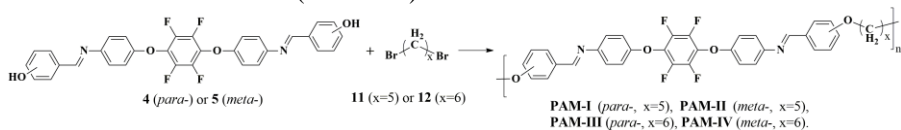
Dihydroxyl-substituted azomethine-containing monomers **4** and **5** with tetrafluorobenzene (TFB) unit were synthesized by a condensation reaction between diamine **1** and isomeric hydroxybenzaldehyde **2** or **3** (Scheme 1).



**Scheme 1.** Synthesis of core-perfluorinated dihydroxyl-substituted azomethine-containing monomers **4** and **5**.

The structure of the synthesized azomethine-containing monomers **4** and **5** was confirmed by FTIR,  $^1\text{H}$ ,  $^{13}\text{C}$ ,  $^{19}\text{F}$  NMR and UV-Vis spectrometry techniques. It should be mentioned that synthesized compounds **4** and **5** can be used as monomers for the production of wide spectrum azomethine-containing polymers.

The novel PAM-I – PAM-IV polymers having aliphatic moiety were prepared by polycondensation reactions of synthesized monomers **4** and **5** with dibromoalkanes **11** and **12** (Scheme 2).



**Scheme 2.** Synthesis of core-perfluorinated PAM-I – PAM-IV.

The conditions for obtaining PAMs were found by changing the temperature and time of the reaction and solvent/monomer concentrations in the reaction medium. Polymers PAM-I – PAM-IV were synthesized with the maximum yields and the highest  $[\eta]$  values by using anhydrous potassium carbonate as a base and monomer concentration in the reaction medium of 10 %. Other synthesis conditions as well as yields and  $[\eta]$  values for PAMs are listed in Table 1.

**Table 1.** The synthesis conditions, intrinsic viscosity values and yields for PAMs

Polymers	Synthesis conditions			Yield, %	[ $\eta$ ], dL/g
	Reaction temperature, °C	Time	Solvent		
PAM-I	100	48 h	DMAc	84	0,13 <sup>a</sup>
PAM-II	100	48 h	DMAc	78	0,24 <sup>b</sup>
PAM-III	100	48 h	DMAc	79	0,16 <sup>a</sup>
PAM-IV	100	48 h	DMAc	75	0,29 <sup>b</sup>

<sup>a</sup>:in H<sub>2</sub>SO<sub>4</sub> at 30 °C;

<sup>b</sup>:in DMF at 30 °C.

The resulting polymers PAM-I and PAM-III are soluble only in the concentrated sulfuric acid, while PAM-II and PAM-IV are soluble in most common organic solvents and insoluble in methanol, ethanol, toluene, benzene, and *n*-hexane. The improved solubility of the polymers PAM-II, PAM-IV in polar organic solvents may be attributed to the simultaneous incorporation of isomeric fragments and flexible aliphatic segments into the polymer chains [7].

The solubility of PAM-II and PAM-IV polymers in THF enabled investigation of their molecular mass distribution by gel permeation chromatography (GPC) using polystyrene standards. According to the GPC measurements, the PAM-IV polymer based on 1,6-dibromohexane has higher molecular weight than the PAM-II compound based on the 1,5-dibromopentane unit. The number-average molecular weight of PAM-II and PAM-IV are 3,400 and 7,600 g/mol respectively.

The values of the polydispersity index were similar: 2.9 for PAM-II and 3.2 for PAM-IV.

The chemical structure of the obtained polymers was confirmed by FTIR, <sup>1</sup>H and <sup>19</sup>F NMR spectrometry techniques.

The <sup>1</sup>H NMR spectra of the soluble polymers (PAM-II and PAM-IV) in CHCl<sub>3</sub> are illustrated in Fig. 1. All

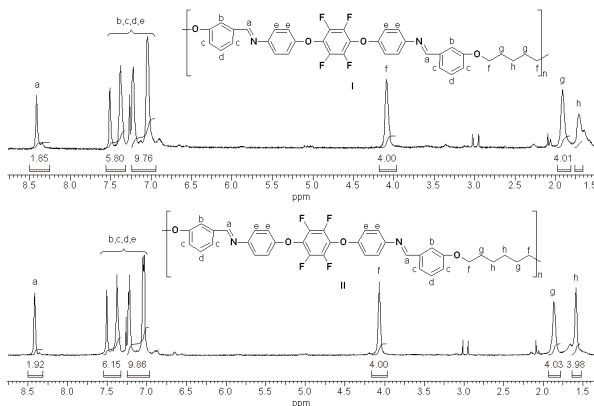


**Fig. 1.** <sup>1</sup>H NMR spectra of PAM-II (I) and PAM-IV (II).

the observed peaks could be readily assigned to the protons in the corresponding repeat units.

The PAMs obtained are characterized by high thermal stability, decomposition temperature which is in the range 381–426 °C and their glass transition temperature is in the range 90–127° C.

In a summary, we have synthesized new core-perfluorinated isomeric dihydroxyl-substituted azomethine-containing monomers with a TFB central unit. Novel polymers with aliphatic moiety different lengths based on these new core-perfluorinated dihydroxyl-substituted azomethine-containing derivatives were also prepared. Our study of the synthesized polymers shows that their solubility, molecular mass characteristics and thermophysical properties are mainly dependent on the isomeric nature polymer's backbone and lengths of the aliphatic spacers in the main chain of the PAMs. These polymers show high thermal stability and high decomposition temperatures. The obtained polymers are promising systems for a wide range of applications as low-dielectric materials, in optical devices and polymers with liquid crystalline properties. These special properties of the core-perfluorinated aromatic polymers require individual consideration will be a subject of our future work.

1. *Kobzar Ya.L., Tkachenko I.M., Shekera O.V., Shevchenko V.V.* The fluorine-containing polyazomethines: synthesis and properties // *Polymer Journal*. 36 (2014) 331-340 (Ukraine).
2. *Ravikumar L., Kalavani S., Vidhyadevi T., Murugasen A., Kirupha S.D., Sivanesan S.* Synthesis, Characterization and Metal Ion Adsorption Studies on Novel Aromatic Poly (Azomethine Amide) s Containing Thiourea Groups // *OJPCHEM*. 4 (2014) 1-11.
3. *Iwan A., Sek D.* Processible polyazomethines and polyketanils: from aerospace to light-emitting diodes and other advanced applications // *Prog. Polym. Sci.* 33 (2008) 289-345.
4. *Tamaseselvy K., Venkatarao K., Kothandaraman H.* Synthesis and characterization of new halogen-containing poly (azomethine-urethane) s // *Makromol. Chem.* 191 (1990) 1231-1242.
5. *Gul A., Akhter Z, Siddiq M., Qureshi R., Bhatti A.S.* Synthesis and physicochemical characterization of poly (azomethine) esters containing aliphatic/aromatic moieties: Electrical studies complemented by DFT calculation // *J. Appl. Polym. Sci.* 131 (2014) 1-8.
6. *Ishikawa H., Toda A., Okada H., Onnagawa H.* Relationship between order parameter and physical constants in fluorinated liquid crystals // *Liquid crystals*. 22 (1997) 743-747.
7. *Abid K.K., Al-barody S.M.* Synthesis, characterisation and liquid crystalline behaviour of some lanthanides complexes containing two azobenzene Schiff base // *Liquid Crystals*. 41 (2014) 1303-1314.

**THERMODYNAMICS OF THE FORMATION,  
THERMOPHYSICAL AND ELECTRICAL PROPERTIES OF  
THE COMPOSITES BASED ON EPOXY POLYMER AND  
CARBON NANOTUBES**

**V.V.Korskanov<sup>1</sup>, I.L.Karpova<sup>1</sup>, V.V.Klepko<sup>1</sup>, N.V.Rukhailo<sup>1</sup>, V.B.Dolgoshey<sup>2</sup>**

*<sup>1</sup>Institute of Macromolecular Chemistry of National Academy of Sciences of Ukraine, 48 Kharkivske shausse, Kyiv 02160, Ukraine*  
[korskanov.v@mail.ru](mailto:korskanov.v@mail.ru)

*<sup>2</sup> Kiev's National University of Construction and Architecture 31 Povitroflotsky Avenue, Kiev, Ukraine, 03680*

Up to now, the most publications was dedicated of the research of the behavior of the some properties composites based on the polymers and carbon nanotubes (CNT's) [1-3]. This paper shows that most of the physical properties of epoxy-CNT's composites are determined by the thermodynamic compatibility of their components.

The epoxy polymer (EP) (based on epoxy resin DER-321 (produced by DOW Chemical (USA) cured with an amine hardener Polypox H354 (produced by UPPC (Germany)), filled with carbon nanotubes have been investigated.

The nanocomposites (NC) with CNTs volume fraction content  $\phi$  from 0.003 to 0.9 were prepared by introducing of nanofillers to DER-321 and dispersed using the ultrasound. After adding hardener of samples were formed on teflon substrates at room temperature during 24 h. Further thermal supplementary curing was carried out at 473 K during 4 hours.

The density, heat capacity, thermal and electrical conductivity and viscoelastic properties of the NC were measured. On the base of experimental results the specific enthalpy, configurational entropy and Gibbs free energies of the NC have been calculated.

The thermodynamics analysis has shown that the maximum of specific energy interaction (SEI) between EP and CNT's in NC was reached at volume content of 0,06÷0,2 % (Fig. 1).

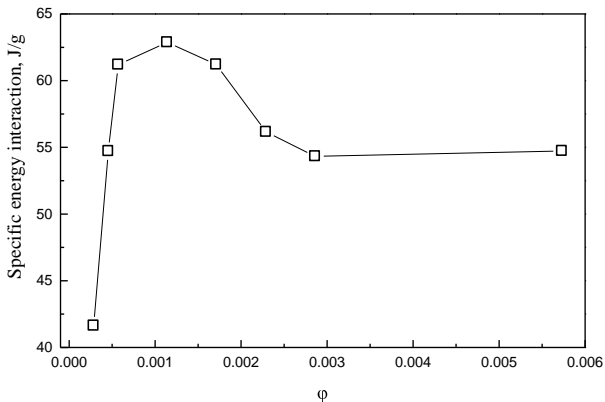


**Fig. 1.** Concentration dependences of the of specific energy interaction between EP and CNT's .

It was found that the SEI determine the thermophysical, electrical and viscoelastic properties of NC.

The very low percolation threshold of electrical conductivity has been found to be around 0.0015 volume fraction of CNTs content (electrical conductivity increased from 1E-16 to 1E-6 S/m in the range from 0,001 to 0,002 volume fraction) (Fig 2a). The experimental data of the thermal conductivity (were measured in temperature interval from 323K to 473K) increased by four times in the range from 0,002 to 0,003 volume fraction (Fig 2b).

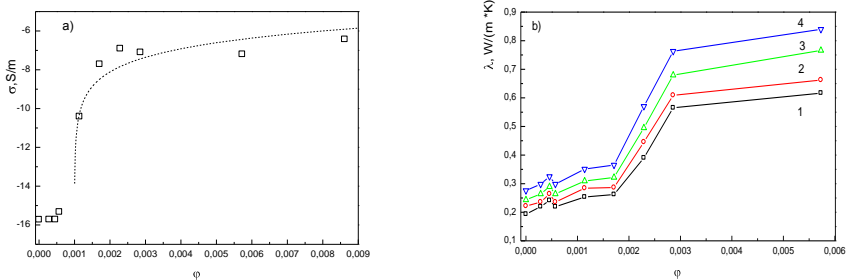


**Fig. 2.** Dependences electrical conductivity (a) and thermal conductivity (b) from volume fraction nanotubes. Temperature: 1 – 323K, 2 – 373K, 3 – 423K, 4 – 473 K.

Depending on the ratio of the components in nanocomposites can be useful as following materials with different properties:

<i>Weight fraction CNT's w, %</i>	<i>Properties</i>	<i>Application field</i>
≤ 0,1	electric conductivity $\sigma \approx 10^{-16}$ Sm/m heat conductivity $\lambda \approx 0,20$ W/(m·K)	insulators low heat conductivity materials
0,1 < w < 0,5	electric conductivity $\sigma \approx 10^{-7}$ Sm/m heat conductivity $\lambda \approx 0,20$ W/(m·K)	semiconductors low heat conductivity materials
0,5 < w < 1,0	electric conductivity $\sigma \approx 10^{-5}$ Sm/m heat conductivity $\lambda \approx 0,8$ W/(m·K)	semiconductors high heat conductivity materials
> 1,0	electric conductivity $\sigma \approx 10^{-5}$ Sm/m heat conductivity $\lambda < 0,1$ W/(m·K)	semiconductors porous materials thermal isolators

1. Hammel E., Tang X., Trampert M., Schmitt T., Mauthner K., Eder A. and Pötschke P. Carbon nanofibers for composite applications// Carbon.– 2004.– V. 42, № 5-6.– P. 1153-1158.
2. Gojny F., Wichmann M., Fiedler B., Schulte K. Influence of different carbon nanotubes on the properties of epoxy matrix composites – A comparative study//Composites Science and Technology. – 2005. – Vol. 65 – P. 2300–2313.
3. Bauhofer W., Kovacs J. A review and analysis of electrical percolation in carbon nanotube polymer composites // Composites Science and Technology. – 2009. – Vol. 69. №10. – P. 1486- 1498.
4. Korskanov V.V., Babkina N.V., Brovko A.A. et. at Viscoelastic, Thermophysics and Relaxation Properties of the Nanofilled Composites based on epoxy polymer // Polymer J. – 2015. – Vol. 37, №2. – C. 3–12.

## **EFFECTS OF POLYURETHANE MATRIX COMPONENT STRUCTURE ON ITS BEAM STRENGTH**

**L. Kosyanchuk, N. Kozak, M. Stratilat, N. Babkina, V. Bezrodnyi**

*Institute of Macromolecular Chemistry of National Academy of Sciences of Ukraine, 48 Kharkivske shausse, Kyiv 02160, Ukraine*  
[lkosyanchuk@ukr.net](mailto:lkosyanchuk@ukr.net)

*Institute of Physics of National Academy of Sciences of Ukraine, 46 Nauki prospekt, Kyiv 03680, Ukraine*  
[bezrod@iop.kiev.ua](mailto:bezrod@iop.kiev.ua)

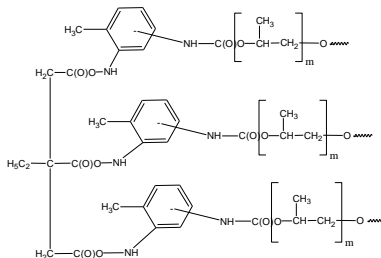
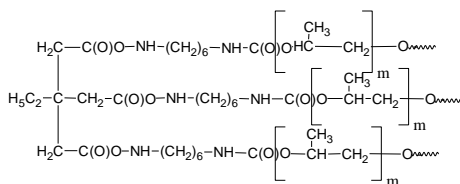
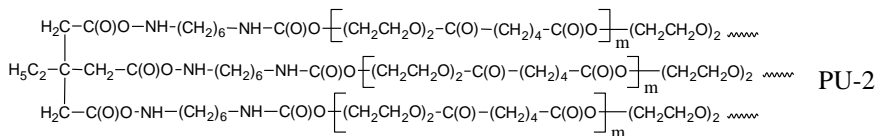
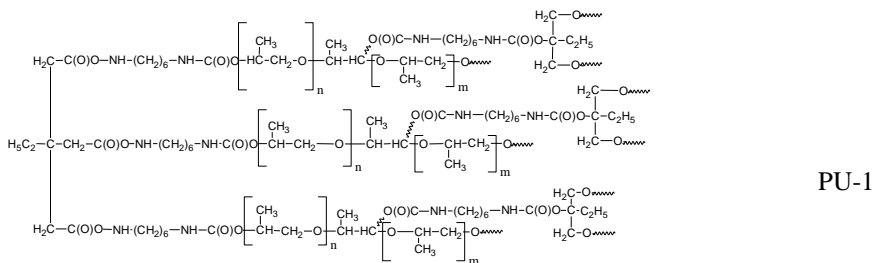
The use of organic dye-doped solid-state laser elements based on polymer matrices is caused by a set of advantages of the latter, compared to their liquid analogues (by compactness, non-toxicity, simplicity of construction and its replacement, possibility of operation in a wide temperature range) [1]. Polymer matrices should satisfy some significant requirements. Besides high optical transparency in a broad spectral region, high solubility for dyes, stability of the latter under storage and operation, they should provide considerable beam strength, i.e. resistance to the powerful light emission. Beam strength of the polymer depends on mobility of its macrochains and penetrability for the low-molecular compounds (decay products, formed under continuous or pulsed influence of laser irradiation) [2]. Linked polyurethanes (PU) can be used as matrices in the dye-doped solid-state laser elements and differ by a type of the diisocyanate component, and also by a structure, molecular weight and functionality of the oligoether part.

The present work deals with the investigations of PU segmental mobility of chains and penetrability by means of the EPR method with a use of a nitroxyl paramagnetic probe TEMPO, and also the study of the linkage density of netlike PU by dynamic mechanical analysis (DMA).

The objects under study were the PU matrices, synthesized from prepolymers of different structure, namely, the ones based on hexamethylene diisocyanate (HMDI) or the mixtures of 2,4-, 2,6-toluene diisocyanate (65/35) (PU-4) and different oligoethers: oligo-diethylene glycol adipate MM800 (ODA-800) (oligoether diol ester) (PU-2), three-functional oligooxy(propylene glycol) MM500 (OPG-500) (polyether triol oligoether) (PU-1), bifunctional oligooxy(propylene

P31

glycol) MM1000 (OPG-1000) (oligoether diol) (PU-3), taken in double equimolar excess of diisocyanate in relation to oligoglycol. Trimethylolpropane (TMP) was used as a linking agent.



The probe was inserted to the PU by means of diffusion process from the saturated vapor of TEMPO. Calculated values of correlation times,  $\tau$ , characterizing mobility of the polymer chains, relative intensity of the probe signal, corresponding to the amount of diffused probe in the polymer, and also  $M_c$  values for all the matrices are presented in Table.

Dynamic characteristics of macro-chains and parameters, affecting the matrix penetrability, and also a linkage degree for the PU, based on HMDI are determined by a structure of the oligoether component.

**Table.** Spin dynamics parameters of the probe and  $M_c$  values in polyurethanes

Sample	Integral intensity, r.u.	$\tau \times 10^{-9}$ , s	$M_c$	Threshold of single-pulse laser damage, $J/cm^2$ ( $\pm 0.5 J/cm^2$ )
PU-1	1.00	20.5	960	12,5
PU-2	5.6	5.1	1800	18,0
PU-3	18.2	1.7	4250	13,5
PU-4	8.5	2.2	3100	20,0

Three-functional OPG-500 compound, having the smallest MM value among the studied oligoethers and the largest linkage degree, is characterized by the lowest values of polymer chain mobility, penetrability for the low-molecular probe from a gas phase and  $M_c$ .

The decrease in functionality of the glycol component in PU-2 leads to the lowering of  $\tau$ , increase of the TEMPO diffusion simplicity and  $M_c$  value. The smaller MM of the glycol component, compared to PU-3 (the smaller theoretical value of  $M_c$ ) and a presence of ester groups in PU-2, more able to form H-bonds with urethane groups, compared with simple ether groups of the glycol component in PU-3, cause larger hindrance of the probe spinning in the PU-2 matrix, decrease of the probe penetrability and smaller  $M_c$  values, compared with PU-3.

Taking into account the values for the lowering of the TEMPO spinning diffusion hindrance, increase in the relative amount of the probe, diffused to the polymer, and  $M_c$  values, the PU matrices can be ranged as follows:

PU-1 – PU-2 – PU-3.

This row is illustrated by the following diagrams:

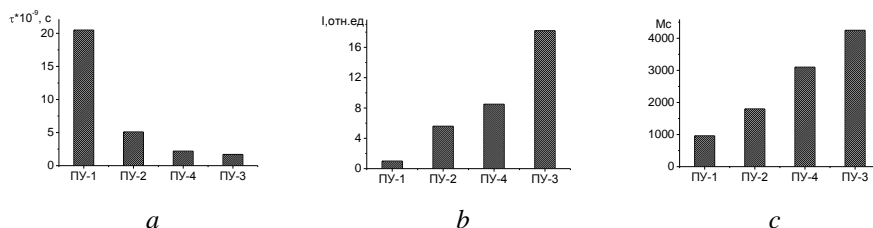


**Fig.** Effects of the polyurethane matrix component structure on the macro-chain dynamics and linkage degree: correlation time (a), relative integral intensity of a signal (b), effective linkage degree (c).

Threshold beam strength of the HMDI based polymers, measured in a regime of single-pulse laser radiation, agrees with the presented above sequence, characterizing the dynamic parameters of the studied matrices and their linkage degree.

The effect of the diisocyanate component type, aliphatic or aromatic one, was analyzed for the PU, based on OPG-1000. After the replacement of the diisocyanate component  $\text{OCN}-(\text{CH}_2)_6-\text{NCO}$  (HMDI) with the  $\text{OCN}-\text{Ph}(\text{CH}_3)-\text{NCO}$  (TDI) one in PU-4, having the same glycol component as PU-3, one should expect higher rigidity and density for PU-4, compared with PU-3.

Actually, this suggestion is proved by calculated values of correlation time  $\tau$ , characterizing hindrance of the probe spinning in PU-4 (Table). They indicate the lower mobility of PU-4 macro-chains, compared with PU-3. In addition, according to the Table data, the TEMPO ability to diffuse in PU-4 is 2.14 times lower, than in PU-3. This is an evidence of significantly denser packing of macro-chains in the polyurethane, based on TDI. The similar decrease is also seen for  $M_c$  values.

One should note, that  $M_c$  values for all initial PU systems, calculated from the data of dynamic mechanic experiments, correlate with both  $\tau$  (a characteristic of segmental mobility) and relative intensity of PU penetrability for the low-molecular probe from a gas phase (Figure), despite the fundamental differences of the methods used.

Measured threshold beam strength of the polymers, based on different diisocyanates correlates also with the parameters of macro-chains mobility, obtained by EPR and DMA methods, penetrability for the low-molecular probe and an effective value of  $M_c$ .

In summary, the carried out investigations allow to predict the material stability under continuous or pulse laser irradiation by selection of the polymer matrix for the solid-state laser elements.

1. Gromov T.A., Dyumaev K.M., Manenkov A.A., Maslyukov A.P., Matyushin G.A., Nechitailo V.S., Prokorov A.M. Efficient plastic host dye lasers // *J Opt Soc Am B* 2 (1985) 1028-1031.
2. Costela A., García-Moreno I., Sastre R. Polymeric solid-state dye lasers: recent developments // *Phys Chem Chem Phys* 5 (2003) 4745-4763.

## CRYSTALLIZATION OF POLYPROPYLENE FROM PARTIALLY DISENTANGLED MELT

**J. Krajenta, A. Pawlak**

*Centre of Molecular and Macromolecular Studies, Polish Academy of Science,  
Sienkiewicza 112, Łódź 90-363, Poland*  
[justynak@cmm.lodz.pl](mailto:justynak@cmm.lodz.pl)

It is known that crystallization of polymers from melt depend on the diffusion of macromolecules to the crystallization front. The movement of macromolecules is limited by the presence of their entanglements with other macromolecules. The crystallization when the number of entanglements was reduced was not fully studied yet. The aim of our investigation is describe formation of spherulitic structure and kinetics of crystallization for semi-crystalline polymer with reduced entanglements in amorphous phase.

The number of entanglements may be reduced by applying specific crystallization procedure [1-3]. Isotactic polypropylene (iPP) with partially disentangled chains was generated through crystallization of iPP from diluted solution in hot mineral oil or in hot xylene. When the temperature decreased a gel was formed inside the flask. The reduced number of macromolecular entanglements in diluted solution was preserved in the gel. The solution with gel was cooled to room temperature and the gel was filtrated and dried. In result was obtained white powder, containing reduced number of macromolecular entanglements [1-2]. The properties and morphology of partially disentangled polypropylene were examined. Characterization of obtained polypropylene powder and for comparison the initial, commercial iPP was made on the basis of DSC measurements, X-ray analysis, rheological measurements and studies of mechanical properties during compression in channel die.

The crystallinity of powder, melting temperature, lamellar thickness were determined from DSC experiments. DSC was also used for studies of isothermal crystallization at 135 °C. The Linkam hot stage connected with polarizing light microscope was applied for studies of spherulitic structure, crystallization kinetics from melts, the regimes of crystallization, in aim to examine the effect of disentanglement on iPP crystallization.

The examples of spherulitic structures for PP powder obtained from xylene solution and for initial PP are shown on Fig 1. It is visible that a nucleation density

was lower in the powder. The growth rate of spherulites was faster for partially disentangled polypropylene, which resulted in largest size of growing spherulites.

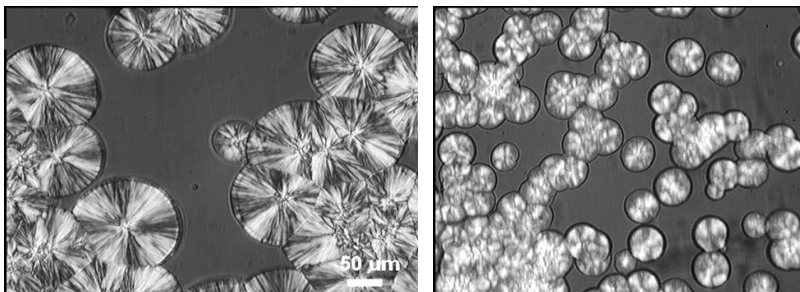


**Fig. 1.** Polarized optical micrographs of iPP<sub>disentangled</sub>(left) and iPP<sub>initial</sub> (right) showing the spherulites growing during isothermal crystallization at 135<sup>o</sup>C. Both samples were kept in the melt state (180<sup>o</sup>C for 1 min) before quenching to 135<sup>o</sup>C.

Figure 2 shows the heat flow in time, measured during the isothermal crystallization of PP powders and initial PP, studied by DSC. As can be seen from Figure 2, the total crystallization time is shorter for iPP from xylene solution (PPX) and for iPP from mineral oil solution (PPO) than for initial polymer (PPI). The lower number of entanglements along the chains causes the higher spherulite growth rate and faster conversion of melt into crystals.

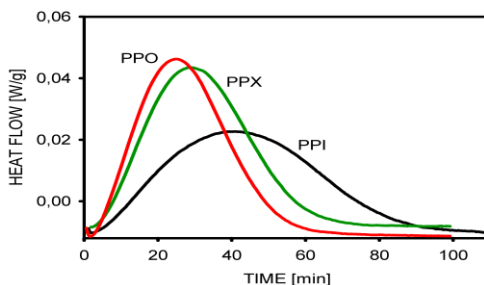


**Fig. 2.** DSC thermograms of PPI (iPP initial), PPX (iPP from xylene solution), PPO (iPP from mineral oil solution) recorded during isothermal crystallization at 135<sup>o</sup>C.

### Acknowledgments

*The studies were financed from funds of the Polish National Science Centre on the basis of the decision number 2012/04/A/ST5/00606. The participation in*

*Workshop was financed from statutory funds of CMMS.*

1. *Krajenta J., Pawlak A., Gałęski A.* Formation of polypropylene nanofibers by solid state deformation blending with molten polyethylene, *Polimery* 10 (2015) 64-66.
2. *Wang X., Liu R., Wu M., Wang Z., Huang Y.* Effect of chain disentanglement on melt crystallization behavior of isotactic polypropylene, *Polymer* 50 (2009) 5824-5827.
3. *Psarski M., Piórkowska E., Gałęski A.* Crystallization of Polyethylene from Melt with Lowered Chain Entanglements, *Macromolecules* 33 (2000) 916-932.

## **CROSSLINKED POLYURETHANES NANOSTRUCTURED**

**N.N. Laskovenko<sup>1</sup>, A.A. Protasov,<sup>2</sup> E.V. Lebedev<sup>1</sup>**

<sup>1</sup>*Institute of Macromolecular Chemistry of National Academy of Sciences of Ukraine, 48 Kharkivske shausse, Kyiv 02160, Ukraine*  
[nilla.laskovenko@gmail.com](mailto:nilla.laskovenko@gmail.com)

<sup>2</sup>*Institute of Hydrobiology National Academy of Sciences of Ukraine Heroes of Stalingrad Ave., 12, 04210, Kiev, Ukraine*  
[protasov@bigmir.net](mailto:protasov@bigmir.net)

### **GOAL OF THE WORK**

Investigation of the process of modification of network polyurethanes with organic-inorganic oligomers to produce nanostructured polymeric materials (Punono).

### **REAL RESEARCH**

Polyurethane based on polyether (PUP) and polyester (PUS) an aromatic polyisocyanate was used as the polymer matrix. Nanostructured organic-inorganic oligomer (NONO) was used as a modifier. NONO has the siloxane structure, and was obtained by classical reaction of hydrolysis-polycondensation of phenyltriethoxysilane with tetraethoxysilane.

RESEARCH METHODS - functional chemical, IR spectroscopy, transmission-optical microscopy, X-ray, optical microscopic analysis. State Standard methods for determining the properties of paints.

### **RESULTS**

It was shown that modified polyurethanes exhibit improved physical and mechanical properties (Table 1). It was found that the studied materials are water-resistant and resistant to aggressive environments (Fig.1, 2).

**Table 1.** Physical -mechanical characteristics of the modified polyurethane

Title  index	Name of polyurethane			
	PUP	PUS	PUSNONO	PUS+Zn(60%)
Hardness relative units, Not less than	0,30	0,45	0,50	0,40
Blow cm, not less than	50	50	50	50
Bending mm, not less than	1	1	1	1
Adhesion, rating, not more	2	1	1	1
$\sigma$ , MPa, not less	23,9	34,0	36,8	38,0
$\epsilon$ ,%, not less	150,0	90,0	85,0	85,5
Mass fraction of the gel fraction,%, not less	95,0	88,5	88,5	87,8

P33

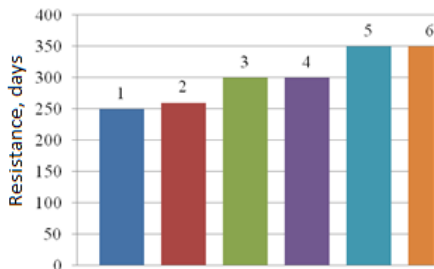
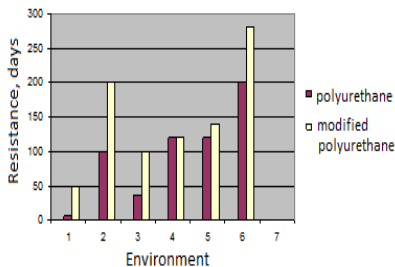


**Fig. 1.** Stable PU coatings in fresh water: 1 PUS; 2 PUS +Zn(60%); 3 PUS +Zn(60%) + NONO (1%); 4 PUP; 5 PUP + Zn(60%); 6 PUP+ Zn(60%) + NONO.

**Fig. 2.** Resistance of polyurethane in the presence of corrosive environments: water: 1-distilled; 2-Maritime; 3 - 20% solution of NaOH; 4 - 20% solution of H<sub>2</sub>SO<sub>4</sub>; 5- 20% solution of CuSO<sub>4</sub>; 6 - 30% solution of NH<sub>4</sub>OH.

Investigations on possibility of using the materials as antifouling coatings were performed. For this purpose, biostability of modified polyurethane was determined and new antiseptics: Titanium - Boron -, amino-containing compounds were used. Studies have shown that polyurethane, which was modified with nano-structured organic-inorganic oligomer, and which has polyesters as hydroxyl-containing component, showed biological stability to the action of bacteria degraders [2]. Studies show the stability of the structure of the films after exposed to cultures of corrosive bacteria (fig.3).



**Fig. 3.** Transmission optical microscopy photos : PU film: A- source; B - after microbiological investigations.

Studies of experiential substrates with different polyurethane coatings in the conditions of the Kanev Reservoir showed that they have some antifouling properties (Fig. 4, 5).

P33



**Fig.4.** Fouling by zooperiphyton of control samples from vinyl plastic.

**Fig. 5.** Absence of fouling on the plates which were coated with PUNONO.

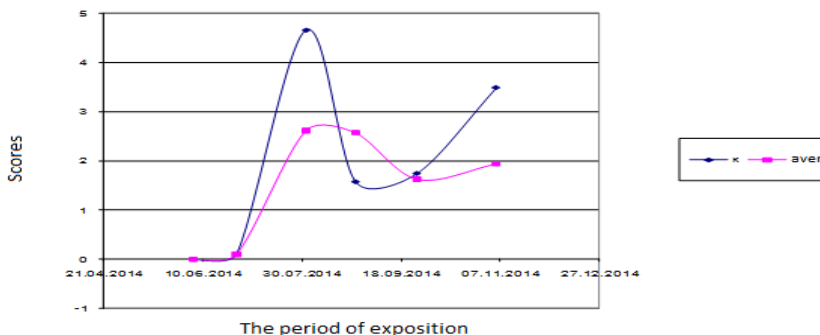


**Fig. 6.** Dynamics of intensity of fouling of substrates (in points) for the different exposures: - control (k) and average value for Sample of PUNONO coatings.

## CONCLUSIONS

Nanostructured polyurethanes were prepared by the modification of polyurethanes by nanostructured organic-inorganic oligomers. Their properties, including antifouling, were investigated. It was investigated and shown, that in time of mass development of zooperiphyton (molluscs, sponges, Dresden and others), the intensity of fouling of studied coatings was only 30% of control. Therefore, further research of nanostructured polyurethanes in this direction may be promising.

1. V.P. Kusnetzova, N.N. Laskovenko, S.I. Omelchenko. Composite polymeric materials, (Institute of Macromolecular Compound Chemistry of National Academy of Sciences of Ukraine, Kyiv). - 2000.- 22.-p. 87-92.
2. Laskovenko N.N., Kopteva G.P., Kusmenko N. Ja. and etc. // «Polymer».-Kyiv.- 2015.- № 5.- in print.

## STRUCTURAL FEATURES OF POLYETHYLENE GLYCOL-CARBON NANOTUBES NANOCOMPOSITES

E. A. Lysenkov<sup>1</sup>, S. I. Bohvan<sup>2</sup>, V. V. Klepko<sup>2</sup>

<sup>1</sup>*Mykolayiv National University named after V.O. Sukhomlynskiy, 24 Nikol'ska Str., Mykolayiv 54030, Ukraine*  
[evalisenkov@mail.ru](mailto:evalisenkov@mail.ru)

<sup>2</sup>*Institute of Macromolecular Chemistry of National Academy of Sciences of Ukraine, 48 Kharkivske shausse, Kyiv 02160, Ukraine*  
[klepko\\_vv@ukr.net](mailto:klepko_vv@ukr.net)

During the last decade polymeric composites, which contain the filler's particles with nanosize are the objects of intensive researches due to their unique properties and wide area of its applications [1]. One of the most perspective materials which used as nanofillers for polymeric nanocomposites are carbon nanotubes (CNT).

The development of materials based on polymeric matrix and CNT is a very difficult process due to thermodynamic and to the kinetic barriers which hinder the good dispersion of nanotubes. A degree of nanotubes' dispersion in a polymer is a determinative for the receipt of materials with improving functional descriptions [2]. The different methods of mixing are used for avoidance of aggregation. A method of mixing in solution is not very much effective due to difficulties in desolvation. The method of CNT surface functionalization results in the improvement of distribution of nanotubes in the nanocomposites, however it worsens their physical properties. Therefore, a study of structure forming in the nanofilled polymeric systems is very actual, because a structure of polymeric nanocomposites determines their properties.

Various methods, such as scanning and transmission electronic microscopy (SEM and TEM accordingly), thermal analysis, Raman spectroscopy and X-ray scattering analysis is used for a study and analysis of structure and morphology of polymeric nanocomposites, filled by CNT. In particular, Small angle X-ray scattering gives information about character of aggregation of individual nanotubes or their bunches and allows to set a structure and sizes of these aggregates. The purpose of this work was a study of features of structure forming of carbon nanotubes in a polymeric matrix in the model nanofilled system based on polypropylene glycol (PPG) and CNT.

Polypropylene glycol (PPG 400) HO[-CH<sub>2</sub>-CH(CH<sub>3</sub>)O-]<sub>n</sub>H ( $n \approx 9$ ) with a molecular mass of  $M_w = 400$  (Aldrich) was used as a fluidic polymer matrix. Its density at  $T = 293$  K was  $\rho_n = 1010$  kg/m<sup>3</sup>. PPG 400 is an oily viscous liquid and it has a pour point of  $\approx 236$  K. Before using PPG 400 was dewatered by heating in vacuum (2 mm) at residual pressure  $p = 270$  Pa and temperature  $T = 263$ -283 K during 5 hours.

The multi-walled CNT were prepared from ethylene using the chemical vapour deposition (CVD) method (TM Spetsmash Ltd., Kyiv, Ukraine) with FeAlMo as a catalyst [3]. They were further treated by alkaline and acidic solutions and washed by distilled water until reaching the distilled water pH values in the filtrate. The typical outer diameter  $d$  of CNT was 20-40 nm, their length  $L$  ranged from 5 to 10  $\mu$ m and mean aspect ratio was  $a = L/d \approx 250 \pm 170$ .

The specific surface area  $S$  of the powders determined by N<sub>2</sub> adsorption was  $S = 130 \pm 5$  m<sup>2</sup>/g. The specific electric conductivity  $\sigma$  of the powder of CNT compressed at 15 TPa was about 10 S cm<sup>-1</sup> along the axis of compression. The density of the CNT was assumed to be the same as the density of pure graphite,  $\rho_n = 2045$  kg/m<sup>3</sup>.

The composites were obtained by adding the appropriate weights of filler to PPG 400 at  $T = 323$  K (viscosity is 30 mPa.s) with subsequent 2 min sonication of the mixture using a UZDN-2T ultrasonic disperser at frequency of 22 kHz and the output power of 150 W. The series of samples with content of CNT within 0.05–1,5 wt% (in further %) were investigated.

Small angle X-ray scattering (SAXS) investigations were done in the diapason of the scattering angles,  $\theta$ , between 0.05° and 4° using a Kratky-camera system. The K $\alpha$  radiation was selected with a filter and data, measured by step scanning with a scintillation counter, were obtained. Previous treatment of SAXS curves was conducted with the use of the program FFSAXS [4].

The microscopy images of composites placed inside a sandwich-type cell (cell thickness was 50  $\mu$ m) were obtained with optical microscope (Ningbo Sunny Instruments Co., Ltd, China). The microscope detector unit was interfaced with a digital camera and a personal computer.

The features of structure forming of CNT in a polymeric matrix based on polypropylene glycol are studied. Two levels of fractal aggregation for the probed nanocomposites was fixed by the method of small angle X-ray scattering. It is set that fractals of the first structural level of aggregation for the probed systems are surface-type, and fractals of the second level are mass-type. The fractal dimension of aggregates of the first structural level grows and arrives at a value 3, that specifies on formation of surface-type fractal aggregates with the most rough surface with the increase of CNT content in the system. The value of fractal dimension for the mass fractal structures of the second hierarchical level for the system of PPG-CNT changes from 2,5 to 2,9, that testifies to formation of net from

the clusters of nanotubes and compression of such mass fractal aggregates with the increase of CNT content. The sizes of pores, which appear between separate nanotubes during their aggregation and are the mediated description of closeness of CNT packing in the nanocomposite are expected using the Guinier's approach. It is shown that the size of "pores", which appear between separate nanotubes during their aggregation, decrease from 6,2 nm to 4,7 nm at the increase of nanofiller's content. Such tendency in dependence of pores' diameters on nanotubes content specifies on the compression of structures from CNT and determining the role of aggregation processes of CNT at the formation of the structure of polymeric nanocomposites based on PPG. Using the method of optical microscopy it is set, that the systems of PPG-CNT are characterized with fractal structure.

1. *Paul D. R., Robeson L. M.* Polymer nanotechnology: Nanocomposites // *Polymer* 49 (2008) 3187-3204.
2. *Liff S. M., Kumar N., McKinley G. H.* High-performance elastomeric nanocomposites via solvent-exchange processing // *Nat. Mater.* 6 (2007) 76-83.
3. *Melezhyk A. V., Sementsov Y. I., Yanchenko V. V.* Synthesis of thin carbon nanotubes by coprecipitation of metal oxide catalysts // *Appl. Chem.* 78, (2005) 938-944 (in Russian).
4. *Vonk C.G.* FFSAXS's Program for the Processing of Small-Angle X-ray Scattering Data. – Geleen: DSM (1974) 83.

## STRUCTURE-PROPERTIES RELATIONSHIP IN COMPOSITES BASED ON POLYURETHANE AND SODIUM SILICATE

**T. Malysheva, A. Tolstov**

*Institute of Macromolecular Chemistry of the National Academy of Sciences of  
Ukraine, 48 Kharkivske shausse, Kyiv 02160, Ukraine*  
[Malysheva\\_tat@ukr.net](mailto:Malysheva_tat@ukr.net)

Over the last years organic-inorganic system (OIS) consisting of polyurethane organic phase and sodium silicate based inorganic phase are studied intensively because of great prospective in producing of nanocomposites with high performance properties.

The aim of this work is the study of effect of isocyanate groups content in macrodiisocyanate (MDI)/polyisocyanate blend on interfacial interactions, sorption and mechanical properties of OIS. Hybrid polymer composites were prepared by the joint polycondensation of isocyanate component (MDI and polyisocyanate) with unmodified or polyacrylic acid modified aqueous sodium silicate. MDI with NCO groups content in the range of 3,6-11,8 wt.% was prepared from poly(propylene glycol) of  $M_w$  1000 or 2000 and tolylene diisocyanate (mixture of 2,4/2,6-isomers). OIS prepared via aforementioned technique contain 20 wt.% of inorganic phase. The reaction between NCO groups of organic phase and silanol groups of inorganic phase during formation of the composites is confirmed by FTIR [1]. It is stated out that the increasing isocyanate groups content in MDI is caused to increasing hydrophobic urethane-silicate layer content at the interface layer, decreasing water sorption ability and improving mechanical characteristics of composites obtained.

1. *Malysheva T.L., Tolstov A.L.* Peculiarities of influence of chemical structure of organic constituent on interfacial interactions in organic-inorganic system based on sodium silicate // *Voprosy khimii i khimicheskoi tehnologii*. 1 (2015) 62-67.

## COHESIVE-ADHESIVE PROPERTIES OF THE COMPOSITES BASED ON OF POLYURETHANE ELASTOMER AND VINYLCHLORIDE POLYMER

T. Malysheva

*Institute of Macromolecular Chemistry of National Academy of Sciences of Ukraine, 48 Kharkivske shausse, Kyiv 02160, Ukraine*  
[Malysheva\\_tat@ukr.net](mailto:Malysheva_tat@ukr.net)

Nowadays, great attention attracts the studies of interfacial interactions in polymer/polymer systems, which realize in obtaining nanocomposites with novel functional characteristics. The chemical structure of polyurethanes (PU) has an impact on phase separation processes, compatibility with vinyl chloride based polymer and cohesive-adhesive properties of the composites. Strong hydrogen bonding (H-bonding) network between polar groups of PU and poly(vinyl chloride) macromolecules at the interface provides a formation of nanoheterogeneous structure of the blends containing up to 30-40 wt% of PVC and improves the tensile properties of the final composites.

The influence of chemical structure of semi-crystalline polyurethane elastomer and vinyl chloride based polymer (like poly(vinyl chloride-co-vinyl acetate), chlorinated poly(vinyl chloride)) on supramolecular structure, cohesion and adhesion properties of the composites has been studied. It was shown that strong interfacial H-bonding between carbonyl groups of PU based on poly(1,4-butanediol adipate) and  $\alpha$ -hydrogens of chlorinated polymers in the blends initiates a formation of a mixed phase with loosely packed macromolecules and result in reducing the mechanical and adhesion strength of the composites. The strengthening of intramolecular H-bonds in elastomer by increasing polar urethane-urea segments content or the replacement of poly(1,4-butanediol adipate) segments onto less compatible poly(ethylene glycol adipate-co-1,4-butanediol adipate) ones suppress the interface interactions and the formation of mixed phase. It leads to improvement of cohesion and adhesion properties of the composites. The composites with 30 wt.% of poly(vinyl chloride-co-vinyl acetate) are characterized by nanoheterogeneous structure and enhanced adhesion properties compared with neat PU.

## **STRUCTURE AND ELECTROPHYSICAL PROPERTIES OF POLYMERS BASED ON EPOXY OLIGOMER AND HETEROPOLYACID**

**O. K. Matkovska<sup>1</sup>, Ye. P. Mamunya<sup>1</sup>, M. V. Iurzhenko<sup>1</sup>, O. V. Zinchenko<sup>1</sup>,  
E. V. Lebedev<sup>1</sup>, G. Boiteux<sup>2</sup>, A. Serghei<sup>2</sup>**

<sup>1</sup>*Institute of Macromolecular Chemistry of National Academy of Sciences of Ukraine, 48 Kharkivske shausse, Kyiv 02160, Ukraine*  
[omatkovska@ukr.net](mailto:omatkovska@ukr.net)

<sup>2</sup>*Université Lyon 1, Ingénierie des Matériaux Polymères, UMR CNRS 5223, 43 Boulevard du 11 Novembre 1918, 69622 Villeurbanne, France*  
[gisele.boiteux@univ-lyon1.fr](mailto:gisele.boiteux@univ-lyon1.fr)

Epoxy composites are widely used for different applications in many technical areas due to their valuable properties. The characteristics of epoxy composites depend on type of curing agent. It is known that Lewis acids can be used as hardeners, however a mechanism of curing is not studied enough although such a type of hardener can provide high characteristics of epoxy composite.

The research is devoted to the study of the structure formation regularities and their influence on the electrophysical properties of polymers based on epoxy oligomer (EO) and heteropolyacid (HPA). HPA causes the reaction of homopolymerization of EO and, except of it, is a source of protons. It is found that solvent of HPA (water) in the initial mixture is determinative factor that has an influence on the structure and electrical properties of the EO/HPA polymer. Using of electrometric and DRS methods it has shown the effect of water concentration on the structural organization of the systems. Water content from 1 to 7 parts in mass leads to structural heterogeneity and increasing the water content up to 9 parts leads to homogeneous structure of the polymer network. For the first time it has been discovered three-stage curing process of systems by the electrometric method. Constants of rate of conductivity change are in range from  $1.4 \cdot 10^{-3}$  to  $4.2 \cdot 10^{-5} \text{ s}^{-1}$ . Electrical and structural models of the epoxy polymer conductivity and morphological model which explains the formation of heterogeneous structure of polymer matrix have been worked out. It is shown that dependence of conductivity on temperature makes agree with VTF theory that point out the influence free volume on the proton transfer process in the EO/HPA polymer.

## NOVEL NONLINEAR OPTICAL CROSSLINKED POLYMERS BASED ON GLYCIDYL SUBSTITUTED QUERCETIN

**D. O. Mishurov<sup>1</sup>, A. D. Roshal<sup>2</sup>, O. O. Brovko<sup>3</sup>**

<sup>1</sup>*National Technical University «Kharkiv Polytechnic Institute», 21, Frunze str., Kharkiv 61002, Ukraine  
[mda1975@mail.ru](mailto:mda1975@mail.ru)*

<sup>2</sup>*Institute of Chemistry is at the Kharkiv National University by name of V.N. Karazin, 4, sq. Freedom, Kharkov 61022, Ukraine*

<sup>3</sup>*Institute of Macromolecular Chemistry of National Academy of Sciences of Ukraine, 48 Kharkivske shausse, Kyiv 02160, Ukraine*

In last decades, the photonics and optoelectronics are most developing fields of science and technology. This development would not be possible without creation of new functional optical-transparently polymeric materials having effective nonlinear optical (NLO) properties [1, 2].

One of the ways to obtain such polymeric NLO materials is the synthesis of multifunctional chromophore-containing monomers with their further cross-linking. These monomers have to be of high molecular second-order polarizabilities that determine the macroscopic NLO response of the polymers.

This work is devoted to synthesis of polymers based on di-, tri- and tetraglycidyl derivatives of quercetin (GDQ). The estimation of molecular second-order polarizabilities ( $\beta$ ) of chromophore-containing monomers using solvatochromic method based on the quantum-mechanical two-level model [3] was carried out. Macroscopic second-order polarizabilities of polymer networks ( $\chi^{(2)}$ ) were determined using one-dimensional rigid oriented gas model [4].

The glycidyl derivatives of quercetin were first obtained. The synthesis was carried out by reaction of quercetin (Q) with epichlorohydrin (ECH). The optimization of reaction conditions aimed to improve the yield of target products was made. It was found that not-catalytic dehydration of quercetin hydroxyl groups results in very low yields of the reaction products.

Our investigations showed that quaternary ammonium salts are the most effective catalysts for mentioned process. The synthesis of GDQ was carried out in the presence of N-Alkyl-N-benzyl-N,N-dimethylammonium chloride ( $M_w = 367.5$ , Sigma-Aldrich Chemicals) under various molar Q/ECH ratios. The obtained GDQ were identified using FTIR and  $^1\text{H}$  NMR methods.

The studies of polymer networks obtained from GDQ have demonstrated high values of their macroscopic quadratic polarizabilities and temporal stability of NLO properties.

1. Dhanya R., Kishore V. C., Sudha Kartha C., Sreekumar K., Rani J. Ground state and excited state dipole moments of alkyl substituted *para*-nitroaniline derivatives // Spectrochim Acta A. 71 (2008) 1355–1359.
2. Mallakpour S., Zadehnazari A. Advances in synthetic optically active condensation polymers // Express Polymer Lett. 5 (2011) 142–181.
3. Paley M. S., Harris J. M., Looser H., Baumert J. C., Bjorklund G. C., Jundt D., Twieg R. J. A solvatochromic method for determining second-order polarizabilities of organic molecules. J Org Chem. 54 (1989) 3774–3778
4. Xie H-Q., Liu Z.-H.; Huang X.-D., Guo J.-S. Synthesis and non-linear optical properties of four polyurethanes containing different chromophore groups // Eur. Polymer J. 37 (2001) 497-505

## ULTRAFINE FIBERS OF CELLULOSE ACETATE BUTYRATE ELECTROSPUN FROM 2- METHOXYETHANOL – DIMETHYLFORMAMIDE SYSTEMS

**L. Olaru, A. L. Matricala, N. Olaru**

*“Petru Poni” Institute of Macromolecular Chemistry, 41A Grigore Ghica Voda  
Alley, Iasi 700487, Romania*  
[lolaru@icmpp.ro](mailto:lolaru@icmpp.ro)

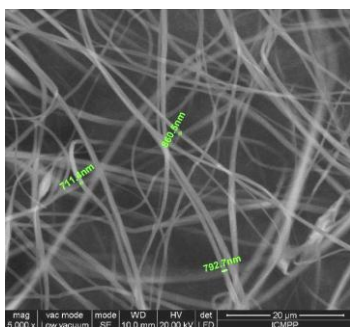
Polymer nanocomposites containing zinc oxide (ZnO) are intensively investigated for their remarkable performances in various fields as optics, electronics, semiconducting materials, biomedicine, photocatalysis. For example, a highly efficient and friendly depollution of waste waters can be performed by means of ZnO-containing materials, which exhibit photocatalytic activity for degradation of many organic pollutants [1]. Flexible polymeric nanofibers produced via the electrospinning procedure are used as substrates for growing of ZnO nanostructures.

New composites of ZnO nanocrystals grown on cellulose acetate butyrate (CAB) nanofiber mats have been recently performed and their photocatalytic activity was demonstrated over two organic dyes [2]. In the first step of this process, CAB nanofiber mats with a zinc salt, like acetate, embedded in the polymer matrix – as a precursor for growing of ZnO nanocrystals – are obtained by electrospinning from polymer solutions containing zinc acetate.

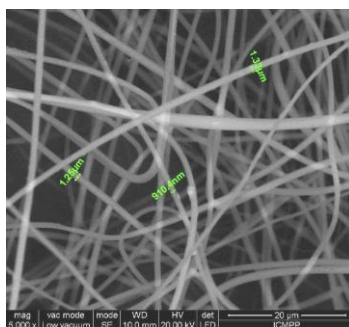
The choice of a suitable solvent for this purpose may cause some problems since such a solvent has to meet the requirements of a good electrospinning solution and the necessity of dissolving the metal salt. In this study, mixtures of 2-methoxyethanol and dimethylformamide (DMF) in various proportions are investigated in an attempt to find adequate solvent system and electrospinning conditions for obtaining of smooth CAB nanofibers without beads and containing zinc acetate in the polymer matrix.

We have shown that 2-methoxyethanol is an adequate solvent for electrospinning of CAB and can provide smooth nanofibers without beads by electrospinning from solutions with polymer concentrations higher than 25 wt.% (Fig.1, a, b), but it cannot dissolve sufficient amount of zinc acetate when it is used without a cosolvent. Fiber diameters increase at higher polymer concentration.

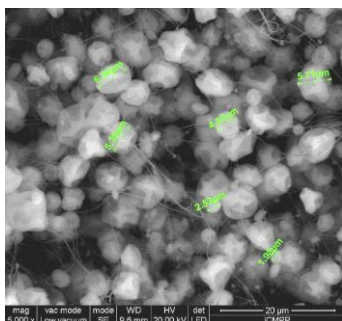
Dimethylformamide is also a solvent for CAB and other cellulose esters, but from its CAB solutions only beads connected by extremely fine fibers can be obtained even for higher polymer concentration (Fig. 1, c, d). An explanation for this behavior may consist in the higher surface tension of this solvent as compared with 2-methoxyethanol. In turn, DMF can dissolve sufficient amount of zinc acetate, which is a precursor for growing of ZnO nanocrystals in metal oxide - polymer composite.



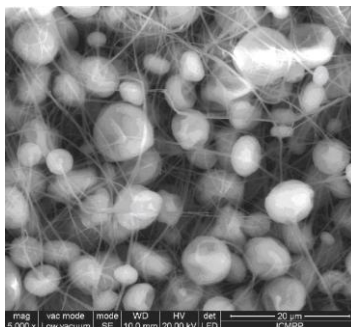
(a)



(b)



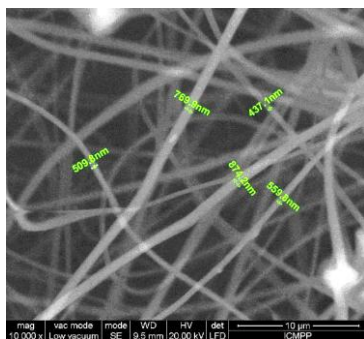
(c)



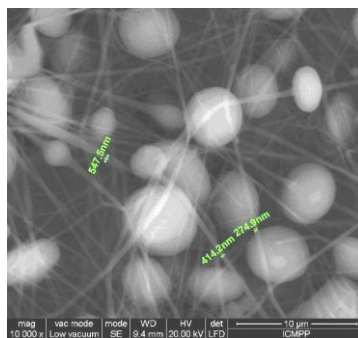
(d)

**Fig. 1.** Nanostructures of CAB obtained from solutions in 2-methoxyethanol at CAB concentrations of 26 wt.% (a) and 32 wt.% (b), and from solutions in DMF at CAB concentrations of 26 wt.% (c) and 32 wt.% (d).

The morphologies of CAB nanostructures obtained in the studied solvent mixtures – as revealed by SEM analysis – are dependent on the composition of the solvent system and on polymer concentration. It was observed that 1:1 (v/v) composition of the solvent mixture is suitable for obtaining of smooth nanofiber mats at 32 wt.% polymer concentration (Fig. 2, a), while lower CAB concentration gave spheres connected by ultrafine fibers (Fig. 2, b). With respect to fiber diameters, which is also dependent on polymer concentration, the above mentioned solvent mixture ensures diameters even lower than those produced in 2-methoxyethanol at 26 wt.%, as shown in Fig. 2, a and Fig. 1, a, respectively.



(a)



(b)

**Fig. 2.** Nanostructures of CAB obtained from solutions in mixtures 2-methoxyethanol – DMF 1:1 (v/v) at 32 wt.% (a) and 29 wt.% (b) polymer concentration.

The morphology of the beads also varied with the composition of the solvent system. At higher proportion of DMF in the mixture, the surface of the beads becomes more irregular due to a combined effect of lower volatility and higher surface tension of this solvent as compared with 2-methoxyethanol. It is also notable that solutions of CAB in mixtures of 2-methoxyethanol and DMF exhibit a better spinnability than those performed in 2-methoxyethanol alone.

The results of this study (including those not depicted in this abstract) show that mixtures of 2-methoxyethanol and DMF in approximately equal proportions are suitable solvent systems for synthesis of smooth electrospun CAB nanofibers with metal salts as precursors for hybrid composites.

1. *Liu H., Yang J., Liang J., Huang Y., Tang C.* ZnO Nanofiber and Nanoparticle Synthesized Through Electrospinning and Their Photocatalytic Activity Under Visible Light // *J Am Ceram Soc.* 91 (2008) 1287 - 1291 .
2. *Olaru N., Calin G., Olaru L.* Zinc Oxide Nanocrystals Grown on Cellulose Acetate Butyrate Nanofiber Mats and Their Potential Photocatalytic Activity for Dye Degradation // *Ind Eng Chem Res.* 53 (2014) 17968 - 17975.

## NICKEL DOPED TIN OXIDE NANOFIBERS PREPARED BY ELECTROSPINNING FOR HUMIDITY SENSING

P. Pascariu<sup>1</sup>, A. Airinei<sup>1</sup>, N. Olaru<sup>1</sup>, F. Tudorache<sup>2</sup>

<sup>1</sup>"Petru Poni" Institute of Macromolecular Chemistry, Aleea Grigore Ghica Voda, 41A, Iași 700487, Romania  
[pascariu\\_petronela@yahoo.com](mailto:pascariu_petronela@yahoo.com)

<sup>2</sup> Interdisciplinary Research Department – Field Science & RAMTECH, Alexandru Ioan Cuza University of Iasi, Bd. Carol I Nr. 11, Iasi 700506, Romania

Nanosized metal oxide materials have been attracted much attention because of their promising environmental capabilities of monitoring applications, especially as active materials for humidity and gas sensors. Generally a humidity sensor has to present fast response and recovery time, high sensitivity, good stability, negligible hysteresis over utilization periods, and possibly a broad operating range for both humidity and temperature, and low cost [1, 2].

In this work, NiO-SnO<sub>2</sub> nanofibers were fabricated via electrospinning technique combined with calcination at 600 °C. The NiO-SnO<sub>2</sub> nanofiber based sensor has sensitive response to relative humidity in air at room temperature. The crystallinity, structure and morphology of the electrospun NiO-SnO<sub>2</sub> nanofibers were discussed. XRD data revealed that NiO-SnO<sub>2</sub> nanofibers with pure tetragonal rutile structure for SnO<sub>2</sub> and cubic phase corresponding for NiO structure were obtained.

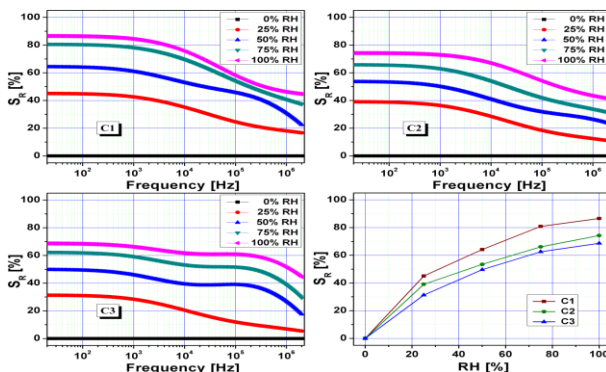


Fig. Humidity sensor sensitivity of NiO-SnO<sub>2</sub> nanofibers.

The emission characteristics are determined by structural defects and oxygen vacancies and depend on the nickel level in nanofibers. These nanofibers having the advantages of porous structures and Ni doping gave excellent performances for humidity sensors. The effect of relative humidity on electrical resistance of sensing element was studied in the humidity range of 0 to 100% RH. The significant effective surface of these nanofibers increases the conduction in the presence of water vapor which is reflected in a important sensitivity to humidity of NiO-SnO<sub>2</sub> nanostructures.

1. *Sin N. D. M., Tahar M. F., Hamat M. H., Rusop M.*, Enhancement of nanocomposite for humidity sensor application, In: *Recent Trends in Nanotechnology and Materials Science*, F. L. Gaol, J. Webb, Eds., Springer Int. Publ. Switzerland. (2014) 15-30.
2. *Kim H. R., Haensch A., Kim I. D., Barsan N., Weimar U., Lee J. H.*, The role of NiO doping in reducing the impact of humidity on the performance of SnO<sub>2</sub>-based gas sensors: synthesis strategies, and phenomenological and spectroscopic studies, *Adv. Funct. Mater.* 21 (2011) 4456–4463.

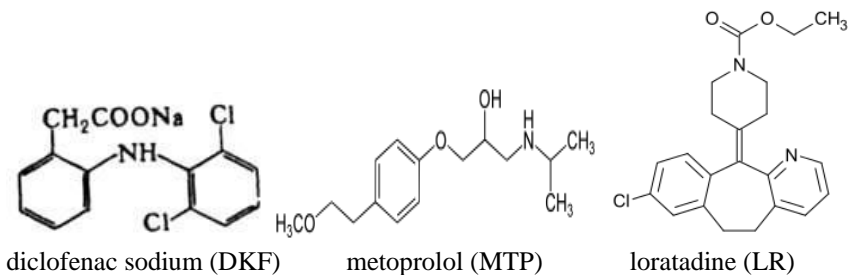
## **β-CYCLODEXTRIN-CONTAINING POLYMER SYSTEM WITH CONTROLLED RELEASE OF DRUGS**

**S.V. Riabov, L.A. Orel, L.V. Kobrina, S.I. Sinelnikov**

*Institute of Macromolecular Chemistry the National Academy of Sciences of  
Ukraine, 48 Kharkivske shausse, Kyiv 02160, Ukraine*

[Sergii.Riabov@gmail.com](mailto:Sergii.Riabov@gmail.com)

Recently, much attention is paid to the development of polymeric matrices with controlled release of drugs. In such systems polymeric carrier and active agent form a complex, which in addition to the set of physiological activity, has adjustable pharmacokinetics [1]. In this respect, a promising components in creating polymer matrices for drug delivery are cyclodextrins (CD), which form inclusion complexes with a various organic substrates, allowing to solve problems such as maintaining constant concentrations of biologically active substances in the blood, drugs release in a long time, protection compounds with short half-life, stability of drugs, reducing the frequency of dosing and elimination of side effects of drugs [2-6]. In the work presented, we investigated a desorption kinetics of drugs from cyclodextrins-containing polymer matrices and established the impact of β-CD functionalized derivatives on their desorption. Therefore, we synthesized cross-linked polymers based on acrylamide (AAM), bis-acrylamide (bis-AAM) and β-CD derivatives like maleate β-CD (β-CD-Mal) and methacrylate β-CD (β-CD-Met), in which biologically active molecules of different sizes, being capable to form inclusion complexes with β-CD or its derivatives, were incorporated. Their structural formulas are given below:

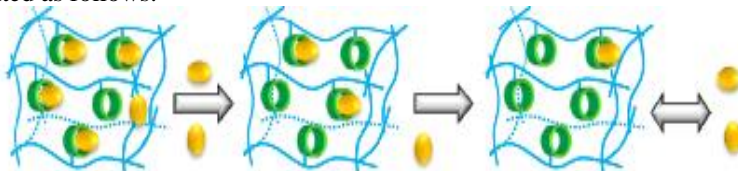


Drugs investigated were introduced into the polymer matrices in two ways: encapsulation (directly during the synthesis of polymer) and swelling (in the already synthesized polymer). The concentration of released compounds was

P41

monitored by means of UV spectroscopy, calculating the amount of drug in solution using the calibration graph. Absorbance for calculating concentrations was measured at maximum absorption with a wavelength region (for DKF – 274 nm, MTP – 275 nm, LR – 247 nm, respectively).

The general scheme of desorption drugs from polymeric carrier can be represented as follows:



In the IR-spectrum of the synthesized copolymer AAm-bis-AAm (without of  $\beta$ -CD moieties) one can see the characteristic absorption bands of amide groups ( $\nu$ C=O and  $\delta$ NH<sub>2</sub>) at 1653 and 1620 cm<sup>-1</sup> respectively, and  $\delta$ NH shoulder at 1528 cm<sup>-1</sup>, in turn, in spectrum of synthesized copolymers AAm-bis-AAm having  $\beta$ -CD-Mal fragments there are absorption bands at 1000-1100 cm<sup>-1</sup>, corresponding vibrations  $\nu$ C–O of glycoside ring and glycoside bridge of  $\beta$ -CD and band absorption at  $\nu$  1724 cm<sup>-1</sup>, which related to  $\nu$ C=O ester fragment.

In order to study the desorption of drugs from polymer samples the experiments involving the drug release kinetics were conducted. The research results are presented in table 1, indicating that presence of  $\beta$ -CD derivative in the polymer matrix resulted in slowing of drugs desorption almost in 2 times for LR and MTP, and for DKF in 4 times. Method of drug's introduction into the polymer matrix (by swelling – sample P-3 or encapsulation – sample P-2) has a little effect on the value of its desorption.

**Table 1.** LP desorption from polymers in water

Polymer samples	Content of the $\beta$ -CD	Type of drugs	Desorption, per day, g / l
P-1	–	LR	0,291
P-2	+	LR	0,132
P-3*	+	LR	0,133
P-4	–	DKF	0,052
P-5	+	DKF	0,012
P-6	–	MTP	0,650
P-7	+	MTP	0,380
P-8**	+	MTP	0,190

\* drugs were introduced into the polymers by swelling in alcohol solution.

\*\* polymer based on  $\beta$ -CD-Met only, other - on  $\beta$ -CD-Mal were obtained.

It was interesting to compare desorption behavior of samples, having different amount of drugs filled in matrix, that contained or did not contain  $\beta$ -CD-Mal. For this purpose, into polymer samples different quantities of MTP (from 0.29 to 0.6 ml of 11% MTP's solution) were injected. As can be seen from table 2, while  $\beta$ -CD derivative is presented in the polymer, MTP desorption proceeds in smaller extent and slower in time.

**Table 2.** MTP desorption in water from polymer samples with different degrees of MTP's filling

Sample	The degree of filling of the matrix		
	minimum	average	maximum
	Desorption MTP, per day, g / l		
Polymer (model)	0,225	0,882	1,1625
Polymer + $\beta$ -CD-Mal	0,474	0,329	0,507

Since the drugs investigated are mainly oral route of use, it was important to examine the influence of acidity medium on their release. So, we also determined the effect of different  $\beta$ -CD derivatives, incorporating in the polymers onto the desorption of drugs (MTP was applied as drug). Analysis of the data obtained leads us to conclusion that changes a medium from the neutral to the acidic one does not significantly affect on the desorption capability of the MTP, at the same time, the presence of  $\beta$ -CD-Met derivative in the polymer matrix slows desorption process of drug stronger compared to the  $\beta$ -CD-Mal derivative.

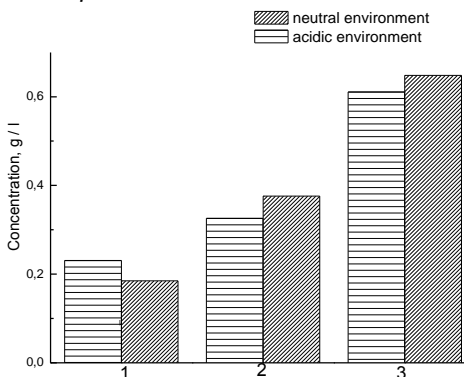


**Fig.** Release MTP from polymers in different medium: sample P-8 (1), sample P-7 (2), sample P-6 (3).

Thus, based on the results obtained, it can be concluded that the incorporating of the  $\beta$ -CD derivatives into polymer matrix results in slowing of drugs release (loratadine, diclofenac sodium, metoprolol succinate). It is of interest for developing of a new drugs-polymer complexes with sustained release and incorporating of the cyclodextrin functionalized polymers may help to reduce overall toxicity drugs and to improve their stabilization during storage.

1. Plate N.A., Vasiliev V.E. Physiologically active polymers. - M.: Chemistry, 1986. – 294.
2. Glangchai L. C., Calderera-Moore M., Li Shi, Roy K. Nanoimprint lithography based fabrication of shape-specific, enzymatically-triggered smart nanoparticles // *J. Control. Release.* 125 (2008) 263–272.
3. Mundargi R.C., Babu V. R., Rangaswamy V., et al. Nano/micro technologies for delivering macromolecular therapeutics using poly(D,LL lactide-co-glycolide) and its derivatives // *Ibid.* 125 (2008) 193–209.
4. Di Benedetto L. J., Huang J. S. Poly(alkylenetartrates) as controlled release agents // *Polym. Degrad. Stability.* 45 (1994) 249–257.
5. De Scheerder I. K., Wilczek K. L., Verbeken E. V. et al. Biocompatibility of polymer-coated oversized metallic stents implanted in normal porcine coronary arteries // *Atherosclerosis.* 114 (1995) 105–114.
6. Bajpai A. K., Shukla S. K., Bhanu S., Kankane S. Responsive polymers in controlled drug delivery // *Progr. Polym. Sci.* 33 (2008) 1088–1118.

**BACTERIAL CELLULOSE-POLYANILINE COMPOSITE  
FOR HEXAVALENT CHROMIUM REMOVAL**

**O. A. Aksenovska<sup>1</sup>, Y. V. Sheludko<sup>1</sup>, V. O. Yevdokymenko<sup>1</sup>, N. D. Didiv<sup>1</sup>,  
O. P. Tarasyuk<sup>1</sup>, I. Y. Zayets<sup>2</sup>, N. O. Kozyrovska<sup>2</sup>, S. P. Rogalsky<sup>1</sup>**

*<sup>1</sup>Institute of Bioorganic Chemistry and Petrochemistry of National Academy of Sciences of Ukraine, 50 Kharkivske shausse, Kyiv 02160, Ukraine*  
[rogalsky@bpci.kiev.ua](mailto:rogalsky@bpci.kiev.ua)

*<sup>2</sup>Institute of Molecular Biology and Genetics of National Academy of Sciences of Ukraine, 150, Zabolotnoho Str., Kyiv 03680, Ukraine*

Chromium is a common pollutant in groundwater because it is widely used in electroplating, metal finishing, leather tanning, dye and textile industries etc. [1]. In aqueous solution Cr is known to exist in two oxidation states such as trivalent Cr(III) and hexavalent Cr(VI). Cr(VI) is acutely toxic, carcinogenic and mutagenic to living organisms whereas Cr(III) is less toxic and does not readily migrate in groundwater [1]. Therefore, the most effective approaches for removal of Cr(VI) from polluted solutions are based on the reduction of Cr(VI) to Cr(III) followed by adsorption of Cr(III) on a solid adsorbent surface. Various natural or synthetic materials, such as zero-valent iron or Fe (II) particles, cellulose or polyamines are reported as widely used electron donors and adsorbents for Cr(VI) removal [2]. Among the polyamines, conducting polymer polyaniline (PANI) has been paid increasing attention for heavy metals removal due to the high content of amine groups, as well as high efficiency and reversibility. Thus, PANI powders may be a good candidate for highly efficient Cr(VI) removal due to their large specific surface area, low cost and easy bulk production [3]. However, recycling the PANI powders after treatment is still a challenge due to its small particle size. The surface coating of PANI on the cost effective, easily separated and reusable substrates, including magnetite (Fe<sub>3</sub>O<sub>4</sub>) nanoparticles, carbon fiber fabric and cellulose was demonstrated a good strategy for solving this problem [2]. Cellulose was shown to be especially promising material for cost-effectively treating Cr(VI) pollution since it can act as an electron donor for the Cr(VI) reduction and also contains a lot of active adsorption sites for Cr(III) adsorption [4]. However, the adsorption capacity of the neat cellulose is not high enough to achieve fast Cr(VI) removal and therefore needs improvement. Thus, the surface modification of cellulose with polymers containing amino groups, particularly PANI has been

clearly demonstrated as effective approach to improve its removal rate and removal capacity against chromium ions [5].

In this study, bacterial cellulose (BC) has been used as support for PANI deposition in order to develop new efficient composite for hexavalent chromium removal. BC is a natural hydrogel synthesized by acetic and other bacteria [6]. Being chemically identical to plant cellulose, BC displays important structural peculiarities. Thus, it has high chemical purity and forms three-dimensional ultrafine network of ribbon-shaped nanofibers which are about two orders of magnitude smaller than plant cellulose fibers [6]. The nano-morphology of BC results in a large surface area and highly porous matrix having enormous water holding capacity (to 99%). At the same time BC hydrogels display high wet strength and elasticity. It was found that PANI can be easily synthesized on the surface of BC nanofibers and assembled into novel electrically conducting 3D network [5]. It is natural to assume that the specific morphology of BC/PANI composite may cause its high efficacy for Cr(VI) removal.

BC hydrogel was synthesized with the help of *Komagataeibacter xylinus* bacteria in the cultural medium contained (w/v): 2% glucose, 0.5% yeast extract, 0.5% peptone, 0.25% disodium hydrogen phosphate, 0.18% citric acid (pH 6.0). The culture was incubated within 7 days at 30 °C under stationary conditions to get a BC-pellicle (Fig. 1, a).

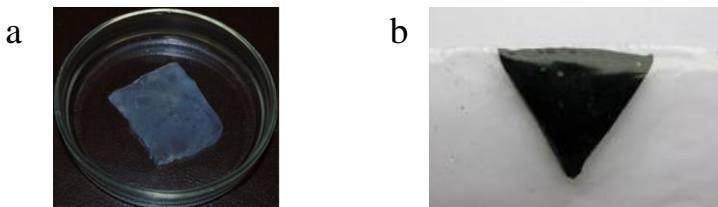


**Fig. 1.** Bacterial cellulose pellicle (a) and BC/PANI composite (b).

BC/PANI composite was obtained using the modified method described in [5]. The scheme of PANI formation in the BC hydrogel is shown in Fig. 2. BC pellicle (10 g, water content 99 wt%) was immersed into 100 ml of water solution of aniline hydrochloride (1 wt%) for 24 h. The wet BC film impregnated with a monomer was immersed into 50 ml of 0.1 M ammonium persulfate solution in 1 M sulfuric acid cooled to 0-5 °C. The dark green composite film (Fig. 1, b) obtained after the reaction time of 4 h was taken out of the solution and washed with distilled water and with methanol consequently. Further, it was immersed into 50 ml of 3% KOH solution for 24 h to convert PANI salt into basic form. The BC/PANI pellicle was dried at 100-120 °C for 24 h. The PANI content in a composite calculated from elemental analysis data was 20 wt%.



For the studying of Cr(VI) removal, the BC/PANI composite with dry weight of 0.01 g was added to 30 ml of Na<sub>2</sub>CrO<sub>4</sub> water solution containing 5 mg/l of Cr(VI) adjusted to PH of 3 by addition of sulfuric acid. In such conditions, only slight stoichiometric excess of PANI (1.3) to Cr(VI) has been used. The mixture was stirred at room temperature and solution probes were taken after different treatment time for spectrophotometric determination of Cr(VI) concentration. The optical density at 540 nm was measured in the presence of diphenylcarbazide [4]. The removal ratio was calculated as following:  $R = 100(C_0 - C_t)/C_0$ , where  $C_0$  is the initial concentration of Cr(VI) in solution and  $C_t$  is the concentration of Cr(VI) after a certain time of exposure to BC/PANI composite. According to the obtained results, the concentration of Cr(VI) in the treated solution decreased on 88% after 60 min exposure, whereas 98% Cr(VI) removal was detected after 90 min. In the comparison experiment, the neat PANI (0.002 g) was used for Cr(VI) removal instead of BC/PANI composite with the same PANI content. The removal ratio of 93% was achieved after 60 min which is similar to those for BC/PANI composite.

Thus, the results of this study indicate on high efficacy of BC/PANI composites for detoxification of Cr(VI) contaminated water. The main advantage of BC based material is much higher surface area which allow fast Cr(VI) reduction. as well as efficient Cr(III) adsorption from water solutions.

1. *Costa M.* Potential hazards of hexavalent chromate in our drinking water // *Toxicol Appl Pharmacol.* 188 (2003) 1–5.
2. *Qiu B., Xu C., Sun D., Wan Q., Gu H., Zhang X., Weeks B. L., Hopper J., Ho T. C., Guo Z., Wei S.* Polyaniline coating with various substrates for hexavalent chromium removal // *Appl Surf Sci.* 334 (2015) 7-14.
3. *Olad A., Nabavi R.* Application of polyaniline for the reduction of toxic Cr(VI) in water // *J Hazard Mater.* 147 (2007) 845-851.
4. *Lin Y.-C., Wang S.-L.* Chromium(VI) reactions of polysaccharide biopolymers // *Chem Eng J.* 181– 182 (2012) 479– 485.
5. *Liu X., Qian X., Shen J., Zhou W., An X.* An integrated approach for Cr(VI)-detoxification with polyaniline/cellulose fiber composite prepared using hydrogen peroxide as oxidant // *Biores Tech.* 124 (2012) 516-519.
6. *Ul-Islam M., Khan T., Park JK.* Water holding and release properties of bacterial cellulose obtained by in situ and ex situ modification. *Carbohydr. Polym.* 2012; 88: 596-603.

## FEATURES OF GLASS TRANSITION PROCESS IN PENTON - AgI SYSTEM

**M. I. Shut, M. A. Rokitskiy, G. V. Rokitskaya, A. M. Shut, T. G. Sichkar**

*National Pedagogical Dragomanov University, 9 Pirogova Str., Kyiv 01601,  
Ukraine*  
[maksal@bigmir.net](mailto:maksal@bigmir.net)

### **Introduction**

Due to a number of properties, in particular, weathering and resistance to weathering and aggressive environments, low gas and vapor penetrability polymer materials are widely used as coatings. However, under varying conditions of temperature durability of products polymeric coating surfaces using is limited to the difference of temperature coefficients of linear expansion (TCLE) of substrate and coating. For example, TCLE of metals and plastics often differ by more than an order of magnitude.

One of the directions of solving this problem could be the approaching of values of coating and substrate surface TCLE. This can be accomplished by using as a coating of polymer composite materials (PCM) with fillers that have almost zero or negative TCLE, and through optimum selection of composite heat treatment.

Optimum filler for such systems, in our view, can be silver iodide (AgI), that is characterized by a negative and stable in a wide temperature range (86 - 420 K) TCLE value. As polymer matrix, due to the symmetrical arrangement along the main chain of chloromethyl groups, which provide stable and high chemical resistance, penton is the most appropriate [1].

This paper is dedicated to the research of thermal expansion peculiarities of penton - AgI PCM system and determination of parameters of the glass transition in this system by dilatometric method.

### **Experimental**

In the capacity of polymer matrix the powdery penton of industrial production was chosen. Original powder was dispersed by mechanical method with following fractionating by using of laboratory sieves YKC-CJI-200 mark with loops size 50 and 40 micron. Before pressing, penton powder was aged for 24 hours at 323 K for elimination of fugitive low-molecular impurities.

Disperse filler – silver iodide was prepared from ultrapure potassium iodide

KI and silver nitrate  $\text{AgNO}_3$ . Solution of KI was infused under continuous mixing in silver-bath. Mixing of solutions and washing of AgI precipitate were carried out in the dark.

The precipitate were carried over at filter-paper and oven dried at 383 K. Dried AgI was dispersed by mechanical method. Particles dimension was controlled by optical microscope. The AgI outlet purity control was realized using X-ray analysis. X-ray diffraction patterns of investigated specimens were registered using DPOH-4-07 in  $\text{CuK}_\alpha$  emission with nickel filter in reflected rays and Bragg-Brentano observation geometry.

Penton - disperse AgI system specimens were prepared at following thermo-baro-time ( $T-p-t$ ) condition: heating rate 3,5 K/min, aging at 483 K pending 15 min under pressure of 20 MPa, cooling from melt with 0,5 K/min rate, that correspond to better technological conditions of composite recycling with taking into account the filler and polymer matrix properties.

Investigation of penton - AgI system linear expansion in 193 - 493 K temperature rate was carried out using modified linear dilatometer gauge of induction type. As an etalon, an invar alloy was used.

### Results and discussion

For composites containing  $0 \leq \varphi < 100\%$  (vol.) of filler in the temperature range 273 - 343 K, there are four breaks on the curve relative elongation. The first two are related to low temperature component of the glass transition and the other two - with a high temperature component.

The selected temperature dependences of the composite system relative elongation are shown in Fig. 1.

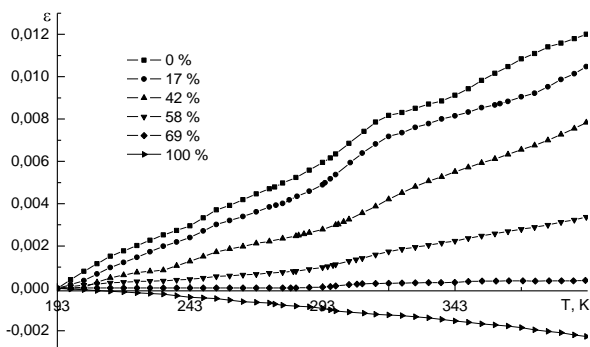


**Fig. 1.** Temperature dependences of the penton - AgI composites relative elongation: 1 - 0 %, 2 - 17 %, 3 - 42 %, 4 - 58 %, 5 - 69 %, 6 - 100 %.

Analysis of composites relative elongation temperature dependences allows to set beginning and ending temperatures of a glass transition components for the polymer matrix and in turn to analyze their concentration dependence.

By the nature of temperature changes  $T = f(\varphi)$  dependences conditionally can be divided into three areas: from 0 to 8 %, from 8 to 42 % and over 42 %.

In the first area, with concentrations from 0 to 8% with content of dispersed AgI increasing some decrease in the glass transition temperature of the beginning of the process is observed which caused by filler structural activity. As the X-ray diffraction research shows, in this concentrations area decrease of the overall penton crystallinity degree is observed. This causes increasing mobility of kinetic units of the polymer chains and promotes their more intense thermal motion.

In the second area, with increasing filler concentration from 8 to 42 %, AgI can play the role of structural nucleus, limiting the mobility of macromolecules individual units near its surface. Therefore beginning temperature of the glass transition process increases.

Further increase of filler content ( $\varphi > 42\%$ ) leads to the appearance of its inhibitory action on the processes of crystal formation in the polymer matrix and therefore, to difficulty of crystallization centers formation and thus to decrease of crystallinity degree and temperature  $T_1$  (third area).

The character of the concentration dependence of ending temperature  $T_2$  of relaxation process is similar to the corresponding beginning temperature  $T_1$  of process. A slight displacement of the temperature  $T_2$  minimum toward the higher concentrations explains the growth of segmental mobility of penton macromolecules due to temperature decrease.

### Conclusions

Thus, due to AgI anomalous negative TCLE value, PCM on its base has TCLE values close to the low molecular materials. In combination of unique thermal conductivity [2] and high chemical and anti-friction penton resistance, above mentioned factor allows to solve the problem of penton and silver iodide composite systems coating durability. In addition, penton - AgI composites are characterized by highly absorptive capacity of ultrasonic and electromagnetic radiation [3,4] which allows using of the systems materials as protective coatings on high-frequency electromagnetic and ultrasonic radiation and significantly expands their application.

1. Shut M.I., Rokitskiy M.A., Rokitskaya G.V., Bashtovyi V.I., Borbich Ju.O. Polymer composite materials based on penton // Scientific Annals of National Pedagogical Dragomanov University, Physical and mathematical sciences, Series 1 (2014) 16 6-23 [in Ukrainian].
2. Rokitskaya G.V., Shut M.I., Rokitskiy M.A., Sichkar T.G. Heat conductivity of polymer composite material based on penton and silver iodide

P43

(AgI) // Proceedings of the 2<sup>nd</sup> CEEP workshop on polymer science. Lasi, Romania, October 24-25 (2014) 215-219.

3. *Shut M.I., Rokitskiy M.A., Rokitskaya G.V., Shut A.M., Levandovskiy V.V.* Physical and mechanical properties of polymer composite materials based on penton and disperse silver iodide // The aerodisperse systems physics 50 (2013) 23-32 [in Ukrainian].

4. *Rokitskiy M.A., Gorbyk P.P., Levandovskiy V.V., Makhno S.M., Kondratenko O.V., Shut M.I.* Electrophysical properties of polymer composites penton - silver iodide system in SF-region // Functional Materials 14 (2007) 1 125-129.

## THE INFLUENCE OF COMPONENT RATIO AND REACTION CONDITIONS ON THE PROPERTIES OF PHOTOCURED EPOXY-ACRYLATE INTERPENETRATING POLYMER NETWORKS

**T. F. Samoilenko, N. V. Iarova, O. O. Brovko**

*Institute of Macromolecular Chemistry of National Academy of Sciences of Ukraine, 48 Kharkivske shausse, Kyiv 02160, Ukraine*  
[s\\_t\\_f@gmail.com](mailto:s_t_f@gmail.com)

At the present stage of development of chemistry and chemical technology the combination of different components in one composite material is an attractive way to obtain new materials with the improved properties. One of the important types of polymer composite materials is an interpenetrating polymer network (IPN), in which the best characteristics of both polymer networks are retained [1]. The aim of this research was to form simultaneous epoxy-acrylate IPNs on the base of acrylic component triethylene glycol dimethacrylate (TEGDM) and epoxy components of different chemical structure: cycloaliphatic triepoxide 1-(2',3'-epoxypropoxymethyl)-1-(2'',3''-epoxypropoxymethyl)-3,4-epoxycyclohexane (E-1), aliphatic diepoxide 1-(2',3'-epoxypropoxy-methyl)-1-(2'',3''-epoxypropoxy-methyl)-cyclohex-3-ene (E-2), and diene bifunctional epoxy resins based on diglycidyl ether of bisphenol A ED-20 (E-3) and Epikote 828 (E-4) in the ratio of 100:0, 50:50, 25:75 and 0:100, and to compare their properties. The polymerization reactions were initiated by means of ultraviolet (UV) radiation of UV-lamp (L) or natural sunlight (S) in a closed (C) or in an opened (O) form, that is, between glass plates or on the glass surface, respectively. A mixture of triphenylsulfonium hexafluorophosphate salts (50% solution in propylene carbonate), 4 wt % of a system, was used as a photoinitiator of both kinds of polymerization (via cationic mechanism of epoxy component and via free radical one of acrylic component). For obtained on the base of the IPNs films such characteristics as gel fraction content, the value of surface hardness and weather resistance were investigated.

The surface hardness of the films, which is represented on a figure, was measured by the pencil test method according to the ASTM D-3363-74. The hardness is determined by the last pencil in a set (ranging from the softest 9B to the hardest 9H) which slate leaves no scratches on its surface.

P44

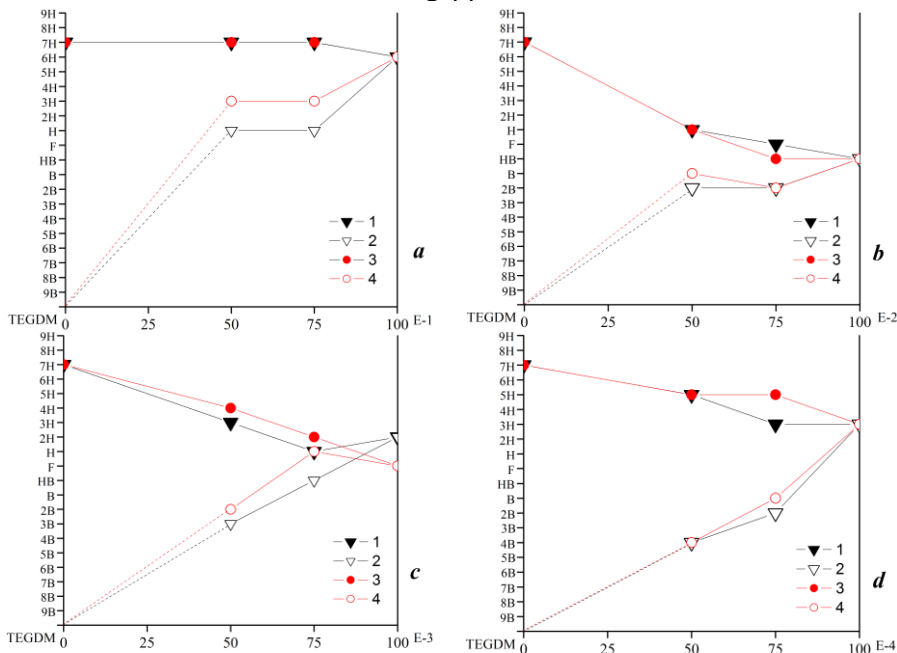


**Fig.** The dependence of surface hardness on the component ratio for IPNs on the base of E-1 (a), E-2 (b), E-3 (c) i E-4 (d), obtained by means of UV-lamp (1, 2) and sunlight (3, 4) in a closed and in an opened form, respectively.

The values of hardness estimated for the samples irradiated with a UV-lamp and sunlight (other factors being equal) almost coincide, which testifies to the effectiveness of applying the sun as a source of UV-radiation for polymerization of given systems. At the same time for the samples cured in the presence of air (fig., curves 2 and 4) and without it (fig., curves 1 and 3) significant differences in the hardness are observed. It is attributed to the oxygen inhibitory effect on the polymerization of TEGDM via free radical mechanism [2]. With the increase of acrylic component in a sample cured in an opened form the hardness of the film descends, while neat TEGDM does not polymerize at all and its hardness tends to be null. Epoxy component in this case serves as a barrier for oxygen diffusion to the system and allows acrylates to polymerize in the presence of air [3]. Among the applied epoxy resins E-1 has the greatest hardness and E-2 has the lowest one, but nevertheless IPNs on the base of E-2 are the least sensitive to reaction conditions, whereas IPNs on the base of E-4 are the most sensitive to them.

The content of gel fraction of obtained samples, which characterizes the completeness of their curing, was calculated by the results of extraction in boiling

acetone for 24 hours and is shown in tables 1 i 2.

**Table 1.** Gel fraction content in the IPNs on the base of aliphatic and cycloaliphatic epoxy resins

Condi- tions / ratio		TEGDM	TEGDM : E-1 = 50:50	TEGDM : E-1 = 25:75	E-1	TEGDM : E-2 = 50:50	TEGDM : E-2 = 25:75	E-2
C	L	99.45	98.5	99.42	100	94.8	94.97	95.06
	S	99.16	97.39	99.4	100	93.89	94.48	95.41
O	L	–	90.7	97.08	100	96.33	95.92	95.16
	S	–	85.22	100	100	92.34	96.25	95.45

**Table 2.** Gel fraction content in the IPNs on the base of diane epoxy resins

Conditions / ratio		TEGDM : E-3 = 50:50	TEGDM : E-3 = 25:75	E-3	TEGDM : E-4 = 50:50	TEGDM : E-4 = 25:75	E-4
C	L	95.08	88.39	92.99	96.16	96.02	97.19
	S	96.4	96.94	94.48	95.08	95.51	97.23
O	L	75.68	91	92.78	79.21	96.38	97.2
	S	93.59	95.92	94.57	94.06	94.77	97.13

High values of gel fraction content means that the degree of conversion of the functional groups in compounds during photopolymerization is also high.

The weather resistance of the obtained films was determined in a climatic cell, in which they were held in strict conditions (humidity – 98%, temperature – 60°C, radiation of UV-lamp with the maximum light intensity at 240 nm) for a month. Changes in mass of the samples after climatic cell are demonstrated in tables 3 ra 4 for IPNs on the base of aliphatic, cycloaliphatic and diane epoxy resins, respectively.

**Table 3.** Changes in mass of the samples of IPNs on the base of aliphatic and cycloaliphatic epoxy resins after climatic cell

Condi- tions / ratio		TEGDM	TEGDM : E-1 = 50:50	TEGDM : E-1 = 25:75	E-1	TEGDM : E-2 = 50:50	TEGDM : E-2 = 25:75	E-2
C	L	2.49	0.18	+1.39	+1.73	1.63	2	2.33
	S	2.47	0.66	+1.2	+1.8	0.48	1.94	2.35
O	L	–	1.94	+1.63	+1.71	1.72	1.64	2.29
	S	–	2.83	+1.31	+1.78	1.98	1.68	2.32

**Table 4.** Changes in mass of the samples of IPNs on the base of diane epoxy resins after climatic cell

Conditions / ratio		TEGDM : E-3 = 50:50	TEGDM : E-3 = 25:75	E-3	TEGDM : E-4 = 50:50	TEGDM : E-4 = 25:75	E-4
C	L	1.68	0.95	0.52	1.06	0.31	+0.48
	S	1.72	0.94	0.31	1.85	0.28	+0.45
O	L	2.45	1.51	0.6	1.07	1.24	+0.39
	S	2.47	1.47	0.55	3.79	1.15	+0.37

The mass of all samples changes slightly, which in general demonstrates their fine weather resistance. For neat epoxy resins, especially for E-1 and E-4, weight increase is observed (marked as a sign «+» in the tables), that corresponds to humidity absorption. For neat TEGDM weight loss is noticed indicating that the reactions of destruction pass. Combination of both components in one IPN allows producing materials with the improved characteristics, namely with minimal changes in sample mass during their operation in weather conditions. For the samples obtained in opened form, weight loss is higher that supplements the results of hardness measuring and also confirms the inhibitory effect of atmospheric oxygen on the polymerization of acrylic component via free radical mechanism.

All in all, the results of the investigation show, that photochemical curing of simultaneous epoxy-acrylate IPNs is an easy and effective way to produce materials with new properties, which, to some extent, may be regulated by varying chemical structure of the components, their ratio and polymerization conditions.

1. *De Brito M., Allonas X., Croutxe-Barghorna C. et al* Kinetic study of photoinduced quasi-simultaneous interpenetrating polymer networks // *Progress in Organic Coatings*. 73 (2012) 186-193.
2. *Decker C., Viet T. N. T., Decker D., Weber-Koehl E.* UV-radiation curing of acrylate/epoxide systems // *Polymer*. 42 (2001) 5531-5541.
3. *Samoilenko T.* The investigation of the curing completeness of epoxy-acrylate formulations depending on their content // *Abstract proceedings of the Eight All-Ukrainian scientific conference of students, post-graduate students and young scientists with international participation «Chemical problems of today», Donetsk.* (2014) 151.

## BIOLOGICALLY ACTIVE METAL CONTAINING POLYURETHANES

**Yu. V. Savelyev, A. N. Gonchar, T.V. Travinskaya**

*Institute of Macromolecular Chemistry, Natl. Acad. of Sci. of Ukraine.  
Kharkovskoe shosse 48, 02160, Kiev, Ukraine*

[lexgon@ukr.net](mailto:lexgon@ukr.net)

Materials containing metal particles of nanometer size exhibit unique physical and chemical properties, and in recent years, they are the objects of intense research. Composites “metal nanoparticle / polymer matrix” are of particular interest since they open the opportunities for structural and functional materials of new generation.

In our work we prepared a biologically active metal containing polyurethane materials based on colloid solutions of silver and copper in polyether.

Preparation of colloidal solutions of metals (Ag, Cu) in the polyether was carried out by Electron beam physical vapor deposition (EB- PVD). This method relates to physical highly productive methods of metals’ nanoparticles obtaining which enables to produce metal (Ag, Cu) colloid solutions with a concentration up to 1000 ppm.

Biological study of metal containing polyurethane nanomaterials have shown that polyurethanes containing Cu and Ag nanometals exhibit bactericidal properties in relation to both gram-positive and gram-negative bacteria, and Candida fungi. These polyurethanes are also bacteriostatically effect on fungi - micromycets.

It was found that during 14 days of cultivation there were no biodegradation products of polymer samples detected in the culture medium, and they did not exhibit toxicity on the cells of tissue culture.

Obtained biologically active metal containing polyurethane materials can be processed into goods for medical purposes (catheters, drains, films, grids and so on) by standard methods of polyurethane processing, as the presence of metal nanoparticles in their structure does not affect the physical properties of the polymer.

## SORPTION / DIFFUSION BEHAVIOR OF NANOSTRUCTURED POLYACRYLAMIDE/SILOXANE HYDROGELS

**O.V. Slisenko, I.M. Bei, V.L. Budzinska, V.V. Levchenko, Ye.P. Mamunya**

*Institute of Macromolecular Chemistry of National Academy of Sciences of Ukraine, 48 Kharkivske shausse, Kyiv 02160, Ukraine*  
[olgasilenko@ukr.net](mailto:olgasilenko@ukr.net)

Creation of new nanocomposite hydrogels with high mechanical and sorption characteristics attracts much scientific interest last years. Few methods of preparation of the organic-inorganic composite hydrogels (OIC) namely introduction of polymer particles [1], nanoclay minerals [2] and carbon nanotubes [3] into the polymers or monomers followed by subsequent cross-linking into (semi)-interpenetrating (sIPN/IPN) polymer networks [4], or formation of independently cross-linked double network hydrogels [5] are widely used. Changing the composition of OIC can provide improved physical-chemical characteristics and resistance to cracks formation of the materials obtained.

A novel nanostructured composite was developed by one-pot polymerization of the organic and inorganic precursors. An organic polymer network was created by polymerization of acrylamide (AAm) in a presence of N,N'-methylene-(bisacrylamide) as a crosslinker, while an inorganic siloxane network was formed in a process of catalytically-induced polycondensation of the aqueous sodium silicate precursor. A series of polyacrylamide/siloxane (PAAm/SiO<sub>2</sub>) hydrogels with different SiO<sub>2</sub> content (up to 35 wt.%) have been successfully prepared by *in situ* polymerization technique. To determine an effect of chemical structure of the OIC hydrogels on its lyophilic characteristics a swelling behavior of materials obtained was studied in details.

FTIR spectral analysis of OICs indicates formation of network structure of the hydrogels obtained by controlled combining both organic (PAAm) and inorganic (silicate) networks. The thermograms of PAAm/SiO<sub>2</sub> nanostructured materials have shown their enhanced thermal stability in comparison with neat organic hydrogel (PAAm) due to formation of thermally stable hybrid hydrogen bonding network between polar amide groups of PAAm and siloxane fragments of inorganic network.

From the analysis of swelling behavior of the hydrogels it was established

that water sorption of individual PAAm has an extreme type of sorption curve, i.e. kinetic curve has well defined maximum after which desorption of water is observed. At the beginning of sorption process the rate of sorption is rather high and is in accordance with Fickian law (Fig.1). PAAm/SiO<sub>2</sub> nanostructured hydrogels corresponds to two-stage swelling model: (1) a rapid increase of the solvent content in the composite that takes place due to PAAm saturation and then after some quasi-equilibrium (2) the solvent concentration increased much slowly. Diffusion coefficient (D) for the composites at the first stage was calculated using “half-saturation” time in accordance with [6].

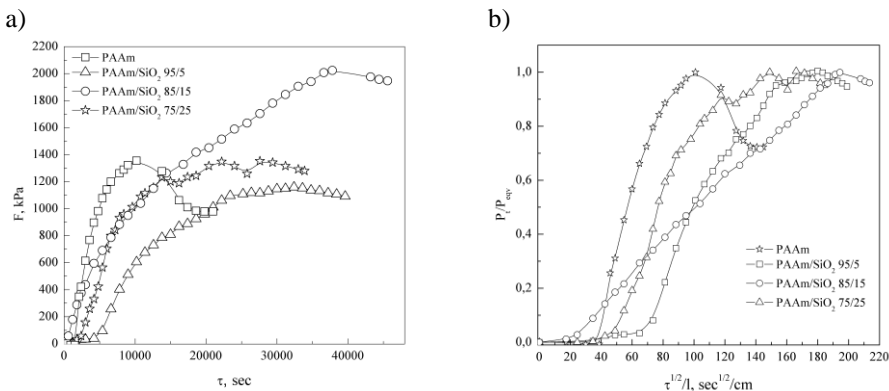


**Fig. 1.** Time-swelling pressure (a) and Fickian sorption curves (b) for PAAm/SiO<sub>2</sub> composites with SiO<sub>2</sub> content: 0, 5, 15 and 25 wt.%.

The D values decreased with increasing inorganic content. However for PAAm/SiO<sub>2</sub> = 75/25 composition it increased again. The equilibrium swelling of the composite hydrogels was much larger than that of the PAAm hydrogel. Even the smallest swelling ratio of PAAm/SiO<sub>2</sub> = 95/5 sample was approximately 3.5 times higher than that of the neat PAAm.

Thus, novel nanostructured hydrogels consisting of organic PAAm and inorganic siloxane networks were synthesized by facile one-pot *in situ* polymerization approach. Spectral study indicates formation of network structure of hydrogel composites obtained. Both DSC and TGA measurements confirm a presence of mixed organic-inorganic hybrid phase that enhances the thermal stability of hydrogel materials. The measured swelling pressures ( $P_{eq}$ ) of PAAm/SiO<sub>2</sub> composites were determined in the range of 1100-2000 kPa. Swelling degree of hybrid composite hydrogels depends on components ratio and reaches 2700 %.

1. *Huang T., Xu H.G., Jiao K.X., Zhu L.P., Brown H.R., Wang H.L.* A novel hydrogel with high mechanical strength: a macromolecular microsphere composite hydrogel // *Advanced Materials*. 19 (2007) 1622–6.
2. *Haraguchi K., Takehisa T.* Nanocomposite hydrogels: a unique organic–inorganic network structure with extraordinary mechanical, optical, and swelling/de-swelling properties // *Advanced Materials*. 14 (2002) 1120–4.
3. *Tong X., Zheng J.G., Lu Y.C., Zhang Z.F., Cheng H.M.* Swelling and mechanical behaviors of carbon nanotube/poly (vinyl alcohol) hybrid hydrogels // *Materials Letters*. 61 (2007) 1704–6.
4. *Lee W.F., Chen Y.J.* Studies on preparation and swelling properties of the N-isopropylacrylamide/chitosan semi-IPN and IPN hydrogels // *JAPS*. 82 (2001) 2487–96.
5. *Gong J.P., Katsuyama Y., Kurokawa T., Osada Y.* Double-network hydrogels with extremely high mechanical strength // *Advanced Materials*. 15 (2003) 1155–8.
6. *Schwob J.M., Guyot C., Richard J.* The effect of latex/polymer properties on blister resistance of coated papers // *Tappi Journal (Coating Conference)* (1991) 65-72.

## **HYPERBRANCHED PROTIC OLIGOMERIC ANIONIC LIQUIDS**

**O. A. Sobko, A. V. Stryutskyi, N. S. Klymenko, M. A. Gumenna,  
A. A. Fomenko, V. V. Klepko, V. V. Shevchenko**

*Institute of Macromolecular Chemistry of National Academy of Sciences of Ukraine, 48 Kharkivske shausse, Kyiv 02160, Ukraine*  
[lgsobko@meta.ua](mailto:lgsobko@meta.ua)

Ionic liquids (ILs) are well known for their exceptional physical properties, such as non-volatility, high thermal and chemical stability, high ionic conductivity, non-flammability, wide electrochemical window and tunable solubility [1].

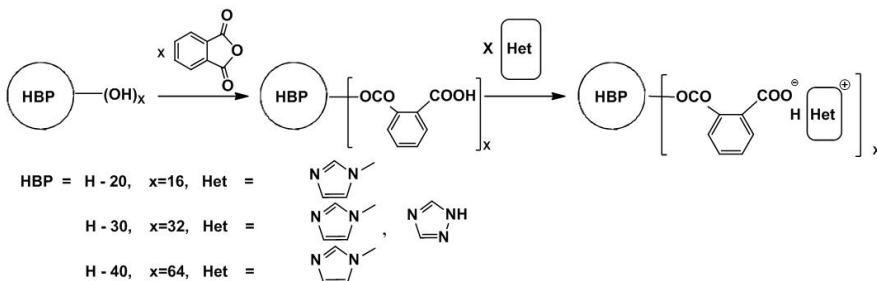
Polymerized ILs or as they are known as polymeric ILs combine the unique properties of the monomer ionic liquids with the macroproperties of polymeric systems, but lose the ability to exist in the liquid state in a wide temperature range [2, 3]. Therefore, it is most reasonable to classify such compounds as polymeric analogs of ionic liquids [2].

At the same time the oligomeric form of ILs, which is intermediate between monomeric and polymeric ILs, is poorly highlighted in literature and the term oligomeric ionic liquids (OILs) was proposed by us for these class of compounds in analogy with polymeric ILs [4,5]. OILs are of great interest in scientific and practical aspects due to a combination of unique properties of ionic liquids with the peculiarities of the oligomeric state of matter [4,5].

In this area promising are the development of methods for the synthesis of the hyperbranched OILs terminated with ionic groups. The globular shape of such OILs enables low viscosity and their multifunctionality provides high density of ionic groups on the molecule surface at relatively low molecular weight[6-8].

In this study the method of synthesis of hyperbranched protic anion carboxylate OILs terminated with methylimidazolium and triazolium cations was developed. The synthesis of these compounds is based on complete acylation of the aliphatic polyester polyols Boltorn® of three generations (H-20, H-30, H-40) with phthalic anhydride followed by neutralizing the resulting oligomeric acid by N-methylimidazole and 1,2,4-triazole.

P47



Synthesized OILs were characterized by FTIR and <sup>1</sup>H NMR spectroscopy. They are solid materials with low temperature of transition in viscous state in the temperature range 40-60°C. These compounds soluble in polar organic solvents. According to DSC glass transition temperatures of the OILs are about -15°C. The synthesized OILs is thermostable up to 150-180°C.

It was found with use of dielectric relaxation spectroscopy that the proton conductivity of these compounds is in the range 10<sup>-5</sup>-10<sup>-4</sup> S/cm at 100-120°C under anhydrous conditions. It is shown that the conductivity of these OILs depends on the generation number of polyether polyols that were used in the synthesis (with increasing generation numbers a conductivity decrease was observed). In addition, the conductivity depends on the counterion (conductivity of triazolium OIL is higher than that of methylimidazolium OIL).

1. Hallett J.P., Welton T. Room-temperature ionic liquids: solvents for synthesis and catalysis // Chem Rev. 111 (2011) 3508-3576.
2. Shaplov A.S., Ponkratov D.O., Vlasov P.S., Lozinskaya E.I., Komarova L.I., Malyshkina I.A., Vidal F., M. Nguyen G.T., Armand M., Wandrey C., Vygodskii Ya.S. Synthesis and properties of polymeric analogs of ionic liquids. Polym Sci B. 55(2013) 122-138.
3. Yuan J., Meccerreyes D., Antonietti M. Poly(ionic liquid)s: an update // Progr Polymer Sci. 38 (2013) 1009-10036.
4. Shevchenko V.V., Strytsky A.V., Klymenko N.S., Gumenna M.A., Fomenko A.A., Bliznyuk V.N., Trachevsky V.V., Davydenko V.V., Tsukruk V.V. Protic and aprotic anionic oligomeric ionic liquids // Polymer. 55 (2014) 3349-3359.
5. Shevchenko V.V., Strytsky A.V., Klymenko N.S., Gumennaya M.A., Fomenko A.A., Trachevsky V.V., Davydenko V.V., Bliznyuk V.N., Dorokhin A.V. Protic cationic oligomeric ionic liquids of the urethane type // Polymer Sci B. 56 (2014) 583-592.
6. Peleshanko S., Tsukruk V.V. The architectures and surface behavior of highly branched molecules // Prog Polym Sci. 33 (2008) 523-580.
7. McKee M.G., Unal S., Wilkes G. L. et al. Branched polyesters: recent

P47

advances in synthesis and performance // *Ibid.* 30 (2005) 507–539.

8. *Kerscher B., Appel A.-K., Thomann R. et al.* Treelike polymeric ionic liquids grafted onto graphene nanosheets // *Macromolecules.* 46 (2013) 4395-4402.

## **ALKOXYSILYL PROTIC OLIGOMERIC IONIC LIQUID AND ORGANIC-INORGANIC PROTON-EXCHANGE MEMBRANES BASED ON IT**

**A. V. Stryutskiy<sup>1</sup>, N. S. Klimenko<sup>1</sup>, M. A. Gumenna<sup>1</sup>, Yu. V. Yakovlev<sup>1</sup>,  
O. A. Sobko<sup>1</sup>, S. I. Lobok<sup>1</sup>, V. V. Korskanov<sup>1</sup>, S. N. Ostapiuk<sup>1</sup>, E.A. Lysenkov<sup>2</sup>,  
V. V. Klepko<sup>1</sup>, V. V. Shevchenko<sup>1</sup>**

*<sup>1</sup>Institute of Macromolecular Chemistry of National Academy of Sciences of Ukraine, 48 Kharkivske shausse, Kyiv 02160, Ukraine*  
[stryutskiy@ukr.net](mailto:stryutskiy@ukr.net)

*<sup>2</sup>Mykolayiv National University V.O. Sukhomlynskiy, 24 Nikolska Str., Mykolayiv 54030, Ukraine*  
[calisenkov@mail.ru](mailto:calisenkov@mail.ru)

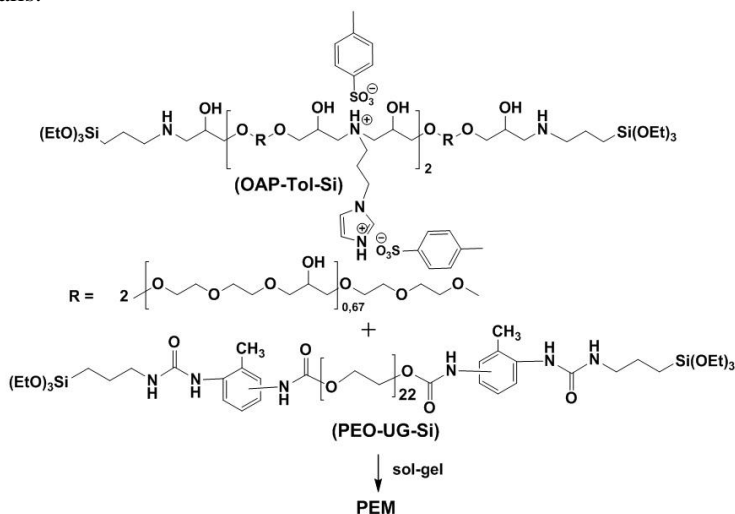
One of the main directions of a polymer electrolyte fuel cells development is to impart them with ability to operate under anhydrous conditions at temperatures above 100°C [1]. A promising solution for this problem is the creation of nanostructured hybrid organic-inorganic polymeric proton-exchange membranes (PEM) via sol-gel method [2,3]. Presence of inorganic silsesquioxane framework as a part of such membranes provides their high thermal stability and mechanical strength and the organic component gives them the necessary flexibility [2]. Another approach to improve the efficiency of polymer electrolyte fuel cells is a replacement of aqueous proton-exchange medium in PEMs with anhydrous one [2]. The use of ionic liquids as such alternative water-free proton-exchange media, which, however, tend to diffuse from the bulk membrane, is very promising [2,4]. At the same time the direction of use for PEM synthesis of protic oligomeric ionic liquids (OILs), which combine the high conductivity of low molecular ionic liquids and the high viscosity of oligomeric compounds, preventing their diffusion [5], and oligoether ion-conductive component remains undeveloped.

In the present study a method for the synthesis of alkoxy-silyl protic OIL (OAP-Tol-Si), which combines the ability to sol-gel transformations, proton-donor and proton-conducting properties, and a method for producing the organic-inorganic PEMs based on that OIL were developed.

Synthesis of OIL OAP-Tol-Si was performed by reaction of excess of

aliphatic epoxy oligomer with 1(3-aminopropyl) imidazole followed by blocking of terminal epoxy groups of the obtained oligomer with 3-aminopropyltriethoxysilane and neutralization of basic groups with 4-toluenesulfonic acid. It should be emphasized that the presence of triethoxysilyl groups as a part of OIL gives it the ability to hydrolytic condensation. The imidazolium tosylate ionic liquid groups provide the proton-donor properties and being combined with the oxyethylene component the proton-conductive properties of the synthesized OIL. As a cooligomer for the PEMs synthesis the oligoethyleneoxyde derivative (PEO-UG-Si) MM 1000 with urethaneurea triethoxysilyl terminal fragments was used.

PEMs synthesis was carried out both by hydrolytic homopolycondensation of OIL OAP-Tol-Si obtained in this work and by joint condensation of it with the oligomer PEO1000-UG-Si at their ratios of 25: 75; 50: 50; 75: 25 respectively. The sol-gel process was carried out using 0.1 N HCl in amount providing a stoichiometric ratio of water to ethoxy groups. The synthesized materials are transparent flexible films that are insoluble in organic solvents, dilute acids and alkalis.



Chemical structure of the synthesized OIL and POMs based on it was studied by FTIR spectroscopy. According to DSC results these membranes are amorphous and their T<sub>g</sub> values are in the negative temperature region. In this case a decrease in T<sub>g</sub> with increase in content of the oligoethyleneoxyde cooligomer PEO1000-UG-Si was observed which is due to the influence of flexible oligoether fragments. The synthesized membranes are thermally stable up to (230-250)°C and the values of their static exchange capacity depending on the content of OIL are (0,48-1,88) mequiv/g. The proton conductivity of the synthesized materials under anhydrous conditions was studied with use of dielectric relaxation spectroscopy

and amounts ( $10^{-5}$ - $10^{-4}$ ) S/cm at temperatures of 100-120°C. The increase in conductivity and thermal stability of POMs was observed with increase of OIL content in their composition.

1. Luo W.-H., Zhao L.-H. Inorganic-organic hybrid membranes with anhydrous proton conduction prepared from tetraethoxysilane, 3-glycidyloxypropyltrimethoxysilane, trimethyl phosphate and diethylethylammonium trifluoromethanesulfonate // J Membr Sci. 451 (2014) 32-39.
2. Shevchenko V.V., Stryutskii A.V., Klimenko N.S. Polymeric organic-inorganic proton-exchange membranes for fuel cells produced by the sol-gel method // Theor Exp Chem. 47 (2011) 67-92.
3. Membreno D., Smith L., Dunn B. Silica sol-gel chemistry: creating materials and architectures for energy generation and storage // J Sol-Gel Sci Technol. 70 (2014) 203-215.
4. Shevchenko V.V., Stryutskii A.V., Bliznyuk V.N., Klimenko N.S., Shevchuk A.V., Lysenkov E.A., Gomza Yu.P. Synthesis, structure, and properties of anhydrous organic-inorganic proton-exchange membranes based on sulfonated derivatives of octahedral oligosilsesquioxanes and  $\alpha,\omega$ -di(triethoxysilyl) oligo(oxyethylene urethane urea) // Polymer Sci B. 56 (2014) 216-228.
5. Shevchenko V.V., Stryutsky A.V., Klymenko N.S., Gumennaya M.A., Fomenko A.A., Trachevsky V.V., Davydenko V.V., Bliznyuk V.N., Dorokhin A.V. Protic cationic oligomeric ionic liquids of the urethane type // Polymer Sci B. 56 (2014) 583-592.

## IONIC LIQUIDS BASED ON POLYMERIC QUATERNARY SALTS OF AMMONIUM (MORPHOLINE DERIVATIVES)

O. S. Sverdlikov'ska, M. V. Burmistr

*State higher educational establishment «Ukrainian state university of chemical technology», 8, Gagarina str., Dnipropetrovsk 49005, Ukraine*  
[osverdlikovska@rambler.ru](mailto:osverdlikovska@rambler.ru)

Ionic liquids (IL) are melts of organic salts that are liquid at a wide temperature range [1]. The unique physical and chemical properties of IL determine their applicability in various fields of science and technology [1-5].

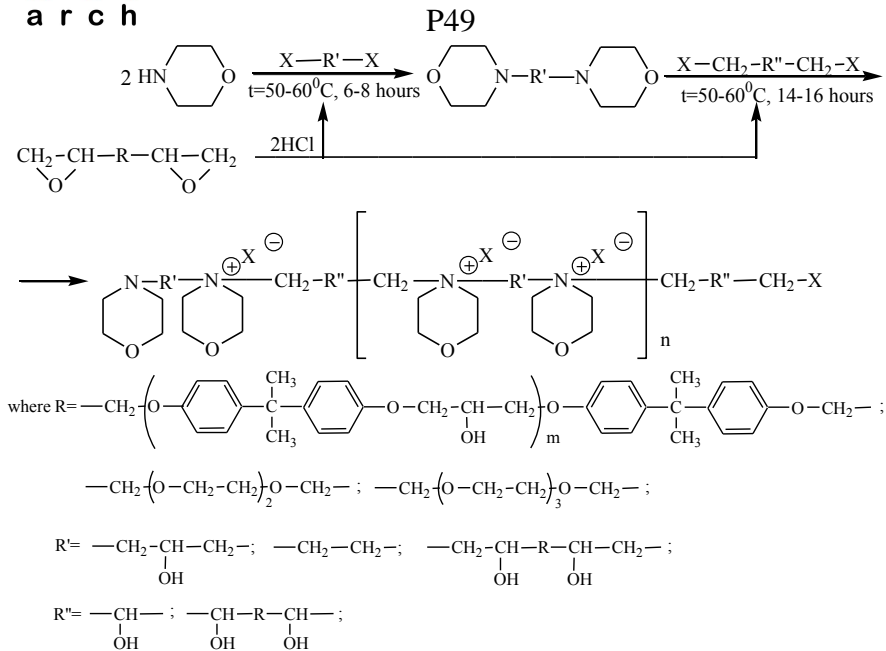
Introduction of the latest science and technology, the emergence of new technologies, materials and energy sources have led to revolutionary changes in society. Mankind has entered the era of scientific and technological revolution that strengthened the human impact on nature. So important is to solve environmental problems. One way to solve many environmental problems associated with emissions from chemical plants, is the use of "green chemistry" – low temperature, thermo stable IL, workable in the temperature range up  $-65^{\circ}\text{C}$  to  $+65^{\circ}\text{C}$  [4]. IL are expensive for a wide range of areas of use, therefore reducing the cost of these compounds is important.

It have been known a large number of works about IL with different organic anionic and cationic organic or inorganic parts. The special interest are promising thermostable low temperature IL based on mono- and bisfunctional quaternary salts of ammonium (morpholine derivatives) with high ionic conductivity [6].

The polyionens (PI) are particular interest among the high-molecular compounds [7]. The unique properties of the impact and effectiveness of PI on different systems and processes associated with a molecular weight and topological structure of macromolecules; charge distributed in the chain of the macromolecule; and functional groups.

Therefore directed synthesis of polymeric quaternary salts of ammonium (morpholine derivatives) – ionic liquids (ILPQASM) is a new type of scientific and practical interest.

In order to continue research synthesis poliquaternary ammonium bases based on morpholine were studied the reactions of polycondensation equimolecular amounts of tertiary diamines based on morpholine and aliphatic alkyl aromatic dihalides. Synthesis have been conducted by Fig. 1:



X= Cl, Br.

**Fig. 1.** Synthesis PQASM.

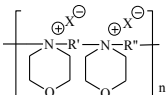
When planning a synthesis the scheme using morpholine for the synthesis of tertiary diamine was chosen. The tertiary diamine has been obtained by a reaction of morpholine with dihalide. The reaction of synthesis (at twice the excess morpholine) has been held at 50-60<sup>0</sup>C for 6-8 hours. As an initial monomers for the synthesis of target PQASM with high yields were identified tertiary diamines based morpholine and 1,3-dihlorpropanol-2, dibromethane, bishalide derivatives ED-20, TEG-1, DEG-1. It has been established [10, 11] that the reactions of bishalide derivatives with morpholine occur by nucleophilic substitution of chlorine atoms in the amino group.

As dihalides (as for the synthesis of tertiary diamines, and as a monomer for the synthesis PQAS) have been used 1,3-dihlorpropanol-2, dibromethane and dihalide derivatives of biepoxyde compounds such as alkylaromatic, and aliphatic structure. The synthesis bishalides has been carried out by known techniques [12], which occurs by nucleophilic attack of unsubstituted agent, spatially more accessible hydrogen atom. The protonation biepoxyde compounds of the oxygen atom occurs on the rapid and reversible first stage with the formation okson-ring. In the second slow stage, the nucleophilic attack of halide ion of proton form of biepoxyde compounds.

The synthesis of PQAS based on morpholine and alkylaromatic, aliphatic dihalides has been performed by Menshutkina reaction (Figure 1). The estimated number of tertiary diamine has been mixed with equimolecular number of dihalide. The initial monomers have been dissolved in acetone. The synthesis was been carried out at a temperature of 50-60<sup>0</sup>C within 14-16 hours. The synthesized PQASM are water-soluble compounds, so the addition of water in the reaction mixture leads to a shift of the equilibrium towards the formation PQAS. It is known that this type of interaction occurring on the mechanism of bimolecular nucleophilic substitution.

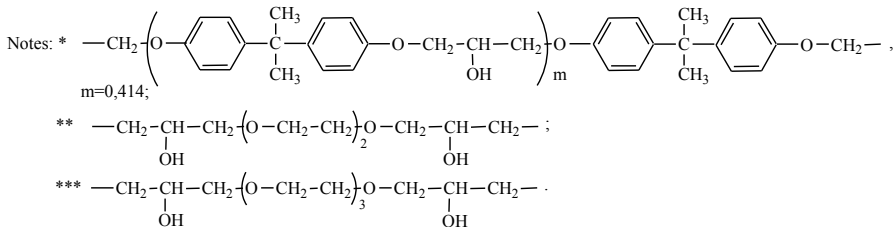
The properties of synthesized PQASM are shown in Table 1. The synthesized PQASM are low-temperature amber color IL of a new type.

**Table 1.** The properties of synthesized PQASM of general formula



R'	R''	X	n	Refractive index ( $d_{20}^{20}$ )	Density ( $d_{20}^{20}$ ), kg/m <sup>3</sup>
$\text{---CH}_2\text{---CH---CH}_2\text{---}$   OH	*	Cl	9	1,5280	910
$\text{---CH}_2\text{---CH---CH}_2\text{---}$   OH	**	Cl	12	1,5210	930
$\text{---CH}_2\text{---CH---}$   OH	***	Cl	15	1,5250	850
*	**	Cl	11	1,5245	920
*	$\text{---CH}_2\text{---CH---CH}_2\text{---}$   OH	Cl	7	1,2956	1115
**	$\text{---CH}_2\text{---CH---CH}_2\text{---}$   OH	Cl	13	1,4132	730
***	$\text{---CH}_2\text{---CH---CH}_2\text{---}$   OH	Cl	10	1,2830	1429
**	*	Cl	11	—	—
$\text{---CH}_2\text{---CH}_2\text{---}$	$\text{---CH}_2\text{---CH---CH}_2\text{---}$   OH	Cl	15	1,1900	—
$\text{---CH}_2\text{---CH}_2\text{---}$	*	Cl	10	1,3910	1248
$\text{---CH}_2\text{---CH}_2\text{---}$	**	Cl	14	1,2200	—
$\text{---CH}_2\text{---CH}_2\text{---}$	***	Cl	19	1,2957	1590
$\text{---CH}_2\text{---CH---CH}_2\text{---}$   OH	$\text{---CH}_2\text{---CH}_2\text{---}$	Br	13	—	—
*	$\text{---CH}_2\text{---CH}_2\text{---}$	Br	16	0,3200	—
**	$\text{---CH}_2\text{---CH}_2\text{---}$	Br	26	1,3433	1419
***	$\text{---CH}_2\text{---CH}_2\text{---}$	Br	23	0,4700	—

P49



The resistance to thermo-oxidative destruction, physical and chemical properties of PQASM has been studied. It is established that the synthesized PQASM thermally stable up to 100–150<sup>0</sup>C.

The ionic conductivity of new PQSAM has been studied (Fig. 2).

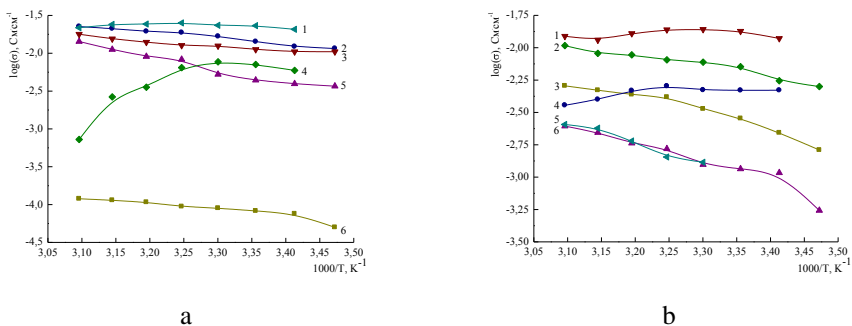


**Fig. 2.** Temperature (1000/T) dependence of ionic conductivity ( $\log \sigma$ ) ILPQSM: 1a–C-7-1, 2a–C-1-7, 3a–C-9-1, 4a–C-1-8, 5a–C-8-1, 6a–C-1-9; 1b–C-13-7, 2b–C-13-8, 3b–C-7-13, 4b–C-8-13, 5b–C-13-9, 6b–C-9-13

New promising low temperature PQASM are a new type of ionic liquids with high ionic conductivity ( $10^{-6}$ – $10^{-2} \text{ Cm}\cdot\text{cm}^{-1}$ ) has been synthesized for the first time.

PQASM can be recommended for use as a component of liquid and polymer electrolytes for electrochemical devices of a new type.

1. N.V. Shvedene, D.V. Chernyshev, I.V. Pletnev. Ionic liquids in electrochemical sensors // Journal. Rush. chem. Society of D.I. Mendeleev. – 2008. – T. LH. – № 2. – P.80-91. (In Russ.)
2. N.V. Ignatiev, W. Welz-Biermann, H. Wilner. New promising ionic liquids // Journal. Rush. chem. Society D.I. Mendeleev. – 2004. – T. XLVIII. – № 6. – P.36-39. (In Russ.)
3. Y.S. Profitable, E.I. Lozinskaya, A.S. Shapley. Synthesis of polymers in ionic liquids // Journal. Rush. chem. Society D.I. Mendeleev. – 2004. – T. XLVIII. – № 6. – P. 40-50. (In Russ.)

4. L.M. Kustov. Ionic liquids – a breakthrough into a new dimension? // Chemistry and Life. – 2007. – № 11. – P.36-41. (In Russ.)
5. V.V. Dotsenko. Ionic liquids: new prospects for refractometric analysis // Ukrainian Metrology journal. – 2008. – № 3. – P.53-57. (In Russ.)
6. E.P. Mamunya, E.V. Lebedev, M.V. Yurzhenko, V.V. Levchenko, O.V. Chervakov, D.C. Matkovskaya, O.S. Sverdlikovska. Ionic liquid. Polymer electroactive materials – 2013. – P. 151-229. (In Ukr.)
7. M.V. Burmistr, E.M. Burmistr. Alkylaromatic polyionenes. – Dnepropetrovsk: UGHTU, 2005. – 131 p. (In Russ.)
8. L.A. Kazitsyna, N.B. Kupletskaya. Application of UV, IR and NMR spectroscopy in organic chemistry. – M.: Higher. Sch., 1971. – 264 p. (In Russ.)
9. J. Shestak. Theory of thermal analysis: Per. from English. – M.: Mir, 1987. – 456 p. (In Russ.)
10. S.Z. Kaplan, N. Zakharov, A.S. Zvontsova, N.V. Chrome-Borisov, S.P. Kozhevnikov, L.V. Pavlyuchenkova. Morpholine derivatives. IV. The interaction of methyl iodide and halogen acids with derivatives oksiziklobutana containing morfolinometil substituents // Chemistry of Heterocyclic Compounds. – 1974. – № 10. – P.1320-1324. (In Russ.)
11. Henry R.A, Dean W.M. // J. Am. Chem Soc. – 1952. – № 1. – P.257.
12. V.H. Shapka. Synthesis and properties of polyelectrolyte of cationic type based on epoxide compounds: Dis... Cand. chem. Sciences: 02.00.06. – Dnepropetrovsk, 1987. – 179 p. (In Russ.)

## MULTI-COMPONENT POLYMER SYSTEMS COMPRISING DIFFERENT BIO-BASED FILLERS

**E0/C0Vgce .T0Dqf ,tn w.'N0Tq w.'P0Vwf qtcej k'F0Tq w**

*“Petru Poni” Institute of Macromolecular Chemistry, 41A Grigore Ghica Voda Alley, Iasi 700487, Romania*

*G/o chI"cf ft gu r'ecv gcec B leo r r0 q"*

Nowadays, ecological concern has resulted in a renewed interest in natural composite materials and issues such as recyclable features and environmental protection are becoming increasingly important for the introduction of new materials and products. At this moment, eco-design concept is applied to more and more materials and products. The development of advanced polymer materials for various sustainable applications requires the obtainment of polymer composites from low-cost, environmental friendly, renewable and biodegradable resources (with natural biopolymers in their structure), with main focus upon enhanced multifunctional properties (e.g. thermal stability, impact resistance, water resistance, photo-stability) and reduced impact as pollution effects under environmental disposal conditions [1-5]. Multi-component polymer systems comprising different biobased fillers (hardwood sawdust, softwood needles, hardwood lignin) within plasticized starch matrix have been obtained. Particle size analysis, Fourier Transform Infrared (FTIR) spectroscopy, X-ray diffraction, scanning electron microscopy (SEM), and TG/DTG/DTA simultaneous thermal analysis methods were used for polymer systems characterization.

*Acknowledgements.* This work was supported by a grant of the Romanian National Authority for Scientific Research CNCS-UEFISCDI Project number PN-II-ID-PCE-2011-3-0187.

1. *Faruk O., Bledzki A.K., Fink H.P., Sain M.* Progress report on natural fiber reinforced composites // *Macromol Mater Eng.* 299 (2014) 9–26.
2. *Isogai A.* Wood nanocelluloses: fundamentals and applications as new bio-based nanomaterials // *J Wood Sci.* 59 (2013) 449–459.
3. *Huber T., Müssig J., Curnow O., Pang S., Bickerton S., Staiger M.P.* A critical review of all-cellulose composites// *J Mater Sci.* 47 (2012) 1171–1186.
4. *Blaker J.J., Lee K.Y., Bismarck A.* Hierarchical composites made entirely from renewable resources // *J Biobased Mater Bioenergy.* 5 (2011) 1-16.
5. *Habibi Y., Lucia L.A., Rojas O.J.* Cellulose nanocrystals: chemistry, self-assembly, and applications // *Chem Rev.* 110 (2010) 3479–3500.

## ULTRAFAST SPECTROSCOPY. STUDY OF THE NON-RADIATIVE PROCESS

**I. R. Tigoianu<sup>1</sup> and M. Chergui<sup>2</sup>**

<sup>1</sup>*"Petru Poni" Institute of Macromolecular Chemistry, Aleea Grigore Ghica Voda, 41A, Iasi-700487, Romania*

<sup>2</sup>*Laboratoire De Spectroscopie Ultrarapide, École Polytechnique Fédérale De Lausanne, ISIC, FSB, CH-1015 Lausanne, Switzerland*

In this presentation, the ultrafast spectroscopy (ultrafast fluorescence up-conversion and transient absorption spectroscopy) was used for to understand, learn about these techniques and to investigate and characterize the non-radiative processes, that consist of different mechanisms such as internal conversion (IC, non-radiative transitions between states of similar spin) and intersystem crossings (ISC, transitions between states of different symmetries) [1].

Fluorescence up-conversion [2] on the fs time scale that measures only the fluorescence of the sample is a complementary tool to transient absorption spectroscopy where we have present contributions from the ground state bleach (GSB) and excited state absorption (ESA) for to address relaxation dynamics in molecular systems.

The ultrafast spectroscopy can be used not only for the fundamental information about photophysics of molecular systems, but also for the present and potential applications that offer these systems in the field of solar energy conversion, light emitting devices, etc.

1. *Chergui M.* On the interplay between charge, spin and structural dynamics in transition metal complexes. *Dalton Trans.* 41 (2012) 13022-13029.
2. *Cannizzo A., Bram O., Zgrablic G., Tortschanoff A., Ajdarzadeh Oskouei A., Van Mourik F., and Chergui M.* Femtosecond fluorescence upconversion setup with broadband detection in the ultraviolet. *Optics Letters* 32, (2007) 3555-3557.

## SYNTHESIS OF STAR-SHAPED MOLECULES BASED ON POLYHEDRAL OLIGOMERIC SILSESQUIOXANE AND AZOBENZENE DYE WITH TRIMETHYLSILYLOXYMETHYLENE GROUPS

**I. M. Tkachenko, Ya. L. Kobzar, A. V. Sidorenko,  
O.V. Shekera, V.V. Shevchenko**

*Institute of Macromolecular Chemistry of National Academy of Sciences of  
Ukraine, 48 Kharkivske shausse, Kyiv 02160, Ukraine*  
[tkachenko\\_im@i.ua](mailto:tkachenko_im@i.ua)

Organic-inorganic oligomeric silsesquioxanes with a general formula  $\text{RSiO}_{3/2}$  are widely used to improve the thermal, mechanical, and optical properties of nanocomposite materials [1-3]. Conjugation of organic chromophores to polyhedral oligomeric silsesquioxane (POSS) core was shown to increase the thermo- and photostability of dyes and enhance optical properties. Furthermore, the bulky POSS core disrupts the stacking of conjugated molecules, therefore increasing fluorescence efficiency. The amorphous character of these conjugates results in solution processability, which makes it possible to manufacture nanocomposites by versatile wet chemistry approaches [3-5].

Organic dyes containing an azobenzene fragment are used extensively as tunable chromophores and light-responsive moieties due to reversible trans-cis photoisomerization [6]. Therefore, attachment of photoresponsive azo dyes to POSS (Azo-POSS) may result in novel hybrid materials with broad applications. Several recent studies demonstrated the utility of this approach by grafting simple azobenzenes onto cubic POSS cages [3, 7, 8].

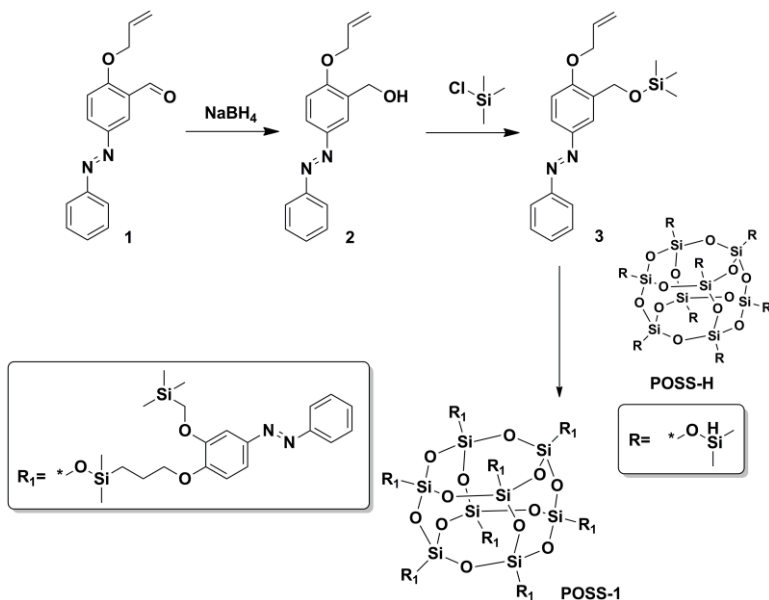
Recently, to elucidate the role of azobenzene conjugation, we utilized two Azo-POSS compounds, with different spacer lengths between the inorganic core and the azobenzene moiety [3, 7]. As is known, the linker length has a pronounced effect on thermal cis-to-trans relaxation [9]. It was shown the branched conjugate with a long spacer between the core and the azobenzene branches (Azo-POSS 1) undergoes photoisomerization in solution but not in an ultrathin solid film due to the aggregation of azo dyes. The thin film of Azo-POSS conjugate with a shorter spacer between the core and the azobenzene moieties (Azo-POSS 2), however, exhibited a pronounced change in intensity of the  $\pi-\pi^*$  transition at 350 nm, indicating efficient trans-to-cis isomerization [7].

On the other hand, atomic force microscopic revealed that Azo-POSS 1

yielded a smooth film, but Azo-POSS 2 under the same conditions gave a somewhat less uniform film. In this case, formation of crystalline domains and up to 30 nm deep cavities was observed on the film surface [7]. Incorporation of bulky groups into chromophore of POSS molecules can prevent of Azo-POSS conjugate crystallization. Additionally, these chemical groups can serve as so-called suitable isolation groups or SIG groups. SIG groups are introduced to decrease the intermolecular dipole–dipole interaction of chromophore fragments [10].

Therefore, the aim of this study was to synthesize new azobenzene dye having side bulky trimethylsilyloxymethylene (TMSOM) groups as well as to prepare highly substituted Azo-POSS structure based on obtained azo-dye via hydrosilylation coupling.

Synthesis of azo-dye 3 containing TMSOM units was accomplished by reaction of aldehyde groups of dye 1 with NaBH<sub>4</sub> followed by interaction of the newly obtained OH-substituted dye 2 with trimethylchlorosilane (Scheme). Substituted POSS-Azo-dye conjugate (POSS-1) was prepared using a hydrosilylation approach with octakis(dimethylsilyloxy)silsesquioxane (POSS-H) as a scaffold for the attachment of azo-dye 3 bearing reactive allyloxy groups (Scheme).



**Scheme.** The route of synthesis of compounds 2, 3 and POSS-1.

It should be noted that the protection of OH groups of dye 2 is essential because OH groups react with Si-H bonds under the conditions used (O-silylation) [11]. So, in addition to serving as a protective group, trimethylsilyl (TMS) groups as part of TMSOM fragments serve as SIG groups, in other words, TMS protecting groups serve dual purposes.

The molecular structure of the synthesized dye 2, dye 3 and POSS-1 was confirmed with FTIR, UV-Vis, <sup>1</sup>H and <sup>13</sup>C NMR spectroscopy, i.e. the results were consistent with the structure of the compounds shown in Scheme. It should be noted that <sup>1</sup>H NMR spectroscopy indicated nearly complete modification of the octavalent POSS core with azo dyes

Compounds 2 and 3 have a typical azobenzene absorbance with a strong  $\pi-\pi^*$  band at 348 nm and a weaker  $n-\pi^*$  transition at around 430 nm. The UV-vis spectra of compounds 3 and POSS-1 in chloroform solutions are very similar. The absence of a pronounced shift of absorbance peak positions before and after dye conjugation to the POSS core indicates that in dilute solution aggregation is insignificant.

In a summary, we have developed synthetic routes for new hydroxyl- and TMSOM-containing azo-dyes. Based on dye with TMSOM groups, a highly substituted Azo-POSS (POSS-1) was synthesized. The structure of the synthesized compounds was determined by FTIR, UV-Vis, <sup>1</sup>H NMR and <sup>13</sup>C NMR spectrometry techniques.

### Acknowledgments

*This work was supported by grant of the National Academy of Sciences of Ukraine No 0115U005242.*

1. Zhang W. A., Muller A. H. E. Architecture, self-assembly and properties of well-defined hybrid polymers based on polyhedral oligomeric silsesquioxane (POSS) // Prog. Polym. Sci. 38 (2013) 1121–1162.
2. Kuo, S. W., Chang, F. C. POSS related polymer nanocomposites // Prog. Polym. Sci. 36 (2011) 1649–1696.
3. Ledin P. A., Tkachenko I. M., Xu W., Choi I., Shevchenko V. V., Tsukruk V. V. Star-shaped molecules with polyhedral oligomeric silsesquioxane core and azobenzene dye arms // Langmuir, 30 (2014) 8856–8865.
4. Pu K. Y., Li K., Liu B. Cationic oligofluorene-substituted polyhedral oligomeric silsesquioxane as light-harvesting unimolecular nanoparticle for fluorescence amplification in cellular imaging // Adv. Mater. 22 (2010) 643–646.
5. Lo M. Y., Zhen C., Lauters M., Jabbour G. E., Sellinger A. Organic–inorganic hybrids based on pyrene functionalized octavinylsilsesquioxane cores for application in OLEDs // J. Am. Chem. Soc.

129 (2007) 5808–5809.

6. *Merino E.* Synthesis of azobenzenes: The coloured pieces of molecular materials // *Chem. Soc. Rev.* 40 (2011) 3835–3853.

7. *Ledin P. A., Russell M., Geldmeier J. A., Tkachenko I. M., Mahmoud M. A., Shevchenko V.V., Tsukruk V. V.* Light-Responsive Plasmonic Arrays Consisting of Silver Nanocubes and a Photoisomerizable Matrix // *ACS Appl. Mater. Interfaces* 7 (2015) 4902-4912.

8. *Chi H., Mya K. Y., Lin, T. T., He C. B., Wang F. K., Chin W. S.* Thermally stable azobenzene dyes through hybridization with POSS // *New J. Chem.* 37 (2013) 735–742.

9. *Miniewicz A., Girones J., Karpinski P., Mossety-Leszczak B., Galina H., Dutkiewicz M.* Photochromic and Nonlinear Optical Properties of Azo-Functionalized POSS Nanoparticles Dispersed in Nematic Liquid Crystals // *J. Mater. Chem. C* 2 (2014) 432–440.

10. *V.V. Shevchenko, A.V. Sidorenko, V.N. Bliznyuk, I.M. Tkachenko, O.V. Shekera, N.N. Smirnov, I.A. Maslyanitsyn, V.D. Shigorin, A.V. Yakimansky, V.V. Tsukruk.* Synthesis and properties of hydroxylated core-fluorinated diamines and polyurethanes based on them with azobenzene nonlinear optical chromophores in the backbone // *Polymer* 54 (2013) 6516-6525.

11. *Marciniac B., Maciejewski H., Pietraszuk C., Pawluc P., Gulinski J.* *Hydrosilylation* (2009). John Wiley & Sons, Inc.

## THE INFLUENCE OF THE ORGANIC-INORGANIC SILICA BASED MODIFIER ON THE EPOXY POLYMER PROPERTIES

**M.G. Tkalich, L.A. Gorbach, O.O. Brovko**

*Institute of Macromolecular Chemistry of National Academy of Sciences of Ukraine, 48 Kharkivske shausse, Kyiv 02160, Ukraine*  
[tkalich.maksym@gmail.com](mailto:tkalich.maksym@gmail.com)

The aim of work was to investigate the influence of the ratio of the initial reagents of epoxy resin ED-20 and organic-inorganic silica based modifier (functionalized by epoxy group (Ep-Si)) on adhesion and viscoelastic properties of cured epoxide composition. The trifunctional triethanolamine (TEA) was used as hardener, which provides the formation of low defective 3D networks. The amount of Ep -Si was varied in interval of 0.5-20 wt %.

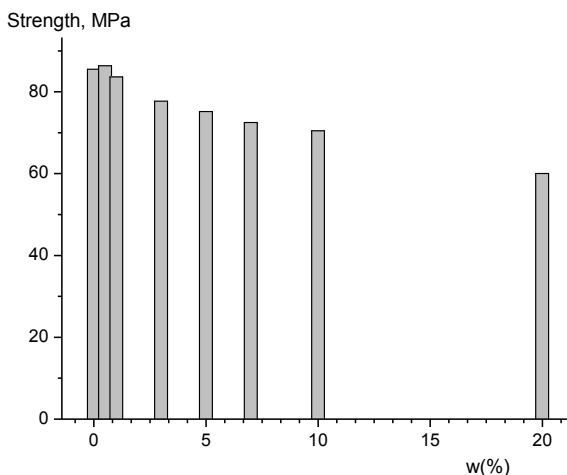


**Fig. 1.** Influence of the amount of Ep -Si on overall strength.

By using dynamic mechanical analysis method the viscoelastic behavior of free epoxy films and films modified by different amount of (Ep-Si) was studied on the dynamic mechanical analyzer TA Instruments Q800 in the temperature interval

P53

of 20-160 °C, with the rate of heating 3 °C/min, on the frequency 10 hz by tensile stress mode. The overall strength was investigated by tensile stress mode with a constant displacement rate,  $\delta=10\text{mm/min}$ .

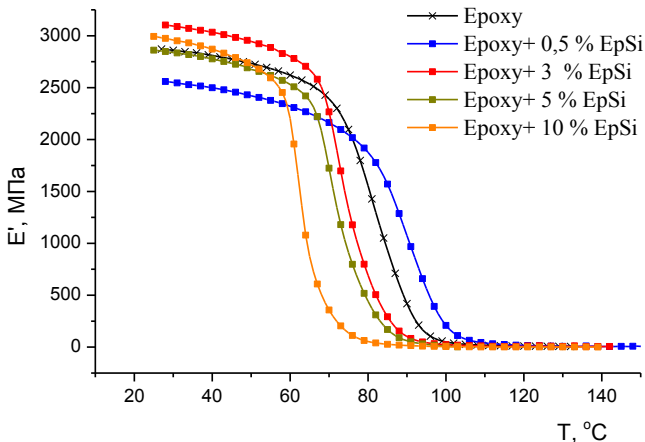


Fig. 2. Temperature dependence of the  $E'$  for epoxy.

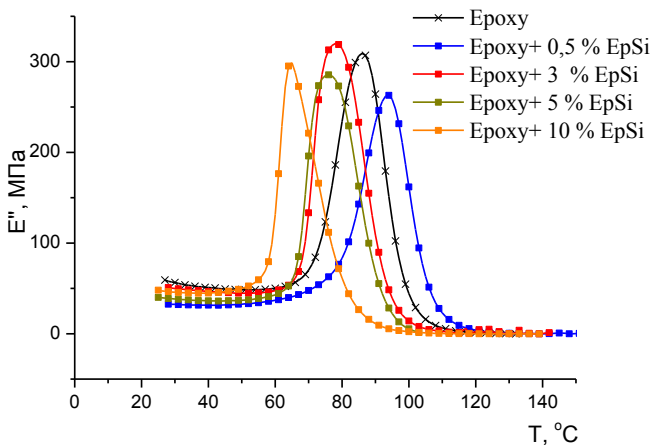


Fig. 3. Temperature dependence of the  $E''$  for epoxy.

The experimental results which was obtained are presented on fig.1 are show the influence of organic-inorganic silica based modifier on adhesion

## P53

characteristics of cured epoxide composition. The dramatic drop of adhesion strength was observed for adhesive layers having amount of Ep -Si less than 1 wt % and more slowly decrease occurred in case of increasing number of modifier.

It was determined that amount of Ep -Si influenced both adhesion and viscoelastic behavior of epoxides (Fig. 2,3). It was shown that adhesion strength and glass temperature of cured epoxide composition, which content 0,5 wt % of organic-inorganic Ep -Si, has too high value compared with the non-modified. Further increases of amount of modifier are decreasing of glass temperature and adhesion strength.

Accordingly, the clear correlation between both adhesion and viscoelastic properties of epoxide composition was determined. It was established that the optimal amount of Ep -Si is 0.5 wt%, that product the best of physic-mechanical properties of epoxide polymer.

## LYOPHILICITY AND OPTICAL PROPERTIES OF CROSS-LINKED COPOLYMERS OF BUTYL METHACRYLATE WITH IMPREGNATED ZnO NANOPARTICLES

**A.L. Tolstov, O.V. Gres, E.V. Lebedev**

*Institute of Macromolecular Chemistry of the National Academy of Sciences of Ukraine, 48 Kharkivske shausse, 02160 Kyiv, Ukraine*  
[tolstov.aleksandr@rambler.ru](mailto:tolstov.aleksandr@rambler.ru)

Polymeric materials loaded with zinc oxide (ZnO) found wide application in various fields of civil life. It has become due to exhaustive properties of the inorganic filler. Introducing micrometer sized ZnO powder into polymers provides improved strength, bactericidal, antifouling, electromagnetic, heat-conductive properties of the final composites [1]. Transfer from micro- to nano-sized ZnO leads to appearing novel optical properties (luminescence, UV-absorbance, high transparency) of the materials [2, 3]. Long exploitation term of polymers filled with ZnO nanoparticles (nZnO) could be achieved by stabilization of inorganic nano-dispersed constituent via functional features of polymeric matrix or additional stabilizers.

In this work we proposed complex approach for stabilization of nZnO in solution by soluble polymeric stabilizer followed by impregnation of stabilized nZnO into a surface of polymeric matrices. Sol of nZnO was synthesized by polyol approach from zinc acetate and ethylene glycol in a presence of poly(N-vinylpyrrolidone) (PVP) as extra stabilizer. Averaged nZnO size in the sol was found as  $16.1 \pm 1.5$  nm (Fig. 1).

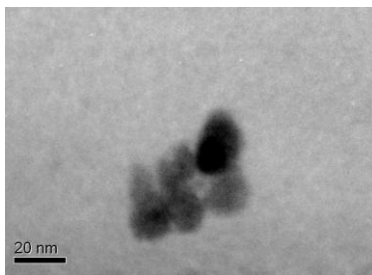


**Fig. 1.** TEM micrograph of PVP-stabilized nZnO sol.

Copolymers of butyl methacrylate (BMA), N-vinylpyrrolidone (VP) and N,N-dimethylaminoethyl methacrylate (DMAEM) cross-linked with ethylene glycol dimethacrylate (EGDMA) have been synthesized by free radical photo-initiated polymerization and used as polymeric matrices for impregnation of nZnO. Composition of the copolymers obtained was presented in Table 1. Polymer films with a thickness of 200  $\mu$ m were used for the

**Table 1.** Composition and lyophilic characteristics of BMA-based (co)polymers

Sample <sup>a)</sup>	Composition, wt%				Equilibrium sorption, wt%		
	BMA	EGDMA	VP	DMAEM	EG	EGME	IPA
PBMA <sup>5</sup>	95	5	-	-	0.4	13.3	13.3
PBMA <sup>1</sup>	99	1	-	-	0.4	43.0	42.8
P(BMA-VP)	90	5	5	-	0.5	30.1	16.5
P(BMA-DMAEM)	90	5	-	5	0.2	19.8	10.1

<sup>a)</sup> Superscript indices indicate cross-link level (EGDMA cross-linker content).

It was experimentally found that EG is good solvent for preparation of nZnO sol but very poor solvent to achieve good results for impregnation of nZnO into surface layer of polymeric matrices (equilibrium swelling of all (co)polymers in EG do not exceed 0.5 wt%). According to handbook data a solubility parameter ( $\delta$ ) for PBMA is 36.8 J/cm<sup>3</sup>. As a result we have tried to select the solvents with  $\delta$  values closed to PBMA to achieve a moderate swelling of polymers in experimental conditions. The second requirement for the solvents is to be good diluents for nZnO sol that will provide a stability of nanosystem. Among different solvents isopropyl alcohol (IPA) with  $\delta$  of 36.8 J/cm<sup>3</sup> and ethylene glycol monoethyl ether (EGME) with  $\delta$  of 44 J/cm<sup>3</sup> were selected ( $\delta$  value of EG is about 61 J/cm<sup>3</sup> that is too high for BMA-based copolymers).

Prior to immobilization of nZnO onto polymeric substrates the lyophilic properties of pure PBMA with different cross-links density and the copolymers are studied to evaluate the best co-solvent for nZnO sol. The kinetics of sorption of solvents selected is presented in Fig. 2.

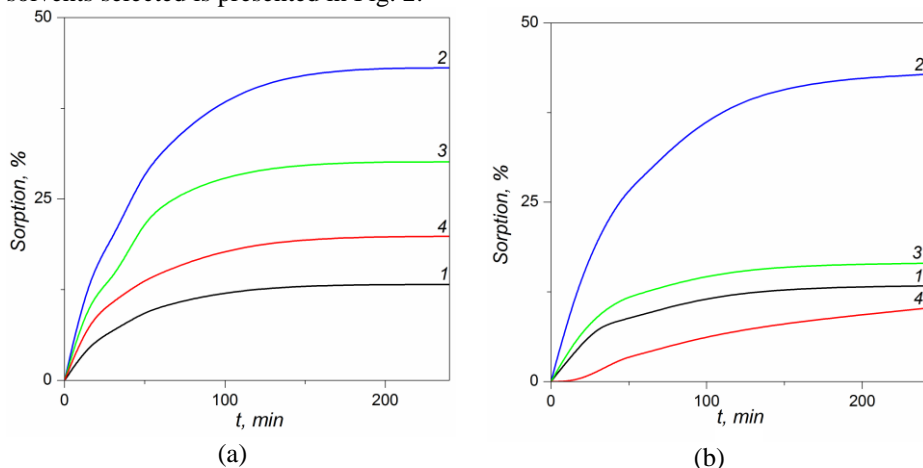


**Fig. 2.** Kinetics of sorption of EGME (a) and IPA (b) by polymer films: (1) PBMA<sup>5</sup>, (2) PBMA<sup>1</sup>, (3) P(BMA-VP), (4) P(BMA-DMAEM).

Equilibrium sorption degrees for all polymers are summarized in Table 1. It was found that swelling behavior of polymer films is highly depend on chemical structure of the polymer and a nature of the solvent. In spite of very close  $\delta$  value of PBMA and IPA the maximum equilibrium swelling of the copolymers was observed when EGME used as solvent. Moreover, introducing EGME into nZnO sol do not change a stability of ZnO nanodispersion.

In accordance with aforementioned results nZnO sol was diluted with EGME (EG/EGME = 1/1 v/v;  $C_{nZnO} = 3.1$  mg/mL;  $C_{PVP} = 2.9$  mg/mL) followed by deposition of the mixture onto a surface of polymer films. Specific nZnO content in polymers of  $0.2$  mg/cm<sup>2</sup> was achieved by dropping appropriate quantity of nZnO sol and temperature-controlled treatment for uniform deposition of active constituent.

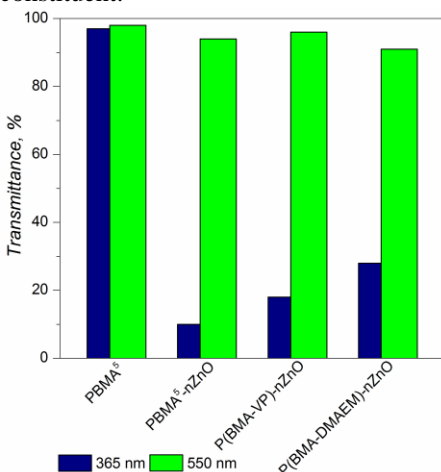


**Fig. 3.** UV-absorbance data of the polymers with immobilized nZnO at fixed wave length.

nZnO and PVP stabilizer). At the same time for P(BMA-DMAEM)-nZnO composition a moderate level of UV absorbance and good transparency in visible region was observed. Probably the main reason of such impact is high reactivity of DMAEM (complexation of  $Zn^{2+}$  by amine-containing ligands [4] and its reducing properties [5]). Intermediate level of UV absorbance for P(BMA-DMAEM)-nZnO system at high transparence in visible region is brought about by effect of polar component of the matrix (VP) on stability of PVP-stabilized inorganic nanophase.

Thus in this work we propose an efficient method for preparation of optically active polymeric nanocomposites with enhanced absorbance at UV region and excellent transparency for visible light. An impact of chemical structure of polymer matrices on optical characteristics of the materials was identified and discussed. Sorption behavior of cross-linked polymer matrices in the media with

Optical properties of polymer films with impregnated nZnO at fixed wave length (UV-A region at  $\lambda = 365$  nm and visible region at  $\lambda = 550$  nm) were measured and the results are collected in Fig. 3. It is shown that reference sample (PBMA without nZnO) is characterized by high transparency at both UV-A and visible region. Impregnation of nZnO provides increased absorbance of UV radiation and excellent transparency at visible region. Highest level of UV absorbance was identified for PBMA<sup>5</sup>-nZnO composite (PBMA matrix is practically inert to both

different solubility parameters was studied as well.

1. *Madelung O.* Semiconductors: Data Handbook, 2004.
2. *Pearton S.J., Norton D.P., Ip K., Heo Y.W., Steiner T.* Recent progress in processing and properties of ZnO // Prog. Mater. Sci. 50 (2009) 293-340.
3. *Tolstov A.L., Gres O.V.* Polymeric systems containing nano- and microstructured zinc oxide // Theoret. Experim. Chem. 48 (2013) 353-366.
4. *Börner J.* Zinc complexes with N-donor ligands and their application as catalysts in the polymerisation of cyclic esters // PhD thesis in Natural Sciences, Paderborn, 2009.
5. *Pliss E.M., Aleksandrov A.L., Mogilevich M.M.* Mechanism of initiated oxidation of dimethylaminoethyl methacrylate // Bull. Acad. Sci. USSR 25 (1976) 2633-2635.

## NEW POLYMERIC NETWORKS BASED ON POLY(VINYL FURFURAL) CROSSLINKED WITH MALEIMIDE MONOMERS CONTAINING TRIBUTHYLTIN CARBOXYLATE FOR ANTIMICROBIAL MEMBRANES

C. Gaina<sup>1</sup>, V. Gaina<sup>1</sup>, O. Ursache<sup>1</sup>, I. Lipovan<sup>2</sup>

<sup>1</sup>“Petru Poni” Institute of Macromolecular Chemistry, 41A Grigore Ghica Voda Alley, Iasi 700487, Romania

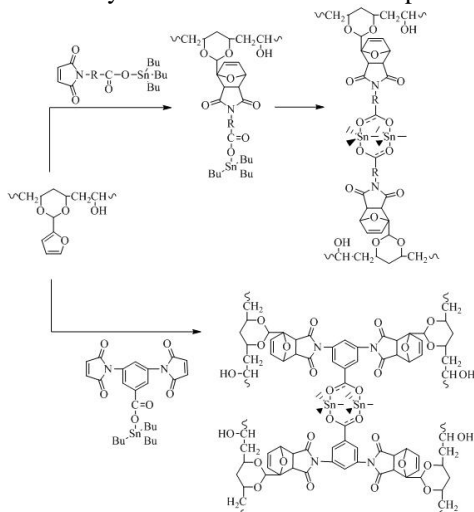
[oana.buliga@icmpp.ro](mailto:oana.buliga@icmpp.ro)

<sup>2</sup> Ion Ionescu de la Brad University of Agricultural Sciences and Veterinary Medicine, 3 Mihail Sadoveanu Alley, Iasi, 700490, Romania

The membranes were obtained by the Diels-Alder cycloaddition reaction of poly(vinyl furfural) with (bis)maleimides [1,2] functionalized with tributhylytin carboxylate groups. Two procedures were used for obtaining films or porous membranes (by phase inversion method).

The structure of the membranes was confirmed by the ATR-FTIR spectroscopy. The morphology of the membranes and the thermal stability were studied. A qualitative study of the antimicrobial activity was also conducted.

A general route for the synthesis of membranes is represented below:



1. Gaina C., Ursache O., Gaina V., Buruiana E., Ionita D. Investigation on

P55

the thermal properties of new thermo-reversible networks based on poly(vinyl furfural) and multifunctional maleimide compounds // *Express Polym Lett.* 6 (2012) 129-141.

2. *Ursache O., Gaina C., Gaina V., Tudorachi N., Bargan A., Varganici C. D., Rosu D.* Studies on Diels-Alder thermoresponsive networks based on ether-urethane bismaleimide functionalized poly(vinyl alcohol) // *J Therm Anal Calorim.* 118 (2014) 1471-1481

## **GUANIDINECONTAINING POLYACRYLAMIDE HYDROGEL**

**M.Ya.Vortman<sup>1</sup>, P.V.Vakulyuk<sup>2</sup>, I.M.Furtat<sup>2</sup>, A.F.Burban<sup>2</sup>,  
V.N.Lemeshko<sup>1</sup>, S.A.Trygub<sup>1</sup>, T.S.Ivanova<sup>1</sup>, V.V.Shevchenko<sup>1</sup>**

<sup>1</sup>*Institute of Macromolecular Chemistry NAN of Ukraine, Kiev, Ukraine*  
[vmar1962@i.ua](mailto:vmar1962@i.ua)

<sup>2</sup>*National University Kievo-Mogilyanskaya Academy, Kiev, Ukraine*

Polyacrylamide hydrogels due to extent of swelling and nontoxicity found a broad application for creation of drug delivery systems of prolonged action. pH-Sensitivity of hydrogels allows to carry out controlled delivery of drug due to existence of ionic groups. One of the ways of such groups introduction is copolymerization of acrylic monomers with those containing cationic or anionic groups. In this regard undoubted interest is represented cationic oligomer derivatives of guanidine which possesses also antimicrobial activity.

The aim of this work - is development of methods of the synthesis of pH-sensitive guanidine polyacrylamide hydrogel for drug delivery systems.

Synthesis of polyacrylamide hydrogel was carried out by radical copolymerization of acrylamide and methylene-bis-acrylamide in water in the presence of guanidine acrylic oligomer and ammonium persulphate. In final hydrogel the guanidine-containing acrylic oligomer performs the function of the ionic cross-linking agent which provides pH-sensitive in the range pH 4-6.

The linear oligomer was synthesized by reaction of aliphatic oligoepoxyde, guanidine and metacrylic acid at a molar ratio of components 2:1:2. At the first stage the aliphatic oligoepoxyde – diglycidyl ether of diethyleneglycole was treated with guanidinhydrochloride at molar ratio of components 2:1. As a result the oligomer with end epoxy groups was obtained. At the second stage the obtained product was reacted with 2 moles of metacrylic acid.

The obtained guanidine acrylate oligomer represents a yellow resin substance, soluble in alcohol, methylethylketone, dimethylformamide.

The structure of the obtained compounds was characterized by IR-spectroscopy.

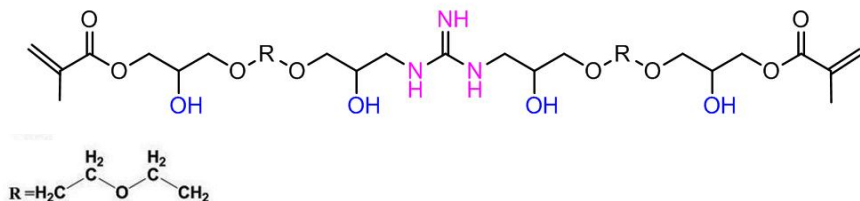


**Fig. 1.** Guanidine acrylic oligomer.

Also initial polyacrylamide hydrogel was synthesized in water by radical copolymerization of acrylamide and methylene-bis-acrylamide as a cross-linking agent. An extent of swelling and ability of release of drug were studied for initial polyacrylate systems and guanidine-containing acrylic oligomer.



The scheme of synthesis of polyacrylamide hydrogel matrix, containing guanidine acrylic oligomer



Polyacrylate matrix    acrylic oligomer    final hydrogel

The scheme of inclusion of covalently bound additives in a hydrophilic polyacrylate matrix

Guanidincontaining hydrogel was used for prolongation of drug on the benzylpenitsilline model. Obtained polymer was inserted to a water solution of drug during on 48 hours. Extent of swelling of polyacrylamide hydrogel and the quantity of sorbed benzylpenitsilline was studied. Then the quantity of desorbed benzylpenitsilline was studied by the insertion of guanidincontaining hydrogel with the sorbed drug in water during on 48 hours.

When guanidine acrylic oligoether was used as ionic cross-linking agent the swelling coefficient falls a little both in water and in biological environments.

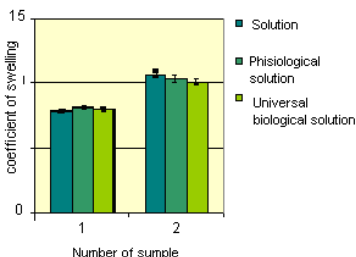


**Fig.2.** Dependence of extent of swelling of polyacrylate systems in environment with a different ionic force  
1- acrylic oligomer as a cross-linked agent  
2 – initial polyacrylate matrix

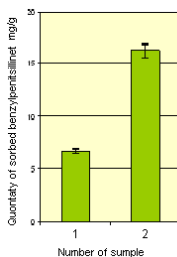


**Fig.3.** Quantity of sorbed benzylpenitsilline  
1- acrylic oligomer as cross-linked agent  
2 – initial polyacrylate matrix

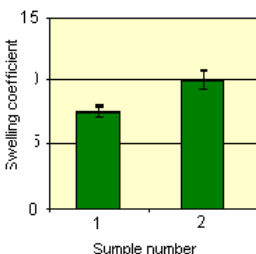


**Fig. 4.** Swelling coefficient  
1 – acrylic oligomer as cross-linked agent  
2 – initial polyacrylate matrix

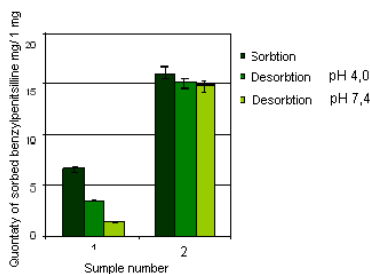


**Fig. 5.** Quantity of desorbed benzylpenitsilline polyacrylate matrix  
1- acrylic oligomer as cross-linked agent  
2 – initial polyacrylate matrix

Influence of pH on ability to release the model drug of the synthesized hydrophilic polyacrylate guanidine systems was studied. It was established that guanidine acrylic oligomer confers to hydrophilic polyacrylate systems pH-sensitivity in the sour environment which is shown at sorbtion and desorbition of drug. The maximum sorbtion and desorbition of drug with use of the guanidine acrylic oligomer was observed at pH 4,0. The initial polyacrylate matrix is not pH

## P56

sensitive: swelling coefficient, sorbtion and desorbtion of medicine doesn't depend on pH value.

The synthesis method of guanidine acrylic oligomer as component of the polyacrylamide hydrogel support was developed. Such oligomer carries out a function of the ionic cross-linked agent in final hydrogel and provides good swelling in biological environments and pH-sensitivity within 4-6. The hydrogel support with use of a guanidine acrylic oligomer provides the prolonged release of drug on model of a benzylpenitsilline with possibility of transdermal use.

## GAS SEPARATION PROPERTIES OF 6FDA-BASED COPOLYIMIDES WITH PHOSPHOROUS-CONTAINING PENDANT UNITS

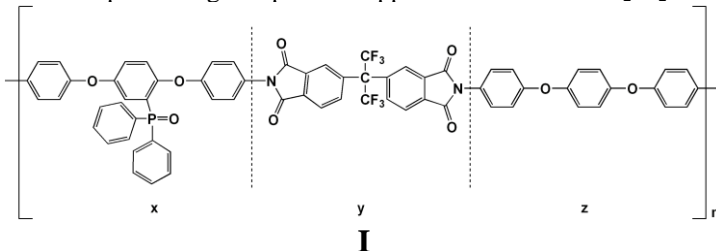
**M. Wójtowicz<sup>1</sup>, A. Wolińska-Grabczyk<sup>1</sup>, A. Jankowski<sup>1</sup>,  
I. D. Carja<sup>2</sup>, D. Serbezeanu<sup>2</sup>, M. Bruma<sup>2</sup>, N. M. Belomoina<sup>3</sup>**

<sup>1</sup> Centre of Polymer and Carbon Materials, Polish Academy of Sciences, M. Curie-Skłodowska 34, 41-819 Zabrze  
[mwojtowicz@cmpw-pan.edu.pl](mailto:mwojtowicz@cmpw-pan.edu.pl)

<sup>2</sup> “Petru Poni” Institute of Macromolecular Chemistry, Romanian Academy, Aleea Grigore Ghica Voda 41A, Iasi- 700487, Romania

<sup>3</sup> Nesmeyanov Institute of Organoelement Compounds, Vavilov Str 28, Russian Academy of Sciences, Moscow-119991, Russia

Gas transport properties of the 4,4-hexafluoroisopropylidene-diphtalic anhydride (6FDA) based aromatic polyimides and copolyimides with phosphorous containing pendant groups (**I**) are reported and compared with properties of the polyimide analogue without pendant groups. Variations in the polymer chain composition were achieved at the synthesis stage by using a mixture of diamine monomers with or without pendant groups in different molar ratios. The effect of the phosphorous containing pendant groups on gas transport has been examined for N<sub>2</sub>, O<sub>2</sub>, He and CO<sub>2</sub> at 35°C under an applied upstream pressure of 6 bar. The polyimide containing bulky pendant groups was more permeable and slightly more selective comparing to its pendant group free analogue. Unexpectedly, the copolyimides appeared to be significantly more selective (about 30 for CO<sub>2</sub>/N<sub>2</sub>) than the both polyimides (less than 20 for CO<sub>2</sub>/N<sub>2</sub>). Moreover, a strong increase in permselectivity has not been achieved at the expense of permeability, which remained within the range of 3 to 6 Barrer. The both transport parameters suggest that this group of copolyimides may constitute membrane materials with promising performances for potential gas separation applications such as CO<sub>2</sub>/N<sub>2</sub> or CO<sub>2</sub>/CH<sub>4</sub>.



**Acknowledgements**

*The financial support offered by CNCSIS-UEFISCDI, Project no. 28/29.04.2013, code PNII-RU-TE-2012-3-0123 is gratefully acknowledged.*

## CORRELATION BETWEEN GAS PERMEABILITY IN HOMO- AND COPOLYIMIDES BASED ON HEXAFLUOROISOPROPYLIDENE AND ALICYCLIC DIANHYDRIDES AND THEIR FRACTIONAL FREE VOLUME

**M. Wójtowicz<sup>1</sup>, A. Wolińska-Grabczyk<sup>1</sup>, A. Jankowski<sup>1</sup> D. Popovici<sup>2</sup>,  
C. Hulubei<sup>2</sup>, M. Bruma<sup>2</sup>**

<sup>1</sup> Centre of Polymer and Carbon Materials, Polish Academy of Sciences, M. Curie-Skłodowska 34, 41-819 Zabrze  
[mwojtowicz@cmpw-pan.edu.pl](mailto:mwojtowicz@cmpw-pan.edu.pl)

<sup>2</sup> “Petru Poni” Institute of Macromolecular Chemistry, Aleea Grigore Ghica Voda 41A, Iasi- 700487, Romania

Varying systematically the molecular structure of homo- and copolyimides, the correlation between their fractional free volume (FFV) and gas permeability have been studied. The polymers were synthesized by a polycondensation reaction using 4,4'-(hexafluoroisopropylidene)diphthalic anhydride (6FDA) or its mixture with bicyclo[2.2.2]oct-7-ene-2,3,5,6-tetracarboxylic dianhydride (BCDA) in 1:1 molar ratio, and various diamines containing different functional groups (Fig. 1). Permeability coefficients ( $P$ ) were determined for pure gases: N<sub>2</sub>, O<sub>2</sub>, He and CO<sub>2</sub>. The FFV of the polymers were determined by the group contribution method developed by Bondi using experimental values of density. It was found that for a given permeant  $\log P$  is a linear function of  $1/\text{FFV}$  as predicted by a free volume theory. However, the deviations from this relationship appeared to be more pronounced when both homo- and copolyimides were considered. In this instance, transport of the gases can be much better described by a model taking into account cohesive energy density of the materials.

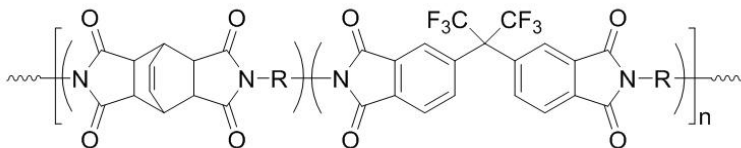


**Fig. 1.** General structure of copolyimides.



Romanian Academy



# THE 3<sup>rd</sup> CEEPN WORKSHOP ON POLYMER SCIENCE

*Polymer Architectures - from concept to design*

**Pol  
Sci  
arch**

September 23-26, 2015

**“Petru Poni” Institute of Macromolecular Chemistry  
Iasi, Romania**



**Organized in the frame of the bilateral Romanian-Ukrainian interacademic project entitled “Development of multifunctional organic and organic-inorganic polymeric materials on the base of components with different chemical nature”, 2012-2016.**